

SALINITY MANAGEMENT IN RIVER BASINS;
MODELLING AND MANAGEMENT OF THE
SALT-AFFECTED JARREH RESERVOIR (IRAN)

CENTRALE LANDBOUWCATALOGUS



0000 0454 6491

Promotor: dr. ir. W.H. van der Molen
emeritus hoogleraar in de agrohydrologie

Co-promotor: ir. J.H.G. Verhagen
toegevoegd docent,
vakgroep Theoretische Produktie Ecologie

K. Shiati

**SALINITY MANAGEMENT IN RIVER BASINS;
MODELLING AND MANAGEMENT OF THE
SALT-AFFECTED JARREH RESERVOIR (IRAN)**

Proefschrift

ter verkrijging van de graad van
doctor in de landbouw- en milieuwetenschappen
op gezag van de rector magnificus,
dr. H.C. van der Plas,
in het openbaar te verdedigen
op maandag 24 juni 1991
des namiddags te vier uur in de Aula
van de Landbouwuniversiteit te Wageningen

وَجَعَلْنَا مِنَ الْمَاءِ كُلَّ شَيْءٍ حَيًّا

از آب هرچیزی را زنده گردانیدیم

And with water we have made all living things.
The Koran

BIBLIOTHEEK
LANDBOUWUNIVERSITEIT
WAGENINGEN

To my parents

111002/01 1431

STATEMENTS

- 1. The brackish water resources of arid and semi-arid countries play a determining role in future agricultural development.
- 2. "Primary salinization" reflects an age-old situation. Human activities aggravate this problem by introducing "Secondary salinization".

This thesis

- 3. Salinity is a water quality problem with a regional character. Therefore, its solution needs a comprehensive regional approach based on implementation of a series of catchment management, engineering and agricultural measures.

This thesis

- 4. The effects of water quality on irrigation are serious, but perhaps more serious is the effect of irrigation on water quality.

Kandiah, A., 1987. Water quality in food production. Water Quality Bulletin, 12, pp. 3-13.

- 5. The conventional guidelines for assessing water suitability for irrigation are conservative and inadequate.
- 6. The successful long-term use of brackish water for irrigation depends on adoption of appropriate crop, soil and water management practices.
- 7. Stratification in reservoirs should no longer be considered as harmful or negative vis-a-vis water quality. Selective withdrawal from stratified reservoirs may be used to beneficially control water quality.

This thesis, and Kaplan, E., 1981. Multiobjective reservoir optimization via lake stratification modeling and constrained nonlinear programming. In: Unny, T.E., and McBean, E.A. (eds), Proceedings of International Symposium on Real-Time Operation of Hydrosystems, University of Waterloo, Ontario, Canada, June 24-28, 1981, pp. 563-581.

- 8. Assisting the developing countries to achieve a sustainable agricultural growth will help the developed countries to alleviate growing problems of land and water resources pollution.
- 9. In development cooperation, higher priority should be given to training, technical education and research programmes.
- 10. There was a Door to which I found no Key.
There was a Veil past which I could not see.
Some little Talk awhile of ME and THEE
There seemed-and then no more of THEE and ME.

Omar Khayyam (1048-1122) - translation by Edward J. Fitzgerald

K. Shiati
Salinity management in river basins;
modelling and management of the salt-affected Jarreh Reservoir (Iran).
Wageningen, 24 June 1991

ABSTRACT

Shiati, K., 1991. Salinity management in river basins; modelling and management of the salt-affected Jarreh Reservoir (Iran). Doctoral thesis, Wageningen Agricultural University, Wageningen, The Netherlands, ix+183 p., 61 Figures, 9 photographs and 20 Tables (Summary and Conclusions in English, Dutch and Farsi).

The sources and origin of salts in the basin of the two salt-affected Shapur and Dalaki rivers (Southern Iran) and the processes involved in salinization have been studied. The extent of water deterioration have been identified by examining spatial changes in the rivers water quality. Among salinity management measures pertaining to water quality, the engineering measures are investigated. It appears that the construction and management of the planned Jarreh Reservoir on the Shapur River is the most feasible one.

The dynamic reservoir simulation model, DYRESM (Imberger, et al., 1978, Version 6.4) is adapted to simulate the salinity/temperature distribution, long-term behaviour and response to various management policies in this reservoir. A simplified method to account for the effect of sediment particles on density of inflows and the inflowing processes in mild bed slope reservoirs is introduced. The method applies only to the steady motion of a turbidity current that is neither depositing nor eroding sediments. The vertical propagation of sediment has not been modelled. This applies to those substances (like dissolved salt) that are not reacting physically or (bio)chemically with suspended particles.

Various management options to minimize the salinity build-up in the reservoir are examined. Among these, the diversion of the most saline part of the summer flows to a point downstream of the last irrigation intakes will result in a significant water quality improvement. At the end of a 5-year simulation, only a weak salinity gradient remains in the reservoir. Based on simulations, using 15 years of data, and the salt balance calculation, the long-term behaviour of the Jarreh Reservoir is studied. It is shown that the salinity in the reservoir is largely determined by annual variability in the river discharge.

KEY WORDS: river basin, salinity, salt diapirism, salt-affected reservoir, density, stratification, sediment particles, sediment-laden inflow, salinity management, Southern Iran

SEARCHED

INDEXED

COPIED

ACKNOWLEDGEMENTS

I am most grateful to Professor Dr. W.H. van der Molen for providing the opportunity for me to carry out the present studies under his supervision and guidance. I very much appreciate his continued encouragement and his valuable criticisms and authoritative corrections of the manuscript. I am greatly indebted to my co-supervisor Ir. J.H.G. Verhagen for his inspiration, suggestions and detailed comments.

I wish to thank the staff of the Department of Hydrology, Soil Physics and Hydraulics for their kind and continued cooperation. Particularly, I wish to thank Professor Dr. J.J. Bogardi, Dr. J. van Hoorn, and Dr. R.W.R. Koopmans for reading parts of the text and for their valuable comments and drs. P.J.J.F. Torfs for his assistance with the DYRESM computer program.

I would like to thank Professor J.C. Patterson, head of Environmental Modelling, Center for Water Research, University of Western Australia for providing the computer model DYRESM and also his later comments on the results.

I express my gratitude to Dr. S.M. Hassanizadeh of the National Institute of Public Health and Environmental Protection (RIVM) for his encouragement, valuable comments, and textual corrections.

My sincere gratitude to Ir. G.J.G. Kok of Royal Dutch Consulting Engineers and Architects, HASKONING and Ir. S. Groot of Delft Hydraulics for their advices and valuable comments on parts of the manuscript.

I would like to express my gratitude to my colleagues in Yekom Consulting Engineers, Particularly Mr. H. Shantia and late A. Ghotbi who kindly made the necessary arrangements for my temporarily leave.

Special thanks should also go to Mr. P.J.F. Link for his assistance with the text processing. I acknowledge the help of Mrs. H.J. van Werven in preparation of the manuscript for printing. The drawing were made by A. Van't Veer whose work was most worthwhile.

Finally, I would like to thank Roya, Elnaz and Ashkan for the leisure time I spent, not with them, but in research work, and whose patience and graciousness made this publication possible.

LIST OF CONTENTS

INTRODUCTION	1
<u>PART I - SALINIZATION IN THE SHAPUR AND DALAKI RIVER BASINS</u>	
1. BASIN CHARACTERISTICS	4
1.1 Drainage basins	4
1.2 Geology of the Shapur-Dalaki catchment	5
1.3 Geomorphological processes and river systems	7
1.3.1 Shapur river	7
1.3.2 Dalaki river	10
1.4 Climate	10
1.4.1 Precipitation	10
1.4.2 Temperature	11
1.4.3 Evaporation	11
1.4.4 Relative humidity	11
1.4.5 Wind	11
1.5 Hydrology	12
1.5.1 Groundwater	12
1.5.2 River flow	12
1.5.3 Water quality	16
1.6 Agriculture and land use	17
1.7 Water resources development	17
References	21
2. SALINITY AND SEDIMENT TRANSPORT IN THE SHAPUR AND DALAKI BASIN	
2.1 Salinity in the Shapur-Dalaki basin	23
2.1.1 Introduction	23
2.1.2 Origin of salinity	24
2.1.3 Salt appearance	25
2.1.4 Sources of salinity	31
2.1.5 Comparison of salinization in river basins	40
2.1.6 Conclusions	41
2.2 Dissolved and suspended matter transport in the basin	43
2.2.1 Introduction	43
2.2.2 Suspended materials	43
2.2.3 Dissolved materials	44
2.3 Relations between river discharge, suspended matter and dissolved matter in the basin	47
2.3.1 Introduction	47
2.3.2 Available data	48
2.3.3 Suspended matter	48
2.3.4 Total dissolved solids	51
2.3.5 Relationships between the components of dissolved matter	54
References	56

PART II - SALINITY MANAGEMENT IN THE SHAPUR AND DALAKI RIVER BASIN

3. A REGIONAL APPROACH TO SALINITY MANAGEMENT IN RIVER BASINS. A CASE STUDY IN SOUTHERN IRAN

Abstract	
3.1 Introduction	60
3.2 Area description	61
3.2.1 Catchment and river system	61
3.2.2 Salinity of the river waters	63
3.3 Salinity control methods in the Shapur and Dalaki basin	65
3.3.1 Strategies	65
3.3.2 Salt disposal methods	65
3.3.3 Salt mitigation methods	68
3.3.4 Other salt mitigation measures	70
3.4 Summary and conclusions	73
References	73

4. BEHAVIOUR OF A SALT-AFFECTED RESERVOIR

4.1 Introduction	75
References	78
4.2 An estimator for the density of a sediment-induced stratified fluid	80
Abstract	
4.2.1 Introduction	80
4.2.2 Temperature and dissolved salt effects $\rho(T,S)$	80
4.2.3 Silt effect $\rho(s)$	81
4.2.4 Temperature, salt, and suspended particles effect $\rho(T,S,s)$	81
References	83

5. MODELLING RESERVOIR WATER QUALITY AFFECTED BY SALT, TEMPERATURE AND SEDIMENT

5.1 Behaviour of sediment-laden stratified flows	85
Summary	
5.1.1 Introduction	85
5.1.2 Analysis of a sediment-laden inflow into a reservoir	86
5.1.3 Application of the model to the Jarreh Reservoir	93
5.1.4 Conclusions	93
References	95
5.2 Numerical simulation of reservoir behaviour	96
5.2.1 Introduction	96
5.2.2 Numerical model	97
5.2.3 Inflow dynamics and algorithm	99
5.2.4 Model inputs	101
5.2.5 Simulation results	105
5.2.6 Effect on output salinity	109
5.2.7 Validation of one-dimensional assumption	113
5.2.8 Conclusions	115

References	116
6. MANAGEMENT OF A SALT-AFFECTED RESERVOIR	
6.1 Introduction	119
6.2 Strategies and measures	121
6.3 Determination of excess water for by-passing or scouring	121
6.4 The effect of by-passing policy	123
6.5 The effect of scouring policy	127
6.6 Salinity trend in the reservoir	130
6.7 Conclusions	136
References	138
RECOMMENDATIONS FOR FURTHER RESEARCH	139
SUMMARY AND CONCLUSIONS	140
SAMENVATTING	147
خلاصہ و نتیجہ گیری	154
Appendix 1. SALINITY AND SALINIZATION	160
A1.1 Major properties of salt structure	160
A1.2 Cause of salinization	160
A1.3 Water resources salinity classification	160
A1.4 References list on salt diapirism in the study area	161
Appendix 2. TURBIDITY CURRENT RELATIONSHIPS	164
A2.1 Governing two-dimensional equations	164
A2.2 Equations on mild bed slopes	171
A2.3 Recasting the equations for triangular cross-section	172
A2.4 Dilution by entrainment (triangular cross-section)	173
Appendix 3. NUMERICAL MODEL DYRESM	174
A3.1 Model description	174
A3.2 Model structure	174
A3.3 Model constants	176
Appendix 4. DIFFUSION OF SALT FROM RESERVOIR BOTTOM	180
CURRICULUM VITAE	183

INTRODUCTION

Southern Iran, with an average total annual rainfall of 300 mm, about 10 per cent of the total annual potential evaporation, is considered as an arid region. If water is available, however, the climate and land resources permit irrigated agriculture. Apart from the water scarcity, the quality (salinity) problem of surface water resources constitutes the main obstacle for developing the region's water and land resources. The problem is largely associated with the geomorphology and hydrology of the natural river basin and is hardly influenced by human activities (natural salinization). Considerable amounts of Iran's brackish surface water resources, about 6700×10^6 m^3 Yr^{-1} , are flowing in the southern part of the country (e.g. Mond river, Shapur and Dalaki rivers, Shur river). They often form the sole sources for irrigation. Therefore, any quality improvement of these vast brackish water resources could have a great beneficial influence on agricultural and regional development.

Although the factors causing natural salinity are essentially unchangeable, regional solutions exist which can control or mitigate the salinity effects by implementing a combination of catchment, engineering and agricultural management measures. As an attempt to alleviate the salinity problem, an investigation program was started for the basin of two salt-affected rivers, Shapur and Dalaki in Southern Iran.

Shapur-Dalaki basin ($52^{\circ}20'$, $50^{\circ}45'$ - $30^{\circ}02'$, $28^{\circ}45'$) has an area of approximately 10 000 km^2 , with geographical area of plains about 160 000 ha, and an average total annual discharge of about 1000×10^6 m^3 . Average total dissolved solids for the Shapur and Dalaki rivers in the summer and at their last water offtakes (Borazjan coastal plain) reaches up to 3700-4000 mg/l. Such high salinities impose significant agricultural constraints. These qualitative problems stem from the existence of salty springs (salinity up to 150 dS/m), formations interbedded with salt and gypsum as well as a number of extruded salt plugs which gradually deteriorate the quality of the river waters. High levels of abundance of sodium and chloride ions in the river's water, compel farmers to grow a specific group of plants with sufficient tolerance to salinity (date palm, wheat and barley) and also to implement a number of agricultural management measures (Photo 1). Obviously, the use of brackish water results in a low yield (about 40 kg of dates per tree) and other secondary effects (Photo 2).

The region contains a number of water bearing limestones (Asmari and Sarvak formations), but the alluvial materials in the plains are rather poor in terms of groundwater resources. Only in the periphery of some plains it is possible to develop, to a limited extent, the groundwater resources. Consequently, the brackish rivers are the only available sources for irrigation.

Shapur and Dalaki rivers have a torrential regime. Reservoirs are needed to

provide storage space to alleviate the hydrological events and to provide water for irrigation. There is a plan to construct a storage dam in the (brackish) Shapur river at Jarreh, near its confluence with the Dalaki river to irrigate 13 000 ha of the coastal areas. There are great concerns about the behaviour of the salt-affected Jarreh Reservoir. A comprehensive study of the role of this reservoir on water quality of the river had yet to be carried out. The present study was initiated by the need to investigate some of these issues prior to the construction of the dam.

The objectives of this research are:

- To identify the origin and sources of salinity in the basin and especially the processes involved in this salinization.
- To determine the contribution of polluting sources in salt accretion and the extent of salinity in the rivers.
- To develop methods and to formulate measures to reduce the salinity of the river waters.
- To model the water quality (salinity) of the salt-affected Jarreh Reservoir, its behaviour upon a large time span as well as its response to different management policies.

Catchment and agricultural management measures are not of interest in this study. The former is less effective in the sparsely-vegetated Shapur-Dalaki basin since the existing of salty formations hamper the plant growth and the latter have been extensively researched and documented.

Records collected since 1974 by the staff of Water Resources Investigation Bureau of Surface Water Section of Ministry of Energy, Meteorological Organization, and Yekom Consulting Engineers of Iran form an essential background to this thesis.

The subject matter of this thesis is divided into two parts. The first part deals with salinization processes and extent of salinity in the basin. The characteristics of the basin are described in Chapter 1. Origin, appearance and sources of salinity in the basin and spatial variation in river water salinity are dealt with in Section 2.1. The dissolved and suspended matter transport in the basin and the processes which are involved are presented in Section 2.2. In Section 2.3, the relationships between river discharge, suspended matter and dissolved matter developed by regression analysis are presented. This relations are used to estimate the future inputs into the Jarreh Reservoir.

Part two deals with the regional approach to salinity management in the river basin and some new aspects related to modelling and management of a salt-affected reservoir.

In Chapter 3 the salinity management measures pertaining to water quality are classified and described quantitatively. Chapters 4 and 5 are devoted to taking into account the effect of sediment content of inflows in modelling reservoir quality. In Section 4.2 a procedure is developed to calculate the water density as a function of temperature, dissolved salts and sediment particles. Section 5.1 deals with the behaviour

of sediment-laden inflows into a reservoir and the equations which describe their characteristics. In Section 5.2, the Jarreh Reservoir water quality as affected by temperature, salinity and sediment particles is modelled. Finally, the response of Jarreh Reservoir to some managment options as well as salinity trend and salt balance calculations are dealt with in Chapter 6.

In this work the numbering of figures is done by Chapters. The symbols used are defined throughout the text.

1 BASIN CHARACTERISTICS

1.1 DRAINAGE BASINS

The Shapur and Dalaki river basins are located in south-west Iran (long. $52^{\circ}20'$, $50^{\circ}45'$ E , lat. $30^{\circ}02'$, $28^{\circ}45'$ N) and cover parts of the Fars and Bushehr provinces (Fig. 1.1). The uplands of the basins are mountainous with a maximum elevation of 3000 m above m.s.l. The altitude decreases to about 20 m at the confluence of both rivers in the coastal plain.

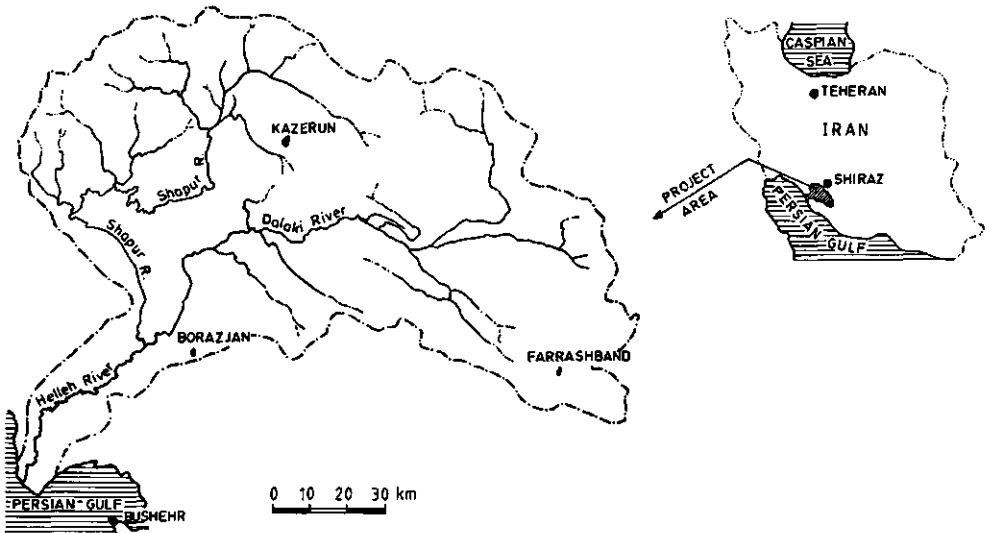


Fig. 1.1 The Shapur-Dalaki basin.

The total drainage area is approximately 10 000 km², of which the Shapur river and its tributaries drain 4110 km² of the northern region and the Dalaki river and its tributaries drain 5800 km² of the southern region. The rivers join to form the Helleh river which debouches into the Persian Gulf. In Fig. 1.2 the longitudinal profiles of the Shapur and Dalaki rivers and their main tributaries are shown.

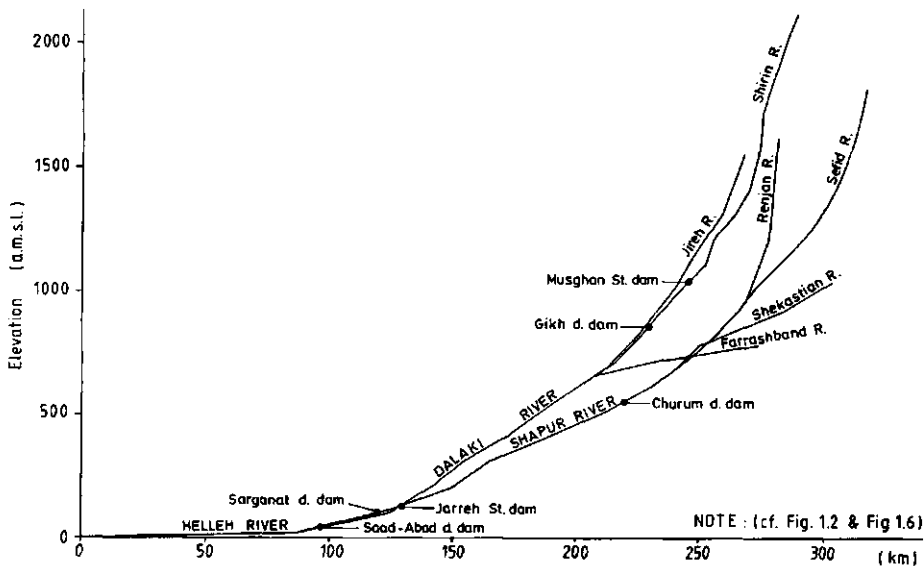


Fig. 1.2 Longitudinal profiles of the Shapur and Dalaki rivers and their main tributaries.

1.2 GEOLOGY OF THE SHAPUR-DALAKI CATCHMENT

The region of the Coastal Fars, where the Shapur-Dalaki river basins are situated, is characterized by very thick sequences of Secondary and Tertiary formations. Up to the Oligocene, these formations are dominantly made up of limestones alternating with occasional marls. On the contrary, the Miocene is characterized by marine shales, marls and some sandstone beds, which indicates the vicinity of an eroding land surface. In the Pliocene, the coastal region of Fars rose above sea level and continental conglomerates started to be formed from limestone pebbles transported from the interior. Quarternary formations lie at the surface in the intermontane basins inland and in the coastal plain.

The successive formations found in this region are listed in Table 1.1, together with their lithology. A geological map of the study area (colored, scale 1:250 000), provided by Yekom Consulting Engineers, Iran, is presented as Annex 1.

In the Late Tertiary, the entire series of older formations were folded into a number of parallel, NW-SE trending long anticlines and synclines, now forming the Zagros Mountains. The thickness of the strata is great, and the distance between these folds is large, of the order of 10-20 km. The emergence

of the area in the early Pliocene was followed by severe erosion; this has given rise to erosion of limestones and subsequent deposition of limestone pebbles, that were later cemented to form the Bakhtyari conglomerates.

Erosion of the softer marls and shales left fewer traces in the river basins, because the resulting clay and silt were mostly transported towards the sea. Such erosion is still very active at present. The Zagros Mountains still have all the characteristics of a young mountain chain: actively downcutting rivers having, in spate, high sediment contents, forming badlands in soft formations and narrow gorges in places where harder strata are traversed.

The erosion of soft rocks has left the harder formations standing out in relief; where the strata are dipping, cuestas have been formed, facing towards the centre of the anticlines. Near the coastal plain, where the dip is monoclinical towards the Persian Gulf, the cuestas are facing inland.

The anticlines still form the hills or mountains, although sometimes soft layers in their centres have been removed by erosion. In that case their harder rims form the highest points in the area. The synclines form long valleys, often drained by subsequent rivers. Locally, they are filled with recent alluvial deposits, in which case these fertile plains are used for intensive agriculture.

In some places, and especially in the centre of some anticlines or at fault lines, salt plugs of Precambrian age have risen from great depths. Three such plugs emerge in the catchment of the Shapur river, and three more in the Dalaki basin. In this arid climate, the salt could rise locally up to the surface, although in other places the domes are covered by a caprock of anhydrite or clay, being a residue from the partly dissolved salt stock.

Table 1.1 Geological formations of the Shapur-Dalaki basin (after James and Wyne, 1965; NIOC, 1977)

Q	Holocene		recent clays, silts and occasional sands
u	Pleistocene		clays, silts, sands, sometimes weakly cemented, forming terraces in coastal plain and intermontane basins
a			
r			
t			
.			
T	Pliocene	Bakhtyari F. Lahbari Member	well-cemented conglomerates more silty, less cemented
e			
r			
t	Miocene	Aghajari F. Mishan F. Guri Member Gachsaran F.	saline siltstones, alternating with occasional sandstone beds marls, silty marls limestone shales with evaporites (gypsum anhydrite, halite)
i			
a			
r			
y			
	Oligocene	Asmari F.	hard limestones, marls
	Eocene	Pabdeh F.	mainly marls
S	Upper Cret.	Guri F. Sarvak F.	marls limestones
e			
c			
o	Lower Cret.	Kazhdumi F.	marls
n			
d	Jurassic	Surmeh F.	dolomites & limestones
.			
	PreCambrian	Hormuz F.	salt plugs

1.3 GEOMORPHOLOGICAL PROCESSES AND RIVER SYSTEMS

In the following, most attention will be given to the Shapur river, because on this river the large Jarreh storage dam is to be constructed. The behaviour of the future reservoir above this dam, especially with regard to its influence on water quality, will be treated in Part II of this thesis. The characteristics of the Dalaki river, therefore, will be given only as far as needed for comparison with Shapur.

1.3.1 Shapur river

The Shapur river basin occupies the north-western part of the Shapur-Dalaki catchment. In the upper reaches of the Shapur basin, the geology is dominated by limestones and marls of Cretaceous to Oligocene age, whereas further downstream the river and its tributaries drain a region that is almost entirely occupied by saline Miocene formations (Annex 1).

The Shapur river and its headwaters originate on the steep southern flank of the Kuh-E Nowdan anticlinal ridge, the highest points of which reach heights of over 3000 m above mean sea level. This ridge mainly consists of Cretaceous limestones (Sarvak formation) and is surrounded by a lowland where the softer Guri and Pabdeh formations have been partly removed by erosion. The hard limestones of the Oligocene Asmari formation stand out as a high rim around the anticline, through the southern part of which the headwaters of the Shapur river have cut spectacular gorges.

Most of these streams are temporary; they join the Sefid river, a consequent seasonal river flowing from east to west in the syncline between the Kuh-E Nowdan anticline and another anticline to the south, that forms the Kuh-E Davan/Kuh-E Morgh mountain ridge. In the west, the flow of the Sefid river becomes permanent and its waters join the Renjan river. Renjan traverses the Kuh-E Davan/ Kuh-E Morgh ridge through a water gap to reach the next synclinal valley, the Kazerun plain. Here it joins the Chenar Shahijan river, draining the NW-part of the upper catchment and together they form the Shapur river. In its upper reach, this river runs southward, following a zone of weakness due to a large fault.

Apart from this flow of surface water, most of the limestones are karstic and supply the headwaters of the Shapur river by springs. On the other hand, also losses from the river basin are possible. From tracer experiments it is known that the Parishan Lake in the Kazerun valley is receiving water from the Dasht Arzhan swamp further north and loses water by subterranean outflow to the Dalaki river further south. Although a comparable subterranean water loss from the Shapur catchment is not excluded, the water balances from both rivers show that it can only form a small proportion of the total flow.

Near the exit of the Kazerun plain, the Pahnak river, draining the southern flanks of Kuh-E Morgh, joins the Shapur river. Shortly below this point, water quantities and qualities are extensively measured at Bushgan Station.

The anticline south of the Kazerun plain, likewise consisting of Cretaceous to Oligocene limestones and marls, plunges towards the north-west. Near its nose, the Shapur leaves this plain. The southern flanks of this anticline, however, are drained by the Dalaki instead of the Shapur. Further downstream, the Shapur catchment consists of formations younger than Oligocene, and most of these are more or less salty. The anticlines in this part of the river catchment become successively lower towards the coastal plain.

Shortly after leaving the Kazerun plain, the Shapur is joined by the Shekastian river, which drains a large area of Miocene shales and evaporites

(Gachsaran formation) in the north-west. As a consequence, its waters contain large amounts of sediments - especially during high discharges - and soluble salts throughout the year.

Only a few kilometers downstream of this junction, the Shapur river traverses an area with two large emergent salt diapirs. They form heavily eroded hills where gypsum, anhydrite and clay form a partial cover on Precambrian evaporites (Hormuz formation) that have risen from great depths. Part of the salt has reached the surface. There are sinkholes and solution tunnels in several places, and a few saline springs occur in the neighbouring river valley.

Beyond this point the Shapur river cuts through the Rudak anticline, formed by the Agha-Jari formation. Where hard sandstone layers are present in this formation, rapids and gorges occur. At one of such points, near the entry of the river into the Khesht plain, the Churum diversion dam is now under construction. The waters, to be taken from the river at this point, will be used to irrigate 6000 hectares in the Khesht plain. The latter is an alluvial basin situated in the Khesht syncline between the Rudak and Takab anticlines. Only a few hard layers within the Agha-Jari formation, hardly forming a watershed, separate this plain from the valley of the nearby Dalaki river, which flows on a level 200 meters below the plain. This demonstrates that the present topography of this area is a very recent feature.

Just before entering the Khesht plain, the Shapur river changes its southward course to flow in a westerly to north-westerly direction, more or less coinciding with the Khesht syncline and thus avoiding to cross the Takab anticline lying to the south. Curving around the nose of this anticline, the river resumes its southward direction and soon afterwards it has cut a deep gorge through the hard conglomerates of the Pliocene Bakhtyari formation, lying at the southern flank of the Takab anticline. At this point, the strata dip gently towards the south, and the Bakhtyari rocks form a steep northward-facing cuesta rising high above the softer shales of the Lahbari Member.

In the gorge, the Jarreh storage dam will be built to irrigate 13 000 ha. of the coastal area. The bottom of the storage reservoir will mainly consist of slightly salty shales belonging to the Miocene Agha-Jari formation and the Mio-Pliocene Lahbari Member.

The hard formations through which the waters of the Shapur river find their way cause a steep gradient in the river. Together with the large detour made around the Takab anticline this explains why the Shapur, near Khesht, flows on a much higher level than the Dalaki river, which has not encountered comparable obstacles in its middle and lower reaches (cf. Fig. 1.2 and Fig. 1.6).

After this gorge, the Shapur enters the coastal Plain, where it joins the Dalaki to form the Helleh river. Just before this junction, at Saad-Abad, an existing diversion dam is used to irrigate agricultural lands and especially date plantations along the Shapur and Helleh rivers. The latter, flanked by date palms over the first 10 km, finally debouches into the Persian Gulf, just

north-west of Bandar Bushehr.

1.3.2 Dalaki river

The headwaters of the Dalaki river are formed by three streams: the Shirin river, draining the northern part of the basin, the Jireh river coming from the east, and the Farrashband river from the south-west.

Of these, the Shirin is the most important tributary. It originates from a limestone area made up mostly of the Asmari and Sarvak formations. Where the river becomes perennial it traverses a large salt plug, where its waters are contaminated by solution of the evaporites and by the outflow from highly salty springs. After crossing a small alluvial plain near Mosghan, the Shirin has cut a water gap through a limestone anticline. At the southern end of this gorge, Mosghan storage dam has been planned. Slightly further downstream a second large diapir influences Jireh river, and a third salt dome occurs in the basin drained by the Farrashband river. As a consequence the streams in the upper part of the Dalaki system have a higher salinity than the corresponding waters in the Shapur basin.

After the headwaters join to form the Dalaki river, this stream mainly follows synclinal valleys. Short tributaries from the north drain areas where evaporites in the Miocene Gachsaran formation contribute large amounts of salts. Especially the Shur river carries a large salt load. Thus, although the Dalaki basin has far fewer Miocene sediments than the Shapur catchment and especially the Gachsaran formation is limited to a few small areas only (Annex 1), the salt loads and salt concentrations of both rivers are comparable. Further details about river salinity and its causes will be given in Chapter 2.

At Sarqhanat, where the river enters the coastal plain, a new diversion dam, which replaces an older structure, is under construction. From this dam 7000 ha. of the coastal plain will be irrigated. About 25 km further downstream the Dalaki joins the Shapur to form the Helleh river.

1.4 CLIMATE

The climate of the Shapur-Dalaki basin (Table 1.2) can be classified as arid (UNESCO, 1979; Sabeti, 1969): the average annual rainfall is below 20 per cent of the total annual potential evaporation. Only in the highest parts of the basin, where the precipitation is higher, the degree of aridity is less.

Except in occasional wet years, most precipitation is confined to the winter months. The dry season lasts from April to October.

1.4.1 Precipitation

The total annual rainfall decreases southwards towards the coastal plains and the Persian Gulf. Mean values vary between 600 mm in the upper part of the

basins to less than 200 mm along the coast (Fig. 1.3) and they are closely related to the elevation of the terrain. Rainfall occurs mainly during the 6 months of November through April, with a peak in mid-winter. In the mountains, part of the winter precipitation falls as snow. The snow cover, however, does not last beyond the end of March. There is only erratic rainfall during the summer season. Maximum and minimum rainfall occur respectively, in January and July.

Daily values of precipitation are quite variable. In winter, daily amounts of over 40 mm are rather frequent; they give rise to considerable runoff from steep, impermeable and sparsely vegetated hillslopes. There is also considerable variation from year to year. Whereas the wettest year on record (1975-76) had 390 mm measured at Shabankareh Station, the driest year (1962-63) did not give more than 73 mm.

1.4.2 Temperature

In the Shapur-Dalaki basin, a great variation of mean temperature is observed over the year. The mean annual values range between 16 °C in the highest (northern) part of the basin and 24 °C in the south-western coastal plain (Fig. 1.4). The maximum and minimum temperatures occur in July/August and January/February, respectively. Values of mean monthly, mean maximum, and mean minimum temperature are shown in Table 1.2. Frosts are common in the interior, but rare in the coastal plain. Daily variation in temperature is very high in all parts of the basin.

1.4.3 Evaporation

The annual potential water evaporation is high: the total annual evaporation, measured with a Class-A pan, exceeds 3000 mm. After correction for the class-A pan, the mean annual potential evapotranspiration becomes approximately 2000 mm (Table 1.2). Both estimates show a clear seasonal trend with a maximum in summer. Their ratio is almost constant over the year and varies around 0.67. The actual evapotranspiration is much lower; an estimate for the annual value of the basin will be given in section 1.5.2.

1.4.4 Relative humidity

The mean yearly values of relative humidity are around 55%, and follow a clear seasonal trend. The monthly averages are up to 72% in January, decreasing steadily to 40% in summer (Table 1.2).

1.4.5 Wind

Wind velocity has been measured only at Bushehr, along the coast, where it is considerable, ranging from 18 km/hr in March to 12 km/hr in June. No data about wind velocities in other parts of the basin are available, but the

wind is more feeble further inland. In Shiraz, for instance, the average yearly velocity is only 9 km/hr.

1.5 HYDROLOGY

1.5.1 Groundwater

In this arid climate, recharge of groundwater by winter rains or snowmelt is possible in the limestone areas. The permeable character of these rocks and the thin soil cover promote such recharge. Outflow of groundwater to the headwaters of the rivers causes a permanent flow in streams like the Renjan and Shirin rivers. There are plans to develop groundwater abstraction from the karstic limestones of the Asmari formation in the anticlines bordering the Kazerun plain.

On the other hand, the Miocene formations are nearly impermeable. Moreover, surface runoff from these areas is promoted by the steep slopes and the sparse vegetation. Some small springs occur, probably associated with fault zones. They often yield highly saline water. In the coastal plain, sandy aquifers occur locally, but their water is often too salty to be used for irrigation.

1.5.2 River flow

The average annual flows from the Shapur and the Dalaki are listed in Table 1.3. As appears from this table, the catchment areas of both rivers are rather similar in size, and the same holds for the annual discharges. The amount of water removed per year gives no indication for a considerable transfer of water from the Shapur basin to the Dalaki river; on the contrary, the specific discharge is slightly higher for the Shapur. These data can be used to estimate the annual actual evapotranspiration as the difference between precipitation (as derived from Fig. 1.3) and specific discharge.

The variation from year to year is considerable: over the period of observation, the annual discharge varies between 124-1270 Mm³ for the Dalaki river and between 162-992 Mm³ for the Shapur river. The discharges mainly occur during winter, and reach a maximum in February.

Average monthly flows over the period of observation are shown in Fig. 1.5a. It appears that the Shapur has a greater variability over the year than the Dalaki. The monthly flows show a high variability from year to year, still more than the annual totals. An example for the wettest month (February) and driest month (August) in different years is given in Fig. 1.5b and c. These figures confirm the irregularities due to the vagaries of the climate. The flow in both rivers is permanent, even in dry years, which is an indication for a contribution by outflowing groundwater.

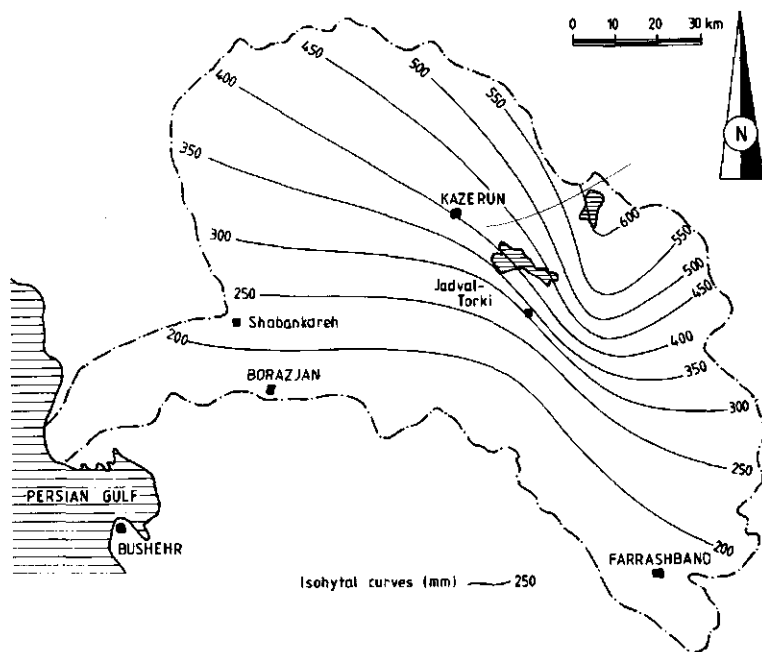


Fig. 1.3 Mean annual precipitation in the Shapur-Dalaki basin.

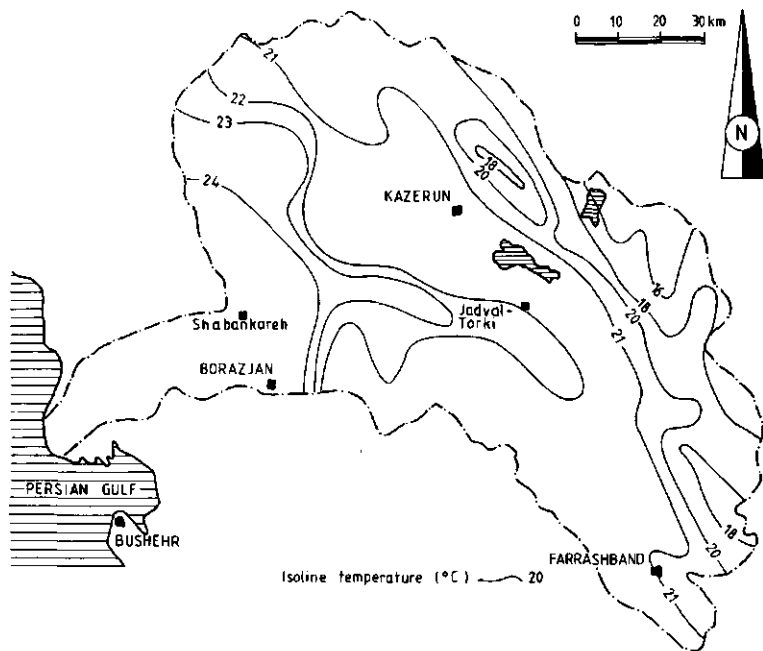


Fig. 1.4 Mean annual temperature in the Shapur-Dalaki basin.

Table 1.2 Climatological data of the Shapur-Dalaki basin
(data: Meteorological Organization of Iran)

stat. no.	O	N	D	J	F	M	A	M	J	J	A	S	year	
of years														

precipitation (mm)														
1	19	2	24	46	70	37	14	16	3	-	-	1	-	213
2	19	4	38	47	128	80	49	41	7	1	-	2	-	447
3	19	5	10	37	80	45	11	30	3	-	-	2	-	223
temperature (°C)														
1	25	27	20	15	14	15	19	24	29	32	34	34	31	25
2	19	24	17	12	10	12	16	20	26	31	33	33	29	22
max. temp. (°C)														
1	19	37	28	22	20	23	28	33	39	43	44	43	41	33
2	19	34	27	20	19	19	23	28	35	40	43	43	39	31
min. temp. (°C)														
1	19	17	13	8	8	8	10	14	18	22	24	25	18	16
2	19	13	8	4	2	4	7	10	17	20	23	22	18	12
relative humidity (%)														
1	25	51	59	72	73	68	59	51	43	44	48	49	50	56
2	19	51	58	67	71	69	60	54	46	39	41	44	47	54
sunshine (hours/month)														
4	10	294	237	204	220	193	243	240	308	341	330	325	305	270
wind velocity (km/hour)														
4	10	15	14	16	17	17	18	16	14	13	12	12	14	15
evaporation Class-A pan (mm)														
1	19	267	160	84	54	75	132	212	351	485	445	418	339	3022
2	19	261	165	87	58	79	117	145	239	405	459	458	405	2876
evapotranspiration calculated from evaporative pan (mm)														
1	19	174	104	59	38	49	86	138	228	315	289	272	220	1972
2	19	191	120	65	46	54	80	99	163	235	335	333	296	2017

Stations:														
1	Shababkareh	E 51 06'	- N 29 23'			elev.	40 m							
2	Kazerun	E 51 40'	- N 29 37'			elev.	860 m							
3	Jadval-Torki	E 51 54'	- N 29 16'			elev.	715 m							
4	Bushehr	E 50 50'	- N 28 59'			elev.	4 m							

Table 1.3 Average annual discharges from the Shapur and Dalaki rivers

		Shapur at Saad-Abad	Dalaki at Sarqhanat
area drained	km ²	3990	5190
annual discharge	Mm ³ /yr	530	425
rainfall on basin	mm/yr	350	300
specific discharge	mm/yr	133	82
actual evapotransp.	mm/yr	217	218

Note:

16 years analysed, period:1961-1978; rainfall from Fig. 1.3.

On a daily scale the irregularities are still more pronounced. Especially the impermeable and mostly steeply sloping shales and siltstones cause an almost immediate runoff after heavy rains. Daily flows in the Shapur at Jarreh are known since 1975. They have been used as inputs into the model simulating the behaviour of the future Jarreh reservoir (Part II).

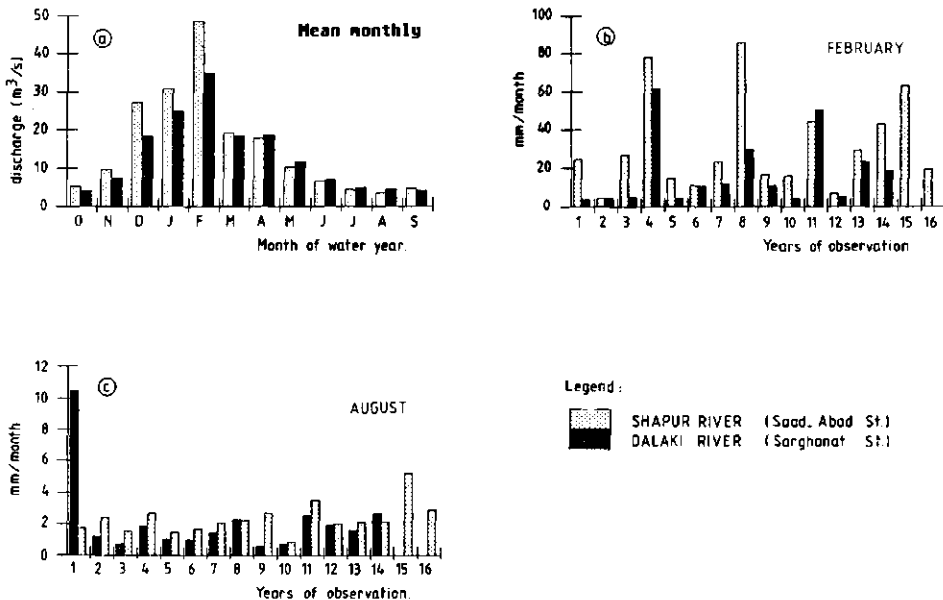


Fig. 1.5 Flow variability for Shapur-Dalaki rivers (1961-1977); (a) mean monthly; (b) wettest month, (c) driest month, data by Ministry of Energy, Iran.

1.5.3 Water quality

The Shapur and Dalaki rivers are primarily originating from karstic springs, which yield waters of excellent quality. Further downstream, they are passing through large areas with salt domes and saline erodible formations. As a consequence, they increasingly become contaminated by salts. The severe erosion of these scarcely vegetated and soft materials results in very high silt contents of this water (cf. section 2.2). If the formations are saline, also salts are liberated during this process, and the runoff carries a considerable salt load, although the concentration during these events remains low due to dilution.

If heavy rains are followed by a dry period, capillary rise will concentrate salts at freshly exposed surfaces, from which they may be dissolved by a following rain. In this way, light rains may result in highly saline runoff from such areas. The Shekastian river (a tributary of the Shapur), for instance, which drains an area largely occupied by the salty Gachsaran formation, has low concentrations but high salt loads during high discharges and high concentrations but lower salt loads at low flows, with a salinity sometimes approximating that of sea water.

The high salt contents form an obstacle to their use for irrigation. The average total dissolved solids of the river waters are listed in Table 1.4. The TDS-contents for the Shapur are higher than for the Dalaki. In both rivers, they increase in a downstream direction.

Table 1.4. Average total dissolved solids (TDS) for the Shapur and Dalaki rivers

	summer (ppm)	winter (ppm)
Shapur:		
Khesht	2720-2780	1740-1800
Jarreh	3700-4000	2130-2440
Dalaki:		
Jireh	1540-1830	920-1380
Sarghanat	3680-3800	1850-2110

In Chapter 2, more details will be given about the origin and chemical composition of the salts in the river waters and about the plans to reduce their high concentrations.

1.6 AGRICULTURE AND LAND USE

In the Shapur and Dalaki basin, agriculture has been practised for centuries. The inland basins, filled with fertile alluvial soils and parts of the coastal plain are intensively cultivated (Fig. 1.6), whereas the steep hills and mountains and the saline parts of the coastal plains are used for grazing, mainly with sheep.

The following limitations are found to impede the agricultural development of the alluvial plains:

- shortage of water
- salinity of water
- adverse chemical and physical soil properties

According to Yekom Consult. Engrs., 1980, out of 86 000 ha. of irrigable lands about 46 000 ha could actually be irrigated after full implementation of water resources development projects.

High salinity - of sodium chloride type - only allows the farmers to grow crops that have sufficient tolerance to salinity (date palm, barley, wheat and alfalfa).

Soil salinity and sodicity in the coastal plain near Borazjan are major constraints to successful farming in this area. Most of the saline-sodic soils in this plain suffer from high water tables and inadequate drainage. Only along the main rivers, where the natural levees provide sufficient natural drainage, highly productive date plantations are found (Photograph 1). Elsewhere, drainage is needed to prevent waterlogging and salinization, such as shown in Photograph 2.

1.7 WATER RESOURCES DEVELOPMENT

The Shapur and Dalaki rivers possess a regime of flash floods in winter, whereas during the summer drought their flow falls to very low values (Fig. 1.5a). Therefore, only a storage dam will be able to regulate the flow of the river needed to create the conditions necessary for developing the agricultural resources. In addition, as will be shown in Chap. 5, salinity can be regulated and improved by careful management of such reservoirs. Table 1.5 shows the feasible water resource developments for the Shapur-Dalaki basin as proposed by Yekom Consult. Engrs. (1980). Fig. 1.6 shows the agricultural zones and the proposed water resources development projects in the basin.

There is limited potentiality for developing groundwater resources in the alluvial plains due to both quantity and quality of such waters. On the other hand, relatively abundant reserves of groundwater exist in the karstic Asmari limestone formations, especially in the Sarbalesh anticline, south of the Kazerun plain (Annex 1), where about 50 Mm³ will be abstracted in the near future. The total safe yield of this aquifer is estimated at 200 Mm³/year.

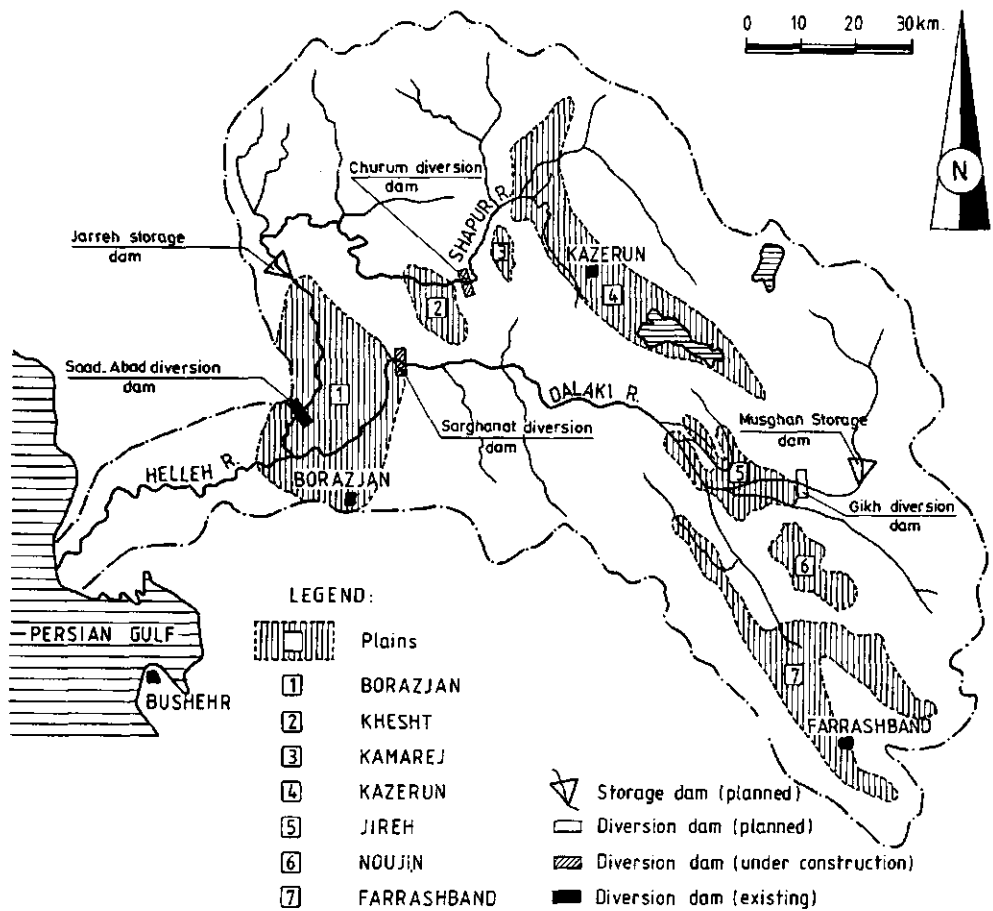


Fig. 1.6 Agricultural zones and proposed water resources development projects in the Shapur-Dalaki basin.

Table 1.5. Water resources development projects for Shapur-Dalaki basin (source: Yekom Consult. Eng., 1980)

river basin	reservoir	height (m)	stored volume (Mm ³)	level of project	irrigated area (ha.)	water use (Mm ³)
surface water:						
SHAPUR	Jarreh s. dam	97	470	phase II		
	Churum d. dam	12	-	under const.		
	Irrig. & Drain. network in Khesht plain			under cons.	5600 (2230)	100 (63)
	Irrig. & Drain. network in			phase II	13000 (3075)	278 (85)
ground water:						
					alluvium	
					23 (18)	
	limestones					200 (0)
surface water:						
DALAKI	Musghan s. dam	93	245	phase I		
	Gikh d. dam	10	-	phase II		
	Sarghanat d. dam	11	-	under const.		
	Irrig. & Drain. network in Jireh plain			phase II	6300 (4470)	112 (165)
	Irrig. & Drain. network in Dalaki plain			under const.	7000 (5340)	180 (160)
ground water:						
					alluvium	
						27 (13)

Note:

In brackets are the values of present use.



Photo 1 Present agriculture in the study area (Borazjan plain). Farmers utilize the brackish water by adopting a series of agricultural management measures: cultivation of salt tolerant crop (date palm); leaching accumulated salt by using basin irrigation method (7*20*1 m), and by irrigation scheduling.



Photo 2 Present agriculture in the study area (Borazjan plain). Soil salinity and alkalinity and low yield are the secondary effect of using brackish water in areas with inadequate drainage.

REFERENCES

James, C.A. and Wyns, J.G., 1965. Stratigraphic nomenclature of Iranian Oil Consortium Agreement Area. Amer. Assoc. Petrol. Geol. Bull., 49:2182-2245.

National Iranian Oil Company, 1977. Explanatory notes to geological map, cross sections and tectonic map of south-central Iran, sheet 5. Tehran, National Iranian Oil Company, Exploration and Production, 1p, scale 1:1000 000.

Sabeti, H., 1969. Barrasi-e Aghalim-e Hayatti-e Iran. University of Tehran, Iran. (in Farsi)

UNESCO, 1979. Map of the world distribution of arid regions. Explanatory Note. MAB Tech. Notes, No. 7.

Yekom Consulting Engineers, 1980. The Shapur and Dalaki rivers salinity control project. vol. (3, 10 and 13), Teheran, Iran. (in Farsi)

2 SALINITY AND SEDIMENT TRANSPORT IN THE SHAPUR AND DALAKI BASIN

2.1 SALINITY IN THE SHAPUR-DALAKI BASIN

Published in part in:

International Association for Hydrological Science (IAHS), publ. No. 185
(Proc. IAHS Third Scientific Assembly, 10-19 May 1989, Baltimore, USA), 201-
210.

2.1 SALINITY IN THE SHAPUR-DALAKI BASIN

2.1.1 Introduction

Salinity is a water quality problem of increasing importance in many irrigated areas. In arid and semi-arid countries this problem is particularly serious because:

- (a) Brackish water is often the only supply available for regional development.
- (b) Increasing population pressure causes more marginal lands to be brought under cultivation and increases the need for using brackish water for irrigation.
- (c) Great efforts are needed to overcome the secondary effects of using saline irrigation water.

According to Sadler et al. (1981) salinity becomes a major obstacle for agricultural development in Western Australia and is widely spread in Western America as pointed out by Miller et al. (1981). The problem remains particularly serious in arid and semiarid countries such as India, Pakistan, Iran, Iraq, Egypt and Tunisia.

Brackish water often accounts for a large portion of the water resources. For instance, in Iran, annually about 6700 Mm³ of such waters flow through 12 major rivers, mostly in the southern part of the country. Any quality improvement of these vast brackish water resources has a great beneficial influence on agricultural and regional development.

Various processes are involved in causing salinity in river basins. Furthermore, the origin, sources and type of salinity are different (Peck, 1978, W. Australia; U.S.B.R., 1974, W. USA; Greenlee et al., 1968, Montana, USA; Van der Molen, 1986, Ebro, Spain; Shaun et al., 1987, Ontario, Canada; Sommerfeldt, 1977, Alberta, Canada).

As an attempt to alleviate salinity problems in river basins a study was carried out of two salt-affected rivers, the Shapur and the Dalaki in Southern Iran. The objectives were:

- (a) To identify the origin and sources of salts that affect the quality of the river water used for irrigation, and especially the processes involved in this salinization;
- (b) To determine the contribution of polluting sources in salt accretion and the extent of salinity in the rivers;
- (c) To develop methods and to implement management measures to reduce the salinity of the river waters.

The first two objectives were accomplished by studying the geological features and especially the presence of salt structures in the basin, monitoring an extensive salt/flow observation network and furthermore by

examining spatial changes of river water quality.

This chapter is the outcome of studying the objectives (a) and (b). The improvement by management measures will be dealt with in Chap. 3.

2.1.2 Origin of salinity

From the Precambrian upto the Pliocene the entire country of Iran was mostly covered by seas which were different in depth, water temperature and lifetime. During regressions conditions were sometimes favourable for the formation of salt deposits (evaporites). They occur either as thick deposits of halite or in the form of halite and gypsum interspersed with layers of marls and some dolomites. In Southern Iran, the salt content of the rivers mainly originates from erosion of three such evaporites, two of which occur in the study area.

i - Precambrian evaporites

Late Precambrian evaporites, known as Hormuz formation (after Hormuz Island in the Persian Gulf) extend from the outer part of the Arabian shield, across the Zagros orogenic belt, on to the internal plateau of Inland Iran (Kent, 1979). They are widespread in the Shapur-Dalaki basin (Fig. 2.1).

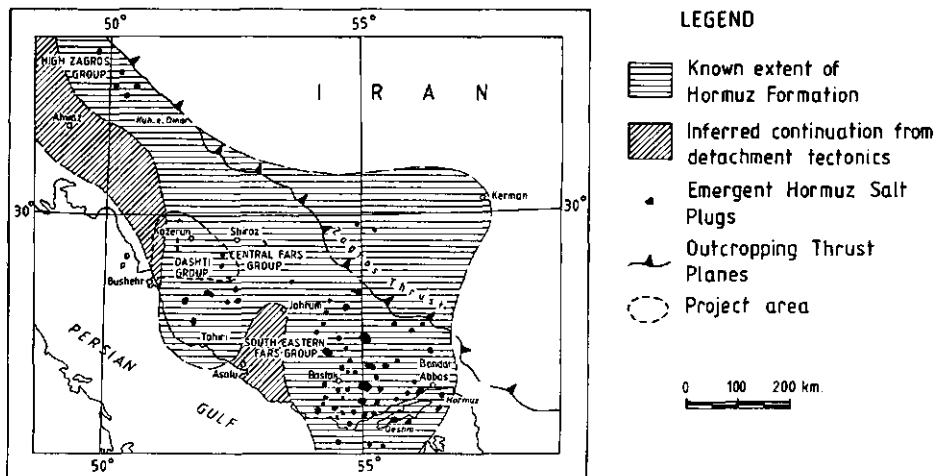


Fig. 2.1 Extent of Hormuz Formation and extrusive Hormuz salt plugs in Southern Iran (after Kent, 1979).

The Hormuz formation is believed to be derived from a widespread unit of interbedded halite, gypsum and non-evaporitic rocks, underlying the phanerozoic rocks of the Zagros mountains at a depth of 2-5 km (Kent, 1958; Kent and Hedberg, 1976; Kent, 1979, 1987). The Hormuz salt itself is usually dull gray and coarsely crystalline; it contains shale and other rock

fragments. From the quantity of gypsum on the weathered outcrops it may be deduced that anhydrite is present in important portion.

ii - Jurassic evaporites

Evaporative conditions during the lower Jurassic resulted in the formation of evaporites with considerable amounts of gypsum and to a lesser degree rock salt and layers of marls and dolomites. Similar evaporites covering the oil-bearing Jurassic limestones, are known in Saudi Arabia as the Arab formation (with anhydrite). The gypsum in this formation changes to halite near Kuwait and to gypsum again in Khark Island and Southern Iran. These evaporites have not been found in the study area.

iii - Miocene evaporites

These formations, which extend over almost the whole of Southern Iran are the main source of the present salinity in the study area (Annex 1). These evaporites cover the oil-bearing Oligocene limestones (mainly Asmari formation) and play a major role in preventing oil to migrate from this reservoir.

Apart from these evaporites, almost all Tertiary formations are saline due to their initial salt content. Erosion of the natural landscape likewise affects the salinity of river waters and sediments displaced over short distances.

2.1.3 Salt appearance

In an evaporative environment salt precipitates as a tabular layer interbedded with other sediments. From this primary stratiform and subhorizontal state, it may be displaced by tectonic processes and appear at the surface in different shapes.

The young salts of Miocene evaporites appear interbedded or interspersed in Tertiary strata affected by folding or tectonic motions. In the Agha-Jari formation, crystallized plates of gypsum occur (Photo 3) whereas the evaporites in the Gachsaran formation are folded together with the strata (Photo 4).

Salt layers of adequate thickness can flow plastically under stresses due to gravity, to imposed tectonic forces, or to a combination of both (Appendix 1, A1.1). The effectiveness of differential stress in driving its deformation depends on such factors as temperature and confining pressure. The presence of impurities is important; water increases diffusive flow, whereas nonevaporitic materials reduce plasticity (Jackson and Talbot, 1986).

In this way, plastic salt flowage has transformed the tabular old salts of the Precambrian Hormuz formation into pillars having a large variety of shapes. In this text they will be denoted as "salt diapir", "salt dome" or "salt plug". These terms will be used interchangeably although the structures

consisting of Hormuz salts all obey the definition of "salt diapir" as given by O'Brien (1968): " a body that has pierced, or appear to have pierced, a shallower overburden". Some of these diapirs appear at the ground surface as "salt plugs" and they may reach a height of thousands of meters above their original position. An outstanding case is the Dashti salt plug, which is a magnificent dome of shining salt with a height of 1300 m, located SE of Bushehr. The main types of large salt structures as distinguished by Jackson and Talbot (1986) are shown in Fig. 2.2.

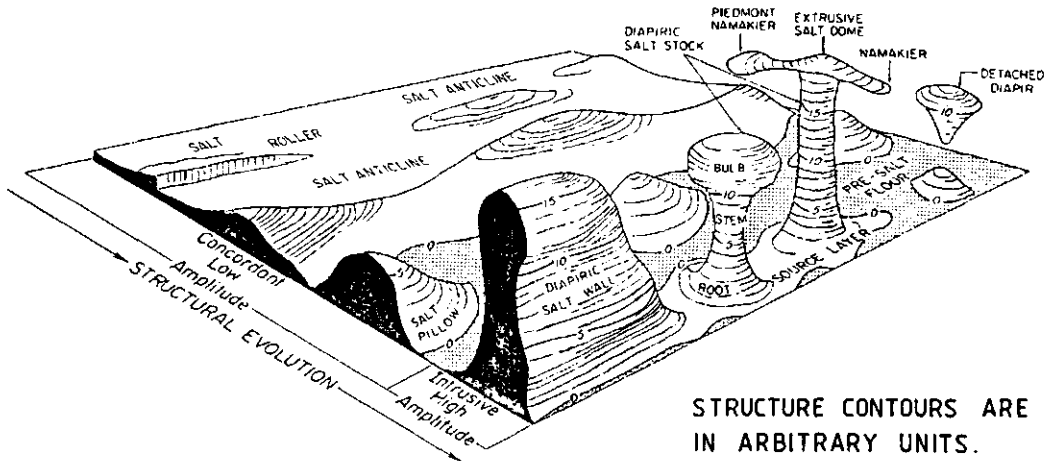


Fig 2.2 The main shapes of large salt structures.
(from Jackson and Talbot, 1986)

Southern Iran is a most favourable area to observe extruded salt plugs (Fig 2.1). In this area 150 salt diapirs are known, six of which are located in the study area. The literature list (Appendix 1, A1.4) gives a rather extensive bibliography of these phenomena, of general interest as well as for this specific area. Intrusion of the majority of the plugs already occurred before the Pliocene Zagros orogeny. This orogeny has been influenced by the pre-existing weak points provided by the salt plugs. Photograph 5 shows the Bachon salt plug in the Dalaki river basin, where water erosion has caused a typical badland topography. Photographs 6 and 7 show the Kamarej salt plug in the Shapur river basin. The salt of this diapir is mined for domestic and industrial purposes. Salt structures are important as:

INTERBEDDED SALT LAYERS IN TERTIARY
EVAPORITES (AGHAJARI FORMATION) 29° 30' - 51° 30'



Photo 3 Crystallized plates of gypsum in Agha-Jari formation (location Khesht plain).



Photo 4 Layering and gypsum outcrops in the Gachsaran formation (location east of Sarmashad).

- traps for hydrocarbons (petroleum);
- possible storage sites for radioactive wastes and other poisons;
- sources of minerals like halite and especially potassium and magnesium salts;
- locations for temporary storage of compressed natural gas.

These applications have provided the main stimulus for an intensive study of their structure, development ("salt diapirism") and dynamics in Southern Iran.

BACHON SALT PLUG : 28°58' - 52°15'

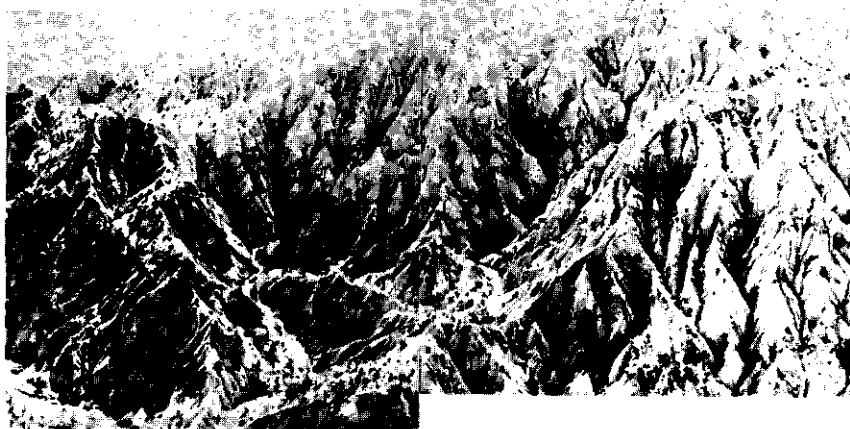


Photo 5 The Bachon salt plug.

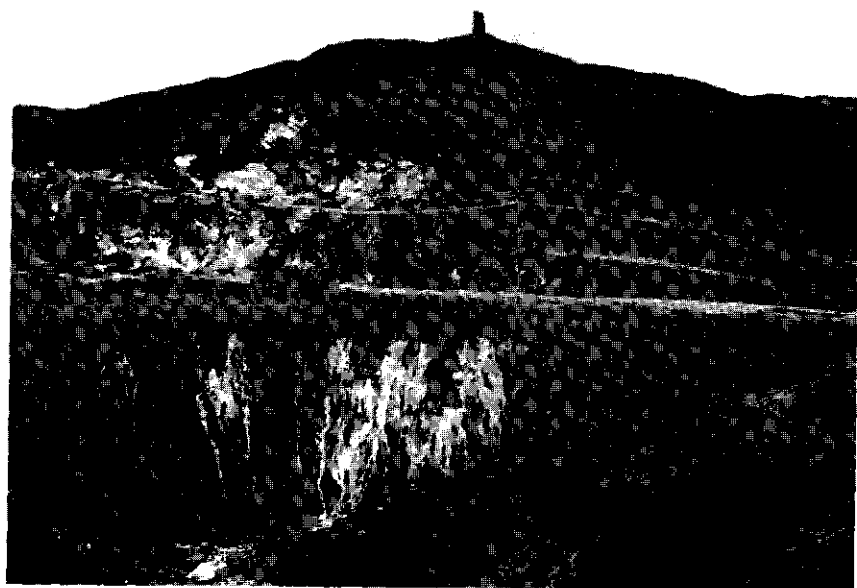


Photo 6 A view of the Kamarej salt plug (29°37' - 51°28').



Photo 7 Salt mining in the Kamarej salt plug.

The salt diapirism in the study area was induced by isostatic pressure from the overburden, by tectonic forces and/or by an igneous intrusion process as schematically shown in Fig 2.3 (Harrison, 1931; O'Brien, 1957; Kent, 1958; Ala, 1974; Kent, 1979 and others).

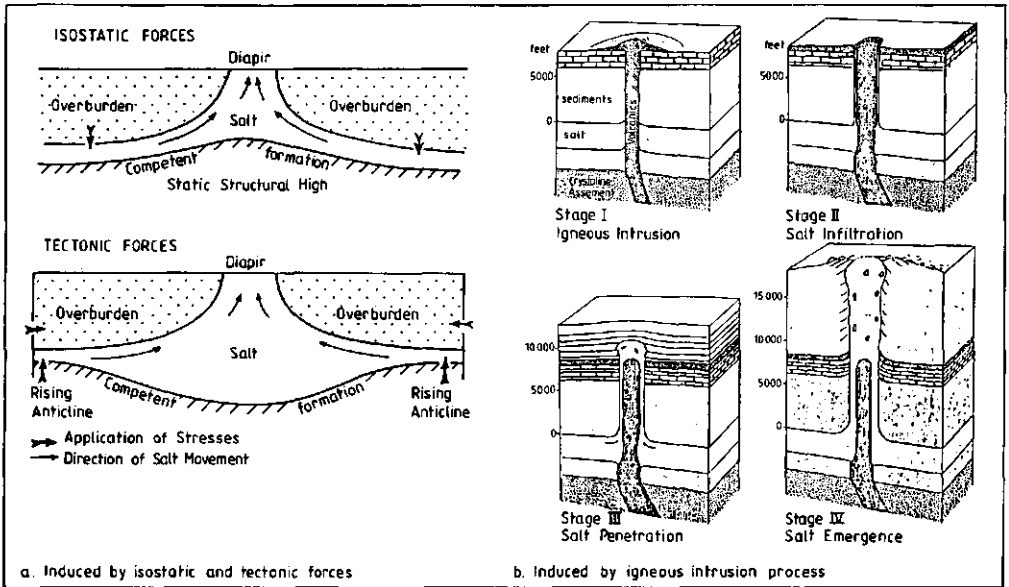


Fig. 2.3 Salt diapirism in the study area (after O'Brien 1957).

The geological activities which are associated with the salt structures give a unique geological character to the study area. A satellite picture of the area taken by the Earth Resources Technological Satellite ERTS (Photo 8) has been used to compare the folded patterns of the Zagros mountains with possible (but non-existent) folded belts on the planet Mars (Mutch et al., 1976). On this picture also the salt domes in the area are clearly visible.

RUMGUN S.P.

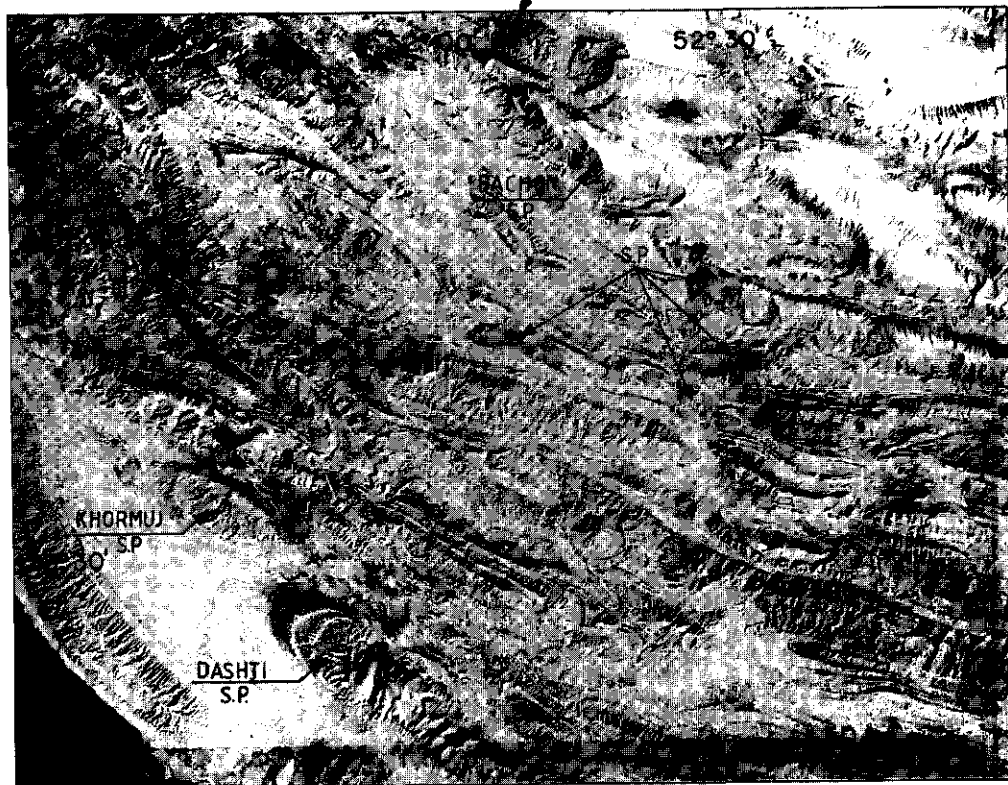


Photo 8 A satellite view from the study area and the appearance of the salt plugs s.p. (after Mutch et al., 1976).

2.1.4 Sources of salinity

The basins of the Shapur and Dalaki rivers have been extensively investigated (Yekom Consult. Engrs., 1980). For this purpose, a network of measuring stations was set up and river flows and water quality have been measured simultaneously since 1961. The network consists of 154 selected points in the main rivers, tributaries and polluting sources (Fig 2.4). Single, seasonal or monthly measurements were carried out in order to investigate the influence of the natural geochemistry as related to the surface hydrology in the basin.

A high standard of water chemical analyses in the cooperating laboratories was maintained by an intercalibration program. The data on water chemical analyses and flow measurements have been provided by Yekom Consulting Engineers, Iran. In these investigations, all major sources of salts have been traced to determine their contribution to the salt loads and the chemical composition of these rivers.

On the basis of the study the polluting sources are categorised as point

or non-point sources. The point sources consist mainly of mineral and salty springs, drains and ghanats, so that at a specific point saline water enters the river. On the other hand, the evaporites, salt plugs and saline groundwater are non-point sources of salinity in the study area. The major sources of salts and their contribution to the salinity of the river water are shown in Table 2.1. Figs. 2.5 and 2.6 show the water chemical composition and the spatial variations of the water quality, respectively.

Fig 2.5 presents an overview of the river water salinities, as measured on August 12, 1975. The size of the icons reflects the salt concentration, their shape the ionic composition (in meq/l). The extremely high concentrations of the Shekastian (Shapur basin) and the Shur (Dalaki basin), during a summer period with low flows, are obvious. It is also clear that sodium and chloride gain in importance as the concentrations become higher. In summer Na and Cl comprise 88-97% of the ions (compared with 84% in sea water). The remaining salts are CaSO₄ and small amounts of bicarbonates.

Table 2.1 Main sources of salinity in the Shapur-Dalaki river basin

basin	source	salt load	
		(1000 tons per year)	(%)
Shapur	Shapur at Bushgan (mainly Ca and Mg-salts)	137	12
	Shekastian river	234	21
	springs near Kamarej salt plug	169	15
	Barang river	188	17
	Tanbakukar river	52	5
	drains & streams between Buraki & Jarreh	119	11
	irrigation return flows between Jarreh & Saad-Abad	217	19
	Total salt load at Sadabad	1116	100
Dalaki	upper reaches (mainly Ca and Mg-salts)	71	5
	Cerezak spring near Runggan salt plug	69	5
	Mosgan spring near Murjan salt plug	45	3
	Jireh river	67	5
	Farashband river	145	10
	Shur river	216	15
	irrigation return flows & sulphur springs in lower reaches (Dalaki-Kolol stretch)	800	57
	Total salt load at confluence with Shapur	1413	100

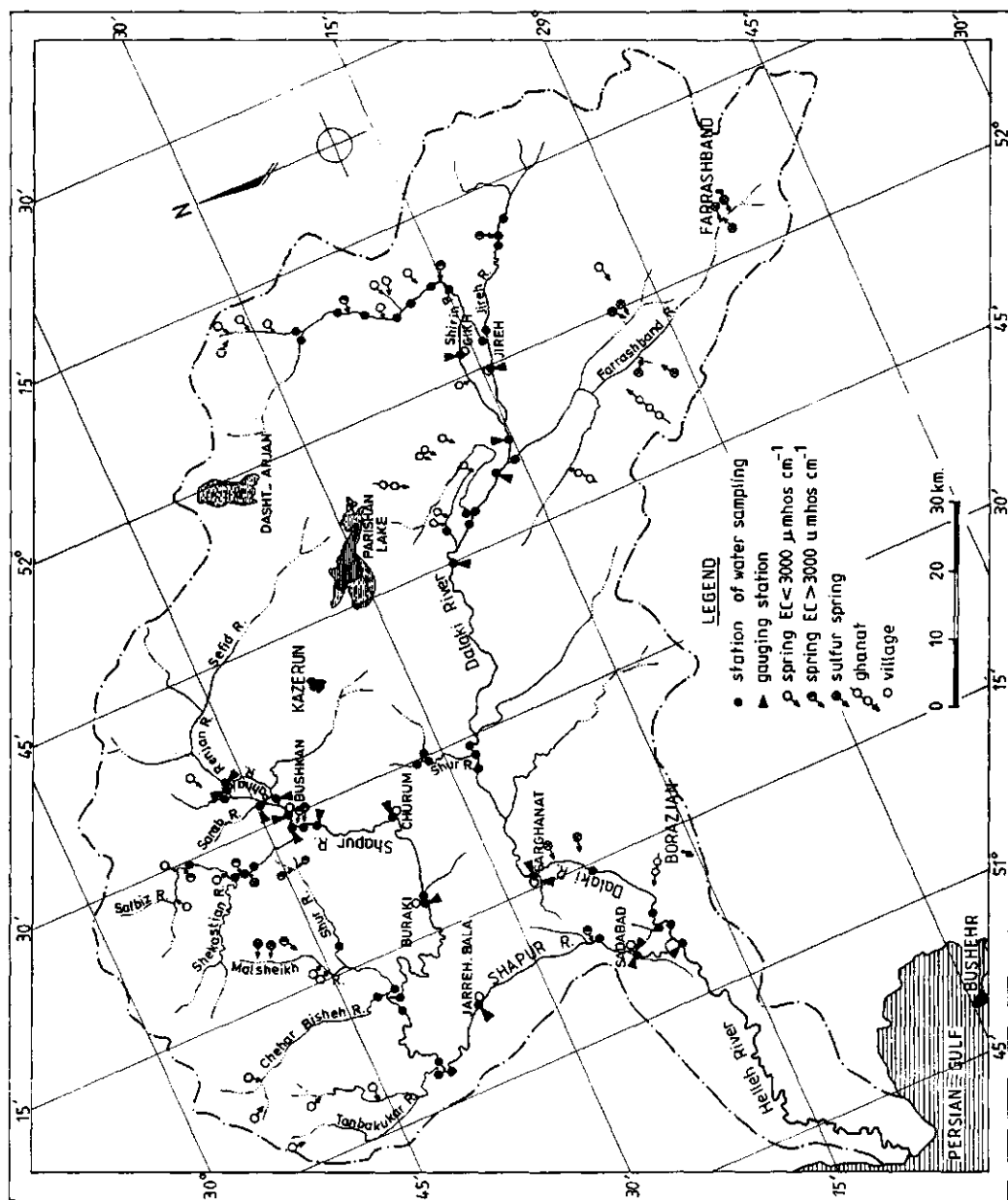


Fig. 2.4 Observation network and polluting sources in the Shapur-Dalaki basin.

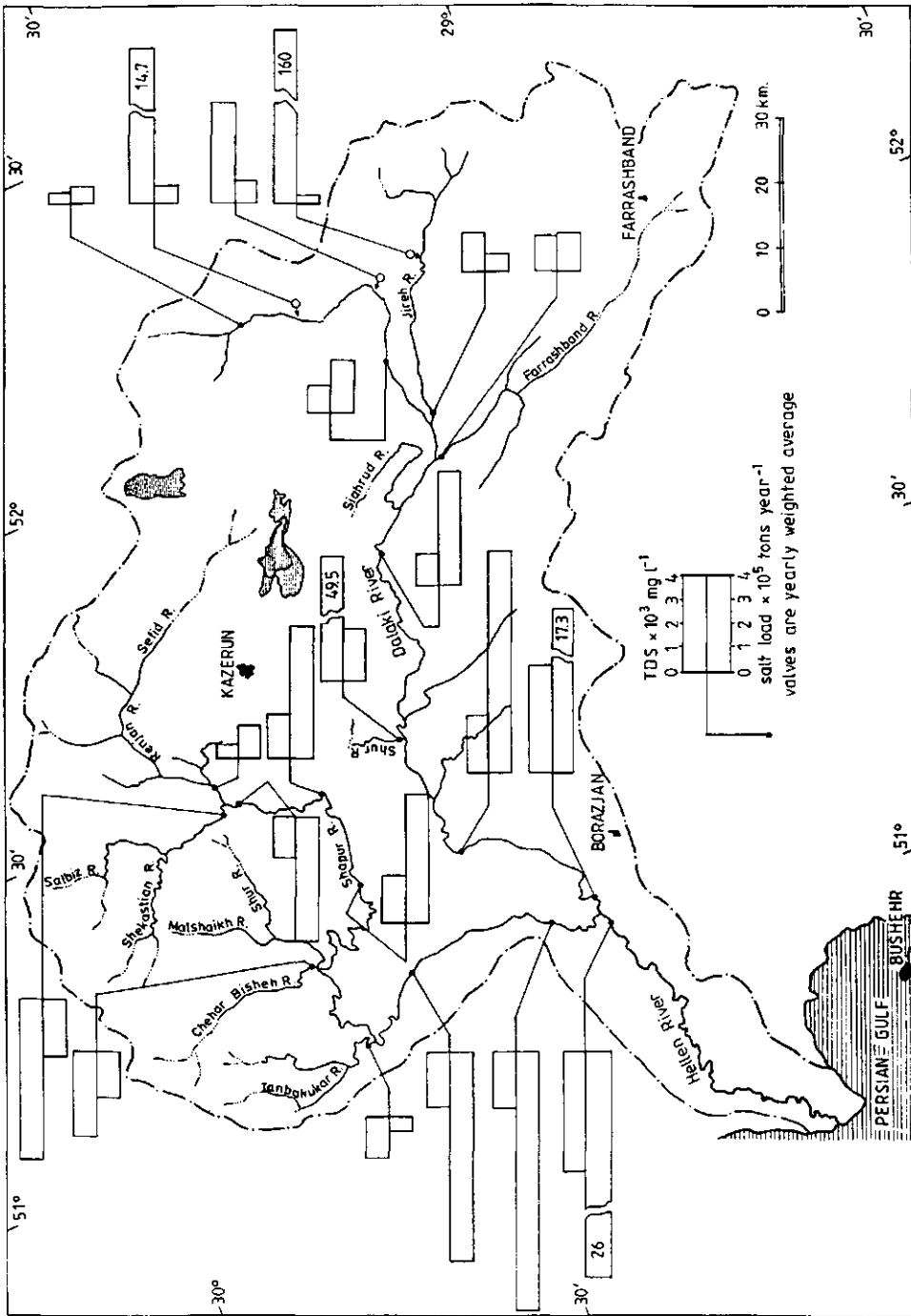


Fig. 2.6 Spatial variation of river's salinity.

2.1.4.1 Shapur river

The tributaries coming from the limestone areas in the north have water of low salt concentration, of which the cations are dominated by calcium and the anions by sulphate and bicarbonate ions. It is this type of water that is diverted at Bushkan for supply to Bandar Bushehr. For all purposes it is of excellent quality.

The Shekastian river, joining the Shapur shortly downstream of this point, has a very high salt content, that is dominated by Na and Cl ions. These salts are derived from the Gachsaran formation. In winter, the period of major discharges, the salt concentrations are moderate, but in summer, during low flows, they may exceed that of sea water (Fig 2.5). Several springs occur in the Shekastian catchment; a reconnaissance, made in March 1976 showed that spring waters issuing from the Asmari limestones have EC-values below 2 dS/m, those from the Mishan beds are slightly above 2, whereas those from the Gachsaran are mostly above 100 dS/m.

The exception is formed by the Gardanbeh spring, located in the Gachsaran area, but yielding fresh water (0.7 mS/cm), which probably issues from the underlying Asmari limestones. In this period the salinity in Shekastian river was around 12 mS/cm. Of this total, the springs sampled contributed not more than around 16%, indicating the importance of diffuse sources like deposits formed by evaporation in the river beds during foregoing dry periods. Over a short distance, the salinity from the Shekastian is still noticeable near the right bank of the Shapur river (Table 2.2, Station 2), but this lateral difference disappears within a few hundreds of meters (Stations 3-4).

Between the confluence with the Shekastian and "Station 70" further downstream, the salt load of the Shapur river increases due to the influence of the Kamarej salt plugs. A sketch of the local geology is given in Fig. 2.7; due to the tectonic movements associated with the diapirs, the situation is far more complicated in detail. Several salt springs are found along the left bank of the river in this area (photo 9). From measurements at these stations it follows that their contribution is more evenly distributed in time than the salt load from Shekastian (Table 2.3). The data for the stations were obtained by measuring EC, multiplying the dS/m by 0.7 to obtain TDS in kg/m³ and again multiplied by the measured river flow.

As can be seen from this table, the Shekastian and Kamarej salt plugs contribute 44 and 31 per cent of the Shapur river salts at Station 70, respectively. Moreover, the contributions of the salt plugs have much less seasonality than the other data, which probably reflects their origin from salt springs slowly dissolving the halite diapirs.

In this area, the river water is more salty near that bank, where the polluting source enters the river (Table 2.2, Station 6). The differences disappear after a few hundred meters due to transversal dispersion in the river. No differences were found over the vertical.

Table 2.2 Salinity of the Shapur river near the Kamarej salt plug
(measurements of Yekom Consult. Engrs., Iran, on 23/3/1977)

station km	EC dS/m				source
	(A)	(B)	(C)	(D)	
1	0.0	1.00	1.03	1.25	1.19
2	0.5	2.70	2.50	2.50	5.00
3	0.8	2.70	2.57	2.89	3.00
4	3.2	2.90	2.88	2.90	2.90
5	4.8	2.90	2.89	2.90	2.91
6	5.2	9.54	3.43	3.45	2.97
7	6.4	4.62	4.61	4.64	4.60

Note: For location of measuring points, see Fig. 2.7.

Table 2.3 Contributions of the Shekastian river and the Kamarej salt plugs (mean annual values, 1961-1977)

month	salt load in 1000 tons			
	Bushgan	Shekastian	Sta.70	Kamarej plugs (1)
Oct.	8.7	13.5	35.4	13.2
Nov.	11.0	16.6	41.4	13.8
Dec.	14.2	27.0	55.8	14.6
Jan.	14.5	30.0	57.9	13.4
Feb.	16.8	43.3	70.4	10.3
Mar.	12.9	21.7	50.7	16.1
Apr.	13.3	19.2	49.6	17.1
May	11.3	15.2	42.8	16.3
Jun.	9.6	13.5	37.6	14.5
Jul.	8.4	11.1	33.1	13.6
Aug.	7.7	11.1	30.8	12.0
Sept.	7.5	12.0	34.4	13.9
Year	136.0	234.2	539.9	168.8
(%)	(25)	(44)	(100)	(31)

(1): Sta. 70 - (Bushgan+Shekastian).

Further downstream, the Barang and Tanbakukar rivers drain a large area with Tertiary strata, part of which belong to the Gachsaran formation. As a consequence, their waters also carry large amounts of salt, comparable to the Shekastian river. Like in the Shekastian, there is a marked seasonal variation in salt load, which is highest in winter during large discharges, whereas in summer small flows with high concentrations occur. The Barang and the

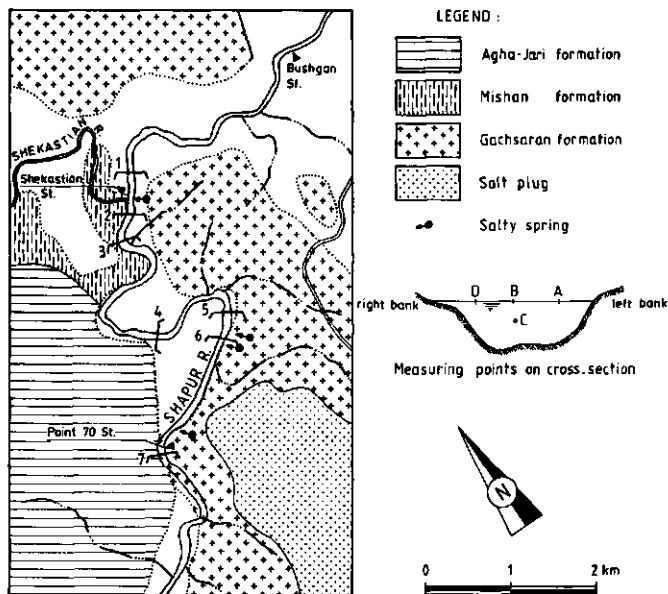
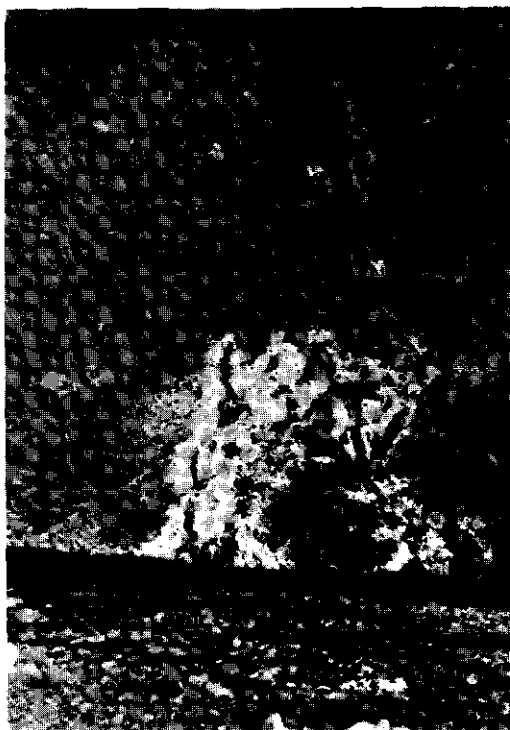


Fig. 2.7 Local geological features and transversal salinity measurements in Shapur R. between Bushgan and Sta. 70.

Photo 9 Salty spring between the Shekastian and point 70 Stations. The spring appears near the river bank from Mishan F., salt is derived from extruded Kamarej salt plugs and the Gachsaran F..



Tanbakukar contribute on average 188 000 and 52 000 tons of salt per year to the Shapur river, respectively.

All sources mentioned above are entirely natural. Irrigation return flows, however, become increasingly important downstream. Their contributions will hardly affect the future Jarreh reser-voir because most of them are located in the coastal plain downstream of the proposed dam. Those entering the Shapur river between Jarreh and the Saad-Abad diversion dam are harmful for the areas irrigated by waters taken at this point.

2.1.4.2 Dalaki river

The upper reaches of the Shirin ("sweet") river, the main tributary of the Dalaki, have water of low salt concentration, of which the cations are dominated by Ca and Mg and the anions by bicarbonate (Fig. 2.5). These components originate mainly from the dissolution of calcite CaCO_3 and dolomite $\text{CaMg}(\text{CO}_3)_2$, forming the Oligocene limestones in this region. Further downstream, after the inflow from three salty springs, the salt concentration markedly increases and NaCl becomes the dominant salt. These springs originate from two emergent salt diapirs which are located 15 km apart from each other. They are known as the Romgan and Murjan salt plugs (Annex 1). These springs contribute annually about 180 000 tons of salt to the Dalaki river.

Until the confluence of the Shur river the changes in water quality are slight (Figs. 2.5 and 2.6). The Shur river, a tributary which drains mainly Tertiary strata along the southern flank of the Sarbalesh anticline, is a major source of deterioration of Dalaki river water. Salt is mainly contributed by springs (Dalaki Shur springs) which appear at the foot of the Guri limestone along a stretch of about 400 m. The salts originate from the Gachsaran formation which is found at the surface nearby and which is also underlying the Guri limestone.

In contrast with the Shekastian, almost all salinity in the Shur river stems from these springs and the effect of diffuse sources (like salty deposits in the river beds) is not significant. The mean annual variation in salt concentration of the Dalaki Shur springs is shown in Table 2.4. The annual average salinity is about 119 g/l; it varies between 60 g/l in February and 198 g/l in August. Table 2.4 also shows that these springs contribute about 210 000 tons of salt per year to the Shur and consequently to the Dalaki river, and that this contribution is rather evenly distributed over the year. These characteristics - point sources, evenly distributed contribution in time - suggest the influence of a (hypothetical) concealed salt diapir rather than the erosion of the Gachsaran beds as a source of these salts.

Table 2.4 Salt contributions of Dalaki Shur springs (annual mean, 1961-1977)

Month	Discharge (l/s)	Salinity (g/l)	Salt load (1000 tons)
Oct.	29	198	15
Nov.	38	168	16
Dec.	42	157	17
Jan.	56	121	18
Feb.	148	60	23
Mar.	113	65	19
Apr.	71	98	19
May	42	160	18
Jun.	37	170	17
Jul.	35	177	17
Aug.	32	187	16
Sept.	29	198	15
Year	56	119	210

Dalaki water is diverted at Sarqhanat by a diversion dam to irrigate the coastal Dalaki plain. Up to this location all polluting sources are entirely natural and not induced by human activities. Further downstream, irrigation return flows contribute considerable amounts of salt to the river. However, their contribution is harmless, since the river water is hardly used downstream of Sarqhanat.

2.1.5 Comparison of salinization in river basins

A comparison of results of the present study with some similar studies in Western Australia (south-west river basins), in Spain (Ebro river basin) and Western USA (Colorado River basin) indicate that the origin, sources, type and causes of salinization are different.

A review about the origin and sources of the salts and the processes which have been involved in the Ebro basin is given by Van der Molen (1986). In this basin the sources of salinity are cyclic salts, erosion of Jurassic diapirs, Tertiary evaporites and formation of sulphate by oxidation of Oligo-Miocene pyrites. The pronounced amount of sulphate and the low bromide content of halite indicate a continental rather than a marine origin of the salts.

In the Colorado River basin the sources of salts are erosion of Tertiary diapirs and glaciation and weathering of marine deposits. The diapirs contribute mainly NaCl but the dominant salt source is Na_2SO_4 from saline seeps (U.S. Dept. of Interior, 1973, 1974; Greenlee, 1968).

In Western Australia, cyclic salt is transported from the ocean to the land via rainfall, and stored in the soil. The clearing of native, deep rooted plants and their replacement with shallow rooted crops allow more water to percolate to the ground water. The water table then rose, and the stored salts were liberated and leached to the streams (a comprehensive review is given by Steering Committee for Research on Land Use and Water Supply, 1989).

Table 2.5 shows the similarities and contrasts of salt problems in these basins. The salinization in the Shapur-Dalaki and Ebro basins are connected mainly with the influence of geomorphology and hydrology of the natural river basin ("primary" or "natural" salinization), whereas in Western Australia salinity is mainly induced by human activities ("secondary salinization").

Table 2.5 Comparison of salt problems in river basins

Basin	Origin/Type of salt	Source of salt	Salinization
Shapur-Dalaki (S. Iran)	marine/NaCl	E.S.P. (Precambrian) E.E. (Miocene)	primary
Ebro (Spain)	continental/ SO ₄ , halite (low bromide)	E.S.P. (Jurassic) E.E. (Oligo-Miocene) O.S.R.	primary
Collie (south-west W. Australia)	cyclic/NaCl	O.S.R.	secondary (agric. clearing)
Colorado (W. USA)	marine/halite Na, SO ₄ (saline seeps, in Montana)	E.S.P. (Tertiary) E.E. (Tertiary)	primary & secondary (irrigat.)

E.S.P. = Erosion of salt plug

E.E. = Erosion of evaporites

O.S.R. = Oceanic salts via rainfall

2.1.6 Conclusions

At present, salinity in the Shapur-Dalaki basin is primarily caused by natural conditions, that have been active for a considerable time. However, human activities such as irrigation development along the downstream reaches (Borazjan Plain) has locally aggravated the problem.

The salts are from marine origin and of the NaCl type. They mainly occur

as evaporites of the Precambrian (Hormuz formation) and the Miocene (mainly the Gachsaran formation). The sources of salinity are erosion of extruded salt plugs and salt-containing formations (diffusive sources) and outflow from salty springs, drains and ghanats (point sources).

The presence of salt structures has played a dominant role in the geological activities in the basin.

Comparison of results with those of Western Australian river basins, the Ebro river basin, and the Colorado river basin show similarities and contrasts in the origin, sources and causes of salinization in these basins.

ACKNOWLEDGEMENT

The author is indebted to Prof. W.H. Van der Molen for his visit to the study area, his comments and constructive criticism of the draft. Ir. S. Van Schaaf and Dr. J.W. van Hoorn are acknowledged for their comments. The salinity measurement data and the geological map of the study area were kindly provided by Yekom Consulting Engineers, Iran.

2.2 DISSOLVED AND SUSPENDED MATTER TRANSPORT IN THE BASIN

2.2.1 Introduction

Mechanical and chemical erosion of salty and soft formations are the dominant processes in the output of sediment and dissolved matter. The output from these processes depends largely upon the water flow through the system and also on the controlling factors such as rainfall intensity, soil type, land use, slope and vegetal cover.

In the study basin the runoff can be divided into base flow and flood flow. The springs, ghanats, drains and seepage form the base flow, whereas the flood flows are generated by surface runoff. The size of flood flows is mainly dependent upon the rainfall characteristics, and there are large differences between floods. In late spring and summer the base flow shows a gradual recession. At the end of the dry season the river flow reaches its lowest values, being about 3-5 m³/s for both Shapur and Dalaki rivers.

The regime of dissolved and suspended matter transport has been investigated by periodic flow measurements and samplings at hydrometrical stations over several years. Moreover, their spatial-temporal distribution can be characterized in relation to water yields, which are available for a longer period of observations.

2.2.2 Suspended materials

Sources

In the region, the vast areas of sparsely vegetated and soft Miocene formations are the main source of suspended matter. In addition, mobilization of sediment from the river bed also yields suspended matter, although on a less spectacular scale. The former process is dominant in winter, whereas the latter is more pronounced in the summer period.

Processes

Raindrops detach and incorporate the soil particles and splash them into the air. On level ground the particles are redistributed more or less uniformly in all directions, but on slopes there is a net downward transport. If the intensity of precipitation exceeds the infiltration rate, overland flow will occur. This flow entrains soil particles and moves them further downslope "sheet erosion" (Linsley et al., 1985). Sheet erosion rarely occurs alone. As a consequence of micro-relief concentration of flow occurs, leading to scouring and "rill erosion". This process of "surface erosion" plays a dominant part in creating large sediment loads in the rivers of the study area.

"Gully erosion", is hardly observed in the region. In this case, erosion is

more rapid in the gullies. A value of 80 kg/m^3 of suspended matter is reported by Schouten (1976) for the Puketuru River basin in New Zealand, where the gullies are the major source of sediment output. In the Shapur-Dalaki basin, gullying occurs especially on the salt domes, where it is initiated by dissolution phenomena and where it leads to formation of badlands, solution tunnels etc.

Besides the above mentioned processes the slow downward creep of soil mass and landslides contribute sediment particles to the streams.

From the plots of observed suspended matter loads against river discharge and against time (Shapur river at Saad-Abad, 1975-1980), as shown in Fig. 2.8, it can be seen that:

- the suspended matter concentration shows a strong positive correlation with the discharge;
- the concentrations of suspended matter are only of geomorphological significance during periods of floods;
- during periods of base flow recession, concentrations are always extremely low (below 50 mg/l).

The maximum measured suspended matter concentration of the Shapur river at Saad-Abad Station during the observation period (1975-1980) reached up to 42 kg/m^3 . Higher values are found in other river basins in Iran: in Qezel Owzan, for instance, a branch of Sefid Rud in Northern Iran, maxima up to 60 kg/m^3 have been recorded (Parhami, 1986). These maxima generally occur during and just after peak discharges. The mean annual sediment discharge of the Shapur at Saad-Abad Station is $4.8 \cdot 10^5 \text{ t/yr}$. Over its drainage basin of 4110 km^2 is approximately $1200 \text{ t/km}^2/\text{yr}$. Much higher values are known from basins of comparable size elsewhere: for the Dali river basin in North Shaanxi in the People's Republic of China and for the Aure river basin in New Guinea (3900 and 4360 km^2) the sediment yields are 16300 and $11000 \text{ t/km}^2/\text{yr}$, respectively (Walling, 1988).

There is a close relation between river flow and sediment concentration, as shown in Fig. 2.8a. From this relation, data can be derived for periods for which river discharges are available, but measurements of suspended sediments are lacking. In a later part of this study, such synthetic data will be used to predict the long-term behaviour of the future Jarreh Reservoir (Part II, Chap. 5).

2.2.3 Dissolved materials

Sources

The sources of dissolved matter have been described in detail in section 2.1. These are:

- 1) extruded salt plugs;
- 2) salty Miocene formations;

- 3) salty groundwater contributed by springs, ghanats, seeps and drains.

The input of dissolved matter by fertilizer applications, mining, etc. is not significant in the region.

Processes

Precipitation water also affects the soil chemically, mainly by dissolving the more readily soluble substances contained within the soil. This process, "chemical erosion" or "chemical soil weathering" (Zachar, 1982) is for an important part temperature-dependent. However, the supply of dissolved matter by this process is mainly depending upon the flowing water and soil types. Molecular diffusion also contributes solubles, but on a much smaller scale since the process is slow.

The effectiveness of such processes differ between winter, the period of high flows, and summer, the period of base flows. A comparison between the chemical composition of river waters in high and low flow periods is shown in Fig. 2.9. It indicates that the high discharges due to winter rainfall cause a drop in mineralization. Also the composition of the dissolved components changes with the season. At high flows, Ca and SO_4 are relatively more prominent, whereas during low discharges Na and Cl are by far the dominant ions. The Ca and SO_4 are supplied by the erosion of the gypsiferous Miocene strata, the Na and Cl mainly by springs in the salty Gachsaran formation and around the salt plugs. These sources contribute small amounts of water throughout the year, but their effect is most pronounced in summer, when they cause a considerable rise in the salt concentration of the river waters. More details will be given in Section 2.3.3.

Several spring waters contain considerable amounts of sulphur compounds, specially hydrogen sulphide. Such "sulphur springs" are stemming from pyrite-bearing formations. On exposure to the atmosphere, their waters are oxidized and a milky suspension of elementary sulphur can often be observed in their outflow channels. Further oxidation will lead to sulphurous and sulphuric acid. The main streams in the Shapur-Dalaki basin, however, are non-acidic, with pH of 7.0-8.5. This indicates that the formation of sulphuric acid by oxidation of sulphur compounds is neutralized by the large amounts of $CaCO_3$ present in the area. Acid-sulphate weathering, as described, among many others, by Van Breemen (1973), Collier et al. (1970) and Schouten (1976), is not active in the study area.

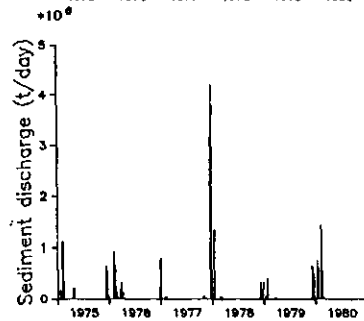
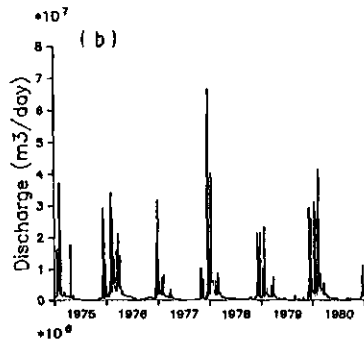
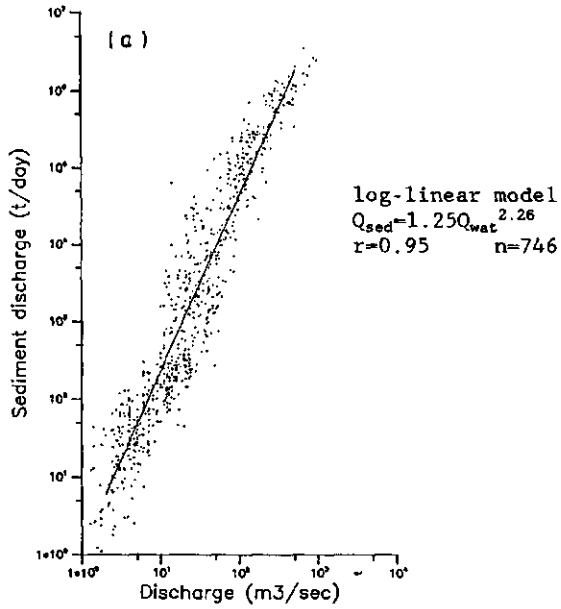


Fig. 2.8 Discharge and suspended matter loads in the Shapur river at Saad-Abad Station; (a) relationship with river flow, (b) against time.

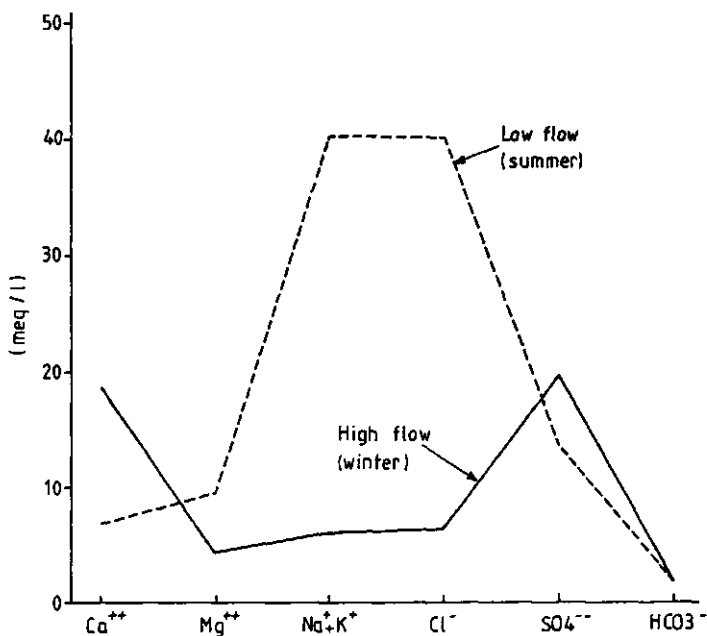


Fig. 2.9 Chemical composition of the Shapur river water (Jarreh Station) in Winter and Summer.

2.3 RELATIONS BETWEEN RIVER DISCHARGE, SUSPENDED MATTER AND DISSOLVED MATTER IN THE SHAPUR AND DALAKI BASIN

2.3.1 Introduction

In most river basins, the concentrations of sediments and total dissolved solids (TDS) show a marked variation in time because of changes in the underlying processes of mobilization and transport. Part of this variation has a seasonal character. Usually there is a close correlation of sediment- and TDS-concentrations with river discharges. Because the latter are easily measurable and are often being observed over long periods, such relationships can be used to obtain data on sediment- and TDS-transport over periods where no data for these quantities are available or to generate long series of data as input for conceptual models. Regression analysis is mostly used for establishing these relationships (e.g. Schouten, 1976).

The obtained relationships are used in estimating the sediment and salt concentrations of the Shapur river at Jarreh Station (Chap. 5).

2.3.2 Available data

For the Shapur-Dalaki river basin data on discharges and suspended load concentrations were provided by the Water Resources Investigation Bureau, Surface Water Section of the Ministry of Energy of Iran. Among these, the data from Saad-Abad Station on the Shapur have been chosen for analysis because they formed the longest and most continuous series. In total, 746 measurements are available for this station, covering the six-year period 1975-1980. Data on TDS-concentrations were provided by Yekom Consulting Engineers, Iran. They consist of a series of instantaneous measurements of TDS and simultaneous river discharges at Jarreh Station on the Shapur extending over the same period.

2.3.3 Suspended matter

The relation between river discharge and sediment load (the product of discharge and sediment concentration) is known as sediment rating curve; it

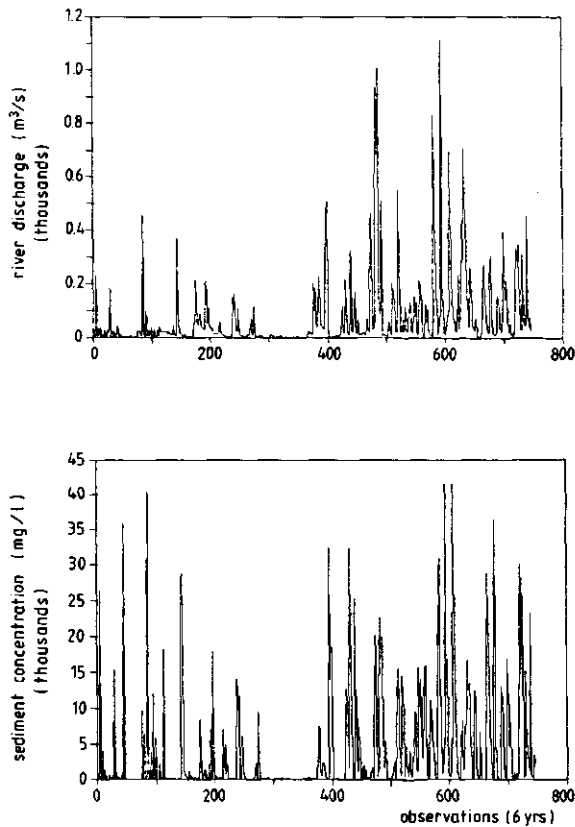


Fig. 2.10 Instantaneous discharge and sediment concentration of Shapur R. at Saad-Abad Station (1975-1980).

is often used to estimate the sediment yield in river basins (e.g. Singh and Chen, 1981). As the rivers under consideration are still in an almost natural condition, Nilson (1977) warning against its use in regulated streams is of no avail.

Fig. 2.10 shows the observed discharges and suspended sediment concentrations for the 746 samples taken at Saad-Abad. It is evident that high river flows are accompanied by high concentrations of suspended solids and that both are extremely variable in time.

For further analysis the annual cycle has been divided into three periods:

- winter (late Sept. - late Febr.), with high discharges due to winter rains;
- spring (late Febr. - late March), with discharges from rains and snowmelt;
- summer (late March - late Sept.), with low baseflow.

The rationale for this subdivision is based on the studies of Rendon-Herrero (1974) and Rendon-Herrero, Singh and Chen (1980) and is further evident from the differences in the scatter diagrams representing the relations between discharges and sediment concentrations (Figs. 2.11a-d; note the differences in scale). Whereas in summer the relation with discharge is almost absent, the winter and spring seasons are characterized by a strong increase in sediment concentration with discharge. In most cases there exists a difference in reaction between the snowmelt period in spring and the rainy winter season (Rendon-Hererro, 1974), but in this region the area affected with snowmelt is too small to bring out this difference (Figs. 11b and 11c).

In winter and spring, the influence of rains and snowmelt producing surface runoff is dominant, whereas in summer mobilization of sediments from the river bed is more important.

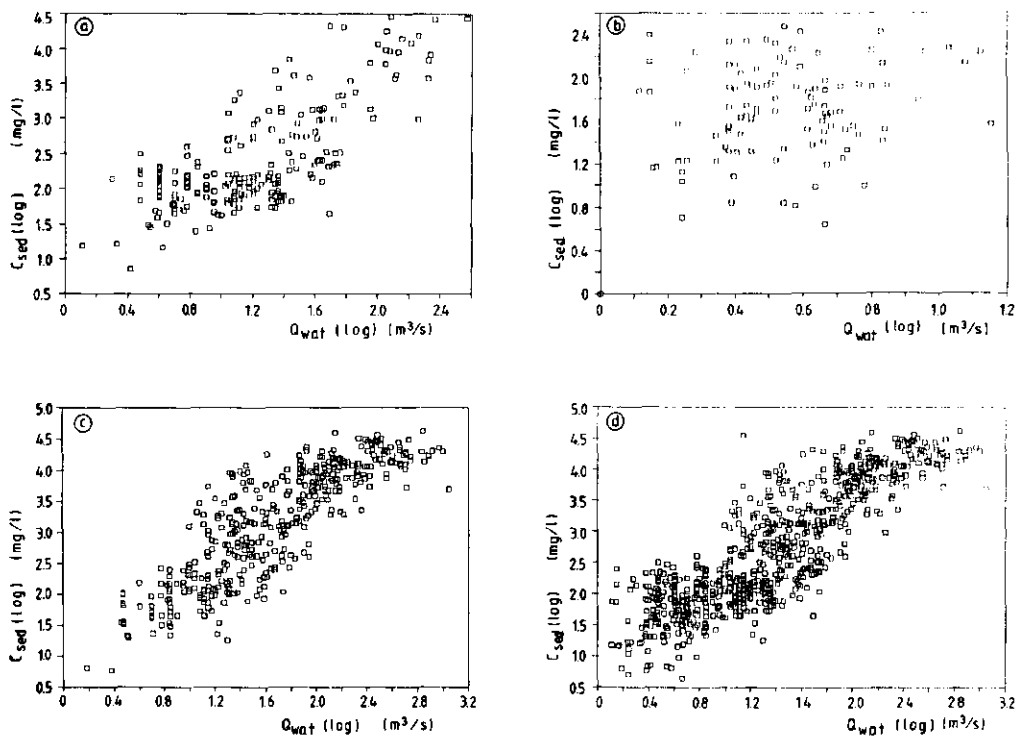


Fig. 2.11 Log transformed scatter diagram of observed river discharge (Q_{wat}) and sediment concentration (C_{sed}): (a) spring period; (b) summer period; (c) winter period, (d) all periods combined.

The overall sediment concentrations as a function of Shapur flows at Saad-Abad Station, presented in Fig. 2.12 were calculated by Karogo (1989) by using the standard regression method outlined by Riggs (1968). The following relationships between sediment concentrations (mg/l) and river discharges (m^3/s) are established:

Q_{wat} (log)	Equation	r
0.0 - 0.35	$\log C_{sed} = 1.7$	
0.35 - 0.95	$\log C_{sed} = 0.613(\log Q_{wat}) - 0.216(\log Q_{wat})^2 + 0.191(\log Q_{wat})^3 + 1.517$	0.79
>0.95	$\log C_{sed} = -0.334(\log Q_{wat}) + 1.368(\log Q_{wat})^2 - 0.317(\log Q_{wat})^3 + 1.44$	0.89

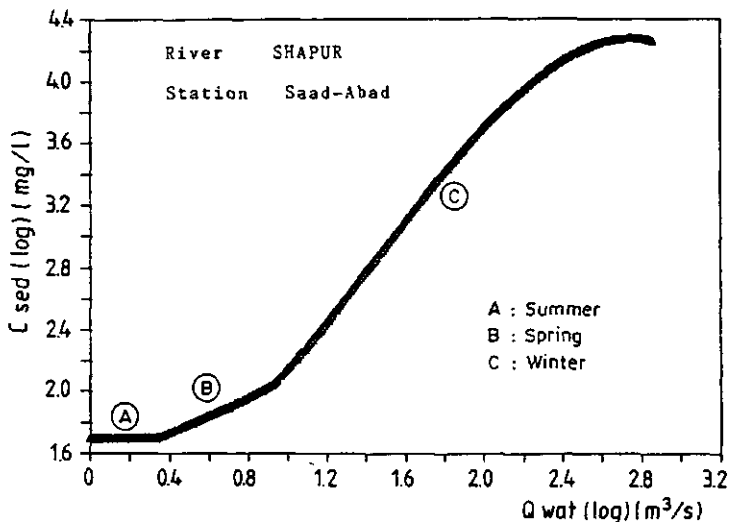


Fig. 2.12 Overall sediment concentration relationships with discharge, Shapur R. at Saad-Abad Station.

2.3.4 Total dissolved solids

Whereas the suspended sediments strongly increase at increasing river flows, the dissolved matter behaves in an opposite way. However, the relation between discharge and dissolved matter is greatly influenced by output sources of these materials and also the dominant processes are involved. The classic relation between river flow and TDS-concentration is an inverse one, and this type has been observed in the study area and e.g. by Guyot et al. (1990) for the Bolivian Highlands. But in south Western Australia, where the solutes in soil are liberated and transported to streams by subsurface runoff, the mineralization is increasing with river discharge (Peck, 1978; Schofield et al., 1988).

The scatter diagram of Fig. 2.13 demonstrates the strong decrease in TDS-concentration at increasing discharge. The graph suggests that TDS consists of two components:

- a "base-concentration", around 1.4 kg/m^3 , mainly Ca+Mg, HCO_3 and SO_4
- a "variable part" VP, decreasing inversely with streamflow, mainly Na and Cl.

This would indicate that the load of the "baseflow component" is proportional to the discharge, whereas the load of the "variable component" is almost constant.

$$Q_{\text{wat}} * \text{VP} = \text{load of VP} = \text{constant}$$

In connection with the origin of the dissolved substances as discussed in

section 2.1 this could mean that the second component stems from salt springs with a rather constant flow throughout the year. In winter, their effects are diminished by the large quantities of surface runoff, but in summer they dominate the composition of the river waters.

The variation of chemical components of the Shapur river at Jarreh Station, as shown in Fig. 2.14 indicates that the concentration of Na and Cl varies between 6-69 meq/l. Whereas Ca, SO₄, Mg, and HCO₃ show less spectacular variation.

The TDS as a function of river discharge for the Shapur river is presented on a logarithmic scale in Fig. 2.15. The following relationships are established:

$$\begin{aligned} \log \text{TDS (mg/l)} &= -0.237 \log Q_{\text{wat}} + 3.624 & (r=0.89 \quad n=75) \\ \log \text{Load (g/s)} &= 0.81 \log Q_{\text{wat}} + 3.57 \end{aligned}$$

which is in fair agreement with the functional relationship that load equals flow times TDS. The relations given above have been used to estimate the future inputs into Jarreh Reservoir.

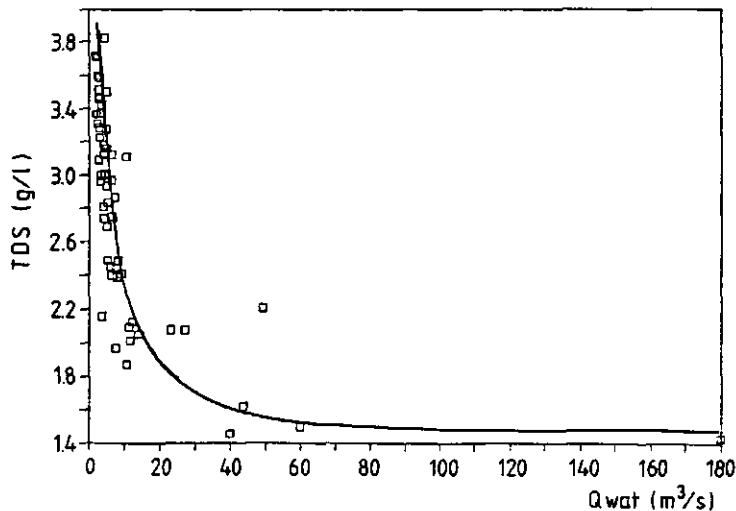


Fig. 2.13 Scatter diagram of observed discharge and TDS, Shapur R. at Jarreh Station.

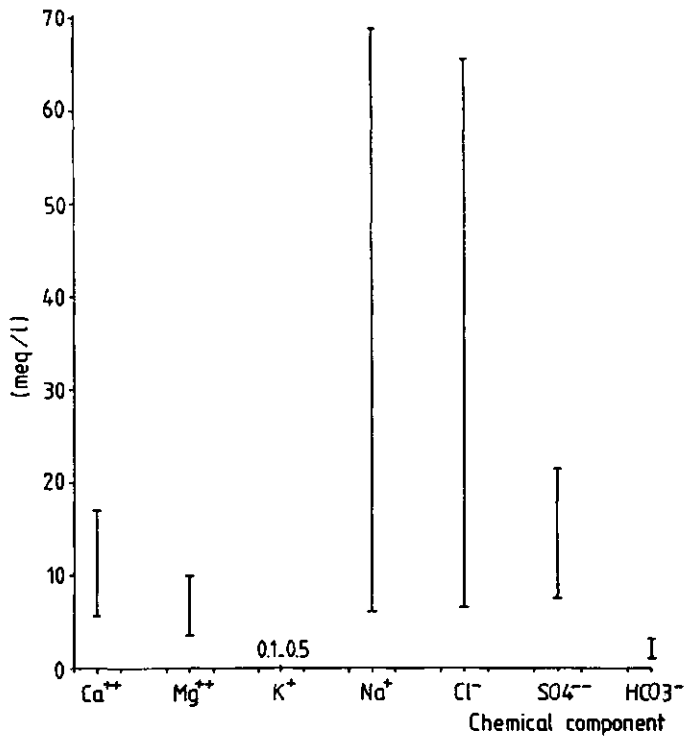


Fig. 2.14 Variation in chemical components of the Shapur R. at Jarreh Station (1975-1980).

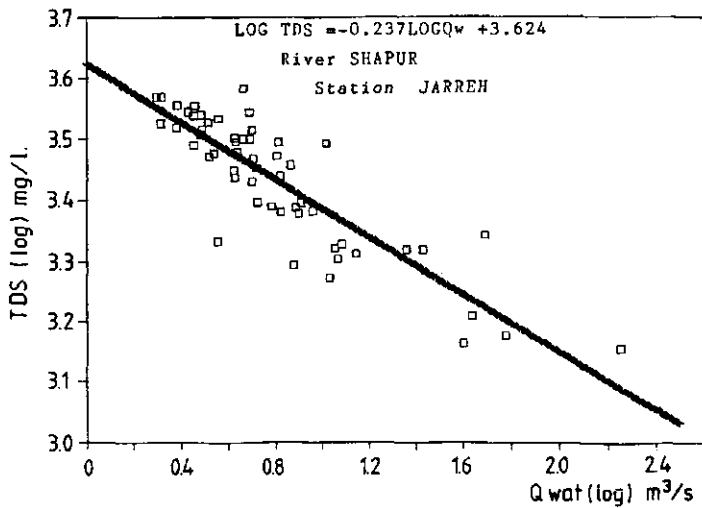


Fig. 2.15 Total dissolved solids related to river discharge for Shapur R. at Jarreh Station.

2.3.5 Relationships between the components of dissolved matter

Most components of the dissolved load have an ionic nature when in solution. Consequently, there is a satisfactory relationship between TDS and electrical conductivity, although it varies with the kinds of ions present. Once these relationships have been established for a particular water type, it is possible to obtain a record on major ion concentrations, suitable for most uses, by only measuring the conductivity. These measurements are simple and inexpensive and it is easy to obtain continuous records for this variable.

The electrical conductivity (EC) of a solution is usually expressed as the reciprocal of the resistance in ohms (mho or Siemens) of an 1 cm³ cube of a solution at 25 °C temperature. The conductivity of fresh water is reported in micromhos/cm or microSiemens/cm (for brackish water the unit of milliSiemens/cm is more commonly used; sometimes it is expressed as deciSiemens/m, dS/m, which has the same numerical value). Provided that the solutions are very diluted, the Kohlrausch law of independent ionic conductivities is valid (Robins, 1972); each ion makes an independent contribution to the total conductivity.

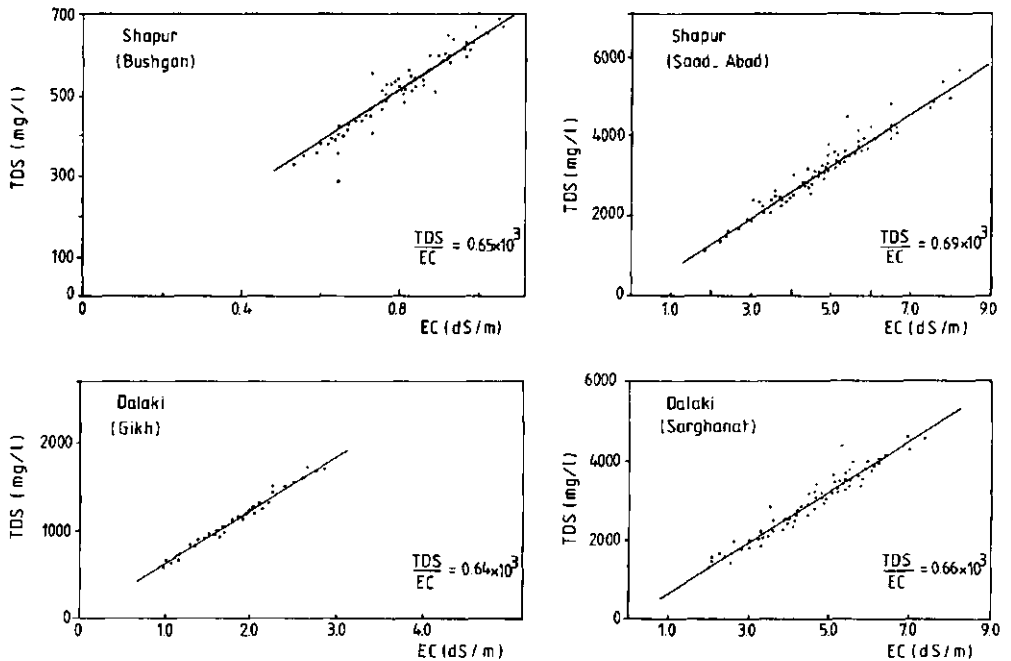


Fig. 2.16 Total dissolved solids (TDS) and electrical conductivity (EC) relations of Shapur and Dalaki rivers.

For the Shapur and Dalaki rivers the relations between main water quality compounds and electrical conductivity at some hydrometrical stations are presented in Figs. 2.16 and 2.17. A long series of conductivity measurements, made during the period 1975-1980 in the Shapur river at Saad-Abad is used to estimate TDS-inputs into the future Jarreh Reservoir.

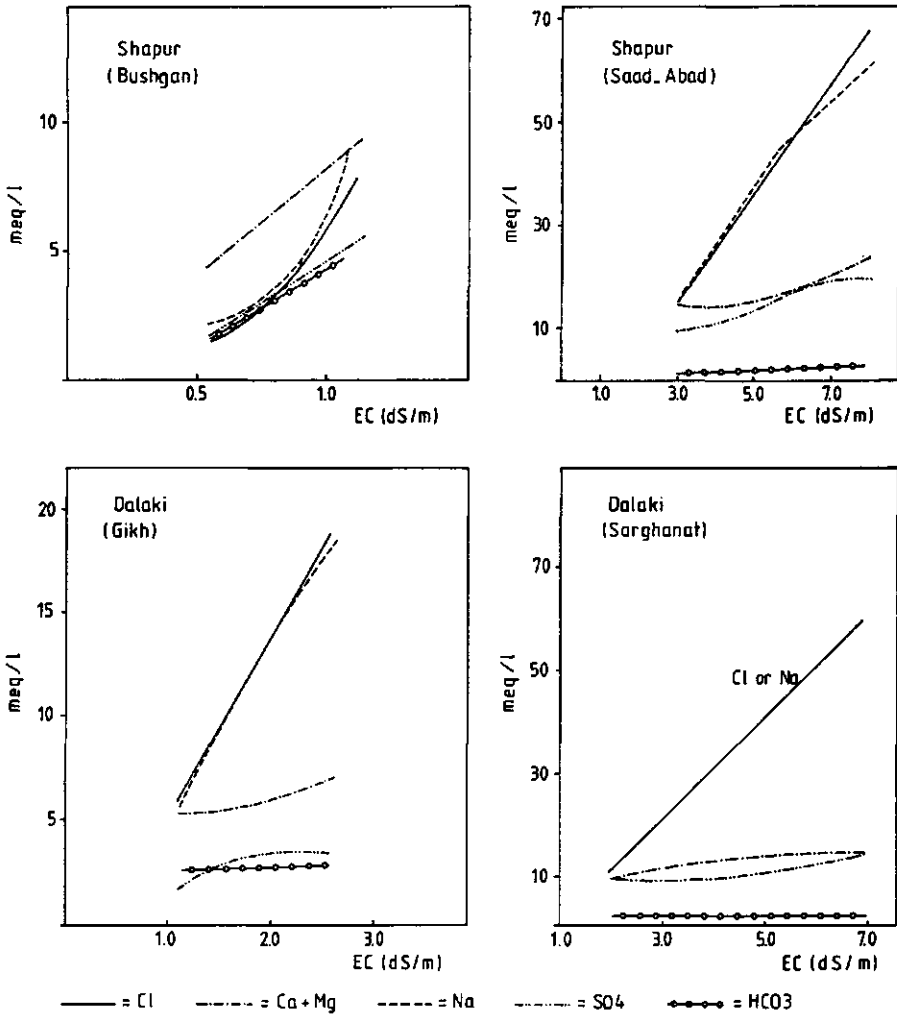


Fig. 2.17 Relations of concentration of dissolved matter components with electrical conductivity for Shapur and Dalaki rivers.

REFERENCES

- Ala, M.A., 1974. Salt diapirism in Southern Iran. *Amer. Assoc. Petrol. Geol. Bull.*, 58:1758-1770.
- Collier, C.R., Pickering, R.J., and Musser, J.J., 1970. Influences of strip mining on the hydrological environment of parts of Beaver Creek basin, Kentucky 1955-56. U.S. Geol. Survey, Prof. Paper 427-c.
- Greenlee, G.M., Pawluk, S., and Bowser, W.E., 1968. Occurrence of soil salinity in the drylands of southwestern Alberta. *Can. J. Soil Sci.*, 48:65-75.
- Guyot, J.L., Roche, M.A., Noriega, L., Calle, H., and Quintanilla, J., 1990. Salinity and sediment transport in the Bolivian Highlands. *Journal of Hydrology*, 113:147-162.
- Harrison, J.V., 1931. Salt domes in Persia. *J. Inst. Petrol. Tech.*, 17:300-320.
- Jackson, M.P.A., and Talbot, C.J., 1986. External shapes, strain rates and dynamics of salt structures. *Geological Society of American Bulletin*, 97:305-323.
- Karogo, P.N., 1989. Sediment rating curves and long-term discharge data generation for river Shapur in Iran. M. Sc. thesis, Dept. of Land and Water Use and Dept. of Catchment Hydrology and Hydraulics, Wageningen Agric. Univ., The Netherlands.
- Kent, P.E., 1958. Recent studies of South Persian salt plugs. *Amer. Assoc. Petrol. Geol. Bull.*, 42:2951-2972.
- Kent, P.E., and Hedberg, H.D., 1976. Salt diapirism in Southern Iran: Discussion. *Amer. Assoc. Petrol. Geol. Bull.*, 60:458.
- Kent, P.E., 1979. The emergent Hormuz salt plugs of Southern Iran. *Journal of Petroleum Geology*, 2:117-144.
- Kent, P.E., 1987. Island salt plugs in the Middle East and their tectonic implications. In: Lerche, L., O'Brien, J.J. eds., *Dynamical Geology of Salt and Related Structures*, Academic Press, 832 pp.
- Lerche, L., O'Brien, J.J. (eds) 1987. *Dynamical geology of salt and related structures*. Academic Press, 832 pp.
- Linsley, R.K., Kohler, M.A., and Paulus, J.L.H., 1985. *Hydrology for engineers*. 5th, McGraw-Hill Book Company, Tokyo.
- Miller, M.R., Brown, P.L., Donovan, J.J., Bergains, R.N., Sondergger, J.L., and Schmidt, F.A., 1981. Saline seep development and control in the North

American Great Plains. Hydrological aspects. Agric. Water Manage., 4:115-139.

Molen, van der W.H., 1980. Water quality: influence of transport and mixing processes. Lecture Notes, Dept. of Land and Water Use, Wageningen Agric. Univ., The Netherlands, 88 pp.

Molen, van der W.H., 1985. Salinity under natural conditions and under rainfed agriculture. Internal Report, Dept. of Land and Water Use, Wageningen Agric. University, The Netherlands, 24 pp.

Molen, van der W.H., 1986. Salinity in the Ebro basin. Internal Report. Dept. of Land and Water Use, Wageningen Agric. University, The Netherlands, 11 pp.

Mutch, T.A., Arvidson, R.E., Head, J.W., Jones, K.L., and Saunders, R.S., 1976. Geology of The Mars. Princeton University Press, Princeton, New Jersey, 399 pp.

O'Brien, C.A.E., 1957. Salt diapirism in South Persia. Geol. Mijnb. N. S., 19:357-37.

O'Brien, G.D., 1968. Survey of diapirs and diapirism. In: Braunstein, J, and O'Brien, G.D., eds., Diapirism and diapirs, Amer. Assoc. Petrol. Geol. Memoir, 8:1-8.

Parhami, F., 1986. Sediment control methods in Sefid-Rud reservoir (Iran). Third International Symposium on River Sedimentation, The University of Mississippi, March 31-April 4.

Peck, A.J., 1978. Salinization of non-irrigated soils and associated streams. Aust. J. Soil Res., 16:157-168.

Rendon-Herrero, O., 1974. Estimation of wash load produced on certain small watersheds. J. of Hydraul. Division, Proceedings of American Society of Civil Engineers, 100:835-848.

Rendon-Herrero, O., Singh, V.P., and Chen, V.J., 1980. ER-ES watershed relationship. Proceedings International Symposium on Water Resources Systems, Dec. 20-22, 1980 at the University of Roorkee, India, Vol. 1, pp. 11-8-41 - 11-8-47.

Riggs, H.C., 1968. Some statistical tools in Hydrology. Techniques of Water-Resources Investigation of the United States Geological Survey, Book 4, Chap. A1, 39 pp.

Robin, J., 1972. Ions in solution 2, an introduction to electro-chemistry. Clarendo Press Oxford.

Sadler, B.S., and Williams, P.J., 1981. The evolution of a regional approach to salinity management in Western Australia. Agric. Water Manage., 4:353-381.

Schouten, C.J.J.H., 1976. Origin and output of suspended and dissolved

material from a catchment in Northland (New Zealand), with particular reference to man-induced changes. Doctoral thesis, University of Amsterdam, The Netherlands.

Singh, V.P., and Chen, V.J., 1981. On the relation between sediment yield and runoff volume. Paper presented at the International Symposium on Rainfall-Runoff Modelling held May 18-21, 1981, at Mississippi State Univ., Mississippi State, Mississippi.

Sommerfeldt, T.G.C., 1977. Warner drainage project. In: Dryland Salinity and Seepage in Alberta. Alberta Dryland Salinity Committee, Lethbridge, Alberta.

Steering Committee for Research on Land Use and Water Supply, 1989. Stream salinity and its reclamation in south-west Western Australia. Water Authority of Western Australia, Rep. No. WH52, 23 pp.

U.S. Department of Interior, Bureau of Reclamation and Office of saline water, 1973. Colorado River International salinity control project. Special Report.

U.S. Department of Interior, Bureau of Reclamation, 1974. Colorado River quality improvement program. Status Report, 125 pp.

Schofield, N.J., Ruprecht, J.K., and Loh, I.C., 1988. The impact of agriculture development on the salinity of surface water resources of south-west Western Australia. Water Authority of Western Australia, Report No. WS 27.

Walling, D.E., 1988. Measuring sediment yield from river basin. In: Lal, R., ed., Soil Erosion Research Methods, Soil and Water Conservation Society, USA., pp. 39-67.

W. Australian Water Resources Council, 1986. Water resource prospectives Western Australia. Report No. 2, Water Resources and Water Use Summary of Data for the year 1985 National Survey. Pub. No. WRC 7/86.

Van Breeman, N., 1973. Soil forming processes in acid-sulphate soils. In: Dost, H., ed., Acid-sulphate Soils (1). Proc. Sympo. on Acid-Sulphate Soils, pp. 223-245.

Yekom Consulting Engineers, 1980. The Shapur and Dalaki rivers salinity control project. vol. (3, 10 and 13), Teheran, Iran. (in Farsi)

Zachar, D., 1982. Soil erosion. Development in Soil Science 10, Elsevier Scientific Company, Amsterdam, The Netherlands.

3 A REGIONAL APPROACH TO SALINITY MANAGEMENT IN RIVER BASINS. A CASE STUDY
IN SOUTHERN IRAN

Published in:

Agricultural Water Management 19 (1991), 27-41

A regional approach to salinity management in river basins. A case study in southern Iran

K. Shati

*Department of Hydrology, Soil Physics and Hydraulics, Wageningen Agricultural University,
Nieuwe Kanaal 11, 6709 PA Wageningen, The Netherlands*

(Accepted 25 June 1990)

ABSTRACT

Shati, K., 1991. A regional approach to salinity management in river basins. A case study in southern Iran. *Agric. Water Manage.*, 19: 27-41.

The present level of salinity in the Shapur and Dalaki river basin (southern Iran) is hardly influenced by human activities and may be denoted as "natural" salinity. This paper aims to describe the engineering measures for the salinity control of the river water in this basin. Among possible salt disposal measures, collection and evaporation of polluted sources in ponds is the most practicable and feasible one. However, greater benefits can be gained by implementation of salt mitigation measures. The model DYRESM was used to simulate the salinity distribution in the planned Jarreh reservoir. Results of the simulation indicate that the Jarreh storage reservoir can regulate and reduce the salt concentration of the irrigation water to a range between 1500 and 2400 mg l⁻¹ compared with between 1000 and 4200 mg l⁻¹ for the original river salinity. Furthermore, the diversion of the most saline inflow in summer also decreases salinity.

INTRODUCTION

Salinity is the greatest water quality problem in arid and semi-arid countries. In several regions, the problem is largely associated with the geomorphology and hydrology of the natural river basin and is then referred to as "natural" or "primary" salinization. Such natural salinity is reported from the United States (Colorado River basin), Spain (Ebro river basin), Romania (Culmatsui river basin), and from Tunisia (Qued Tessa and Medjerda river basins). It is found extensively in southern Iran (e.g., Shapur and Dalaki and Mond river basins).

In many regions human activities aggravate the initial problem by introducing "secondary" salinization. In non-irrigated areas, this is referred to as dry land salting (Peck, 1977). Dry land salting is widespread in southwestern Australia, in the Great Plains region of the United States (Montana, North and South Dakota) and in Canada in the prairie provinces of Alberta, Manitoba and Saskatchewan (Peck, 1977; Miller et al., 1976; Sommerfeldt, 1977).

Regardless of the cause of salinization, the manifestation of the salt problem, i.e., a rise in soil and water salinity is similar.

Considerable amounts of brackish surface and subsurface waters are available in many countries and often form the sole resources for irrigation. For example, in Iran, an amount of 6700 million m^3 per year of surface water with a salinity above 2500 mg l^{-1} is reported to be available.

Although the factors causing natural salinity are essentially unchangeable, regional solutions exist to control or mitigate the salinity effect by adopting a combination of catchment management, engineering and agricultural measures. In an attempt to alleviate the salinity problem, a regional study was carried out in the basin of two salt-affected rivers, Shapur and Dalaki in southern Iran. As part of this study, the salinity management measures pertaining to water quality are classified and described quantitatively.

Catchment management measures are not of interest here because the Shapur and Dalaki basin is characterized by a very scarce natural vegetation due to the existing salty formations which hamper plant growth. The measures related to agricultural management have been extensively researched and documented (e.g., UNESCO, 1970; Van Hoorn, 1971; Doneen and Westcot, 1984; Ayers and Westcot, 1985; Rhoades, 1984, 1985, 1987). In this paper only engineering measures for salinity control of the river water are presented.

AREA DESCRIPTION

Catchment and river system

The Shapur and Dalaki basin ($52^{\circ}20'$, $50^{\circ}45'E$, $30^{\circ}02'$, $28^{\circ}45'N$) is located in the southwestern part of the Zagros mountain range in southern Iran (Fig. 1). The basin has an area of approximately $10,000 \text{ km}^2$. The Shapur and Dalaki are the major rivers in the basin, with an average annual discharge of 530 and 425 million m^3 , respectively. The rivers join to form the Helleh river which enters the Persian Gulf. There are plans to irrigate an area of the coastal plain with water from a reservoir to be constructed in the Shapur river at Jarreh, near its confluence with the Dalaki river.

The basin is mountainous with very sparse vegetation. The highest peaks reach an altitude around 3000 m, although less than 5% of the area lies above 2100 m.

The climate is categorized as arid according to the UNESCO classification (UNESCO, 1979). The annual average rainfall of the area is only about 10% of the total annual potential evaporation. Some climatic data are given in Table 1.

As a consequence of climate, landform and geological setting, river flows are extremely variable. The Helleh river discharges over 80% of its annual flow during winter (December–April).

SALINITY MANAGEMENT IN SOUTHERN IRAN

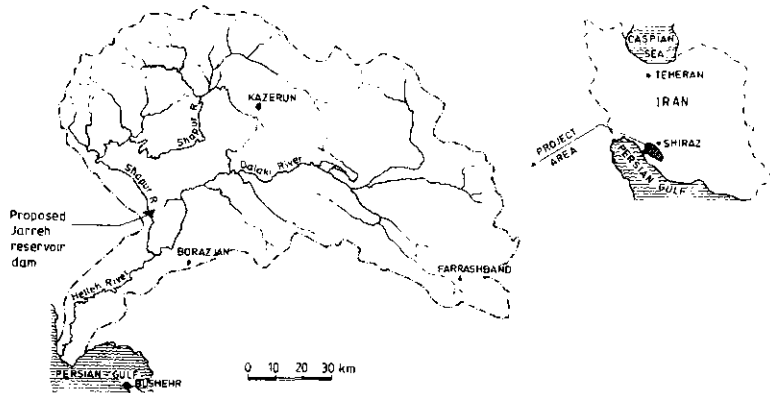


Fig. 1. The Shapur and Dalaki basin.

TABLE I

Mean monthly climatological data of the area.

Month	Rainfall (mm)	Evaporation class A pan (mm)	Temperature (°C)	Relative humidity (%)	Wind at 2 m (km/h)
Oct	2	267	27	51	9
Nov	24	160	20	59	8
Dec	46	84	15	72	10
Jan	70	54	14	73	11
Feb	37	75	15	68	10
Mar	14	132	19	59	11
Apr	16	212	24	51	12
May	3	351	29	43	13
Jun	0	485	32	44	13
Jul	0	445	34	48	11
Aug	1	418	34	49	10
Sep	0	339	31	50	9
Year	213	3022	24	56	11

Analysed over 25 years, period 1952-1978.
Shabankareh Station (51°06'E; 29°23'N).

The region is sparsely populated. Apart from nomadic grazing, few agricultural activities are found, except for a few small irrigation schemes using water from rivers, qanats and springs.

Salinity of the river waters

Origin and sources. The salt in these rivers is derived from marine formations or evaporites (Shiati, 1989). These formations are mainly Late Precambrian evaporites (Hormuz Formation) which locally appear at the surface as emergent salt plugs, and salty gypsiferous marine Miocene strata (Fars Formation), the latter extending over almost the entire study area. These sources contribute their salt to the receiving waters either over a large and extended area (non-point or diffusive sources) or discharge at a specific place (point sources) such as salty or mineral springs and qanats.

Seasonal variation. The mean monthly discharge and the concentration of the total dissolved solids (TDS) of the Shapur river at Jarreh Station is shown in Fig. 2. It shows that TDS varies inversely with the flow. It reaches an annual high value in the summer period (June–September) and falls to an annual low value in winter (December–March). The seasonal variation in ion concentration and its relation with electrical conductivity (EC) are shown in Fig. 3. In summer, Na^+ and Cl^- contribute up to 75% of the total anions and cations but their share decreases to 45% during winter. These temporal variations in discharge and salinity play an important role in the salinity management strategies to be discussed in the next section.

Salt loads. Most of the geological formations present in the area are impermeable or nearly so. Consequently, surface runoff and erosion are common in winter. Summer flows originate mainly from groundwater issuing from springs and old and often disused qanats. The most important processes that affect the salinity of the rivers are:

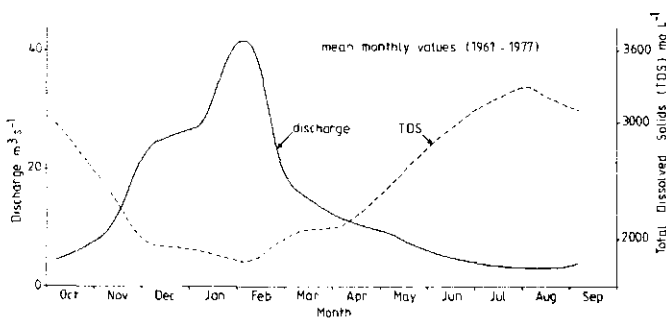


Fig. 2. Seasonal variation of discharge and TDS for the Shapur river at Jarreh Station.

SALINITY MANAGEMENT IN SOUTHERN IRAN

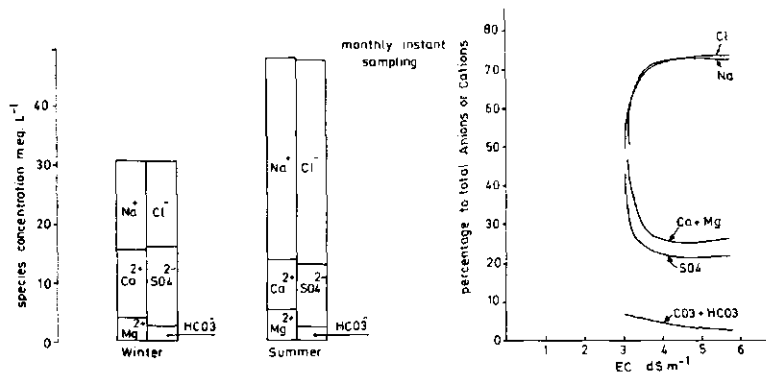


Fig. 3. Seasonal variation in ion concentration and its relation with EC for the Shapur river at Jarreh Station.

- (1) diffusion of salts from nearly impervious saline formations into the water flowing over their surface during rains;
- (2) erosion of such formations, yielding salts as well as sediments from the eroded soil masses;
- (3) salty groundwater from springs and other outlets, flowing throughout the year.

The first two processes dominate in winter. In the upper reaches of the rivers, older formations consisting of hard limestones dominate, and the runoff water remains nearly salt-free. But further downstream, the marine Fars Formation yields large amounts of NaCl and CaSO₄ (the latter especially from the gypsum present in these strata). Due to the high discharges and ineffective salt-transport processes involved, however, the concentration of these compounds in the river water remains relatively low during the rainy season.

The third process adds smaller amounts of water throughout the year, with high concentrations of (mainly) NaCl. In winter, their effects are diminished by the large quantities of surface runoff, but in summer they dominate the composition of the river waters. Snowmelt is not an important source of water in this river basin, for less than 5% of the area is high enough to retain a snow cover for more than a few weeks.

Human activities, other than nomadic grazing, are negligible. The present salinity, therefore, reflects an age-old situation that will be denoted as "natural" in this study.

SALINITY CONTROL METHODS IN THE SHAPUR AND DALAKI BASIN

Strategies

Salinity is a water quality resource problem with a regional character. Therefore, its solution needs a comprehensive regional approach based on implementation of a series of catchment management, engineering and agricultural measures. The solution also depends on the objectives as well as on the local physical conditions. Thus, each basin requires its own special combination of measures and strategies. For example, different solutions have been suggested for North Dakota and Montana (Van Schilfgaarde, 1981), for integrated control of the Colorado River in the United States (USBR, 1974) and for south Western Australia (Sadler and Williams, 1981; Schofield, 1989). These examples, however, differ drastically from the conditions in the study area.

In the Shapur and Dalaki basin a combination of engineering and agricultural management strategies should be adopted. Two engineering strategies can be employed for salinity control: first, to dispose of the salt before it enters the receiving water course and, second, to reduce the salt effect in the river course (e.g. by means of reservoir management).

Salt disposal methods

Several methods of salt disposal have been investigated by Yekom Consulting Engineers (1980); they are summarized in Table 2. Collecting and evaporation of polluted waters in natural ponds is the most practicable and feasible alternative. It takes advantage of the high annual evaporation (3000 mm) of the area. The main obstacles for implementation of this measure are the scattered occurrence and the difficult accessibility of polluting sources, and the difficulty to collect the water and convey it to an evaporation pond, and finally the high cost of implementation. The following four salinity control schemes have been found technically and economically feasible (Fig. 4).

(1) *Shekastian river project (Shapur)*. The project includes a pumping station with a capacity of 100 l s^{-1} , 11 km of pipeline and evaporation basins. The scheme conveys an average of 1.6 million m^3 of salty Shekastian river water during the dry season (May–November) to evaporation basins in the northeast of the Kamarej plain. The implementation of the project will prevent the annual entry of about 53,000 tons of salt into the Shapur river. As a result of the project the annual average salt concentration of the Shapur river is expected to drop by 100 mg l^{-1} , and by about 420 mg l^{-1} during the dry season.

(2) *Tol-Kharaki drain project (Shapur)*. The project includes a pumping station with a capacity of 250 l s^{-1} and a diversion canal of 8 km. The scheme

SALINITY MANAGEMENT IN SOUTHERN IRAN

TABLE 2

Engineering measures for salinity control in the Shapur and Dalaki basin (Yekom, 1980).

	Engineering measures	Applicability	Proposed salt-disposal projects (Ref. Fig. 4)
Salt disposal	Collecting, diverting and evaporation in natural or artificial ponds	Applicable	Shur river project Shekastian river project
	Collecting and desalting	Not applicable	-
	Sealing of springs through grouting with cement, etc.	Not applicable	-
	Recharge through wells into deep aquifers	Not applicable	-
	Evaporation of salty tributaries by use of sequence of dykes and mining the salt	Not applicable (too costly)	-
	Disconnect the recharge (limestone) from the polluting source (salt plugs) by pumping	Applicable	Cerezak spring project
	Diverting the polluting source to a point downstream	Applicable	Tol-Kharaki drain project
	Use of salt water in the chemical industry	Not applicable (too costly)	-
Salinity mitigation	Construction and management of storage reservoirs	Applicable	Jarreh storage res. project
	Desalination	Not applicable (too costly)	-
	Partial storage of saline or fresh water	Not applicable	-
	Blending or cyclic use	Applicable (costly)	Shapur and Zohreh river water blending project

diverts 4.6 million m^3 of Tol-Kharaki drain water during the dry season downstream of the last diversion dam in the Shapur river. The implementation of the project will lower the annual average salt concentration by 50 $mg\ l^{-1}$, and by about 150 $mg\ l^{-1}$ during the dry season, which is equivalent to 31,000 tons of salt.

(3) *Cerezak spring project (Dalaki)*. The project includes the drilling of deep wells in a limestone aquifer. Water will be pumped from the aquifer into the river before being contaminated by a salt plug. The main effect will be a decreased discharge from saline springs into the Shirin river, resulting in a decrease of the salt load by approximately 69,000 tons per annum and the average salt concentration in Dalaki river by 370 $mg\ l^{-1}$.

(4) *Shur river project (Dalaki)*. The project includes a collecting system, a pumping station, 7 km of pipeline, a diversion canal and evaporation basins. The system conveys a total of 1.7 million m^3 of salty spring water to evaporation basins in the south of the Kamarej plain. The implementation of the project will prevent the annual entry of about 225,000 tons of salt to the Dalaki river and lower its average salt concentration by 530 $mg\ l^{-1}$.

The spatial variations of salt concentration (τ_{DS}) in the Shapur and Dalaki rivers, expressed as annual averages, are shown in Fig. 4. In their upper reaches

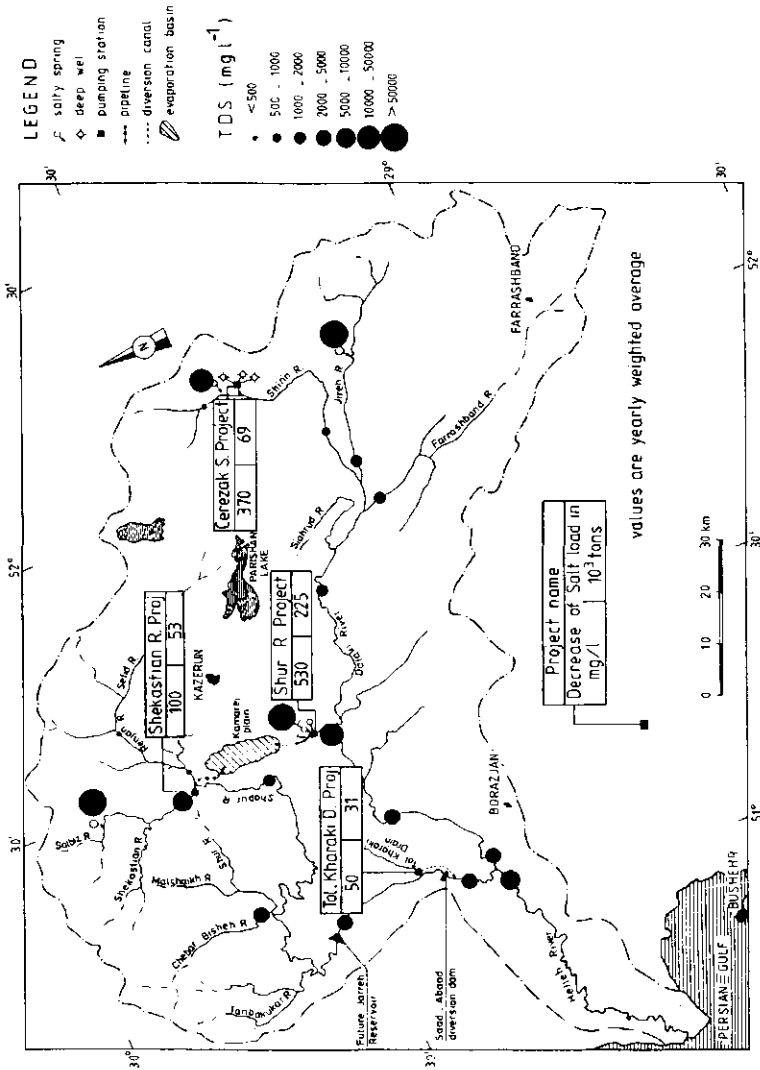


Fig. 4. Spatial variation of salt concentrations in the Shapur and Dataki rivers and the effect of the proposed salinity control projects on river salinity.

the rivers have good quality water ($300\text{--}400\text{ mg l}^{-1}$). However, along their route, due to the effect of point and non-point polluting sources, the water quality deteriorates tenfold, reaching concentrations of $2300\text{--}4500\text{ mg l}^{-1}$, equivalent to 1.1×10^6 and 1.7×10^6 tons of salt before their confluence. Figure 4 also shows the effect of the four salinity control projects that can decrease the average annual salt load of the Shapur and Dalaki river by 82,000 and 294,000 tons, respectively.

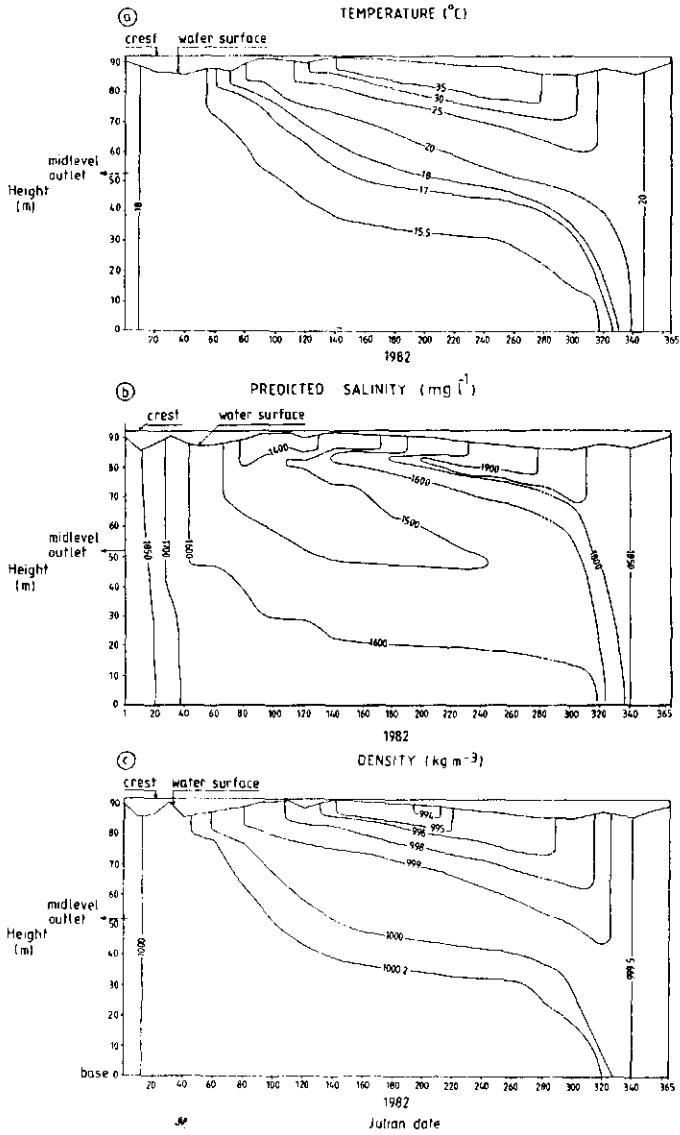
Salt mitigation methods

Construction and management of a storage reservoir

The Shapur and Dalaki rivers have a torrential regime. To use the flow of the river for irrigation in the coastal plain, a reservoir is needed to store flood waters. Thus, the Jarreh reservoir with a capacity of 470 million m^3 has been planned at a location 15 km upstream of the Jarreh-Bala village on the Shapur river. The Jarreh reservoir was used to evaluate the effectiveness of a storage reservoir as salt mitigation measure. This method makes use of the temporal variation in stream discharge and salt concentration and of a phenomenon called stratification which occurs in natural and artificial impoundments.

(i) *Stratification.* Impounded waters are often stratified due to difference in density caused by temperature, dissolved substances and suspended particles. In a stratified reservoir, different layers can be recognized: the warmer and usually fresher top layer (epilimnion); the colder and mostly saltier lower layer (hypolimnion); and an intermediate layer (mesolimnion). The dynamic reservoir simulation model DYRESM (Imberger et al., 1978; Imberger and Patterson, 1981) was used to predict the stratification in the future Jarreh reservoir. DYRESM only models temperature and salinity contribution. However, the model is under modification to account for the effect of inflow of suspended particles as well.

Figure 5 shows the daily averages of the simulated temperature, salinity and density for the year 1982. For this simulation the following situation was assumed: irrigation water was drawn from the midlevel outlet (height 52 m), the bottom outlet (height 23 m) was closed and the excess floods spilled over the top spillways (height 92 m). As can be seen in Fig. 5, during winter the water cools down at the surface. This cooler and heavier water then sinks into deeper layers. Due to this vertical mixing in the reservoir, its contents becomes homogeneous. Stratification due to the increase in solar radiation and heating of the upper water layers starts in spring (date 82080) and builds up until early autumn. In this period the inflowing water is saltier than the water at the surface of the reservoir. The inflow intrudes at the level of the sharp density gradient of the thermocline and builds up a relatively thin layer of water with a salinity increasing from 1400 mg l^{-1} (date 82100) up to about 2000 mg l^{-1} (date 82260). From early autumn onwards the solar radiation



reduces, the upper water layers cool down again, and the stability of the stratification decreases. Due to the influence of wind the homogeneous mixed upper layer becomes deeper until an overturn occurs and the reservoir becomes homogeneous again.

Figure 6 shows the daily averages of the simulated salinity over a period of four years (1982–1985) and the variation in salinity at the midlevel outlet. The summer stratification inhibits the withdrawal of the thin layer of the saltier water at the midlevel outlet. Therefore, the overall salinity in the reservoir increases after each turnover in winter. The predicted salinity at the midlevel outlet and the original salinity are presented in Fig. 7. The regulation of the Shapur river by the Jarreh reservoir will reduce the extremely high salinity in spring and summer. For the years 1982–1985 the salinity of water supplied for irrigation varies between 1500 and 2400 mg l^{-1} in comparison with between 1000 and 4200 for the original salinity of the river.

(ii) *Management of salt-affected reservoirs.* The salinity of the water that will be supplied for irrigation can be further improved by management policies of the reservoir in the following ways:

(1) Manipulating the level of the halocline such that the irrigation water can be supplied from the less saline part of the reservoir for most of the irrigation season, e.g. by a release of water from the bottom outlet.

(2) Releasing the most saline inflow as waste water before mixing occurs, by means of a selective withdrawal structure.

(3) Bypass or diversion of the most saline inflow, e.g. by tunnels or pipes.

The effect of one of the management policies, i.e., the diversion policy is shown in Fig. 8. In this simulation a total of about 50 million m^3 of the most saline river inflow ($\text{TDS} > 3200 \text{ mg l}^{-1}$) was diverted during the summers of 1984 and 1985. The maximum salinity that occurs at the end of 1985 at the midlevel and bottom outlets, decreased about 300 mg l^{-1} .

Other salt mitigation measures

Desalination remains a very costly process and is not likely to be utilized as a salt disposal method in the foreseeable future in southern Iran. This measure was studied for the Dalaki river at the Sarganat Station. The scheme involved a desalting plant with a capacity of 125 million m^3 per year and an salinity of 240 mg l^{-1} , which can be blended with 74 million m^3 of river water resulting in a salt concentration of 1300 mg l^{-1} . The desalting cost was estimated from the desalting cost for the Wellton-Mohawk drain, a tributary of the Colorado River in southern Arizona which is comparable in capacity and salinity (USBR, 1973). It appeared to be prohibitive.

Fig. 5. (a) Simulated temperature, (b) salinity, and (c) density distribution in the Jarreh reservoir for the year 1982.

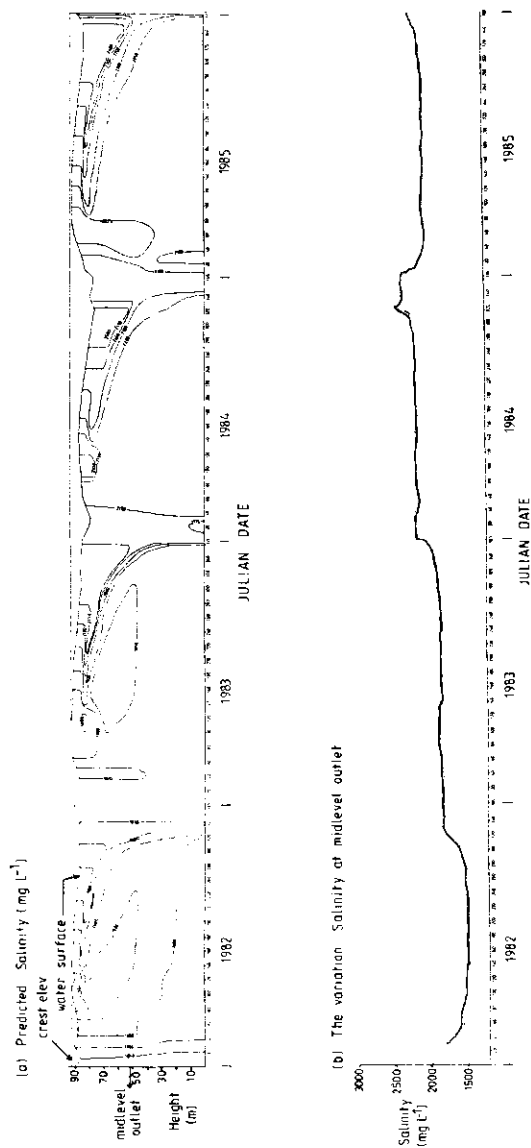


Fig. 6. (a) Simulated salinity in the reservoir, and (b) variation at the midlevel outlet for the years 1982–1985.

SALINITY MANAGEMENT IN SOUTHERN IRAN

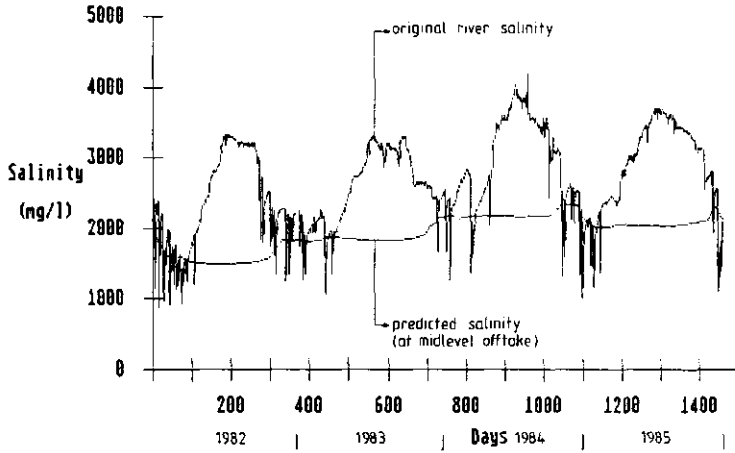


Fig. 7. Predicted salinity and the original river salinity.

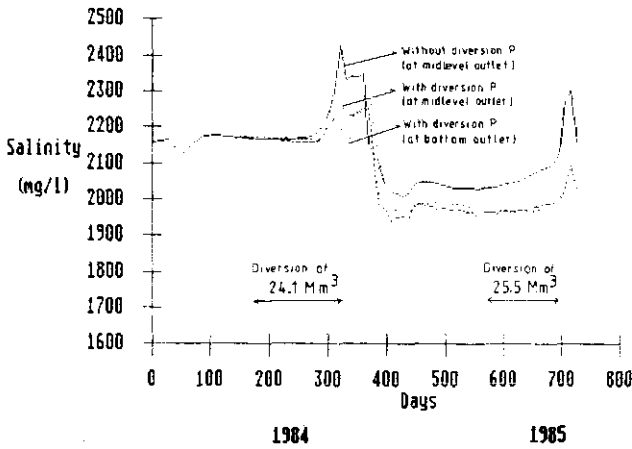


Fig. 8. Management of Jarreh reservoir, diversion policy.

Partial storage of either saline or fresh water cannot be applied because the rivers are brackish for most of the year.

Blending of the Shapur water at the Churum Station with the less salty Zohreh river water is technically feasible but costly. Moreover, Rhoades (1987)

contains that using the two water types cyclically instead of mixed yields greater flexibility and opportunity for crop production.

SUMMARY AND CONCLUSION

In the Shapur and Dalaki basin, engineering measures seem promising for salinity control. Among the measures for salt disposal, collection and evaporation of saline water in ponds appears to be the most practical alternative. Most of the measures studied are unfeasible due to high cost, little effect and technical difficulties. The proposed salinity control schemes reduce the average salt load of the two rivers by 376,000 ton yr⁻¹ (Fig. 4).

Among the measures for salt mitigation, the construction and management of a storage reservoir is the most successful one. The Jarreh storage reservoir can regulate and reduce the salt concentration of the irrigation water to a range between 1500 and 2400 mg l⁻¹ (Fig. 7). The reduction of more than 1800 mg l⁻¹ during spring and especially summer is very valuable because cultivation of moderately tolerant crops (soybean, cowpea, safflower and clover) becomes possible. Furthermore, the diversion of the most saline inflow during summer also decreases salinity (Fig. 8). Finally, careful management of the storage reservoir, making use of the natural stratification processes in its waters, may further improve the quality of the water released.

ACKNOWLEDGEMENTS

The basic hydrometric and meteorological data have been kindly provided by the Water Resources Investigation Bureau, Surface Water Section of Ministry of Energy and Meteorological Organization of Iran, and the salinity data by Yekom Consulting Engineers. Prof. Dr. W.H. van der Molen, Dr. J.W. van Hoorn and Ir. J.H.G. Verhagen are acknowledged for their advice.

REFERENCES

- Ayers, R.S. and Westcot, D.W., 1985. Water quality for agriculture. FAO Irrig. Drain. Pap., 29: 174 pp.
- Doneen, L.D. and Westcot, D.W., 1984. Irrigation practices and water management. FAO Irrig. Drain. Pap., 1: 63 pp.
- Imberger, J., Patterson, J., Hebbert, B. and Loh, L., 1978. Dynamics of reservoir of medium size. J. Hydraulic Div. ASCE., 104: 725-743.
- Imberger, J. and Patterson, J.C., 1981. A dynamic reservoir simulation model. DYRESM. In: H.B. Fischer (Editor), Transport Models for Inland and Coastal Waters. Academic Press, New York, pp. 310-361.
- Miller, M.R., Van der Pluym, H., Holm, H.M., Vasey, E.H., Adams, E.P. and Bahls, L.L., 1976. An overview of the saline-seep program in the states and provinces of the great plains. In:

SALINITY MANAGEMENT IN SOUTHERN IRAN

- Proc. Symp. on Regional Saline-seep Control. Bozeman, Montana. Montana Cooperative Extension Service Bull., 132. pp. 4-17.
- Peck, A.J., 1977. Development and reclamation of secondary salinity. In: Soil Factors in Crop Production in a Semi-Arid Environment. University of Queensland Press, St. Lucia. pp. 301-319.
- Rhoades, J.D., 1984. Using saline waters for irrigation. In: Proc. Int. Workshop on Salt-Affected Soils of Latin America. Maracay, Venezuela. 1983. pp. 22-52.
- Rhoades, J.D., 1985. New strategy for using saline waters for irrigation. In: Proc. ASCE Irrigation and Drainage Spec. Conf., Water Today and Tomorrow, July 24-26, 1984, Flagstaff, AZ.
- Rhoades, J.D., 1987. Use of saline water for irrigation. Water Qual. Bull., 12: 14-20.
- Sadler, B.S. and Williams, P.J., 1981. The evolution of a regional approach to salinity management in Western Australia. Agric. Water Manage., 4: 353-381.
- Schofield, N.J., 1989. Stream salinity and its reclamation in south-west Western Australia. Rep. No. W552. Steering Committee for Research on Land Use and Water Supply. Water Authority of Western Australia, Perth.
- Shiati, K., 1989. The origin and source of salinity in river basin: A regional case study in Southern Iran. In: S. Ragone (Editor), Regional Characterization of Water Quality. Proceedings of a Symposium. May 1989, Baltimore. IAHS Publ., 182 pp. 201-210.
- Sommerfeldt, T.G., 1977. Warner drainage project. In: Dryland Salinity and Seepage in Alberta. Alberta Dryland Salinity Committee, Lethbridge, Alta.
- UNESCO, 1970. Research and training on irrigation with saline water. Tech. Rep. UNDP, Project Tunisia 5, 256 pp.
- UNESCO, 1979. Map of the world distribution of arid regions. Explanatory note. MAB Tech. Notes, No. 7.
- USBR, U.S. Department of Interior, Bureau of Reclamation and Office of Saline Water. 1973. Colorado River International Salinity Control Project. Special Rep.
- USBR, U.S. Department of Interior, Bureau of Reclamation, 1974. Colorado River Quality Improvement Program. Status Rep.
- Van Hoorn, J.W., 1971. Quality of irrigation water, limits of use, and prediction of long-term effects. In: Salinity Seminar Baghdad. FAO Irrig. Drain. Pap., 7: 114-135.
- Van Schilfgaarde, J., 1981. Dryland management for salinity control. Agric. Water Manage., 4: 383-391.
- Yekom Consulting Engineers, 1980. The Shapur and Dalaki Rivers Salinity Control Project, Vols. 3, 10, 13, 14. Tehran, Iran (in Farsi).

4 BEHAVIOUR OF A SALT-AFFECTED RESERVOIR

4.1 INTRODUCTION

Reservoirs are providing storage space to alleviate the consequences of extreme hydrological events (draughts and floods) and provide water for various purposes: e.g. irrigation, hydropower generation, water supply. Reservoirs also play an important role in environmental concerns: they act as sinks for certain residuals carried by river waters, alleviate the extreme variability of conservative water quality parameters (e.g. salinity) of rivers, and improve the water quality by careful management. A phenomenon of considerable influence on water quality is the stratification of the water in reservoirs. In a stratified system, the following water quality profiles are typically observed (Fig. 4.1):

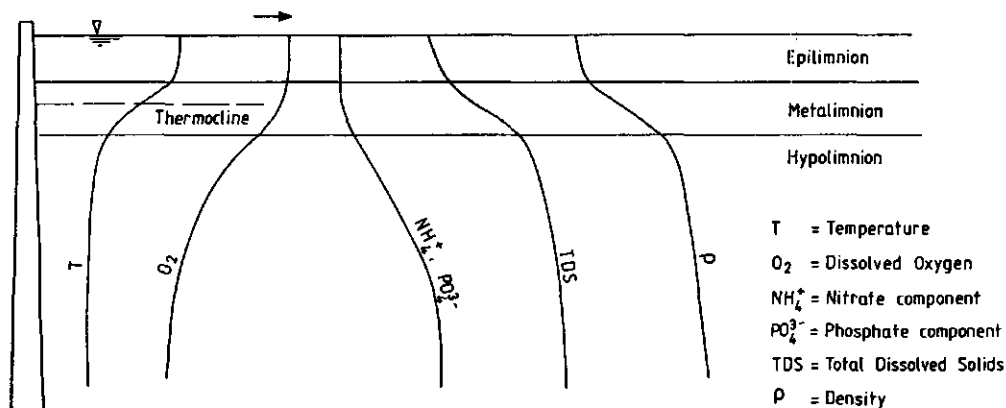


Fig. 4.1 Typical water quality profiles in stratified systems.

Existence of a comparatively heavier, cooler, and often more salty layer at the reservoir bottom, and enriched by products from the mineralization and decomposition of organic matter, brings about marked changes in water quality of the reservoirs. Thus, quality deterioration may occur due to a depletion of dissolved oxygen and an increase in nutrient concentration of the hypolimnion water. In this study, we are concerned only with salinity as a water quality parameter of interest. In the foregoing sections, it was shown that a feasible engineering measure for salinity management in the salt-affected Shapur river basin comprises both construction and management of the Jarreh reservoir. Of course, a much more careful management is required to fulfill various salinity constraints together with criteria associated with different purposes. It is the aim of this study to investigate i) some new aspects of modelling water quality

(salinity) of such reservoirs, ii) their behaviour upon a large time span, and iii) their response to different management policies.

The first objective is accomplished by modifying and extending an existing model for stratified reservoirs, the dynamic reservoir simulation model DYRESM (Imberger et al., 1978), in order to take into account the effect of sediment on physical processes (mixing) in the reservoir (Chap. 5). Chemical and biological processes, running simultaneously with the physical processes are not dealt with in the present work (e.g. Jorgensen, 1980; Jermer, 1987). The second and third objectives are achieved by applying the dynamic reservoir simulation model to simulate the reservoir on a long-term basis (1975-1990), and by examining different management options (Chap. 6). The planned Jarreh Reservoir on the brackish sediment-laden Shapur river, in Southern Iran, is used as a real case throughout this study.

The stratification phenomenon

Deep reservoirs are stratified due to differences in density caused by temperature, soluble salts and/or suspended particles. The thermal stratification can be briefly explained as follows. Most of the solar energy received at the reservoir surface is absorbed as heat. Some of the heat is transmitted downwards by conduction and by turbulent diffusion caused by wave action and the remainder is lost to the atmosphere mainly through evaporation and by long wave radiation exchanges. During summer the surface tends to warm up, and the top water becomes warmer than the bottom water. As a result, three distinctive zones develop: a thin, warm and generally fresher layer with approximately constant temperature at the top (epilimnion), a cold and more salty layer with small gradient at the bottom (hypolimnion), and a zone with steep temperature gradient in between (thermocline or metalimnion). During the autumn, the incident radiation decreases, the temperature of the epilimnion drops, the thickness of the epilimnion increases and the density difference between the epilimnion and hypolimnion decreases. If cooling continues the top layer may become heavier than the water underneath. This condition is not stable, which results in a circulation in the reservoir. This "turnover" is usually assisted by wind drag on the surface. During this period of water circulation, the flow induced by the wind mixes almost the whole volume of the reservoir.

The degree of stratification depends on the densimetric Froude number (F_r), $F_r = U/(g'H)^{1/2}$. If the length and volume of the impoundment are introduced as characteristic parameters F_r becomes:

$$F_r = \left(\frac{L}{H}\right) \left(\frac{Q}{V}\right) \left(\frac{H}{g}\right)^{\frac{1}{2}} \quad (4.1)$$

where

- L = reservoir length (m)
- H = average reservoir depth (m)
- U = average flow-through velocity (m/s)
- Q = discharge (m³/s)
- V = reservoir volume (m³)

- g' = modified acceleration due to gravity (m/s^2), $g' = g(\Delta\rho/\rho)$
- g = acceleration due to gravity (m/s^2)
- ρ = water density (kg/m^3)
- $\Delta\rho$ = density difference over depth H (kg/m^3)

According to Water Resources, Inc. (1969), strongly stratified impoundments are those for which $F_r \leq 1/\pi$, weakly stratified are those for which $0.1 < F_r < 1.0$ and fully mixed impoundments are defined by $F_r > 1$ (Orlob, 1983). According to Catner (1983) if F_r is less than $1/\pi$, stratification is expected, with the degree of stratification increasing with decreasing densimetric Froude number.

Jarreh Reservoir classification and characteristics

Based on geometry, meteorological conditions and hydraulic and nutrient loads, the Jarreh Reservoir can be classified as follows:

- Warm monomictic : with water temperature never below $4^{\circ}C$, winter circulation and summer stagnation (Hutchinson, 1957; Jorgensen, 1980) occur.
- Strongly stratified : with densimetric Froude number $F_r \ll 1/\pi$.
- Time of residence : with an average residence time equal to $V/Q = 470 \text{ Mm}^3 / 430 \text{ Mm}^3 \text{ yr}^{-1} = 1.1 \text{ year}$.
- Due to low concentration of phosphate and nitrate nutrients in the inflows, estimated as 0.02 mg/l and 0.4 mg/l , respectively, and a residence time of a year, the Jarreh Reservoir is expected to be of Oligotrophic-mesotrophic type (the procedure suggested by Jorgensen, 1980 is followed). Future agricultural development in the region (fertilizer application, urbanization, ...etc.) will result in an increase in total phosphate and nitrate concentration of inflows and may cause eutrophication of the reservoir.

REFERENCES

- Canter, L.W., 1983. Impace studies for dams and reservoirs. *International Water Power & Dam Construction*, No. 7, Sutton.
- Hutchinson, G.E., 1957. *A treatise in limnology. Geography, Physics and Chemistry*, Vol. 1, John Wiley & Sons, New York, 1015 pp.
- Imberger, J., Patterson, J.C., Hebbert, R.H.B., and Loh, I., 1978. Dynamics of reservoir of medium size. *J. Hydraul. Div., ASCE*, 104:725-743.
- Jermer, M.K., 1987. *Water resources and water management. Development in Water Science*, Pub. No. 28, Elsevier, The Netherlands, 385 pp.
- Jorgensen, S.E., 1980. *Lake management. Water Development, Supply and Management*, Vol. 14, Pergamon Press, U. K., 167 pp.
- Orlob, G.T. (ed), 1983. *Mathematical modelling of water quality: stream, lakes, and reservoir*. John Wiley & Sons, New York, 518 pp.
- Water Resources Engineers, Inc., 1969. *Mathematical models for prediction of thermal energy changes in impoundments*. US Environmental Protection Agency Water Pollution Control Research Series 16130 EXT, Contract 14-22-422. US Government Printing Office, Washington, DC, 157 pp.

4.2 AN ESTIMATOR FOR THE DENSITY OF A SEDIMENT-INDUCED STRATIFIED FLUID

published in :

Earth Surface Processes and Landforms, 15 (1990), 365-368

SHORT COMMUNICATION

AN ESTIMATOR FOR THE DENSITY OF A SEDIMENT-INDUCED STRATIFIED FLUID

K. SHIATI

Department of Land and Water Use, Wageningen Agricultural University, Nieuwe Kanaal 11, 6709 PA Wageningen, The Netherlands

Received 11 January 1989

Revised 16 October 1989

ABSTRACT

The contribution of dissolved salts and/or sediment particles in altering the fluid density cannot be neglected in studying density stratified flows. In this paper equations are presented to evaluate the density of water as a function of temperature, salt content, and sediment load. A nomograph based on these equations is constructed. The nomograph is applied to estimating the density variations of the Shapur River, a sediment-laden stratified river in Southern Iran. It is illustrated that sediment gives rise to large peaks in density of the river. Such variations are known to be an important factor in geomorphology.

KEY WORDS Density Estimator Stratified river Sediment particles

INTRODUCTION

Sediment loads play an important role in shaping the morphology of rivers and waterways. A sediment-laden stratified inflow (e.g. river) has an impact on physical, chemical, and biological processes in impounded waters. The sediment-laden stratified inflow into lakes or reservoirs forms turbid underflow currents, which constitute an important mechanism in reservoir sedimentation. Engineering practices involving such flows require accurate knowledge of the density of stratified fluids.

The density of a fluid (ρ) is determined by its temperature (T), inorganic soluble solids (S), and suspended particles (s). Under atmospheric pressure it can be expressed as:

$$\rho = f(T, S, s)$$

The combined effects of dissolved salts and temperature on density is investigated by many researchers (e.g. Chen and Millero, 1977a, 1977b; Millero *et al.*, 1976; Fischer *et al.*, 1979) and is tabulated in the literature (e.g. hydrographical tables in Knudsen, 1901; U.S. Navy H.O., 1952). The combined effect of temperature, salt, and sediment on density are not linear and they do not simply add up. Therefore, one should provide estimators of density which allow for the interplay of these three factors. In this study basic equations are presented and based on these, a nomograph is constructed. With the help of this nomograph density can be conveniently estimated for use in practical engineering problems. The use of the nomograph is illustrated by applying it to the Shapur River (Southern Iran).

TEMPERATURE AND DISSOLVED SALT EFFECTS $\rho(T, S)$

The dependence of ρ on temperature is non-linear, because the density of water reaches a maximum at 4°C. Also the relation with salinity is non-linear because of volume contraction in the fluid. The contribution of

0197-9337/90/040365-04\$05.00

© 1990 by John Wiley & Sons, Ltd.

SHORT COMMUNICATION

dissolved salts in the fluid is to increase density, depress the temperature of maximum density, and further more affect on static stability of an impounded water (Chen and Millero, 1977a).

The most commonly used relation for the effect of salt and temperature on density is the empirical expression due to Knudsen (1901):

$$\rho(T, S) = \rho(T, O) + [0.805 - 0.00286(T - 4 + 0.22S)]S \quad (1)$$

where S is the salinity in ‰, T is the water temperature in °C, $\rho(T, O)$ is the density of pure water at different temperatures in kg m^{-3} , and $\rho(T, S)$ is the density at varied salt and temperature in kg m^{-3} . Equation 1 shows that even a nominal amount of dissolved salts increased the density of the fluid. All of the recent studies indicate that Knudsen's tables are reliable to ± 1 ppm in expansibility or thermal expansion and ± 10 ppm in density (Millero *et al.*, 1976).

Fischer *et al.* (1979) developed an estimator for sea water, valid for small range of S as:

$$\sigma(T, S) = \sigma(T, S_0) + \partial\sigma(T, S_0)/\partial S [S - S_0] \quad (2)$$

$$\sigma(T, S) = (\rho(T, S) - 1)1000$$

where S is the salinity in ‰, S_0 is the reference salinity (34‰), T is the temperature in °C, and $\rho(T, S)$ is the fluid density in gms cm^{-3} . $\sigma(T, S_0)$ and $\partial\sigma(T, S_0)/\partial S$ are calculated from a table (Fischer *et al.*, 1979, Table A.2).

Equations 1 and 2 are valid at atmospheric pressure only. More elaborate expressions, correcting density at other pressures, have been obtained by later investigators (e.g. Millero *et al.*, 1976; Chen and Millero, 1977b).

SILT EFFECT $\rho(s)$

The contribution of sediment to ρ is linear for all practical purposes. Consider a fluid element with mass (M) and volume (V) containing sediment particles with density (ρ^s), total volume (v) and total mass (m), then the mass of the suspension and the fluid density (ρ) can be expressed by:

$$M = \rho^s v + \rho_0(V - v) \quad (3)$$

$$\rho = \rho^s(v/V) + \rho_0(1 - v/V) \quad (4)$$

where ρ_0 , the density of sediment-free water, is mostly a function of temperature and salt. Defining c as volumetric concentration of sediment $c = v/V$, Equation 4 can be written as:

$$\rho = \rho^s c + \rho_0(1 - c) \quad (5)$$

Equation 5 can also be written in terms of sediment concentration x , $x = \rho^s c$ as:

$$\rho = x + \rho_0(1 - x/\rho^s) \quad (6)$$

or in terms of submerged specific weight of sediment particles R , $R = (\rho^s - \rho_0)/\rho_0$ as:

$$\rho = \rho_0 + \rho_0 R c \quad (7)$$

TEMPERATURE, SALT, AND SUSPENDED PARTICLES EFFECT $\rho(T, S, s)$

The fluid density ρ is first calculated as a function of salt and temperature and then the contribution of sediment can be added. $\rho(T, S)$ was calculated by Equation 1 and $\rho(T, O)$ by a 4th degree approximation of data on density of pure water given at various temperatures (Handbook of Chemistry and Physics-D171). The additive effect of silt load in changing the density was calculated by Equation 6.

A nomograph based on the empirical equations given above is constructed over a range of values normally encountered, salinity in the range 0–20‰, temperature in the range 0–48°C, and sediment concentration in 0–120 kg m^{-3} as shown in Figure 1. The nomograph is applied to estimating the density variations of the

SHORT COMMUNICATION

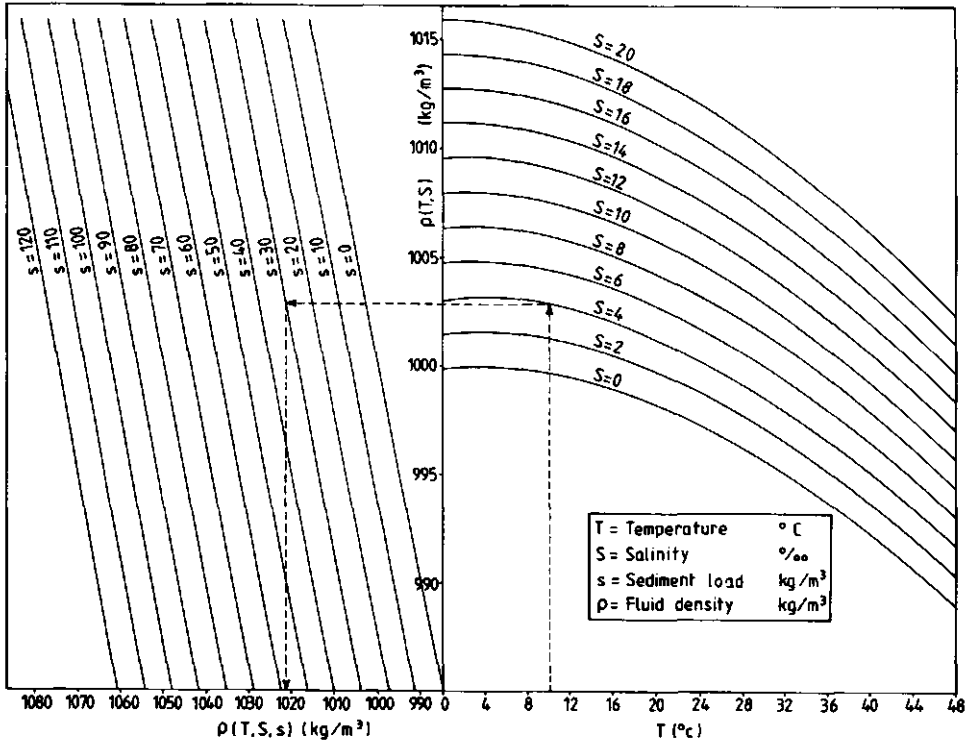


Figure 1. Fluid density for various temperatures, salinities and sediment concentrations

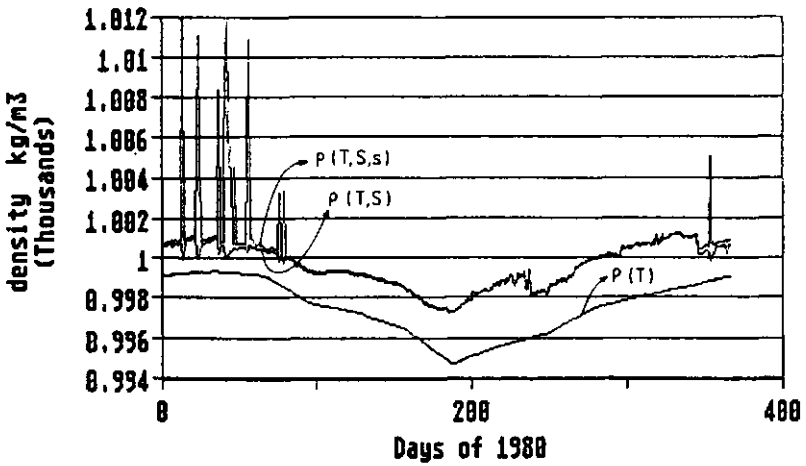


Figure 2. Variation in density of a stratified river (Shapur River, Iran) due to temperature, salt, and sediment load

SHORT COMMUNICATION

Shapur River in Southern Iran (Figure 2). It indicates that, whereas changes in temperature and salinity cause a slowly varying seasonal fluctuation, sharp peaks in density are caused by the heavy sediment loads in this river.

ACKNOWLEDGEMENTS

The author wishes to thank Prof. W. H. van der Molen and Ir. J. H. G. Verhagen for their helpful comments and corrections of the text.

REFERENCES

- Chen, C. T. and Millero, F. J. 1977a. 'Effect of salt content on the temperature of maximum density and on static stability on lake Ontario', *Limnol. Oceanogr.*, **22**, 158-159.
- Chen, C. T. and Millero, F. J. 1977b. 'The use and misuse of pure water PVT properties for lake waters', *Nature*, **266**, 707-708.
- Fischer, H. B., List, E. J., Koh, R. C. Y., Imberger, J., and Brooks, N. H. 1979. *Mixing in Inland and Coastal Waters*, Academic Press, New York, 483 pp.
- Handbook of Chemistry and Physics 1968-1969*, 49th edition, The Chemical Rubber Co.
- Knudsen, M. 1901. *Hydrographical Tables*, G.E.C. Gad, Copenhagen.
- Millero, F. J., Gonzales, A., and Ward, G. K. 1976. 'The density of sea water solutions at one atmosphere as a function of temperature and salinity', *Journal of Marine Research*, **34**, 61-93.
- U.S. Navy Hydrographic Office 1952. 'Tables for sea water density', *H.O. Publication No. 615*, U.S. Navy Hydrograph Office, Washington, D.C.

5 MODELLING RESERVOIR WATER QUALITY AFFECTING BY SALT, TEMPERATURE AND SEDIMENT

5.1 BEHAVIOUR OF SEDIMENT-LADEN STRATIFIED FLOWS

published in :
(slightly modified)

Atelier International sur l' Application des Models Mathematiques a l' Evaluation des Modifications de la Qualite de l' Eau, Tunis, 7-12 Mai 1990, 413-425.

Derivation of equations presented in sections 5.1 and 5.2 are presented in Appendix 2.

MODELLING RESERVOIR WATER QUALITY AFFECTED BY SALT, TEMPERATURE AND SEDIMENT:

BEHAVIOUR OF SEDIMENT-LADEN STRATIFIED FLOWS

Shiati, K. * and Verhagen, J. H. G.**

*Department of Hydrology, Soil Physics and Hydraulics, and
**Department of Theoretical Production Ecology, Wageningen Agricultural University, Nieuwe Kanaal 11, 6709 PA Wageningen, The Netherlands

SUMMARY

A sediment-laden stratified flow influences the physical processes, sedimentation and water quality in a reservoir. In this paper, its characteristics at the plunging region, and the resulting underflow and sediment transport related to such flows are studied. It is shown that in reservoirs, turbidity currents are characterized by a constant Richardson number (R_T) larger than one, a constant velocity (U) and, hence, a normal or steady condition. Accordingly the basic equations (Parker, 1982) may be considerably simplified. Results of field measurements in Latian Reservoir (Iran) are compared with predictions of current velocities obtained from different equations of momentum. Finally, the behaviour of the sediment-laden stratified inflows is compared with that of a conservative gravity current used in the model DYRESM (Imberger et al., 1978) for two inflow conditions into the future Jarreh Reservoir (Iran). It is shown that the sediment load considerably enhances the velocity and the buoyancy force of the underflow current, especially at high river discharges.

INTRODUCTION

The water quality in a reservoir is greatly influenced by a phenomenon called "stratification". Due to density gradients over depth the vertical turbulent mixing is reduced, leading to stagnation, followed by the possibility of oxygen depletion in the lower layers. Deep reservoirs are generally stratified as a result of heat input at the water surface by solar radiation. Vertical mixing is induced by cooling at the surface, by wind energy and by the kinetic energy of inflows and outflows. After some initial mixing, the inflow will penetrate to a depth where its density is in accordance with the density of the environment. Therefore, reservoir stratification is greatly influenced by three main properties of the inflowing water: temperature, soluble substances and suspended matter. If

the river water has a higher density than the contents of the reservoir, underflow will occur along the reservoir bottom.

Underflow caused by inflow devoid of suspended matter is called "conservative gravity current" or "density current". The behaviour of density currents in a reservoir and the effects of temperature and/or soluble substances on the water quality have been extensively studied and modelled (e.g. Hebbert et al., 1979; Imberger et al., 1978). Orlob (1983) gives a detailed review of existing models for predicting water quality and ecological relationships in reservoirs. However, the effect of suspended matter is seldom taken into account. The presence of sediment particles in the inflowing water affects the dynamics of the resulting underflow (now called "turbidity current") and the mixing process in a reservoir. Sediment-laden rivers are most commonly found in arid and semi-arid regions, and their influence on reservoir stratification needs to be fundamentally studied. Shiasi (1990) has shown that, although changes in temperature and salinity cause a slowly-varying seasonal fluctuation in the density of river water, sharp peaks in density may be caused by heavy sediment loads.

The aim of this paper is to study the combined effect of temperature, salt and sediment content of inflowing river water on the mixing process in a reservoir and to model its water quality, especially its salinity. In this Section (5.1), relationships that describe the sediment-laden stratified inflows in a reservoir are derived from the basic equations. Field measurements in Larian Reservoir (Iran) have been used to compare the various momentum equations suggested by different researchers. Next, the behaviour of a conservative gravity current (Hebbert et al., 1979) and a turbidity current (present paper) are compared. In Section 5.2, the dynamic reservoir simulation model, DYRESM (Imberger et al., 1978) has been modified in order to take into account the contribution of sediment particles. Throughout this study the planned Jarreh Reservoir on the brackish sediment-laden Shapur river (Southern Iran) is employed as a real case.

ANALYSIS OF A SEDIMENT-LADEN INFLOW INTO A RESERVOIR

A schematic view of a sediment-laden stream entering a stratified reservoir is shown in Fig. 5.1. There are four regions of flow. First we have the "channel flow" where the sediment-laden stream flows into the nearly stagnant water of a reservoir. The inflow pushes the ambient water ahead until a balance of forces is reached and at that point (called plunge point), it starts to sink beneath the ambient water and forms "underflow". The region of transition from channel flow to underflow is referred to as "plunging region". Two types of underflow can be formed, depending mainly on bottom slope: a supercritical depositing/eroding turbidity current on a steep slope and a steady uniform turbidity current on a mild slope. Turbid underflow travels over the reservoir bottom and is diluted by water entrainment from the ambient water and by deposition of sediment. In a stratified reservoir, the underflow may intrude horizontally at its level of neutral buoyancy to form "interflow" and finally it diffuses into the reservoir water body. The analysis of sediment-laden inflow into a reservoir requires an accurate description of the dynamics of flow in these

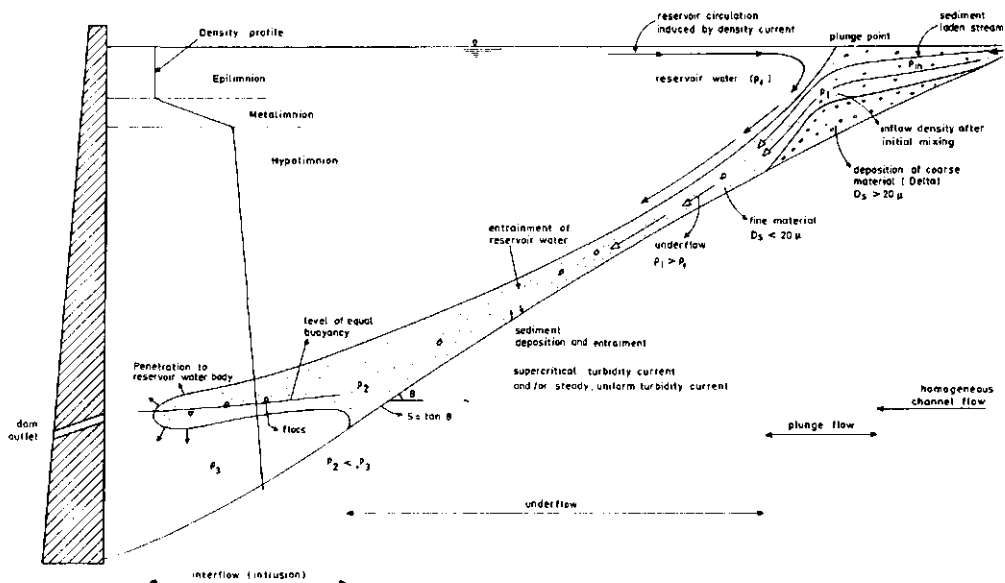


Fig. 5.1 Inflow of sediment-laden river water into a stratified reservoir (schematic).

four regions as well as of the sedimentation pattern throughout the reservoir.

Plunging flow analysis :

The analysis of a turbidity current in the plunging region is complex. Thus far most researchers have neglected the effect of sedimentation in this region. The reader can be referred to Akiyama and Stefan (1987) for a detailed review on the subject. The analysis of the plunging process is directed towards prediction of the depth at the plunge point (h_p). In case of a non-mixing plunging flow Akiyama and Stefan (1984) derived the following equations for h_p on mild (h_{PM}) and steep slopes (h_{PS}), respectively:

$$h_{PM} = \left(\frac{f_c}{SS_2} \right)^{\frac{1}{3}} \left(\frac{Q^2}{e_0 g} \right)^{\frac{1}{3}} \quad (5.1)$$

$$h_{PS} = \left(\frac{1}{S_1} \right)^{\frac{1}{3}} \left(\frac{Q^2}{e_0 g} \right)^{\frac{1}{3}} \quad (5.2)$$

where q is river inflow rate per unit width [L^2T^{-1}], ϵ_0 is the relative density difference between inflow and ambient water [-], S is channel bed slope [-], g is acceleration due to gravity [LT^{-2}], and the dimensionless constants f_t , S_1 , S_2 are total friction factor and profile parameters for which the following values are proposed: $f_t=0.02$; $S_1=0.25$; and $S_2=0.75$, respectively. They showed that on a mild slope the Richardson number downstream of the plunge point could be approximated as:

$$R_I = \frac{f_t}{SS_2} \quad (5.3)$$

which is large compared to one and indicates subcritical flow for this case. Eq. (5.3) is consistent with field measurements in Wellington Reservoir, Australia (Hebbert et al., 1979).

Underflow (turbidity current) analysis :

The steady state, two dimensional, layer-averaged equations which describe the behaviour of turbidity currents on slopes are the equations of conservation of fluid mass, sediment mass, momentum and turbulent kinetic energy. The latter is reduced according to Bagnold's auto-suspension concept, $US/V_s > 1$ (Parker, 1982; Akiyama and Stefan, 1985). These equations are:

i) Equation of fluid mass balance:

$$\frac{d(Uh)}{dx} = E_w U \quad (5.4)$$

ii) Equation of sediment mass balance:

$$\frac{d(UhC)}{dx} = V_s (E_s - C_b) \quad (5.5)$$

iii) Equation of momentum balance in x-direction:

$$\frac{d(U^2h)}{dx} = RgChS - \left(\frac{1}{2}\right) Rg \frac{d(Ch^2)}{dx} - C_b U^2 \quad (5.6)$$

where U is the layer-averaged flow velocity [LT^{-1}], h is layer thickness [L], x is coordinate in downstream direction [L], C is the layer-averaged volumetric concentration of suspended sediment [-], C_b is near-bed sediment concentration ($C_b = r^0 C$) [-], V_s is settling velocity of particles [LT^{-1}], E_w is coefficient of entrainment of water from the quiescent water above the underflow [-], E_s is coefficient of sediment entrainment, r^0 is ratio between near-bottom and average concentration, R is submerged density ratio of the sediment, also denoted as "submerged specific density" ($R = (\rho^s - \rho_w) / \rho_w$)

$[-]$, ρ^s is density of sediment, ρ_w is density of ambient water, and C_D is drag coefficient $[-]$. An important parameter governing the behaviour of stratified flow is the Richardson number, $R_I = RgCh/U^2$. If the Richardson number exceeds unity, the flow is termed subcritical, else supercritical (these terms refer to the mode of flow, with supercritical flow being able to cause erosion of the bottom).

The above mentioned authors found that an appreciable bed slope was required to maintain the current in a supercritical state, which is a necessary condition for erosion to occur. In reservoirs, the bed slope is usually small and the turbidity currents are of the depositing type. To see the consequences of these findings for a practical case, the relations (5.4)–(5.6) were applied to the Jarreh Reservoir ($S=0.0035$) and solved numerically. The results are shown in Fig. 5.2. In Fig. 5.2a it can be seen that the Richardson number (R_I) reaches a value close to unity within a very short distance (a few meters) after which the current becomes subcritical. The case of an eroding/depositing turbidity current was only observed when the bottom slope was fictitiously increased to 4% (Fig. 5.2b), far higher than the existing 0.35 per cent.

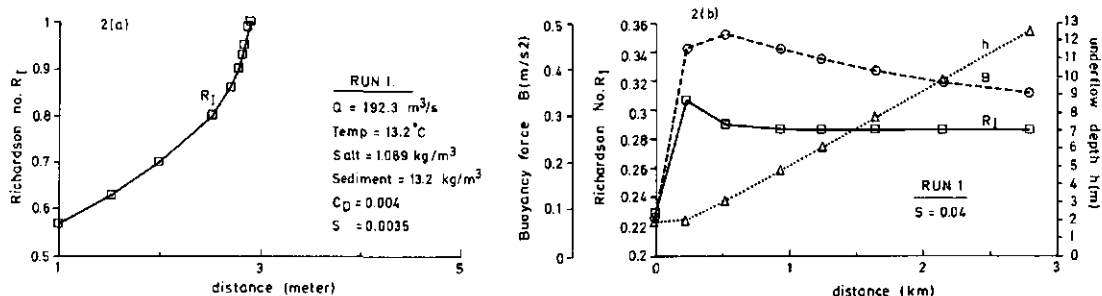


Fig. 5.2 Application of erosive/depositing turbidity current relations to the Jarreh Reservoir (Iran).

Thus, on small bed slope turbidity current is characterized by a large value of R_I ($R_I > 1$). In that case it is not unrealistic to assume that the velocity U does not change with distance (Luthi, 1980; Altinaker et al., 1987). In addition, the assumption is made that all the sediment particles in the turbidity current remain in suspension ($E_s = C_b$) during the time that the underflow is actively moving along the bottom. In that case the equations (5.4)–(5.6) reduce to:

$$\frac{dh}{dx} = E_w \quad (5.7)$$

$$\frac{d(UCh)}{dx} = 0 \quad (5.8)$$

$$E_w + C_D = R_I (S - \frac{1}{2} E_w) \quad (5.9)$$

Luthi (1980); Parker (1982); Graf (1983) have suggested momentum equations similar to eq. (5.9), which are shown in Table 5.1. Graf et al. (1987) and Altinaker et al. (1987) have demonstrated experimentally that the head of a turbidity current on a small slope ($\theta < 2.1^\circ$) slightly decelerates due to a loss of buoyancy flux caused by weak sedimentation. This occurred when the slope was smaller than a critical value. They showed the critical slope to be related to a parameter $(S - V_s/U)$, i.e. Bagnold's criterion for auto-suspension.

Flow properties calculated by various momentum equations for the case of inflow of Shapur river into the Jarreh Reservoir (RUN1, 27/1/1980) are given in Table 5.1. It appeared that the differences in the flow velocity given by these equations are small. However, the equation (5.3), as well as the equations (5.11) and (5.12) that consider a nett settling of sediment particles, resulted in a higher Richardson number and a slightly lower current velocity.

Table 5.1 Flow properties calculated by various momentum equations (Jarreh R., RUN1)

Equation		R_I (-)	U (m s ⁻¹)	State of flow
$C_D = R_I S$ (Parker, 1982)	Eq. 5.10	4.28	0.23	subcritical steady
$E_w + C_D = R_I (S - (E_w/2))$ (present study)	Eq. 5.9	4.59	0.22	subcritical steady
$R_I = E_t / (SS_2)$ (Akiyama & Stefan, 1985)	Eq. 5.3	7.62	0.19	subcritical steady
$E_w + C_D = R_I (S - V_s/U)$ (Luthi, 1980)	Eq. 5.11	7.95	0.19	subcritical steady
$C_D = R_I (S - V_s/U)$ (Graf, 1983, 1987)	Eq. 5.12	7.81	0.19	subcritical steady

Field measurement :

In this section, results of a field study carried out in the Latian Reservoir, Iran are compared with predictions of the velocity obtained from the equations of momentum mentioned above. On April 25, 1984 a flood of 77.4 m³ s⁻¹ was measured in several transects of the inflowing rivers Jaj-Rud and Lavarak at their entrance into the Latian Reservoir (IWRIL, 1984).

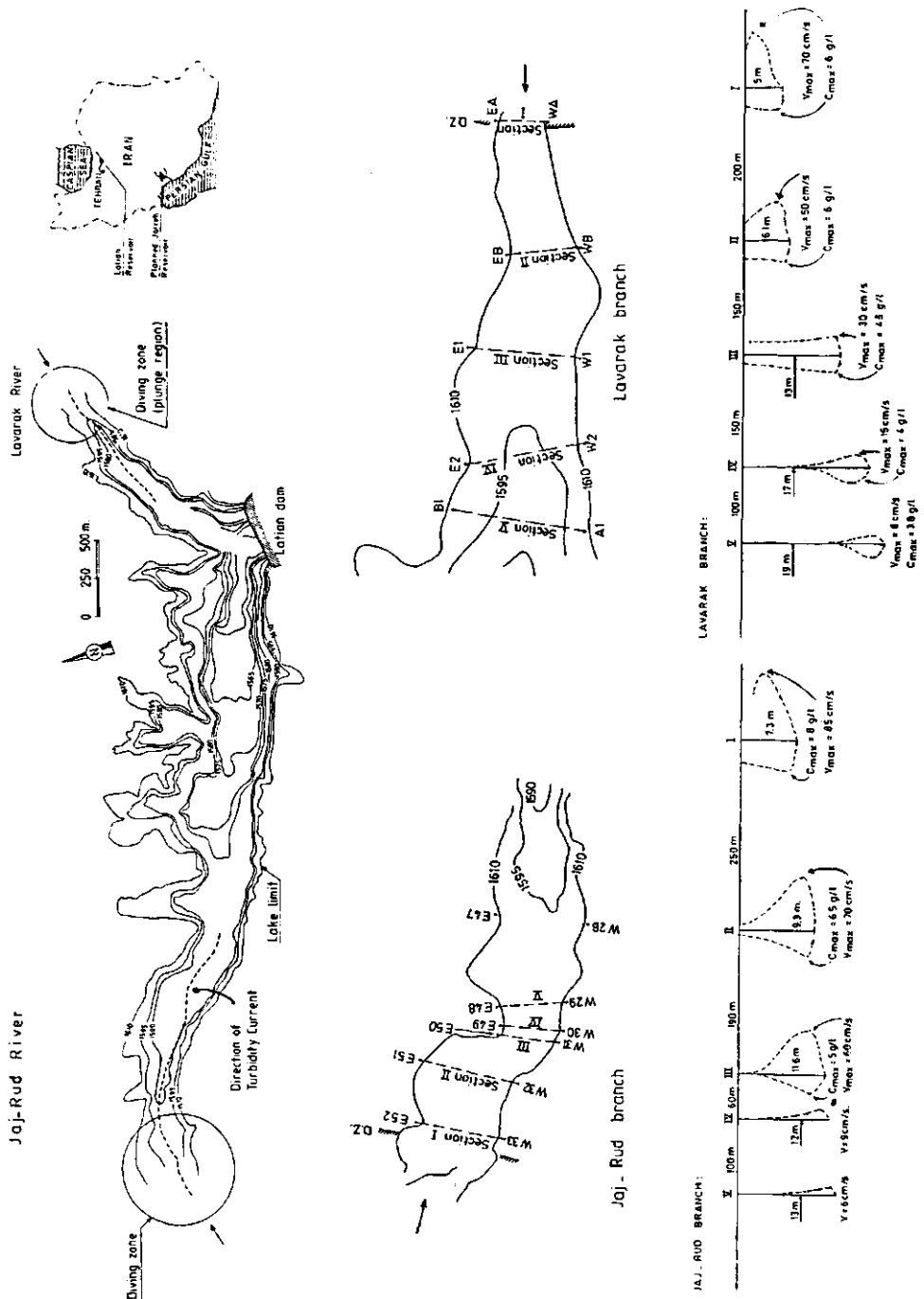


Fig. 5.3 Field measurements of turbidity current in Larian Reservoir (Iran, 25/4/1984).

In Fig. 5.3 the geometry of the reservoir, the direction of the current, the region of submergence (D.Z.) and the measured velocity and concentration profiles at the experimental sections are shown. It appeared that the underflow attains a uniform average velocity of about $6-8 \text{ cm s}^{-1}$ and moves slowly with a thickness of few meters above the bed towards the dam-wall (Fig. 5.3, Sections IV and V). In this experiment, the flood was not strong enough and its duration was too short to follow the current all the way up to the dam-wall, although it was observed at the location of the outlet.

Fig. 5.4 shows that the field measurements are in reasonable agreement with the equations presented in Table 5.1. The expressions of Harleman (1961) for Lake Mead, USA and Fan (1962) for Chinese reservoirs show a discrepancy with the others and resulted in higher underflow velocities. Fig. 5.4 shows also that the simple expression of Akiyama and Stefan (1984) eq. (5.3), which predicts the Richardson number of the underflow for the mild bed slope is rather consistent with the field measurements, although the latter show a more pronounced influence of sediment concentration.

The sediment in a reservoir has the following deposition pattern: the coarse material forms deltas at the head of the reservoir; the finer material forms the bottom sediments, spreading throughout the reservoir; the finest material has a tendency to remain in suspension and travel with the turbidity current. The grain size distribution of particles carried by

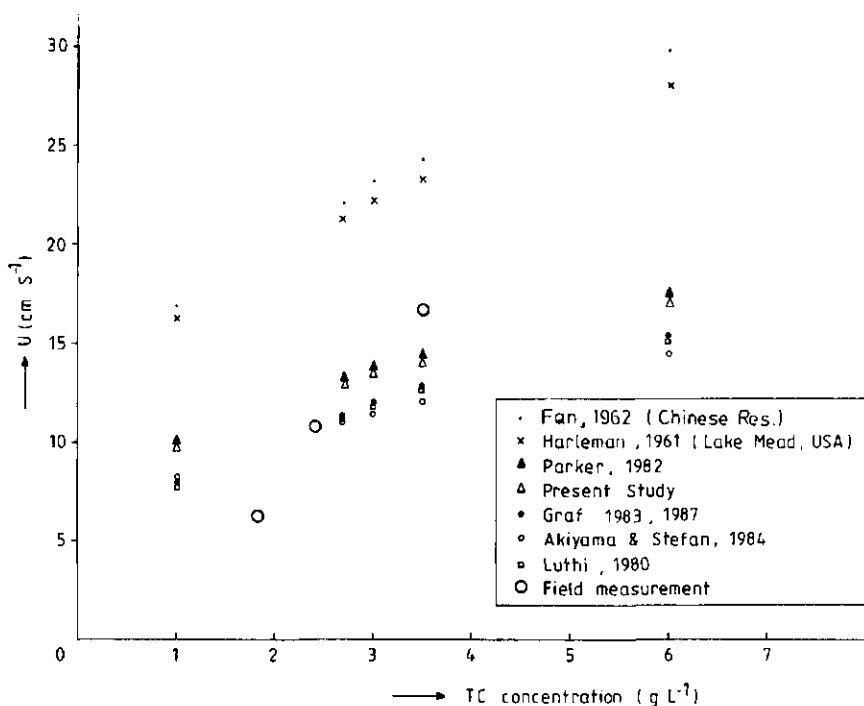


Fig. 5.4. Comparison of calculated velocities and field measurements in the Latian Reservoir (Iran, Lavarak branch, $S=0.007$).

turbidity current in the Latian Reservoir shows a d_{50} and d_{90} in order of 0.004–0.02 mm, respectively, which is consistent with other field measurements (e.g. Lake Mead, USA, Howards, 1953).

APPLICATION OF THE MODEL TO THE JARREH RESERVOIR

The Shapur river valley, in the stretch affected by the reservoir, has relatively narrow channels, an average bottom slope of 3.5 ‰ and a triangular cross-section with a half base angle of about 80°.

Relations (5.7), (5.8) and (5.9) were recast and applied for this reservoir (see Appendix 2). Furthermore, the results are compared with those for conservative gravity currents to show the effect of sediment contribution. For the latter, the work of Hebbert et al. (1979) that is used in DYRESM (Imberger et al., 1978) and developed for Wellington Reservoir, Australia has been used. The results of two computer runs representing a large flood (RUN1) and a normal flow condition (RUN7), respectively, are presented in Fig. 5.5. It appears that the sediment load considerably increases the velocity and the buoyancy force (defined as $B-RgC$) of the current during flood conditions (Fig. 5.5a). During normal flow conditions density and turbidity current relationships lead to more or less similar results (Fig. 5b).

CONCLUSIONS

The expressions (5.7), (5.8) and (5.9) describe the turbidity current on a small bed slope at the equilibrium state. This condition has been checked by using Bagnold's criterion. The equations of turbidity currents at the equilibrium state or equations that consider the settling tendency (V_s/U), like those of Luthi (1980) and Graf et al. (1987) may be assumed to approach conservative density currents in most practical cases. The sediment effect is mainly present in the initial conditions. However, the effect of sediment particles in inflowing water cannot be neglected. The sediment considerably increases the density of the inflow and, consequently, the velocity and the buoyancy force of the underflow and will affect both stratification and mixing processes.

In the light of the field measurements it can be concluded that the larger particles will settle already in the vicinity of the plunging region. The sediment-laden flow will then continue (and decelerate) with small size fractions until it reaches an equilibrium state (with a particle size of about 0.02 mm) and travel downward with negligible deposition during this movement.

ACKNOWLEDGEMENT

The field measurements data of turbidity current in the Latian Reservoir have been kindly provided by the Institute of Water Resources Investigation and Laboratories of the Ministry of Energy of Iran.

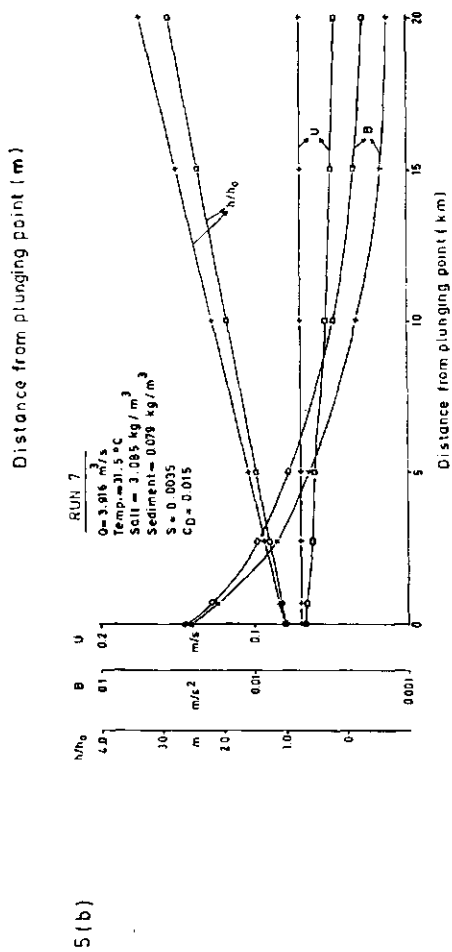
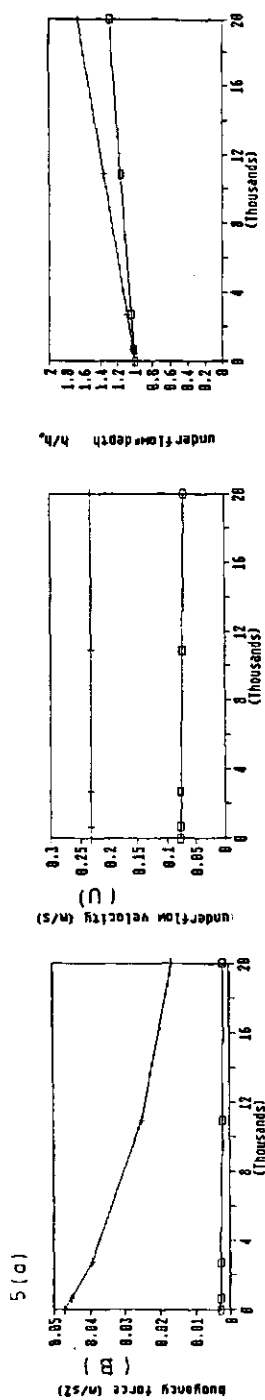


Fig. 5.5 Comparison of flow parameters from density relations (\square) and turbidity current (\rightarrow) for Jarreh Reservoir: (a), RUN1 - flood condition; (b), RUN7 - normal flow condition.

REFERENCES

- Akiyama, J., and Stefan, H., 1984. Plunging flow into a reservoir: theory. *Journal of Hydraulic Engineering*, 110:484-499.
- Akiyama, J., and Stefan, H., 1985. Turbidity current with erosion and deposition. *Journal of Hydraulic Engineering*, 111:1473-1496.
- Akiyama, J., and Stefan, H., 1987. Gravity currents in lakes, reservoirs and coastal Regions: Two-layer stratified flow analysis. Project Report No. 253, St. Anthony Falls Hydraulic Laboratory, Univ. of Minnesota, Minneapolis, Min.
- Altinaker, M.S., Graf, W.H., and Hopfinger, E.J., 1987. Hydraulics of the head of a turbidity current. *Laboratories d'Hydraulique, Ecole Polytechnique Federale Lausanne, Switzerland*.
- Fan, Jia-hua, 1962. An approximate method for calculating the density currents in reservoirs. *Scientia Sinica*, 11:707-722.
- Graf, W.H., 1983. The behaviour of silt-laden current. *Water Power and Dam Construction*, 35:33-38.
- Graf, W.H., Altinaker, M.S., and Hopfinger, E. J., 1987. The head of a weakly depositing turbidity current on a small slope. *Rapport Annuel, Laboratoire d'Hydraulique, Ecole Polytechnique Federale de Lausanne, Switzerland*.
- Harleman, D.R.F., 1961. Stratified flow. *Handbook of fluid Dynamics*, V. Streeter, ed., McGraw-Hill Book Co., Inc., N. Y.
- Howards, C.S., 1953. Density currents in Lake Mead, *Proc. of the Minnesota International Hydraulics Convention*, pp. 355-368.
- Imberger, J., Patterson, J.C., Hebbert, R.H.B., and Loh, I., 1978. Dynamics of reservoir of medium size. *J. Hydraul. Div., ASCE*, 104:725-743.
- Institute of Water Resources Investigation and Laboratories, 1984. Investigation of turbidity current in the Latian Reservoir. Ministry of Energy, Report No., 67, Tehran, Iran. (In Farsi)
- Luthi, S., 1980. Some new aspect of two-dimensional turbidity currents. *Sedimentology*, 28:97-105.
- Parker, G., 1982. Conditions for the ignition of catastrophically erosive turbidity currents. *Mar. Geol.*, 46:307-327.
- Shiati, K., 1990. An estimator for density of a sediment-induced stratified fluid. *Earth Surface Processes and Landforms*, 15:365-368.
- Orlob, G.T. (ed), 1983. *Mathematical modeling of water quality: stream, lakes, and reservoir*. John Wiley & Sons, N. Y., 518 pp.

5.2 NUMERICAL SIMULATION OF RESERVOIR BEHAVIOUR

5.2.1 Introduction

Most reservoirs, especially those which are deep and have a long residence time, tend to develop a vertical density structure characterized by a well-mixed epilimnion, a metalimnion with a substantial density gradient, and a weakly stratified lower region called the hypolimnion. This vertical density structure depends on the vertical distribution of temperature, salinity and suspended matter. The stratification in reservoirs is the result of meteorological conditions in the area and of the features of the inflowing and outflowing waters.

The inflowing water usually has a temperature and salinity different from that of the stored water in the reservoir. Besides, the inflowing water may carry suspended matter. These factors determine the density of the inflowing water.

The sediment effect on the density of inflowing water can be observed from Fig. 5.6, which shows the water density of Shapur river with and without the effect of the sediment content for the year 1982. It appears that the effect of sediments is pronounced only during the winter period (December–April). Sharp peaks in density are caused by heavy sediment loads during flood events; they are accompanied by dips in salinity, resulting of a lower density of the sediment-free water at the same time. In the dry season (May–November), the amount of sediment particles in the inflowing water is almost negligible and the water density is almost entirely determined by temperature and salt concentration.

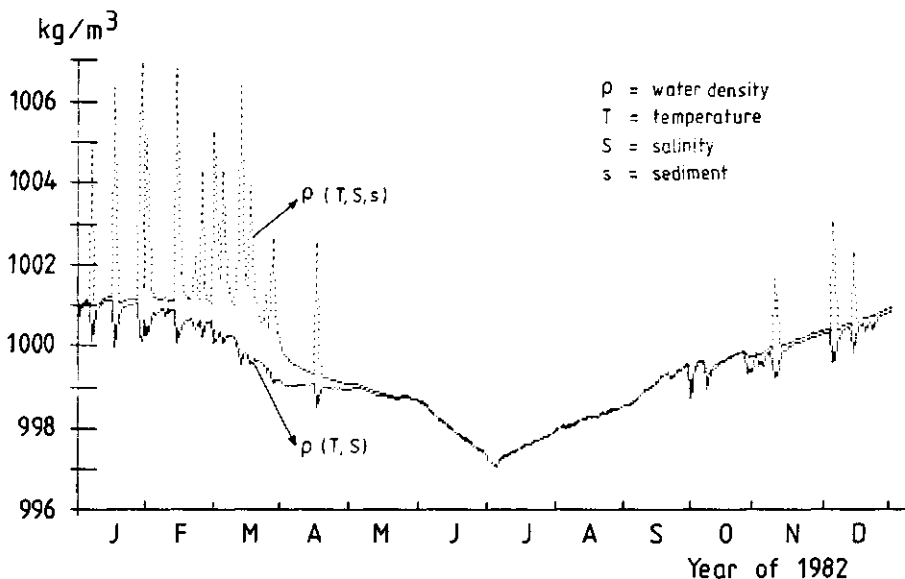


Fig. 5.6 Variation in water density of Shapur R. with and without the effect of sediment.

Numerous models have been developed to simulate the thermal stratification in reservoirs (e.g. WRE model, WRE, Inc., 1969; MIT model, Huber et al., 1972; STRATIF model, Van Pagee et al., 1982; EPAECO model, Gaume and Duke, 1975). Also the combined effect of temperature and salinity on reservoir stratification has been studied and modelled in literature (DYRESM, Imberger et al., 1978).

The purpose of this study is to investigate the contribution of suspended sediment on the inflowing water, and its effect on the quality (salinity) of the reservoir water.

To accomplish the above objective, an algorithm for the behaviour of sediment-laden inflows has been described in Section 5.1. The behaviour of the turbidity current is based on certain assumptions specific to mild bed slopes. These assumptions are: the turbidity current can be characterized by a constant Richardson number larger than one, $R_f > 1$; a constant current velocity and hence a steady flow condition; and finally that particles smaller than 20 microns remain in suspension (with negligible deposition or entrainment), and will settle only after the current has ceased.

Although the new algorithm introduces the combined effect of temperature, salinity and sediment on inflow processes, it does not simulate the turbidity distribution in the reservoir. This restricts the application of our model to predicting the distribution of those dissolved substances which are not reacting (bio)chemically with suspended particulate matter, like salinity. For other compounds like e.g. phosphorus and heavy metals a significant amount will be removed from the water column by settling of suspended matter. To model such reactions one needs also to consider the spatial and temporal distribution of the suspended particles and their adsorption characteristics. These reactions were not included in the present model.

The algorithm is introduced into the reservoir simulation model DYRESM to simulate the salinity structure in the planned Jarreh Reservoir (Southern Iran). The main purpose of this reservoir is to irrigate 13000 ha. of the coastal plain (Fig. 1.6). Simulations are carried out for data of the year 1982. The results show that the sediment particles affect both temperature and salinity (and thus density) distributions in the reservoir by intensifying their gradients. Moreover, it affects the salinity of the water withdrawn from the outlets. However, the latter effect turns out to be small and may not be significant for its use in irrigation.

5.2.2 Numerical model

The dynamic reservoir simulation model DYRESM as developed by Imberger et al. (1978) is used to simulate the salinity in the Jarreh Reservoir. DYRESM is a one-dimensional numerical model for the prediction of temperature and salinity in small- and medium-sized reservoirs and lakes. DYRESM uses a layer concept, according to which the body of the reservoir is divided into horizontal layers (or slabs). These layers are assumed to have spatially uniform properties but variable thickness as inflows, outflows, and mixing processes expand and contract them (Fig. 5.7). The thickness scales of the layers are determined internally by those factors appropriate to the process acting at the time; likewise the time scale of the process determines the time steps of the model within the day. DYRESM

has a fixed time step of one day for inflow and outflow processes and a variable sub-daily time step, between one quarter of an hour and 12 hours for mixing process.

The concepts and architecture of the various processes incorporated have been described in detail in literature. In particular, Imberger, et al. (1978), Patterson et al. (1978), Fischer et al. (1979), Spigel and Imberger (1980), Imberger and Patterson (1981), Imberger (1984) and Patterson et al. (1984) give a detailed description of the model and its construction. It suffices to note here that submodels of five basic processes are incorporated: surface heat and mass exchange, mixed layer dynamics, inflow and outflow dynamics, and hypolimnetic mixing.

DYRESM has been validated on several lakes and reservoirs. Its major development and validation was in Wellington Reservoir (storage= 185×10^6 m³, area= 16 km²), an irrigation supply reservoir situated in the southwest of Western Australia. A quantitative measure of the performance of the model is given by Patterson et al. (1984). For the Wellington Reservoir the average expected errors for the hypolimnion were found to be 0.14 °C in temperature and 25 ppm in salinity, and for the epilimnion, 0.9 °C and 150 ppm. A short description of DYRESM is presented in Appendix 3. In the next

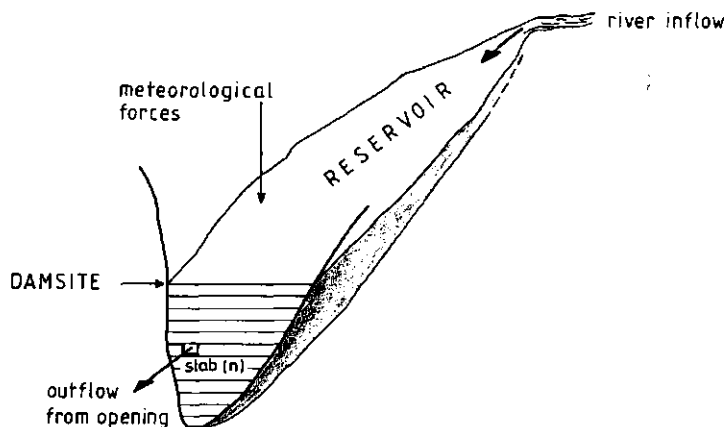


Fig. 5.7 Typical layer in DYRESM model.

section a brief description of the inflow algorithm which takes into account the combined effect of temperature, salinity and sediment on inflow processes is presented.

5.2.3 Inflow dynamics and algorithm

The density of the inflowing water varies with time due to differences in temperature and in dissolved and suspended matter. Besides, deep reservoirs are stratified for most of the year due to the same causes. The inflowing water tends to seek a level at which its density and that of the reservoir are the same. The flow either floats over the reservoir surface if the inflow is lighter or it plunges into the reservoir water if it is heavier than the reservoir water at the surface. It can also mix fully over some depth depending on the density distribution in the reservoir. Typical patterns of inflow are shown in Fig. 5.8 (Fischer, 1979). We will especially consider the case that the inflow has a higher density than the water stored in the reservoir.

In that case, a "plunge line" will be visible, if the entrance point is a well defined drowned river valley. In case of a wide entrance area, the plunge occurs at a single "plunge point". Only the first case is applicable to our problem.

Once the inflowing river has passed the plunge line it will continue to flow down the river channel, entraining reservoir water as it moves towards the dam wall. The entrainment leads to an increase in the underflow volume, thus a decrease in its density. In this way a neutral condition may be achieved, where the density of inflow becomes equal to the density of the surrounding water, and a horizontal penetration (intrusion) of the inflow is assumed to commence. The inflow may continue until it runs out of momentum or until it is stopped by the dam. It may even have enough momentum to climb the face of the dam and flow over the spillways. Such flow of muddy water over the spillway has been reported, among other places, for lake Mead in the USA and lake Matahina in New Zealand (Raudkivi, 1979); it is not expected to occur in Jarreh Reservoir.

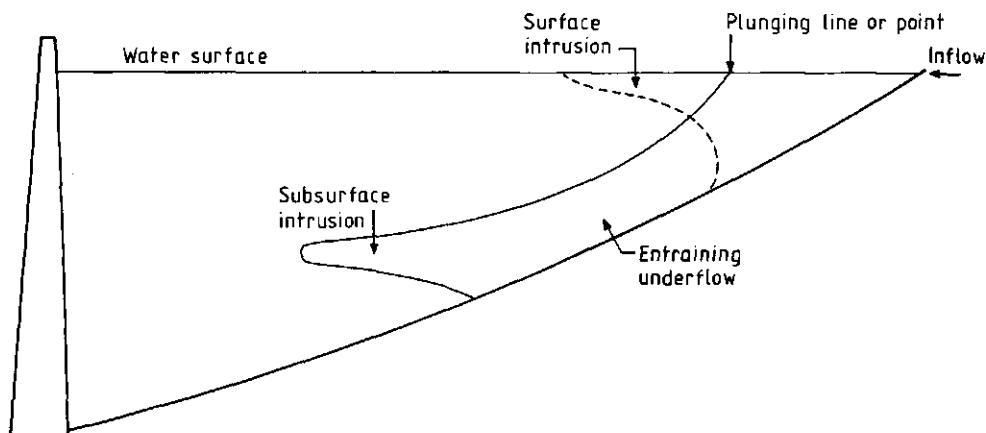


Fig. 5.8 Typical inflow patterns in a reservoir.

Throughout the inflow process, mixing occurs at the plunge region, as well as during underflow and intrusion.

The dynamics of the river discharge entering the main body of the reservoir is modelled by the subroutine INFLOW:

At the beginning, the inflow properties i.e. volume Q , temperature T , salinity S , silt content SED , and density ρ are initialized to the river values. The density of the inflow ρ is calculated as a function of temperature, salinity and sediment load (Shiati, 1990). The inflow density is then compared with that of the top layer ρ_{NS} : if $\rho < \rho_{NS}$ the total volume is added to the top layer, a new surface level and properties are computed, and control is returned to the main program. If, $\rho > \rho_{NS}$, underflow occurs, and a calculation of the initial inflowing depth h_0 and entrainment from the layers adjacent to the underflow are required.

The value of h_0 is approximated from equations (5.1) and (5.3). For Jarreh Reservoir, of triangular cross-section, with a base half angle equal to 80° and a bed slope of $3.5 \text{ }^\circ/00$, the equations (5.1) and (5.3) can be recast into:

$$h_0 = 0.86 \left[\frac{Q^2}{\Delta g} \right]^{\frac{1}{3}} \quad (5.13)$$

where Q is river discharge and Δ is non-dimensional density anomaly $\Delta = (\rho_r - \rho_u) / \rho_r$, ρ_u is the underflow density and ρ_r the reservoir density. This formulation applies only to streams with small bed slope; in the case of larger bed slopes, shear production and mixing at the plunge point must also be considered (Akiyama and Stefan, 1984, 1987).

It should be noted that the underflow density ρ_u is calculated with the assumption that the underflow carries only particles with diameter less than 20 microns; larger particles are assumed to settle in the stretch between inflow point and plunge line, forming a delta in that region (Graf, 1983a, 1983b).

In the preceding chapter it is assumed that the turbidity current velocity does not change with distance. The inflow may thus be routed down along the bottom of the river channel of the stratified reservoir by applying equations (5.7)-(5.9), (after recasting them according to the reservoir geometry) to the vertically averaged inflow variables. The flow depth h , and the amount of dilution $\Delta Q/Q$ due to entrainment as a function of the distance along the river channel x can be written as: (see Appendix 2 for the derivation):

$$h = E_w x + h_0 \quad (5.14)$$

$$\frac{\Delta Q}{Q} = \left(\frac{h}{h_0} \right)^2 - 1 \quad (5.15)$$

The entrainment coefficient of water (E_w) is a function of Richardson's number (R_T). The functional form proposed by Parker et al. (1987) based on

experimental results for simple conservative density currents (Ashida and Egashira, 1977) and turbidity currents is

$$E_w = \frac{0.075}{(1+718R_I^{2.4})^{0.5}} \quad (5.16)$$

This yields a value of $E_w=2.4*10^{-4}$ for Jarreh Reservoir, quite similar to measured value ($1.9*10^{-4}$) in the Wellington Reservoir (Hebbert et al., 1979). Employing the E_w and R_I (from eq. 5.3) to the momentum equation (eq. 5.9) gives a value of $C_D=0.025$ for Jarreh Reservoir. Akiyama and Stefan (1985) suggested a value of $C_D=0.02$ and Hebbert et al. (1979) measured it as 0.015 in his field experiment with simple conservative density currents in Wellington Reservoir.

The entrainment ΔQ from the layers adjacent to the underflow as given by eq. (5.15) is added to the inflow Q . The properties T , S and ρ are adjusted and ρ is compared with the density of the next layer below. If the inflow density is smaller, the level of insertion is taken to be the mid-point of the turbidity current layer. If not, the process is repeated until a neutrally buoyant level is found or until the reservoir bottom is reached. Intrusion into a stratified water body has been studied by Imberger et al. (1976) and employed in the model DYRESM. These studies calculate the length of intrusion to the dam wall(e) and the thickness (2δ) of intrusion (see Appendix 3). The apportionment of the total inflow volume over 2δ is done in such a way that the inflow velocity takes a bell shaped profile.

Once the inflow is inserted, the properties T , S and ρ of the layers are recalculated and control is returned to the main program. It should be noted that at this stage the vertical distribution of sediment particles is not modelled. It is assumed that, once the inflow comes to rest, sediment particles will start to settle on the reservoir bottom in a process known as "pelagic sedimentation". The sedimentation process is enhanced by "flocculation", which, in turn, is stimulated by salinity.

5.2.4 Model inputs

DYRESM uses daily meteorological data (air temperature, wind speed, short-wave radiation, sunshine duration, vapour pressure and rainfall), inflow data (water temperature, river discharge, salinity and sediment content), outflow data (amount of withdrawal from bottom and/or midlevel outlets) and reservoir geometry (width and length at the outlets and crest level, area-volume relationship and bed slope).

The planned Jarreh Reservoir is a medium-size (storage $470*10^6$ m³, area 19.5 km², at the crest level), irrigation supply reservoir in Southern Iran (Fig. 5.9). It will be about 92 m deep at the dam wall and extend some 23 km along the relatively narrow Shapur river valley (average bed slope 3.5 ‰, and a triangular cross section with a half base angle of about 80°). Withdrawal is primarily for irrigation and will occur throughout the year. The average residence time of the water in the reservoir is 1.1 year.

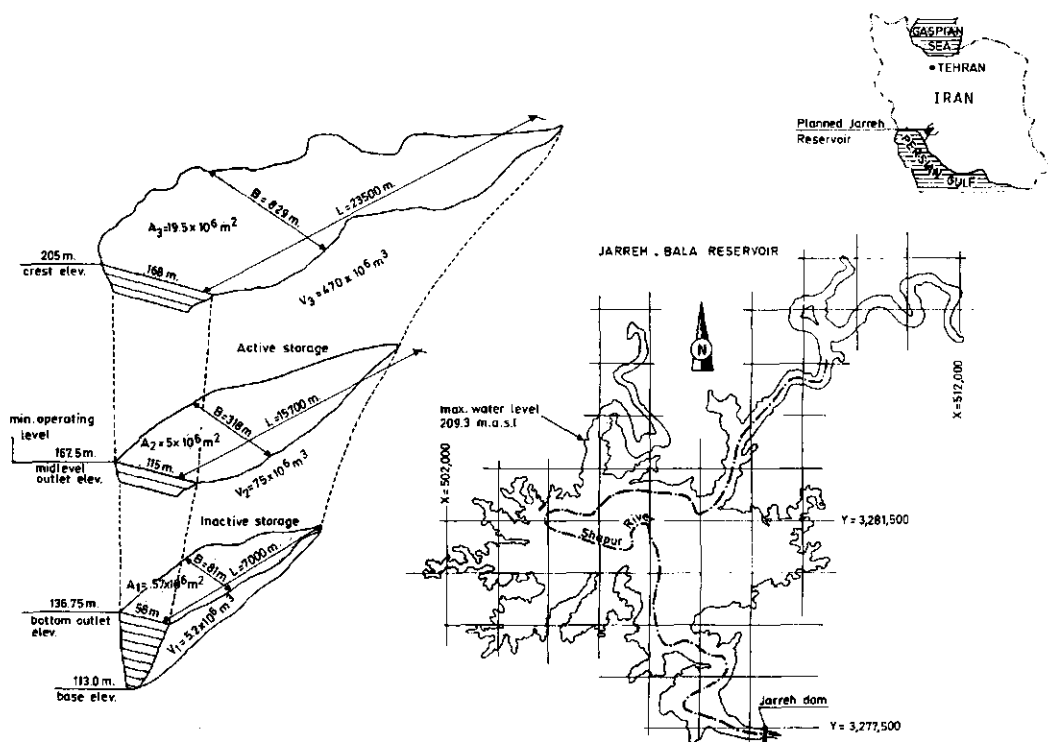
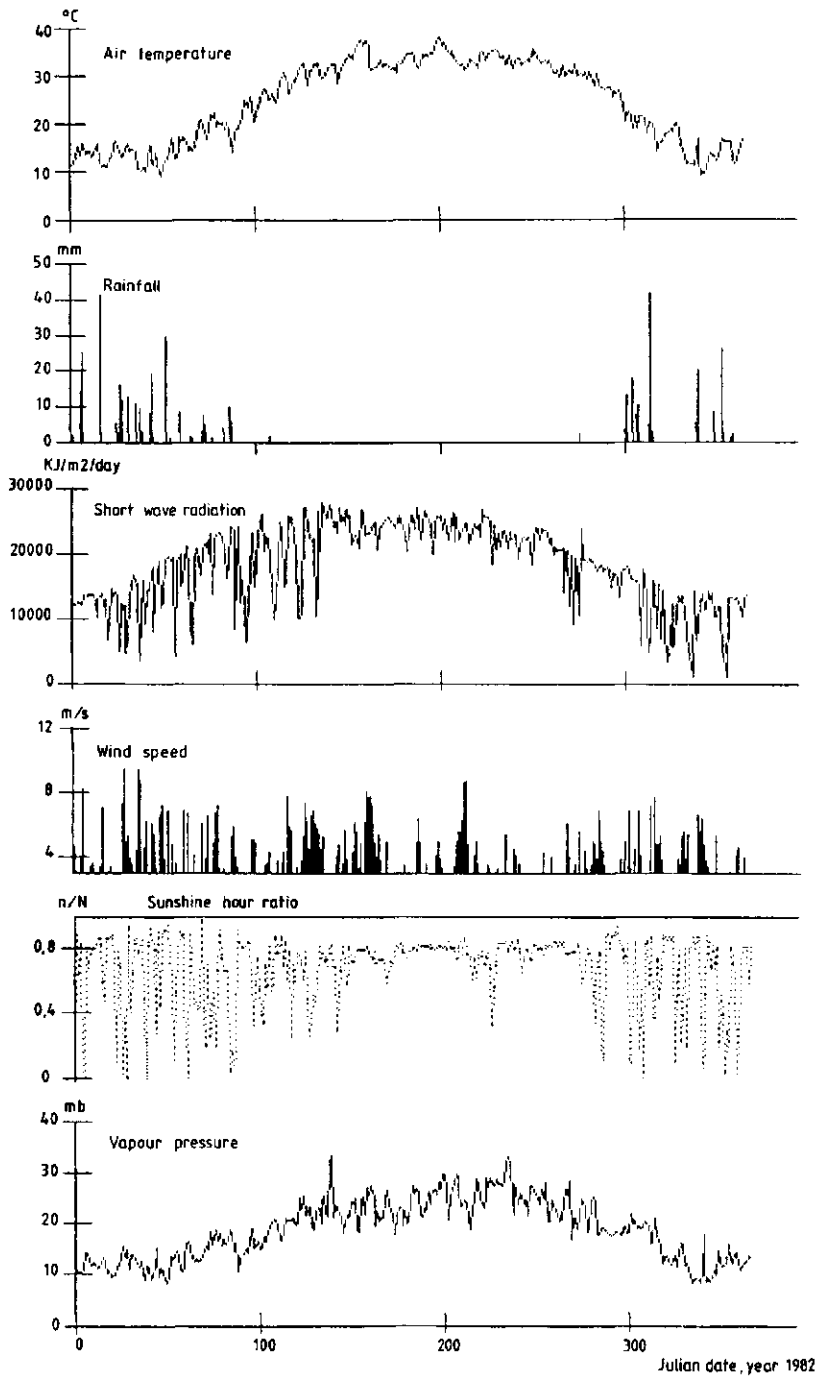


Fig. 5.9 Location and geometry of the Jarreh Reservoir, Southern Iran.

The seasonal course of various inputs into the reservoir over the simulation period (1982) is shown in Fig. 5.10. The rainfall and river discharge are strongly seasonal. Peaks of flow coincide with peak sediment load but have an inverse relationship with salinity. The salinity of the inflow becomes as high as 3500 ppm during the summer period. At the present situation, the salinity of total input to the reservoir is hardly influenced by human activities (Chap. 2). Wind speeds in Fig. 5.10 have been shown only if greater than 3 m/s for the sake of clarity, but the model uses all the data.

Daily inflow data, i.e. discharge, salinity and temperature are gauged at the Jarreh Station on Shapur river. The daily meteorological data were obtained from the nearby stations, Shabankareh and Bushehr Station (see Fig. 1.6). It should be noted that 1982 is the wettest year (annual discharge $1120 \times 10^6 \text{ m}^3$) in a 15 years record. Irrigation demands are, of course, projected values.



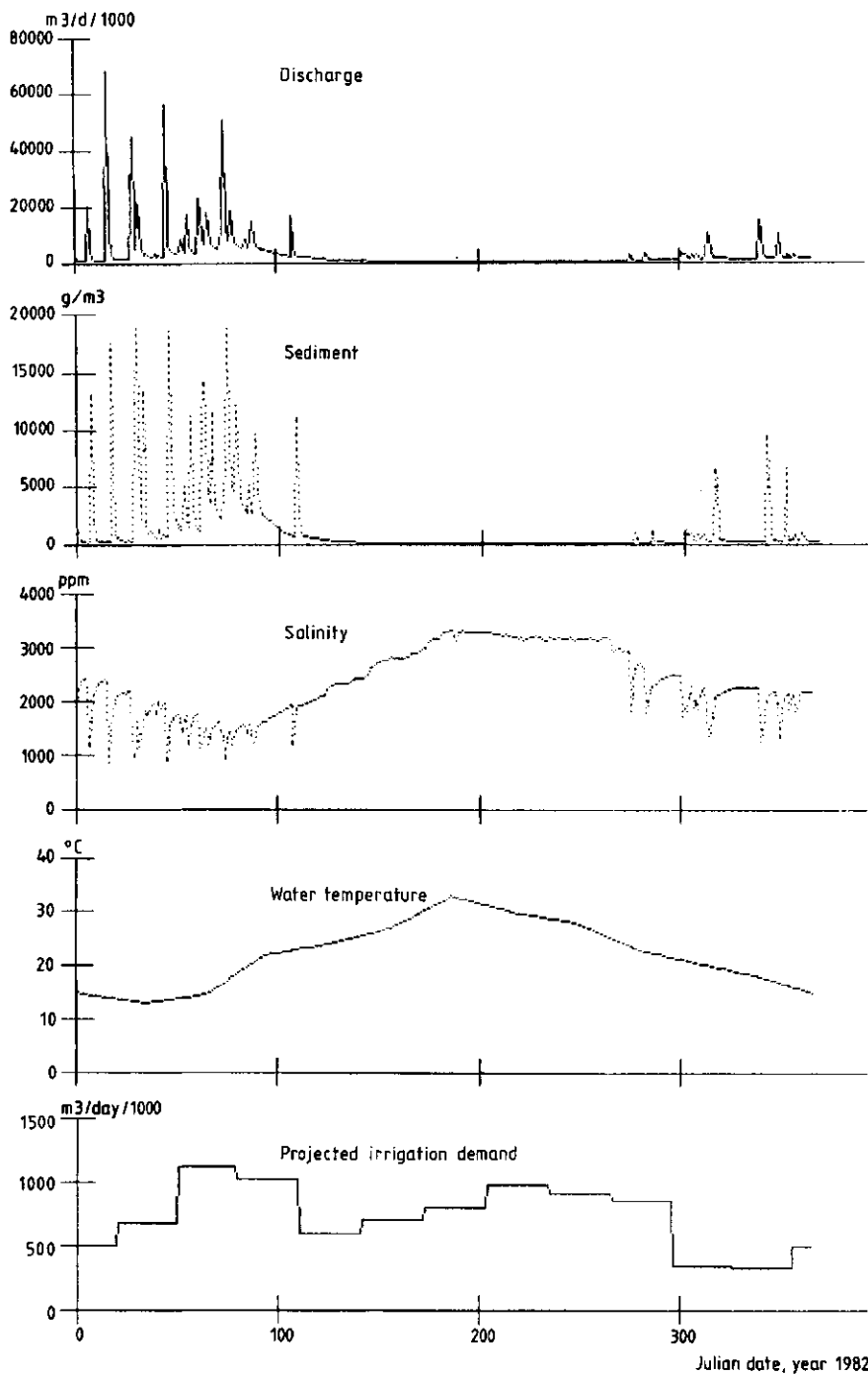


Fig. 5.10 Inflow, meteorological and irrigation demand input data; Shapur R. (Jarreh Station).

5.2.5 Simulation results

DYRESM was run for data of the year 1982 with and without sediment effect. In these simulations the irrigation water is supposed to be withdrawn from the midlevel outlet, located 52 m above the base of the dam. We show the results of these simulations in several forms. Figure 5.11 gives the simulated profiles of temperature, salinity and density for days which represent different seasons. In Fig. 5.12 the predicted iso-halines at the bottom part of the reservoir are shown.

In the following we will give a physical explanation for the behaviour of the presented results.

Simulation without sediment effect

Simulation begins with day 82001 (1st January 1982), with an almost homogeneous initial condition ($T \approx 18$ °C, salinity ≈ 1850 ppm). From previous runs of the model, these values appeared to show annual periodicity. Until day 82027, the inflowing water is saltier and colder than the water in the reservoir, thus, it is more dense. From day 82027 onwards until day 82080, the inflow is less salty than the water in the reservoir, but because it is also colder its density is still higher. The dense winter inflow (January-March) lodges in deeper layers in the reservoir, causing a change in the temperature and salinity of these layers. As a result, the temperature and salinity in the deeper layers of the reservoir reduce between day 82027 to 82080 from 17.8 to 14.4 °C and from 1950 to 1650 ppm, respectively. Because the top layers remain more or less unchanged during this period a weak stratification with density between 999.6-1000.4 kg m⁻³ develops (Fig. 5.11 a-b, day 82080).

Summer stratification builds up until autumn due to warming up of the surface water. A thermocline forms, protecting waters below from exchange with the upper layers. During this period the inflow enters at the level of the thermocline because sharp density gradients occur there. Since the inflows are salty a relatively thin brackish water layer, with a salinity of up to 2050 ppm is formed (Fig. 5.11a, days 82120 and 82220) at the thermocline.

In late July the reservoir is strongly stratified, with temperatures ranging from 14.5 to 35 °C, salinity from 1470 to 1950 ppm, and density from 995.3 to 1000.4 kg m⁻³ (Figs. 5.11a-b, day 82220).

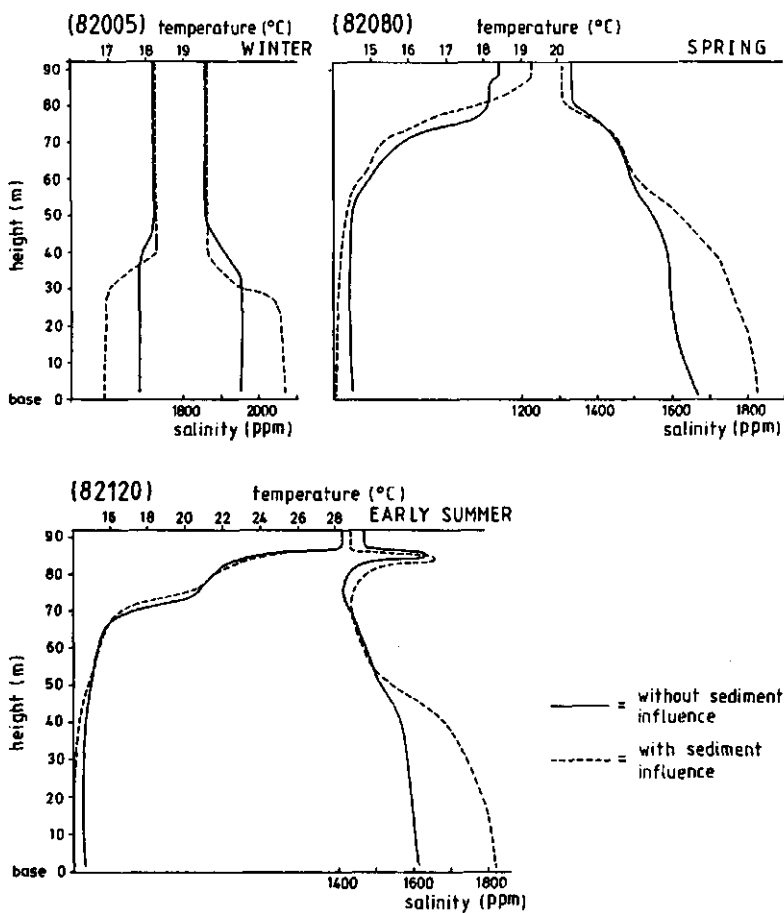
In late autumn the stability of stratification decreases due to the drop in temperature of the surface water. During this period the inflows become also colder and because the adjustment of the temperature in river water to those in the atmosphere goes faster than in the large reservoir, the river water becomes more dense than the reservoir again and intrudes in deeper water layers. The surface wind mixes the surface layers and finally an "overtturn" occurs at the end of autumn (on day 82340) and the reservoir becomes homogeneous again over the top depth of 80 m (Fig. 5.11 a-b, day 82350).

The results show that the temperature regime of the reservoir is determined by the inflows, and by surface heating and cooling. The bottom temperature of the reservoir for most of the year is determined by the temperature of the coldest inflows (14 °C), whereas the surface temperature

is determined by the meteorological forcing. On the other hand, the salinity regime of the reservoir is mainly determined by the vertical density structure in the reservoir and by the inflows.

Simulation including sediment effect

When the effect of sediment is introduced, the density of the inflowing water is notably increased so that the inflow penetrates more rapidly to the bottom layers. Once this dense water reaches the bottom layers, it tends to stay there longer than in case of lighter water. In this way the differences in temperature and salinity of successive water layers will increase. In other words, the presence of sediment intensifies the gradients. This results into more salty and colder bottom water layers, an effect which persists throughout the year (Fig. 5.11a and 5.11b).



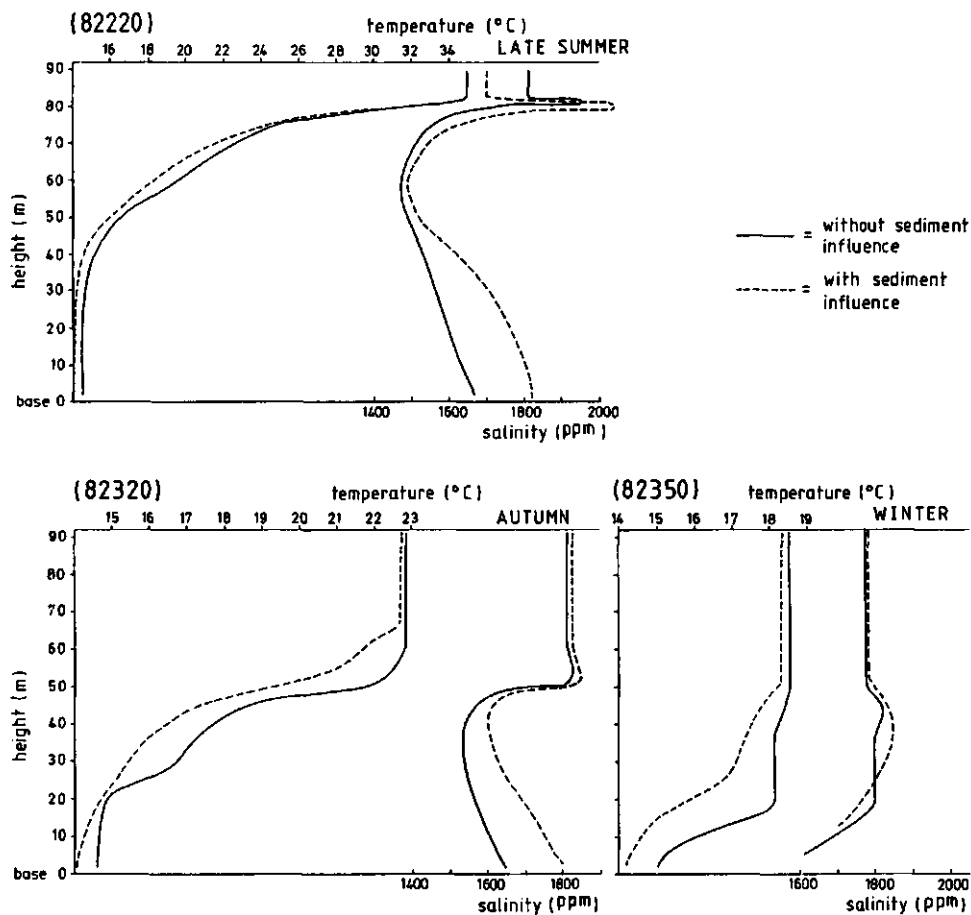


Fig. 5.11(a) Simulated temperature ($^{\circ}\text{C}$) and salinity profiles (ppm) in the Jarreh Reservoir for the year 1982.

Similar results were found by Marjonavic and Orlob (1987) who studied the effect of salinity on thermal stratification.

During the dry season (spring-mid autumn), the effect of sediment is negligible due to small amount of sediment in the inflowing water. In this period the inflow inserts almost at the same level for both simulations.

From late autumn the inflows become sediment-laden and colder and lodge to deeper water layers. The overturn takes place around day 82340 but due to the more intense gradients in temperature and salinity at the hypolimnion, the reservoir becomes homogeneous over the upper 50 m only.

The effect of sediment on the simulated temperature, salinity and density distribution is clearly shown in Figs. 5.11 and 5.12, and is described below.

Temperature

As can be seen from Fig. 5.11(a), when the effect of sediment is taken into account, the bottom water layers are colder than when the sediment effect is neglected. The data show a decrease in temperature of the bottom water layers between 0.5 and 2.5 °C, due to sediment influence.

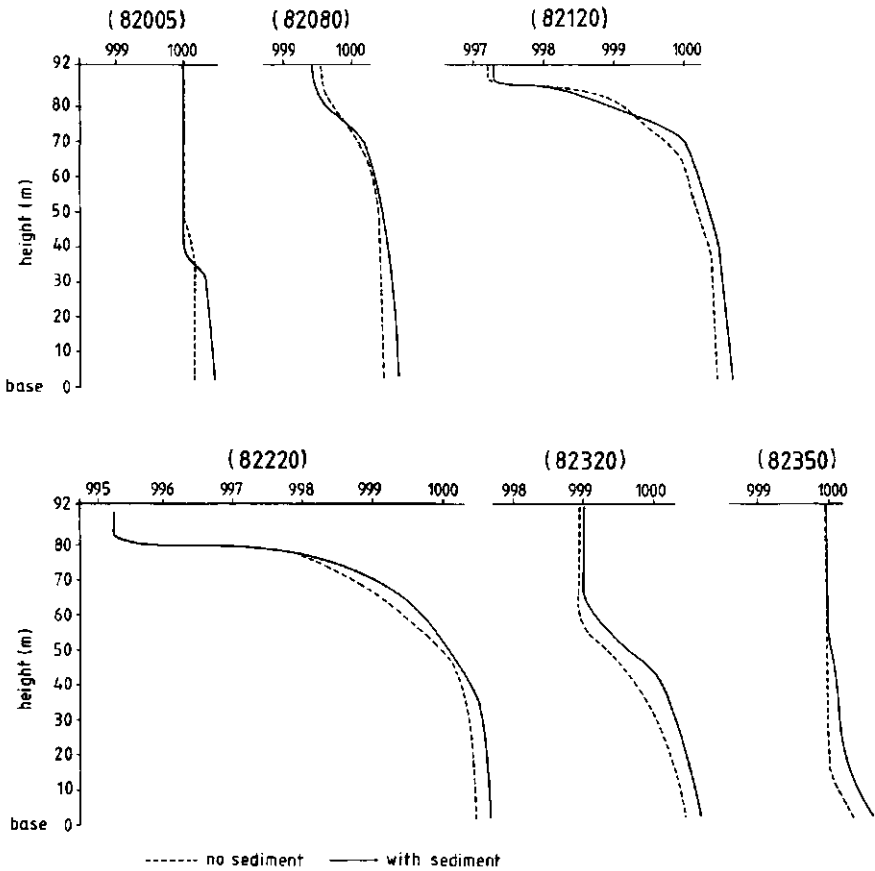


Fig. 5.11(b) Simulated density profiles (kg/m^3) in the Jarreh Reservoir for the year 1982.

Salinity

From Figs. 5.11a and 5.12, it is clear that bottom water layers become more salty due to the sediment effect. The difference in simulated salinity between both cases persists throughout the year and reaches up to about 200 ppm. The salinity at the lower part of Jarreh Reservoir shows the following pattern over the year (Fig. 5.12):

A salty inflow in January (2200–2500 ppm) increases the initial salinity

(1850 ppm) in the deeper layers upto 2000 ppm. The inflow in February and March is less saline (it goes down to 1400 ppm) causing a decrease in salinity in this region. At the end of winter (day 82090) the salinity ranges from 1600 to 1800 ppm. During spring and summer and early autumn these values remain unchanged since the sharp thermocline will protect the deeper layers from salty inflows. In late autumn and winter the salty inflows can lodge again into the deeper part and cause an increase in the salinity up to 1900 ppm (day 82350). At that time the upper 50 meters become mixed.

Density

The vertical density structure will be influenced by the change in vertical temperature and salinity structures. Therefore, a cold and salty water in the bottom region results in an increase in density and thus an intensified stratification. The difference in simulated density between the "with and without sediment" cases reaches up to 0.3 kg m^{-3} in the region below the thermocline. In January, November and December, stratification is weak and cold salty and sediment-laden inflows can lodge into the deeper part of the reservoir and remain there during the rest of the year. With sediment, the enhanced stability will restrict the turnover in winter to the upper 50 meters; below that depth the stagnation persists.

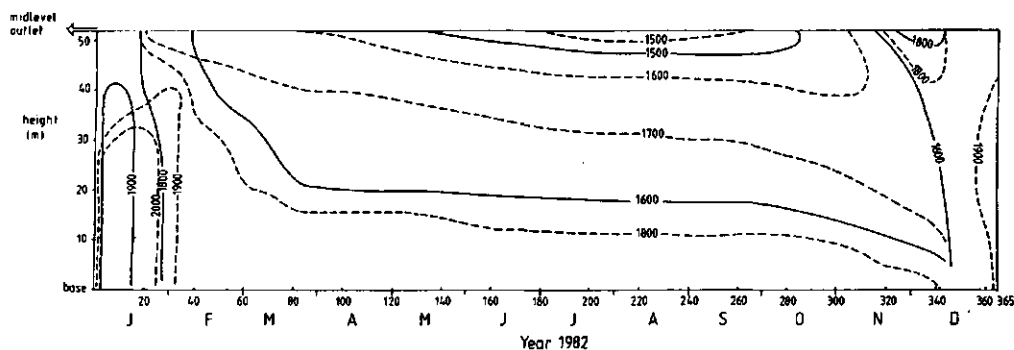


Fig. 5.12 salinity distribution at the lower part of Jarreh R. without (————) and with (-----) sediment effect.

5.2.6 Effect on output salinity

The withdrawal salinity is mainly affected by the stratification in the reservoir. Density stratification inhibits vertical motions within the reservoir, since any water particle displaced vertically into the heavier fluid below or the lighter fluid above will experience a restoring force, which will eventually return it to its original level. As a result of these buoyancy effects, withdrawal water from a stratified reservoir comes from a horizontal layer centered at the level of the outlet. The process is known as selective withdrawal and has been reviewed by Imberger (1980). In case of the absence of stratification, the withdrawal water flows radially towards the outlet, from all directions equally. The present version of

DYRESM uses a selective withdrawal algorithm developed by Hocking et al. (1988).

Jarreh Reservoir can supply irrigation water from two fixed level outlets: midlevel outlet (height 52 m) and bottom level outlet (height 23 m). The average salinity of supplied water as calculated by DYRESM at the bottom and midlevel outlets for both simulations is shown in Fig. 5.13. It can be seen that the salinity of the withdrawal water can increase up to 150 ppm when the effect of sediment is introduced. The effect is more pronounced in the bottom outlet water in winter, because the withdrawal water in that case comes from deeper layers in which salinity is more sediment affected. The difference in salinity of the withdrawal water at the midlevel outlet between both cases is small since this outlet withdraws water from midlevel layers which are less affected by sediment effects.

As noted before, the simulation year 1982 was abnormally wet, and consequently the inflowing water carried relatively large amounts of sediment particles. In order to examine a larger time span, a four years series of daily input data (1982-1985) is run. This data set also includes the driest year on record (1984, annual discharge 289×10^6 m³) which occurred just two years after the wettest year. The results of these simulations are presented as withdrawal salinity at the bottom outlet (Fig. 5.14), and as salt balance of the reservoir (Table 5.3). For the four-year simulation period an increase in supply salinity when the effect of sediment is taken into account can be observed. Nevertheless, the difference in the withdrawal salinity hardly exceeds 150 ppm. The dry year 1984 shows the most striking features. In this period the withdrawal salinity deteriorates to a range 2150 to 2400 ppm in comparison to 1500 to 2000 ppm in the wet year 1982 (Fig. 5.14).

An increase in withdrawal salinity up to 150 ppm is still not significant for its use in irrigation, but somehow it influences the salt balance in the reservoir. Table 5.2 shows the salt balance in the Jarreh Reservoir for the simulation year 1982. It shows that when the effect of sediment is taken into account, an extra amount of 3.1×10^6 kg salt is withdrawn with the irrigation water from the bottom outlet. This means that the amount of salt stored in the reservoir at the end of the year will be overestimated (up to 3×10^6 kg) if sediment effect is not taken into account. For the period 1982 to 1985 (Table 5.3), the withdrawn irrigation water contains an extra amount of 9×10^6 kg of salt. At the same period, less salt (about 6×10^6 kg) has been withdrawn with spilled water. As the result, at the end of simulation, the amount of salt stored in the reservoir decreased by 3×10^6 kg when sediment effect is taken into account. Apparently, this value is negligible when compared with the total salt content of the reservoir (Table 5.3).

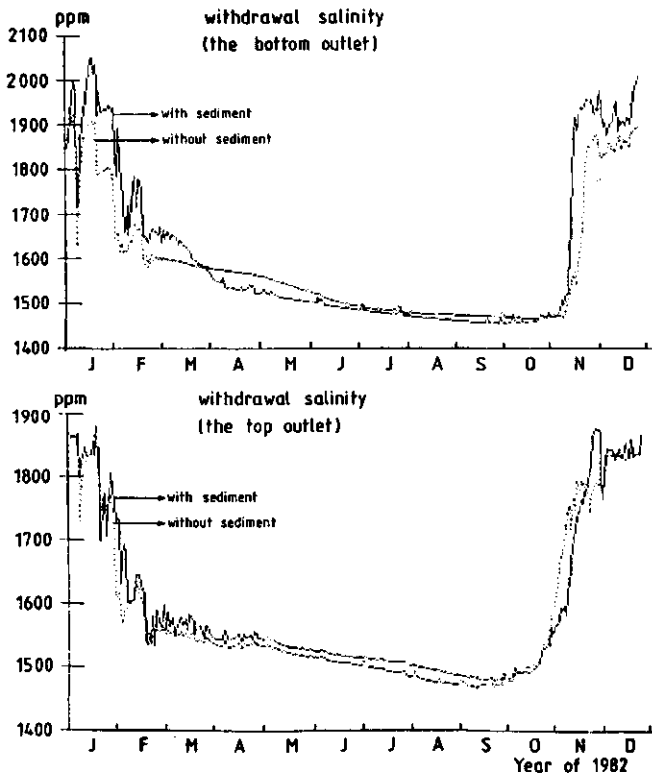


Fig. 5.13 Simulated salinity at the outlets with and without sediment effect.

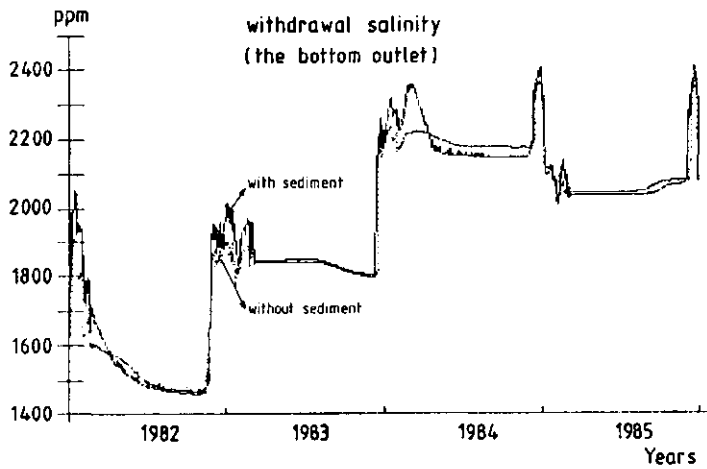


Fig. 5.14 Withdrawal salinity (ppm) at the bottom outlet, simulation period 1982-1985.

Table 5.2 Water and salt balance for Jarreh reservoir in 1982
(withdrawal from bottom outlet)

	Water (10 ⁶ m ³)	salt concentration (ppm)	salt load (10 ⁶ kg)
Reservoir on day 0	450 (450)	1850 (1850)	832 (832)
Inflow	1128 (1128)		1693 (1693)
Spill over spillways	816 (816)		1244 (1243)
Irrigation demand	268 (268)		419 (423)
Evaporation exceed	24 (24)		
Reservoir on day 365	470 (470)	1832 (1827)	862 (859)

Figures in bracketts are with sediment effect.

Table 5.3 Water and salt balance for Jarreh Reservoir in 1982-1985
(withdrawal from bottom outlet)

	water (10 ⁶ m ³)	salt concentration (ppm)	salt load (10 ⁶ kg)
Reservoir on day 0	450 (450)	1850 (1850)	832 (832)
Inflow	2284 (2284)		4000 (4000)
Spillage	1127 (1127)		1829 (1823)
Irrigation demand	1073 (1073)		2061 (2070)
Evaporation exceed	102 (102)		
Reservoir on day 1461	432 (432)	2180 (2173)	942 (939)

Figures in bracketts are with sediment effect.

5.2.7 Validation of one-dimensional assumption

The assumption of one-dimensionality in spatial variation of parameters is usually made in a stratified reservoir. As a result of stratification, vertical motions are inhibited, longitudinal and transverse variations play a secondary role, and the variation over the vertical become the most important contribution to the first-order balances of mass, momentum, and energy.

Therefore, in applying a one-dimensional model, DYRESM, to Jarreh Reservoir one needs to verify whether the conditions for that reservoir are indeed one-dimensional in the sense outlined. The constraints imposed by such a one-dimensional model may best be quantified by defining a series of non dimensional numbers (Orlob, 1983; Patterson et al., 1984). The numbers are based on degree of stratification, basin geometry, surface wind stress, and rates of inflow and outflow:

Wedderburn number (W)

This number compares the hydrostatic pressure gradient force with the friction force in the momentum equation applied to the homogeneous mixed upper layer in the reservoir

$$W = \left(\frac{g'h}{u_*^2} \right) \left(\frac{h}{L} \right) \quad (5.17)$$

where g' is the effective reduced gravity across the thermocline [LT^{-2}], h depth of thermocline [L], L the reservoir length scale [L], and u_* the surface shear velocity [LT^{-1}]. Spigel and Imberger (1980) have shown that for $W > 0(1)$ the departure from one-dimensionality is minimal, that for $0 < (h/L) < W < 0(1)$ the departure is severe but may be successfully parametrized, and for $W < 0(h/L)$ the slope in the thermocline is dictated primarily by wind stress at the water surface and the thermocline can locally reach the bottom or the water surface.

Densimetric (internal) Froude number (F_r)

This number compares the momentum force, represented by an average flow-through velocity, with the internal gravitational force tending to maintain stability:

$$F_r = \frac{U}{\left(\frac{\Delta \rho}{\rho_0} g d \right)^{\frac{1}{2}}} \quad (5.18)$$

where $U=Q/bd$ is the average flow-through velocity [LT^{-1}], Q the river discharge [L^3T^{-1}], d the average depth [L], b the width of the reservoir [L], $\Delta \rho$ is the density difference over depth [ML^{-3}], ρ_0 is the reference density [ML^{-3}], and g is the acceleration due to gravity [LT^{-2}]. If the length and volume of the impoundment are introduced as characteristic parameters, (5.18) becomes

$$F_r = \left(\frac{L}{d}\right) \left(\frac{Q}{V}\right) \left[\frac{\rho_o d}{\Delta\rho g}\right]^{\frac{1}{2}} \quad (5.19)$$

where L is the length [L], and V=Lbd is the volume [L³].

The following criterion is suggested by Water Resources Engineers, Inc. (1969): well-stratified impoundments for which one-dimensional models are best suited are those for which $F_r \ll 1/\pi$; and fully mixed systems are defined by $F_r > 1$. Patterson et al. (1984) suggested to use the value of the internal Froude number for inflow (F_I) and outflow (F_O) as a criterion for one-dimensionality. One-dimensionality is accepted if:

$$F_I = \frac{u}{(g'H)^{\frac{1}{2}}} < 1 \quad (5.20)$$

where u is inflow velocity [LT⁻¹], g' is the reduced gravity between the surface reservoir water and the inflow [LT⁻²], and H is the depth at the reservoir entrance. And in addition if:

$$F_O = \frac{Q}{(g'^{\frac{1}{2}} H^{\frac{5}{2}})} < 1 \quad (5.21)$$

where Q is the outflow discharge [LT⁻³] and g' the reduced gravity between the surface and bottom water and H the reservoir depth.

Ratio of the internal Rossby radius of deformation and reservoir width (R)

This number compares the internal gravitational force with the Coriolis force.

$$R = \frac{(gh)^{\frac{1}{2}}}{fB} \quad (5.22)$$

where g' is the effective reduced gravity over depth h [LT⁻²], h the depth of interface [L], f the Coriolis frequency [T⁻¹], and B is the maximum width of reservoir [L]. $R > 1$ is the criterion for the absence of rotational effects and therefore of the absence of a slope of the interface due to earth rotation.

We now examine the validity of the assumption of one-dimensionality by calculating the values of W, R, F_r , and F_O using the simulation density profiles as shown in Fig. 5.11(b). The computations were performed for days 82005, 82080, 82120, 82220, 82320, and 82350 and are considered as typical for various times of the year. The results are presented in Table 5.4.

Table 5.4 Values of the criteria for one-dimensionality in Jarreh Reservoir

Criteria	----- days of 1982 -----					
	82005	82080	82120	82220	82320	82350
Wedderburn No. (W)	0.88	10.07	260.98	217.91	39.60	10.97
Internal Froude No. (F _r)	0.0025	0.0095	0.0011	0.00016	0.0018	0.0059
(F ₀)	0.0017	0.0015	0.0004	0.00062	0.0004	0.0007
Ratio of Rossby No. and width (R)	0.87	2.0	5.38	7.57	1.98	1.11

The computed values of W for Jarreh Reservoir give a value of $W > 10$ for most of the period. Only during the starting days of simulation (82005), when the stratification was extremely weak, the value of W is smaller than one, but still much greater than the depth/length ratio of the reservoir. Thus the reservoir satisfies the one-dimensionality criterion in this respect.

The computed values of R vary between 0.87-7.57 throughout the simulation year and clearly satisfy the criterion for most of the period. The exception is again for the starting days when the reservoir is almost homogeneous.

The values of F_r, F₀ as presented in Table 5.4 indicate that the reservoir is strongly stratified for most of the period. This analysis leads to the conclusion that the Jarreh Reservoir meets all theoretical constraints of one-dimensionality.

5.2.8 Conclusions

Results of this study lead to the general conclusion that the sediment load of the inflowing water influences the density stratification by intensifying the gradients of salinity and temperature of the lower water layers. As a result the presence of sediment in the inflow leads to colder and more salty deep water layers in the reservoir. For the simulation year 1982 the salinity of the lower water layers increases up to 200 ppm, temperature lowers with 0.5-2.5 °C, and density increases up to 0.3 kg m⁻³.

The sediment effect on withdrawal water salinity - an increase up to 150 ppm at the bottom outlet - is hardly significant for its use in irrigation. However, the total salt content of the reservoir is affected by the change in salinity distribution due to the inflowing sediment.

The influence of sediment has been considered by taking into account its effect on density in the inflow after entry, dilution with the

reservoir water, and intrusion into the reservoir water body. After the flow arrives at the dam wall, the flow will stop and the suspended sediment will settle on the reservoir bottom. The vertical and horizontal propagation of sediment has not been modelled in this approach. This confines the application of the model to dissolved substances only. For water quality variables which depend on (bio)chemical reactions with substances attached to suspended particles, one has to consider the turbidity distribution in the reservoir as well.

Inflow is only one of many significant processes that affect the water quality structures in reservoirs. Therefore, in order to verify the new inflow algorithm a short sequence of data in which the inflow is the dominant process is needed. The present work described the behaviour of a turbid underflow with negligible deposition and entrainment. Further research should incorporate the spatial and temporal distribution of suspended particles as well. Further investigations should also include experiments in both laboratory and field, and especially the latter.

ACKNOWLEDGEMENT

The author wishes to thank Ir. J.H.G. Verhagen for his contribution to this research. The author also wishes to thank Dr. J.C. Patterson, Director of Center for Limnological Modelling, Center for Water Research (CWR), The University of Western Australia for providing DYRESM and for also useful comments on this work. The help of drs. P.J.J.F. Torfs in modification of the model is acknowledged.

REFERENCES

- Akiyama, J., and Stefan, H., 1984. Plunging flow into a reservoir: theory. *Journal of Hydraulic Engineering*, 110:484-499.
- Akiyama, J., and Stefan, H., 1985. Turbidity current with erosion and deposition. *Journal of Hydraulic Engineering*, 111:1473-1496.
- Akiyama, J., and Stefan, H., 1987. Gravity currents in lakes, reservoirs and Coastal Regions: Two-layer stratified flow analysis. Project Report No. 253, St. Anthony Falls Hydraulic Laboratory, Univ. of Minnesota, Minneapolis, Min.
- Ashida, K., and Egashira, S., 1977. Basic study on turbidity currents. *Proc. Japan Soc. of Civ. Eng.*, 237:35-50.
- Fischer, H.B., List, E.J., Koh, R.C., Imberger, J., and Brooks, N.H., 1979. *Mixing in inland and coastal water*. Academic Press, 483 pp.
- Gaume, A.M., and Duke, Jr., J.H., 1975. Computer program documentation for the reservoir ecological model EPAECO. Report to US Environmental Protection Agency, Washington, DC by Water Resources Engineers, Inc.
- Graf, W.H., 1983a. The hydraulics of reservoir sedimentation. *Water Power and Dam Construction*, 35:45-52.

Graf, W.H., 1983b. The behaviour of silt-laden current. *Water Power and Dam Construction*, 35:33-38.

Hebbert, B., Imberger, J., Loh, I., and Patterson, J.C., 1979. Collei River underflow into the Wellington Reservoir. *J. Hydraul. Div. Am. Soc. Civ. Eng.*, 105:533-546.

Hocking, G.C., Sherman, B.S., and Patterson, J.C., 1988. Algorithm for selective withdrawal from stratified reservoir. *Journal of Hydraulic Engineering*, 114:706-719.

Huber, W.C., Harleman, D.R., and Ryan, P.J., 1972. Temperature prediction in stratified reservoirs. *J. Hydraul. Div. Am. Soc. Civ. Eng.*, 98:645-666.

Imberger, J., Thompson, R., and Fandry, C., 1976. Selective withdrawal from a finite rectangular tank. *J. Fluid Mech.*, 78:389-512.

Imberger, J., Patterson, J.C., Hebbert, R.H.B., and Loh, I., 1978. Dynamics of reservoir of medium size. *J. Hydraul. Div., ASCE*, 104:725-743.

Imberger, J., 1980. Selective withdrawal: a review. *Proc. 2d Int. Symp. Stratified Flows, Int. Assoc. Hydr. Res.*, 1, Trondheim, Noeway, 381-400.

Imberger, J., and Patterson, J.C., 1981. A dynamic reservoir simulation model-DYRESM 5. In: H.B. Fischer ed., *Transport Models for Inland and Coastal Waters*, Academic Press, Inc., New York, pp. 310-361.

Imberger, J., 1984. Reservoir dynamics modelling. Prediction in water quality. E.M.O Loughlin, and P. Cullen, eds., *Australian Acad. of Sci.*, Canberra, Australia, pp. 223-248.

Marjonavic, N., and Orlob, G.T., 1987. Effect of density stratification on water quality. In: Graf, W.H., and Lemmin, U., eds., *Lake and Reservoir Hydraulics, Proc.*, xxii Congress International Association for Hydraulic Research, IAHR, Lausanne, pp. 179-186.

Patterson, J.C., Imberger, J., Hebbert, R.H.B., and Loh, I., 1978. *User Guide to DYRESM*. Report No. EFM-3, University of Western Australia, Australia.

Patterson, J.C., Hamblin, P.F., and Imberger, J., 1984. Classification and dynamic simulation of the vertical density structure of lakes. *Limnol. Oceanogr.*, 29:845-861.

Parker, G., Garcia, M., Fukushima, Y., and Yu, W., 1987. Experiments on turbidity current over an erodible bed. *Journal Of Hydraulic Research*, 25:123-147.

Raudkivi, A.J., 1979. *Hydrology: an advanced introduction to hydrological processes and modelling*. Pergamon Press, U. K.

Shiati, K., 1990. An estimator for the density of a sediment-induced stratified fluid. *Earth Surface Processes and Landforms*, 15:365-368.

Spigel, R.H., and Imberger, J., 1980. The classification of mixed-layer dynamics in lakes of small to medium size. *J. Phys. Oceanogr.*, 10:1104-

1121.

Orlob, G.T. (ed), 1983. Mathematical modelling of water quality: stream, lakes, and reservoir. John Wiley & Sons, N. Y.

Water Resources Engineers, Inc., 1969. Mathematical models for prediction of thermal energy changes in impoundments. US Environmental Protection Agency Water Pollution Control Research Series 16130 EXT, Contract 14-22-422. US Government Printing Office, Washington, DC, 157 pp.

Van Pagee, J.A., Groot, S., Klomp, R., and Verhagen, J.H.G., 1982. Some ecological consequences of a projected deep reservoir in the Kabalebo river in Suriname. Hydrobiological Bulletin, 16:241-254.

6 MANAGEMENT OF A SALT-AFFECTED RESERVOIR

6.1 INTRODUCTION

In several arid and semi-arid countries, the main water resources for regional development are from reservoirs constructed on brackish sediment-laden rivers. Such salinity is caused by different processes, as described in Chap. 2, and results in a rise in salinity of the water stored. The presence of saline inflows requires a careful management of such reservoirs.

The models for a stratified reservoir, as described in the foregoing sections, can be used to predict the effects of various measures to be taken. Such simulation studies have been used to find appropriate strategies for the future Jarreh Reservoir in Southern Iran. This storage dam with a capacity of 470 Mm³ on the brackish Shapur river will be constructed to irrigate 13000 ha of a coastal plain. The catchment of Shapur river is suffering from salinity caused by natural processes (Chap. 2). Due to this, approximately 1.2*10⁶ tons of salt are brought into the reservoir in an average year. The river discharge and salinity of the Shapur river at the damsite (Jarreh Station) are shown for the period 1975-1990 in Fig. 6.1. It shows that the salinity (TDS) of the river is strongly influenced by both long term and seasonal variations in stream flow. For example, the high annual inflows of 1982 (discharge 1127 Mm³, 2.12 times the median) averaged 1500 mg/l TDS whereas the inflows of 1984, a dry year (discharge 280 Mm³, 0.54 times the median) averaged 2180 mg/l in salinity. On a seasonal basis, the flood flows (winter period) are generally less saline. Low flows (summer period), however, are in part due to groundwater flows and remain highly saline. For the recorded period the salinity of the inflowing water varies between 750-4200 ppm.

The high variability of both the discharge and the salinity of the Shapur river have compounded the problem. In wet years when the river flows are high, the average salinity of inflow is low and the reservoir is flushed out so that the quality of the impounded water improves. On the other hand, a dry year causes a considerable deterioration of quality, and especially a series of consecutive dry years will deteriorate the quality considerably.

In reservoirs, the temporal variation of salt content as shown in Fig. 6.1 is partially alleviated, and the water quality is mainly controlled by stratification phenomena and retention time (Chap. 5). It is the aim of this study to show how appropriate management strategies can improve the quality of the water to be withdrawn and at the same time minimize the risk of a salinity build-up in the reservoir. Such strategies might be developed by studying the interaction between inflow characteristics, withdrawal policy and stratification in the reservoir.

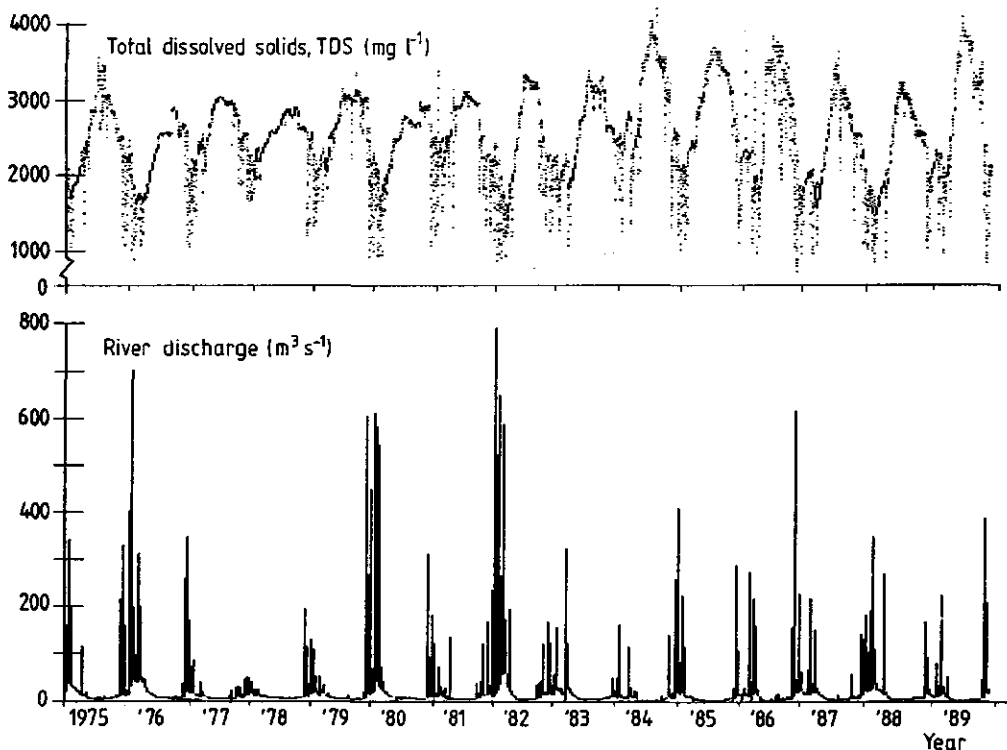


Fig. 6.1 Distribution of river discharge and salinity of the Shapur river at Jarreh Station.

It should be noted that any improvement in the salinity by means of reservoir management will be beneficial, especially during the dry years. As described in Chapter 3, most of the salinity control schemes for reducing salt entrance into the river, upstream of the Jarreh Reservoir were technically and economically unfeasible.

DYRESM is used to investigate the response of the Jarreh Reservoir to various management strategies. Furthermore, it is used to simulate the salt build-up in the reservoir over a long time span. For the former purpose, a five-year period (1982-1986) of daily inflow and meteorological data and for the latter a fifteen-year period (1975-1990) of daily inflow data and an average year of meteorological data (1986) are used.

6.2 STRATEGIES AND MEASURES

Among the factors which influence the reservoir stratification (meteorological, inflow and outflow) only inflows and outflows can be controlled. As a result, only those management options are investigated that are based on the manipulation of both inflow and outflow. Inflow manipulation is achieved by diverting the most saline river inflows (summer inflows) before they reach the body of the reservoir ("by-pass policy"). Outflow manipulation includes release of excess water (subject to safe yield constraints) from the most saline part of the reservoir at appropriate outlets and appropriate times ("scouring policy").

Different strategies of course depend on the management objective; solely to improve the offtake salinity, and/or to improve the average salinity in the reservoir. The objective for Jarreh Reservoir is primarily to maintain the status quo or, if possible, minimize the salinity build-up in the reservoir. The quality of the irrigation supply is not a primary objective because on one hand any improvement in supply salinity is not going to be significant and on the other hand it will be of little importance for the moderately salt tolerant crops that are already being cultivated in the study area.

A general conclusion on the aspects of reservoir management cannot be given; every reservoir of this kind will require its specific management. For example, the results of adopted options for the Jarreh Reservoir show some similarities but also differences with Wellington Reservoir, W. Australia (Patterson et al., 1978; Fischer et al., 1979; Imberger, 1981).

6.3 DETERMINATION OF EXCESS WATER FOR BY-PASSING OR SCOURING

The amount of water that can be diverted or released should be consistent with the demand, inflow and the storage volume. Long-term simulation may lead to the development of operation rules to minimize the amount of spillage and maximize the available water for scouring or diversion (e.g. Loh and Hewer, 1977; Yeh, 1985; He, 1987). Long-term simulation might also lead to improved water quality at the expense of supply quantity.

It should be noted that the simulation techniques used to derive reservoir operating rules should include quality criteria. At present little work has been done to include water quality in the optimization procedure. Instead the state of reservoir system is simply described in terms of a single variable, water volume. The above-mentioned problem i.e. how to couple an optimization algorithm with a simulation model to assess the water quality and account for multiple objectives, are the core of a research is currently undertaken for the Jarreh Reservoir, Iran (Bogardi, 1990).

At present in the Jarreh Reservoir, for the period 1982/1986, different values for diversion or scouring are examined, using a simulation program, RELEAS (Shiati and Torfs, 1990). A schematic description of RELEAS is shown in Fig. 6.2 and Flowchart 2.

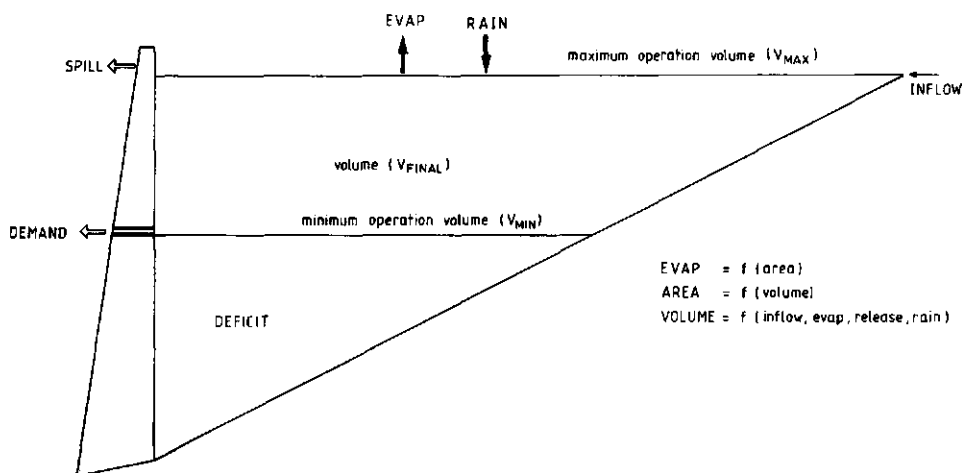


Fig. 6.2 Schematic description of RELEAS.

Various strategies were investigated with this model, to wit:

- DIVERSION I to IV: bypassing of summer flows with high salinity to a point downstream of the last irrigation intakes.

DIVERSION I: diversion of flows with salinity of 3600 ppm TDS and over;

DIVERSION II: same, with cutoff level 3400 ppm;

DIVERSION III: same, with cutoff level 3200 ppm;

DIVERSION IV: same, with cutoff level 3000 ppm.

- SCOUR I to IV: selective withdrawal of water from the reservoir.

SCOUR I: in summer, through midlevel outlet at height 52 m;

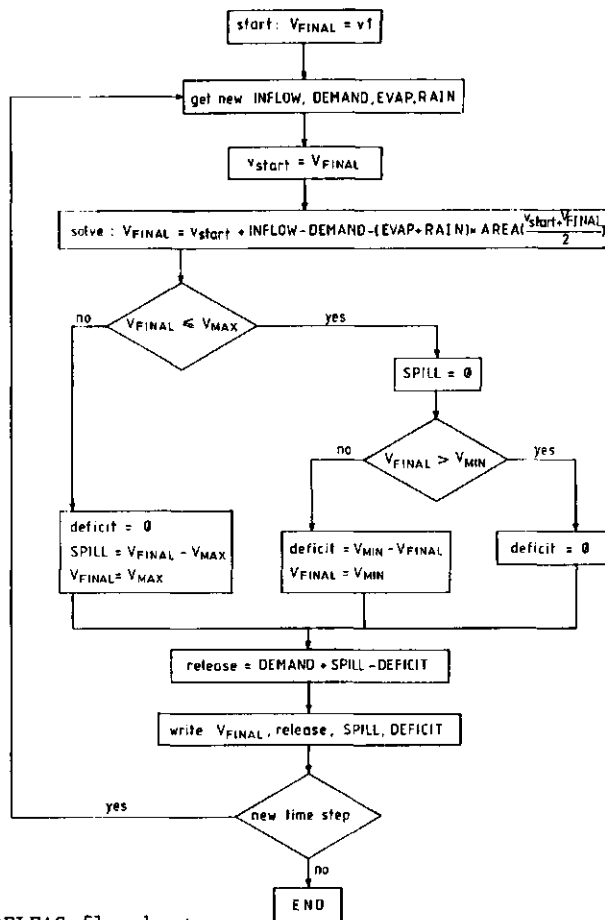
SCOUR II: in summer, through midlevel outlet at height 67 m;

SCOUR IIa: in late summer to early autumn, at height 67 m;

SCOUR III: in summer, through top outlet at height 78 m;

SCOUR IV: combination of SCOUR IIa and DIVERSION IV.

For the amounts and times of diversion and scouring see Table 1.



Flowchart 2. RELEAS flowchart.

6.4 THE EFFECT OF BY-PASSING POLICY

The simulated reservoir volume corresponding to diverting all inflows with a salinity greater than 3000, 3200, 3400, and 3600 ppm is shown in Fig. 6.3, Diversion I-IV. As can be observed, for the simulated period (1982/1986) an amount of 158 Mm³ (corresponding with cutoff salinity 3000 ppm) can be diverted without adversely affecting the reliability of supply. The corresponding volumes to be diverted, the period of diversion and the simulation results for some specific days of the simulation period are shown in Table 6.1. Fig. 6.4 shows the salt content of the reservoir (kg) and the salinity (TDS) of the withdraw water, respectively. These results show that a diversion policy will have a major effect on the salinity of the withdraw water as well as on the overall salinity of the reservoir. When a cutoff salinity of 3000 mg/l is examined (diversion IV) the average salinity of the reservoir on day 84295 is reduced by 7.3% (equivalent to 172 mg/l TDS) and the salinity of released water by 4.6% (equivalent to 100 mg/l TDS). The maximum reduction in supplied salinity (18 %) occurs on day

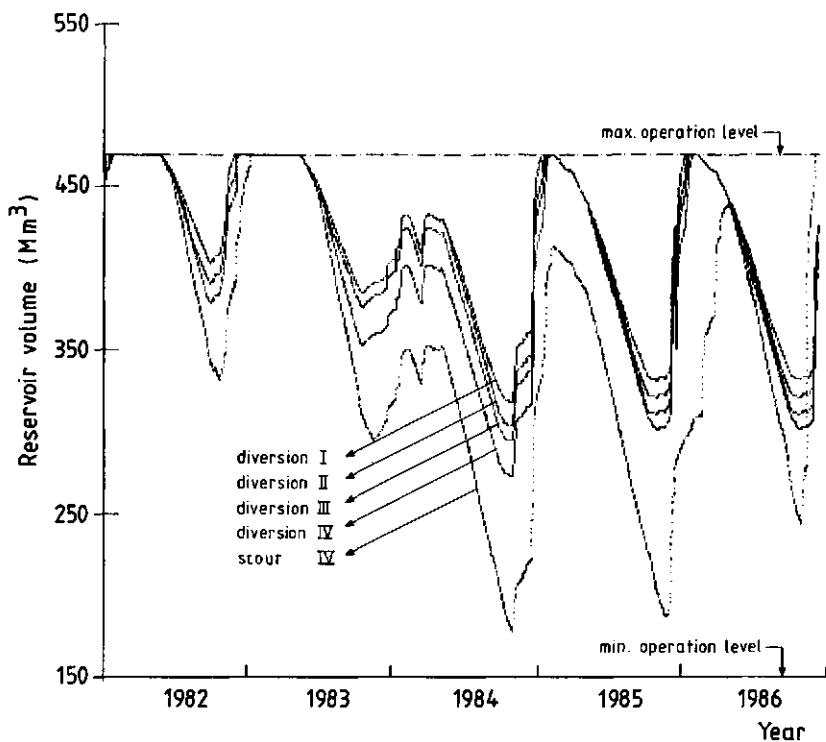


Fig. 6.3. Simulated Jarreh Reservoir volume corresponding to different diversion volumes.

85354, with also 8.7% reduction in average salinity of the reservoir equivalent to 387 and 198 mg/l TDS, respectively. At the end of this simulation the total salt accumulation in the reservoir is reduced by $72 \cdot 10^3$ tons which is 8.5% improvement on the "no policy" results. The price paid for this reduction in salinity is a diversion of $158 \cdot 10^6$ m³ of the river flow during the periods shown in Table 1.

This management policy has a pronounced effect on the salinity distribution in the reservoir (Fig. 6.5). As can be observed from this figure, at the end of simulation the reservoir still is stratified due to temperature gradients, but only a weak salinity gradient remains.

Implementing such a policy does not require elaborate engineering constructions. Of course, the choice of a cutoff salinity 3000 ppm requires larger diversion structures. A preliminary plan for diverting three cubic meters per second of the salty summer inflows (corresponding with cutoff salinity 3000 ppm) includes:

- 1) A submerged intake structure with two slide gates to be operated through a walkway slab. The diversion site is located 22 km upstream of the Jarreh dam site, at an elevation greater than the maximum water level of the reservoir.

2) The saline water is then conveyed to the river at a place downstream of the reservoir command area through two high-pressure plastic pipelines ($\phi=1000$ mm). The length of the pipeline system which conveys saline water to the downstream part of the existing Saad-Abad diversion dam will be about 56 km (Fig. 1.6). The friction slope of the pipes is assumed to be 0.3% and the flow will be regulated by two jet valves at the outlet and will be released to the river after passing an energy dissipator. The system will be operative during 2-4 months in the summer period.

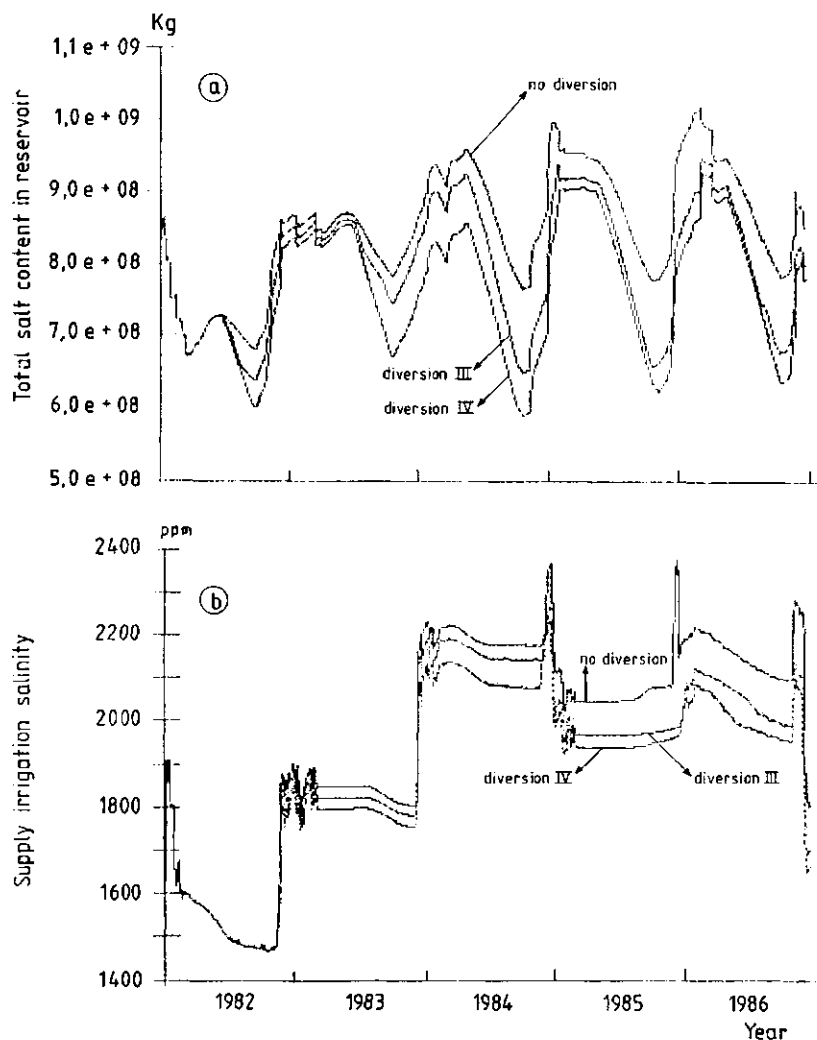


Fig. 6.4. Simulated results of diversion policy; (a) total salt content of reservoir (kg), (b) supply irrigation salinity (ppm).

Table 6.1 Effects of management policies in the Jarreh Reservoir, Southern Iran

Policy	Diversion/Scouring Period	Diversion Volume 10 ⁶ m ³	Scouring Rate m ³ /d/1000	(82001)		(82275)		(83295)		(84295)		(85354)		(86365)							
				S.S. PPM	R.S.C. 10 ⁶ kg	A.R.S. PPM	S.S. PPM	R.S.C. 10 ⁶ kg	A.R.S. PPM	S.S. PPM	R.S.C. 10 ⁶ kg	A.R.S. PPM	S.S. PPM	R.S.C. 10 ⁶ kg	A.R.S. PPM	S.S. PPM	R.S.C. 10 ⁶ kg	A.R.S. PPM			
No Policy	-	-	-	1864	842	1859	1470	683	1768	1810	781	2093	2176	765	2381	2349	867	2273	1804	850	1808
Diverison I	84177-235	7.9	-	-	-	-	-	-	-	-	-	-	-	-	-	-	-	-	-	-	-
	85184-231	7.7	-	-	-	-	-	-	-	-	-	-	-	-	-	-	-	-	-	-	-
	86185-190	0.8	-	-	-	-	-	-	-	-	-	-	-	-	-	-	-	-	-	-	-
	86204-218	2.1	-	-	-	-	-	-	-	-	-	-	-	-	-	-	-	-	-	-	-
Diverison II	84147-283	22.8	-	-	-	-	-	-	-	-	-	-	-	-	-	-	-	-	-	-	-
	85163-265	18.8	-	-	-	-	-	-	-	-	-	-	-	-	-	-	-	-	-	-	-
	86149-190	2.3	-	-	-	-	-	-	-	-	-	-	-	-	-	-	-	-	-	-	-
	86185-236	6.1	-	-	-	-	-	-	-	-	-	-	-	-	-	-	-	-	-	-	-
Diverison III	82181-231	12.9	-	-	-	-	-	-	-	-	-	-	-	-	-	-	-	-	-	-	-
	83184-210	5.5	-	-	-	-	-	-	-	-	-	-	-	-	-	-	-	-	-	-	-
	83266-281	4.0	-	-	-	-	-	-	-	-	-	-	-	-	-	-	-	-	-	-	-
	84139-283	28.9	-	-	-	-	-	-	-	-	-	-	-	-	-	-	-	-	-	-	-
	85149-294	29.1	-	-	-	-	-	-	-	-	-	-	-	-	-	-	-	-	-	-	-
	86142-276	28.7	-	-	-	-	-	-	-	-	-	-	-	-	-	-	-	-	-	-	-
Diverison IV	82173-245	24.9	-	-	-	-	-	-	-	-	-	-	-	-	-	-	-	-	-	-	-
	83181-220	32.3	-	-	-	-	-	-	-	-	-	-	-	-	-	-	-	-	-	-	-
	84139-283	24.9	-	-	-	-	-	-	-	-	-	-	-	-	-	-	-	-	-	-	-
	85137-315	39.4	-	-	-	-	-	-	-	-	-	-	-	-	-	-	-	-	-	-	-
	86142-294	37.3	-	-	-	-	-	-	-	-	-	-	-	-	-	-	-	-	-	-	-
		-	-	-	-	-	-	-	-	-	-	-	-	-	-	-	-	-	-	-	-
Scour I	82230-320	-	277	1864	842	1859	1471	664	1778	1817	760	2108	2193	685	2416	2362	782	2270	1763	851	1768
	83260-350	-	359	-	-	-	-	-	-	-	-	-	-	-	-	-	-	-	-	-	-
	84270-340	-	277	-	-	-	-	-	-	-	-	-	-	-	-	-	-	-	-	-	-
	85270-360	-	438	-	-	-	-	-	-	-	-	-	-	-	-	-	-	-	-	-	-
	86250-340	-	414	-	-	-	-	-	-	-	-	-	-	-	-	-	-	-	-	-	-
Scour II	82230-320	-	277	1864	842	1859	1459	662	1773	1796	757	2100	2177	679	2398	2034	774	2249	1758	828	1762
	83260-350	-	359	-	-	-	-	-	-	-	-	-	-	-	-	-	-	-	-	-	-
	84270-360	-	277	-	-	-	-	-	-	-	-	-	-	-	-	-	-	-	-	-	-
	85220-360	-	438	-	-	-	-	-	-	-	-	-	-	-	-	-	-	-	-	-	-
	86250-340	-	414	-	-	-	-	-	-	-	-	-	-	-	-	-	-	-	-	-	-
		-	-	-	-	-	-	-	-	-	-	-	-	-	-	-	-	-	-	-	-
Scour III	82275-320	-	554	1864	842	1859	1460	680	1764	1812	780	2090	2160	672	2389	2033	763	2237	1751	824	1753
	83300-345	-	718	-	-	-	-	-	-	-	-	-	-	-	-	-	-	-	-	-	-
	84280-325	-	555	-	-	-	-	-	-	-	-	-	-	-	-	-	-	-	-	-	-
	85300-345	-	878	-	-	-	-	-	-	-	-	-	-	-	-	-	-	-	-	-	-
	86290-335	-	829	-	-	-	-	-	-	-	-	-	-	-	-	-	-	-	-	-	-
Scour IV	82180-270	-	273	1864	842	1859	1477	638	1765	1824	711	2063	2145	636	2308	2068	765	2195	1720	824	1724
	83200-290	-	349	-	-	-	-	-	-	-	-	-	-	-	-	-	-	-	-	-	-
	84170-280	-	277	-	-	-	-	-	-	-	-	-	-	-	-	-	-	-	-	-	-
	85200-300	-	384	-	-	-	-	-	-	-	-	-	-	-	-	-	-	-	-	-	-
	86200-300	-	373	-	-	-	-	-	-	-	-	-	-	-	-	-	-	-	-	-	-
Scour V	24.9	554	1864	842	1859	1537	601	1728	1829	661	2036	2129	502	2290	2220	557	2095	1579	733	1560	
	32.3	718	-	-	-	-	-	-	-	-	-	-	-	-	-	-	-	-	-	-	-
	24.9	555	-	-	-	-	-	-	-	-	-	-	-	-	-	-	-	-	-	-	-
	39.4	878	-	-	-	-	-	-	-	-	-	-	-	-	-	-	-	-	-	-	-
	37.3	829	-	-	-	-	-	-	-	-	-	-	-	-	-	-	-	-	-	-	-

1) S.S. = Supply Salinity R.S.L. = Reservoir Salt Content A.R.S. = Average Reservoir Salinity
 2) In brackets are percentage improvements

6.5 THE EFFECT OF SCOURING POLICY

Apart from diversion, advantage can be taken of strong summer stratification in Jarreh Reservoir. In summer, a thin layer of warm and brackish water will form at the top, above the level of the thermocline (Chap. 5). This brackish water layer persists up to late autumn, when a turnover occurs and the water in the reservoir will be mixed. The development of this strong stratification may be used to our advantage by selective withdrawal of this layer. In this respect, much will depend on the flexibility of offtake level selection.

Based on the stratification and a strategy of selective withdrawal, some of the most saline part of the reservoir water can be removed in summer (scoured) before internal mixing distributes it over the remainder of the storage.

A number of options are examined. Furthermore, the policy is tested for the effects of the timing of the scour and the level at which withdrawal take place.

The simulation results are also summarized in Table 6.1. The results are also compared with the simulation results of "no policy" option and the percentage of improvement is cited. For all type of policies tested, the irrigation water is supplied from the bottom outlet (height 32 m) and an amount of $153 \times 10^6 \text{ m}^3$ of water (the same amount as diversion IV) is scoured.

The first class of policies tested, SCOUR I and SCOUR II, is to remove the top brackish water layer during mid summer up to mid autumn in 90 days, before the occurrence of turnover in the reservoir. In SCOUR I, scour takes place from the midlevel outlet at height 52 m, as was envisaged in the feasibility design of the Jarreh dam. However, the final design of the dam fixed the midlevel outlet at a height of 67 m above the base of the dam. SCOUR II simulates scouring at this level. SCOUR IIa shows the effect of the timing of the operation: it was delayed to 45 days after all salt wedges have been fully inserted and after the depth of the brackish layer has deepened with the cooling at the surface and by the increasing wind effect.

The second class of policies tested, SCOUR III, involves the removal of the most saline wedges at the top (about 78 m from the base, see Fig. 6.5), before they participate in mixing. SCOUR IV examines the combined effect of diverting the inflows with salinity greater than 3000 ppm (Diversion IV) and SCOUR IIa. In this case a quantity of $316 \times 10^6 \text{ m}^3$ is removed, which leads to intolerably low reservoir levels (Fig. 6.3, SCOUR IV).

The effectiveness of the scouring policy is shown in Fig. 6.6, where the salinity of the scoured water is illustrated. It is evident that this salinity is consistently less than the salinity of the diverted water, indicating that the policy is not as effective as diversion. The maximum salinity of the scoured water is 2540 mg/l compared with 4000 mg/l of diverted flows.

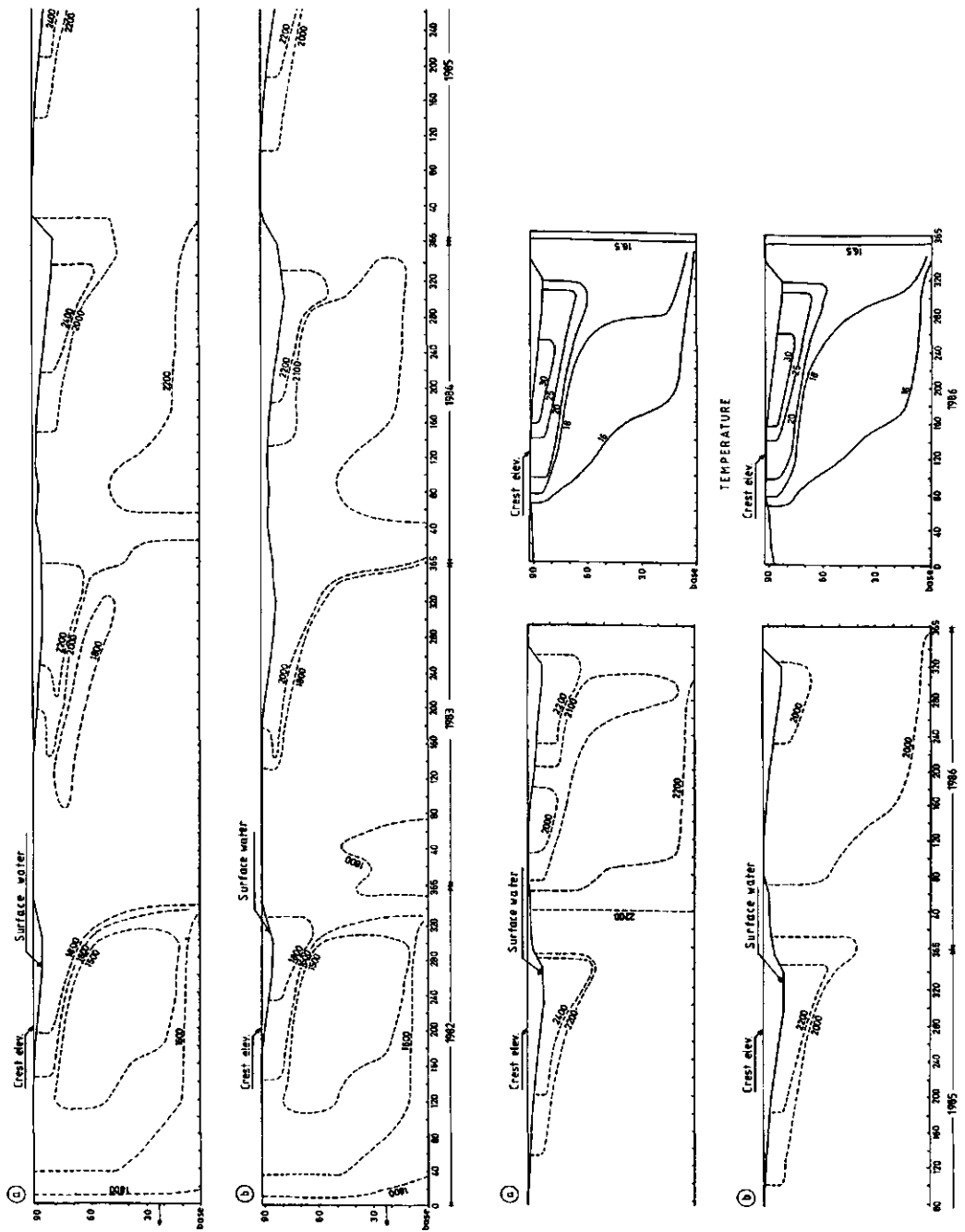
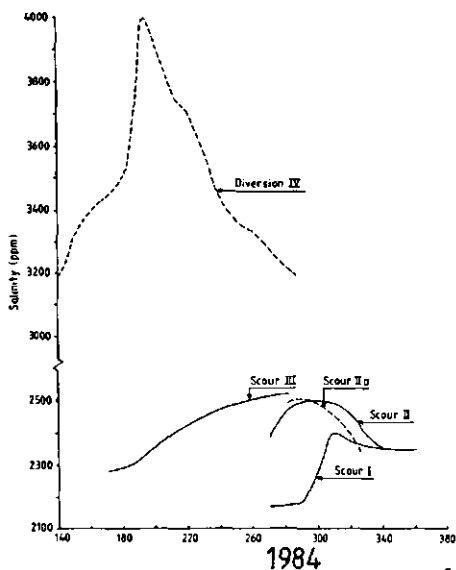
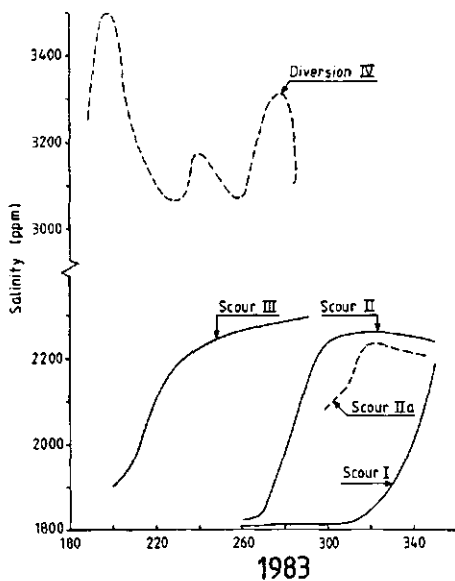
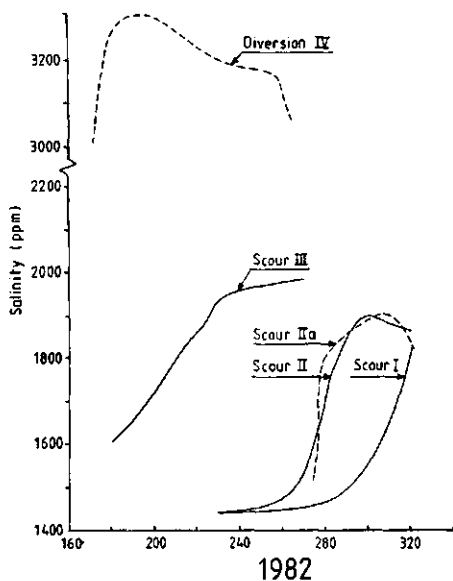


Fig. 6.5 Salinity distribution in Jarreh R. (1982-1986); (a) without diversion policy, (b) with diversion policy "3000" (Division IV).

The results of SCOUR I and to a lesser extent SCOUR II indicated that scouring water from the level of 52 m and 67 m respectively is ineffective, since water was taken from the fresher regions for most part of the period. In both policies scouring took place at outlet levels which are too low in view of the depth at which the highest salinity concentrations occur. SCOUR IIa indicated that it is desirable to delay the scour until the bulk of the high salty summer inflows had been transported to deeper levels in the reservoir during late summer and autumn. More benefit is gained by SCOUR III, which allows removal of summer inflows at a high outlet level prior to their mixing with the surrounding water. As the result of this policy, the



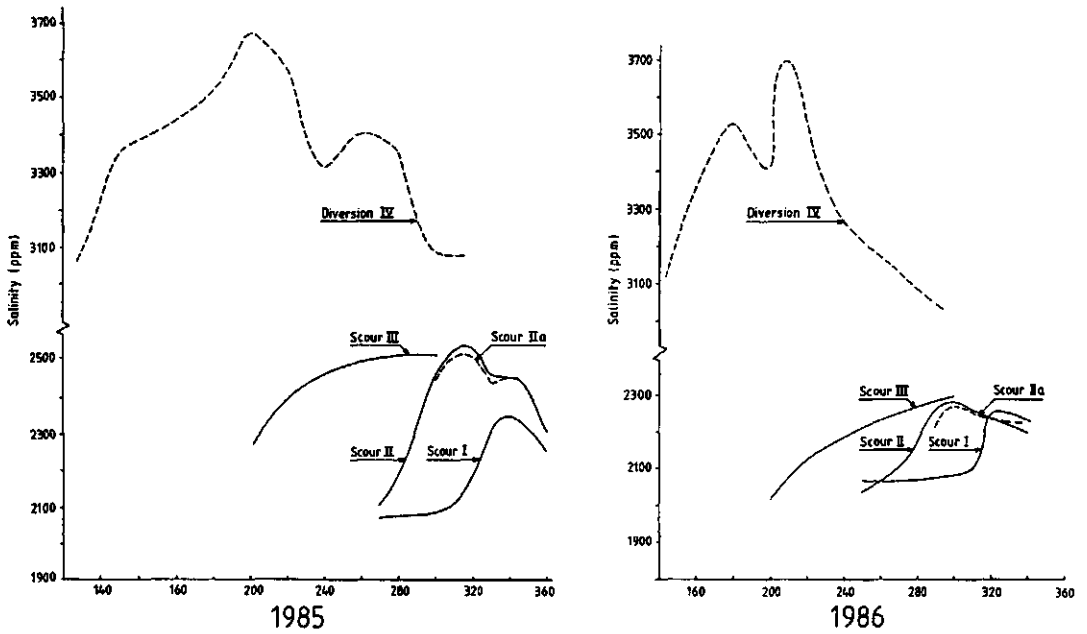


Fig. 6.6 Scouring policy, the salinity of released water.

average salinity of the reservoir at the end of simulation decreases by up to 4.6 % (equivalent to $26 \cdot 10^3$ tons of salt). The maximum improvement on supply salinity 4.6% (equivalent to 85 mg l^{-1} TDS) is gained on day 86365. When a combination of by-passing and scouring policies is tested, SCOUR IV, the salt accumulation in the reservoir is reduced considerably (Table 1). As a result, at the end of simulation (day 86365) the salinity of the reservoir is reduced by 13.7% (equivalent to 248 mg/l TDS), supply salinity by 12.4% (equivalent to 225 mg l^{-1} TDS), and salt accumulation by $117 \cdot 10^3$ tons. However, the large withdrawal in SCOUR IV causes too low reservoir levels.

Although the control of the yearly salinity build-up in the reservoir by SCOUR III and/or SCOUR IV is more effective, their implementation requires the construction of a selective withdrawal outlet structure. A multi-level offtake structure allows the management options to be practised more effectively and more sophisticated options can be employed (e.g. removal of the most saline water for scouring and simultaneous offtake of less saline water for irrigation supply).

6.6 SALINITY TREND IN THE RESERVOIR

It is important to study the behaviour of a salt-affected reservoir on a long-term basis. For this purpose, a salt balance calculation of the reservoir is necessary.

- the water balance in reservoir reads:

$$Q_i = Q_u + B + dV/dt \quad (6.1)$$

- the salt balance in reservoir reads:

$$Q_i C_i = Q_u C_u + dZ/dt \quad (6.2)$$

where

- Q_i = inflow (m^3/s)
- Q_u = outflow (m^3/s)
- B = evaporative excess (m^3/s)
- V = volume of water in reservoir (m^3)
- C = salt concentration in the reservoir (kg/m^3)
- C_i = salt concentration of inflow (kg/m^3)
- C_u = salt concentration of outflow (kg/m^3)
- Z = salt stored in reservoir (kg)
- t = time (s)

For a completely mixed reservoir ($C=C_u$), an analytical solution can be obtained from eqs. (6.1) and (6.2) (see van der Molen, 1980, eq. 8):

$$C = \frac{Q_i C_i}{Q_i - B} + [C_0 - \frac{Q_i C_i}{Q_i - B}] \cdot \left[\frac{V_0}{V_0 + (Q_i - B - Q_u) t} \right]^{\frac{Q_i - B}{Q_i - B - Q_u}} \quad (6.3)$$

However, for a stratified reservoir eq. (6.3) cannot be applied because of $C \neq C_u$. For such a case a numerical solution is often used. In this study a module is added to DYRESM to calculate the total mass content, salt content and average salinity of reservoir as well as outlets water at each daily time step. The following scheme is employed.

$$\text{Total water mass} = \sum_1^{NS} (V_i * \rho_i) \quad (6.4)$$

$$\text{Total salt content} = \sum_1^{NS} (S_i * V_i * \rho_i) \quad (6.5)$$

$$\text{Average salinity} = \frac{\sum_1^{NS} (S_i * V_i * \rho_i)}{\sum_1^{NS} (V_i * \rho_i)} \quad (6.6)$$

where

- V_i = volume of the i-layer (m^3)
- ρ_i = density of the i-layer (kg/m^3)
- S_i = salinity of the i-layer (ppm), and $i = 1, NS$

Another source of salt input is by diffusion from the salty Miocene formation forming the reservoir bottom. The amount of salt input by this

process has been calculated for Jarreh Reservoir; it is presented in Appendix 4. It appears that salt (diffusive) flux is negligible after the first few years.

The salinity trend in the Jarreh Reservoir is obtained by using the 15-year daily inflow data. Daily meteorological data are available only for five years (1982-1986) and not for the whole period of 15 years of inflow data. Therefore, the meteorological data of an average year (1986) are used as being representative for the simulation period. The reason for this standardization is: for the study area, apart from rainfall the variation in meteorological data (sunshine hr, temperature, short wave radiation, vapour pressure) from year to year is usually not very distinctive when compared with inflow data (Fig. 6.7). Moreover, results of a simulation using all the meteorological data available (5 years of 1982-86) show little (and negligible) difference with using data of the representative year of 1986 (Fig. 6.8), indicating the primary role of inflow in determining the reservoir salinity.

The results of the 15-year simulation are shown as total salt content and average salinity of the reservoir, Fig. 6.9, and water and salt balance at the end of the simulation period, Table 6.2. It is evident from Figs. 6.9 and 6.1 that the salt content of the reservoir is primarily determined by the annual variability of inflow. The high and fresh flows of the wet years 1975-76, 1979-80 and 1987-88 flushed out the reservoir and reduced the salt content to its lowest level of about 7.5×10^8 kg and the average salinity to 1550 ppm TDS. On the other hand, the low and saline flows of the dry years 1977-78, 1978-79 and 1983-1984 increased the salt content of the reservoir up to about 1.1×10^9 kg and an average salinity to 2600 ppm.

Under certain conditions, $Q_1 = B$ and $Q_u = 0$ (all incoming water evaporates, no outflow, and reservoir volume remains constant) the salt concentration in a lake or reservoir rises until precipitation of salt occurs (salt lakes, soda lakes and borax lakes of arid regions). Apparently, these conditions do not exist for the Jarreh Reservoir because of $Q_1 \gg B$ and salt mainly is being removed by the outlet water (see Table 6.2). As can be observed, at the end of the 15-year simulation (day 89365), from the total salt input of 1.48×10^{10} kg, only 55×10^6 kg of salt accumulated in reservoir and the rest are removed by the spill and irrigation waters. As can be observed from Fig. 6.9 the reservoir salinity on the simulation period varies in a range between 1500-2600 ppm.

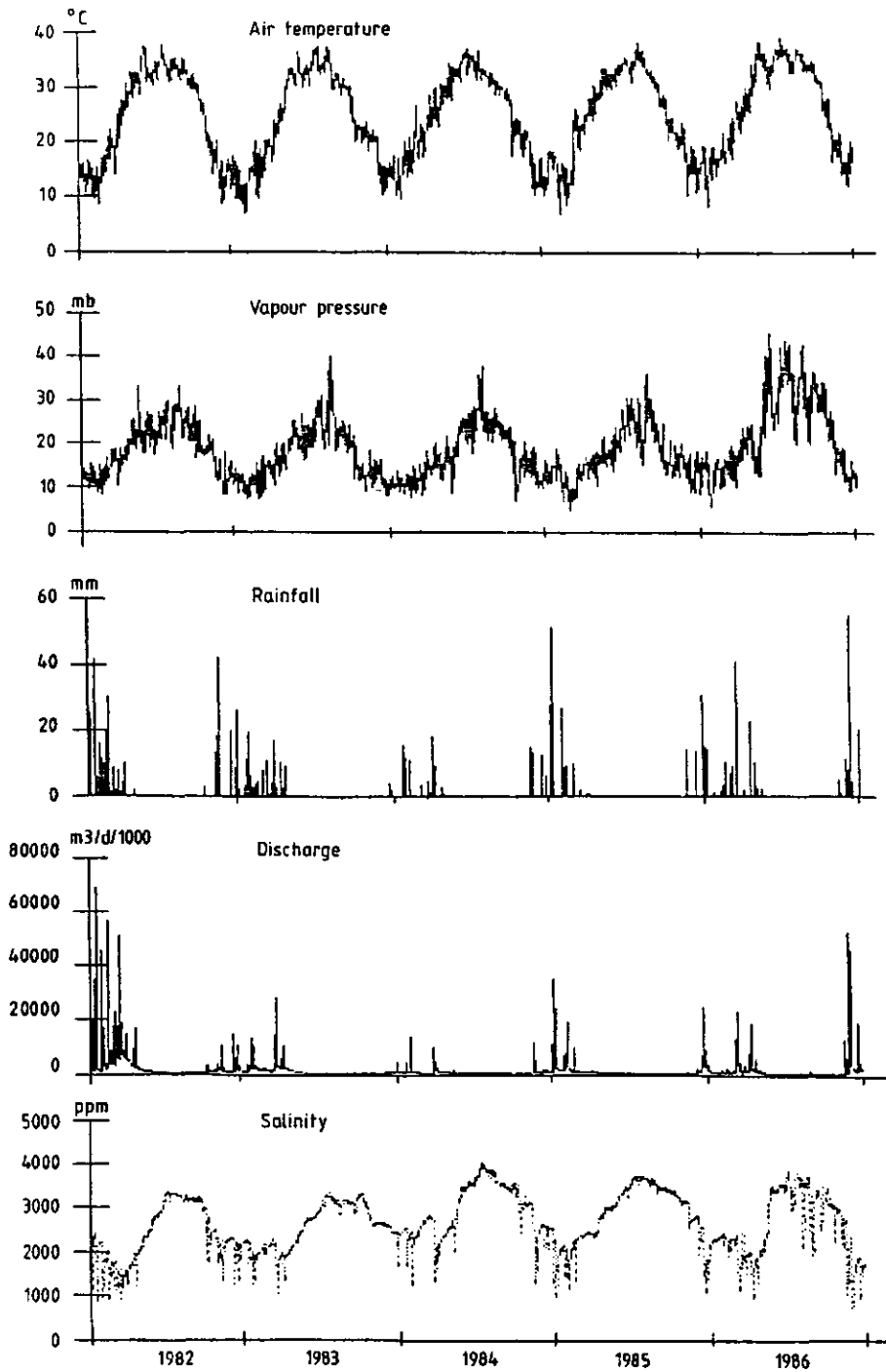


Fig. 6.7 Variation in meteorological and inflow data (1982-1986), Jarreh Station.

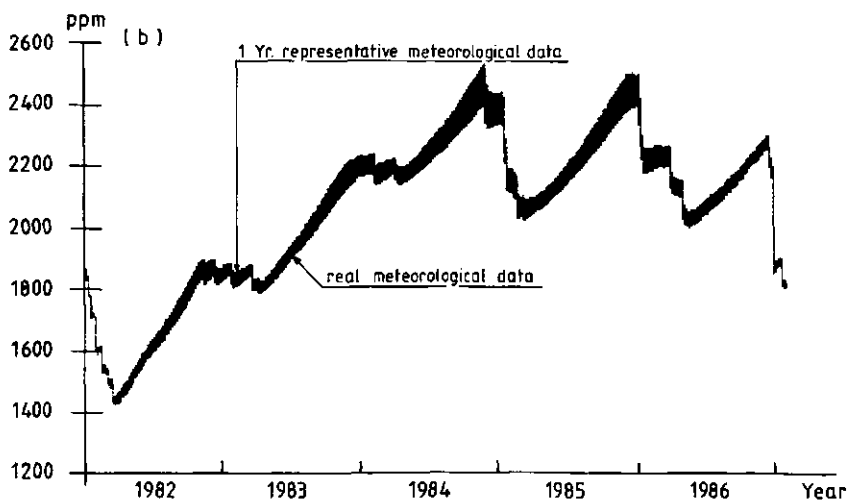
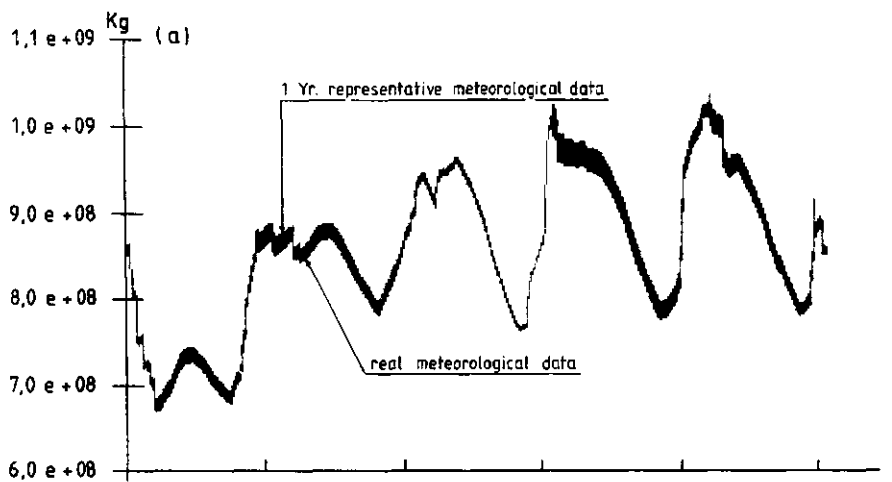


Fig. 6.8 Simulation results using a 5-year and a representative year of meteorological data; (a) total salt content in reservoir, (b) supply salinity.

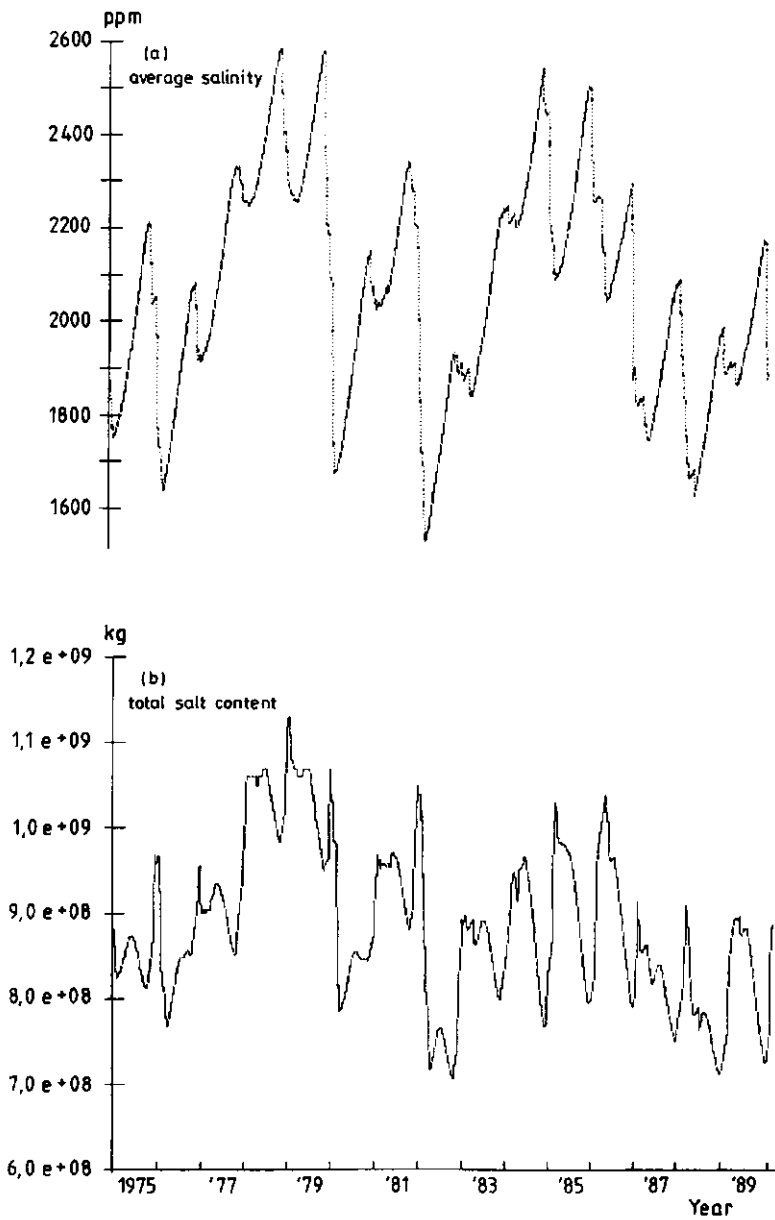


Fig. 6.9 Salinity trend in Jarreh R.; (a) average reservoir salinity (ppm), (b) total salt content (kg).

Table 6.2 Water and salt balance for Jarreh Reservoir, simulation period 1975-1990 (withdrawal from bottom outlet)

	water ($10^6 * m^3$)	salt concentration (ppm)	salt content ($10^6 * kg$)
Reservoir on day 0	450	1850	832
Inflow	8404		14820
Spill	3787		6740
Irrigation	4022		80204
Evaporation excess	574		
Reservoir on day 89365	470	Ave. salinity =1887	887

6.7 CONCLUSIONS

It is clear that the diversion of the most saline part of the inflow will result in significant water quality improvements of both offtake and reservoir. Implementing such a policy for the Jarreh Reservoir does not involve severe engineering constraints.

Control by scouring is less effective at the presently planned offtake levels. However, an alteration of the outlet structures, or use of a multi-level offtake structure would result in more effective implementation of this policy. Nevertheless, this policy will remain always less effective than the diversion policy. Scouring the salt wedges in autumn, is a standard procedure in the management of salinity in Wellington Reservoir, W. Australia (Fischer et al., 1979; Imberger, 1981). This is because for the Australian case the high salinity inflow water is usually cold. Hence saline water lodges in the deeper places and can be easily scoured through the bottom outlet. The above mentioned condition is not to be expected for Jarreh Reservoir, where the most saline inflows remain near the surface at the level of thermocline.

In Fig. 6.10 the average salinity of the reservoir operating policies (with and without implementing the management policy) are compared with the original river salinity for the period 1982-1986. It is evident that the reservoir has alleviated the consequences of extreme river salinity (up to 4000 mg l^{-1}) to an extent acceptable for moderately salt tolerant crops (up to 2400 mg l^{-1}). In this period the reservoir salinity varies in a range between 1450 and 2415 mg l^{-1} . The adopted management policy (diversion of inflows with a salinity greater than 3000 ppm) reduces this figure to about 1430 to 2200 mg l^{-1} .

The salinity trend in Jarreh Reservoir is determined mostly by annual

variability in river discharge. The high and fresh flows of the wet years flushed out the reservoir, whereas the low and salty flows of the dry years deteriorate the quality. This indicates that an equilibrium condition hardly will be achieved, but that the reservoir salinity will vary within a range. For the period 1975-1990 the average reservoir salinity, without management policies varies between 1500-2600 ppm (Fig. 6.9).

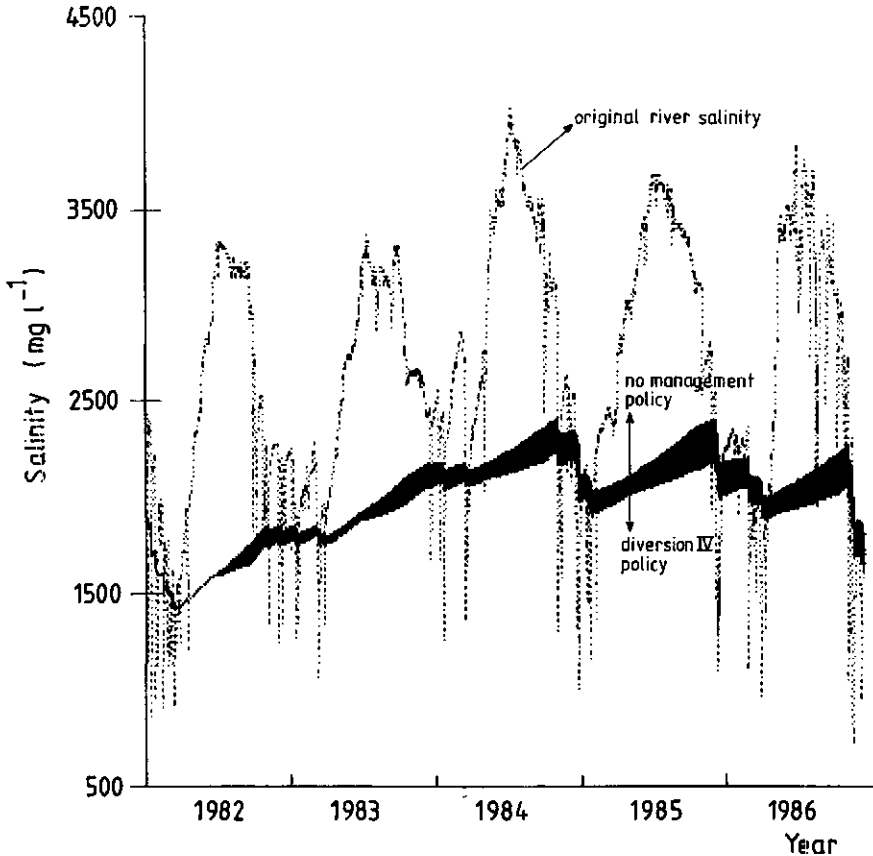


Fig. 6.10 Comparison between the original river salinity and average reservoir salinity with and without management policy.

REFERENCES

- Bogardi, J.J., 1990. Reservoir management under consideration of stratification and hydraulic phenomena. Research Proposal to PhD Program, Dept. of Hydrology, Soil Physics and Hydrology, Wageningen Agric. Univ., The Netherlands.
- Crank, J., 1967. The mathematics of diffusion. vi+347 pp. Oxford University Press (p. 31, eq. 3.13).
- Fischer, H.B., List, E.J., Koh, R.C., Imberger, J., and Brooks, N.H., 1979. Mixing in inland and coastal water. Academic Press, 483 pp.
- He, Q., 1987. Operation policies for a three-reservoir system in Tianjin area, North China. M. Eng. Thesis No. WA-87-7, AIT, Bangkok, Thailand.
- Imberger, J., 1981. The influence of stream salinity on reservoir water quality. Agric. Wat. Manage., 4:255-273.
- Loh, I.C., and Hewer, R.A., 1977. Salinity and flow simulation of a catchment reservoir system. Proc. Hydrology Symposium, I. E. Aust., Brisbane.
- Molen, van der W.H., 1980. Water quality: influence of transport and mixing processes. Lecture Notes, Dept. of Land and Water Use, Wageningen Agric. Univ., The Netherlands, 88 pp.
- Patterson, J., Loh, I., Imberger, J., and Hebbert, B., 1978. Management of a salinity affected reservoir. Proc. Hydrol. Symp. I.E. Aust. pp. 18-22.
- Shiati, K., and Torfs, P.J.J.F., 1990. Simulation of reservoir storage level by model RELEAS. Internal Note, Dept. of Hydrology, Soil Physics and Hydraulics, Wageningen Agric. Univ., The Netherlands.
- Volker, A., 1942. Voorloopige resultaten en conclusies van een onderzoek naar den invloed van grondwaterstromen op de chloorgehalten van het grondwater in de IJsselmeerkom. Unpublished Report, Dienst der Zuiderzeewerken. (in Dutch)
- Yeh, W.W-G., 1985. Reservoir management and operations models: A state-of-the-art review. Water Resour. Res., 12:1797-1818.

RECOMMENDATIONS FOR FURTHER RESEARCH

i - Interaction between sediment particles and physical mixing processes

The presence of sediment particles in the inflowing water affect the density, resulting underflow and thus influence the physical mixing processes in the reservoir. The present work models a steady motion turbidity current with neither depositing nor eroding sediments. That is the temporal variation of sediment particles has not been modelled. The time varying distribution of particles in a reservoir is the result of a complex set of physical and (bio)chemical processes and their mutual interactions. In future studies, a model that describes particles distribution and combines it with the physical mixing processes in a stratified reservoir should be able to handle the particles settling, diffusion and coagulation.

Many investigators who have studied the behaviour of sediment-laden inflows in reservoirs, have verified their theoretical expressions by laboratories experiments. Only a few field measurement is reported. Further research should also emphasize more on comprehensive field measurements.

ii - Management of salt-affected reservoirs

- Development of reservoir operating rules

The only control available over the behaviour of reservoirs are manipulation of inflows and outflows. The amount of water that can be allocated for management purposes should be determined by developing an operating rule (using an optimization technique). The main criteria should be to minimize the amount of spillage and maximize the amount of release. The present study does not include such an optimization.

- Coupling the optimization and water quality model

The optimization techniques which will be used to develop reservoir operating rules should include water quality criterion as well. Various objective functions (such as target salinity and salt load in the reservoir) and constraints (such as selective withdrawal) may be used. At present, a research program is established to investigate the above-mentioned aspects for management of the Jarreh Reservoir at the Department of Hydrology, Soil Physics and Hydraulics of Wageningen Agricultural University.

SUMMARY AND CONCLUSIONS

This thesis presents results of a research on the regional salinization in the Shapur-Dalaki river basin (Southern Iran) and some solutions to reduce the salinity of the water to be used for present and future irrigation systems. The basic data were collected over the period 1974-1990. Special emphasis is given to investigate the origin, sources and extent of salinity and the processes influencing its production and transport. An important part of the study comprises the modelling of the stratification in a future storage reservoir, as affected by temperature, salinity and sediment.

Chapter 1 describes the general characteristics of the basin, and provides the necessary background information.

Two rivers traverse the study area. The northern part is drained by the Shapur river, the southern part by the Dalaki river. The geological features of the basin are characterized by very thick sequences of Secondary and Tertiary formations in which the rivers and their tributaries have incised deep valleys, that are partly filled with alluvium. Up to the Oligocene, the formations are dominantly made up of dolomitic limestones. The Miocene formations consist of marine shales and marls, interbedded with salt and gypsum. At the centres of some anticlines or at fault lines, six salt plugs of Precambrian age have risen from great depths (3-5 km). The main landscape-forming processes were erosion, transport, and deposition under arid climatic conditions. The upstream areas consist of limestones and marls of Cretaceous to Oligocene age, whereas the middle part of the basin is almost entirely occupied by saline Miocene formations (Annex 1). Also the alluvial coastal plain, forming the lower part of the basin, is salty. As a result, the highest salt concentrations in soil and water are found in the downstream part of the basin.

Climate is arid, with temperate winters and dry and very hot summers. Precipitation mainly occurs during winter (December to March), but is far less than the potential evapo-transpiration. The seasonality in climatological factors is great. As a consequence, river flows are extremely variable. The rivers discharge 70-80% of their annual flow during winter, often as flash floods of a few days duration only. The alluvial plains are poor in groundwater resources, and brackish surface waters form the sole resources of irrigation. Irrigated farming is influenced by the water quality. In the downstream plains, where the soil and water resources are most saline, the highly salt tolerant date palm is the main crop. In the inland valleys of the upper part of the basin, wheat, barley and more sensitive crops (like fruit trees and vegetables) are cultivated.

Chapter 2 describes the salinization processes and the extent of salinity in the basin.

Na and Cl form the dominant components of dissolved salts, suggesting a maritime origin. Late Precambrian evaporites (Hormuz formation) and Miocene

formations (especially the Gachsaran formation) are the main sources. The salts of the Miocene appear interbedded or interspersed in Tertiary strata (Photo 3 and 4), whereas the salt of the Precambrian appears at the surface as large plugs formed by salt diapirism (Photo 5 and 6). The presence of these structures has influenced the geological activities in the basin during the Pliocene Zagros Orogeny.

Salt and water monitoring at the observations network indicates that in an average year approximately $2.5 \cdot 10^6$ tons of salt are carried by the Shapur and Dalaki rivers (Table 2.1). The salty tributaries Shekastian (Shapur basin) with a yearly average salinity of 6850 (3700-40 000) mg/l and Shur (Dalaki basin) with a yearly average salinity of 58 000 (26 000-148 000) mg/l are the main sources. The basins of these tributaries are almost entirely formed by the Miocene Gachsaran formation. Extremely salty springs occur (salinities up to 198 000 mg/l have been measured) that issue from Gachsaran strata or from salt diapirs.

The upstream river waters originate from limestone formations, and are of calcium bicarbonate type. After the confluence with the first salty tributaries sodium chloride becomes dominant. At the entrance into the coastal plain Na and Cl comprise 75% of the total ions; the remaining salts are Ca and Mg sulphate and a small amount of bicarbonate. The proportion of Na and Cl in waters from salty springs and tributaries varies between 88-97% and is even higher than the 84% in sea water (Fig. 2.5).

Upstream of the coastal plain, salinity is primarily caused by natural conditions, that have been active for a considerable time. Secondary salinization occurs mainly in the areas downstream of the Saad-Abad and Sarghanat diversion dams. It was introduced by irrigation in the Borazjan coastal plain, where it has caused severe problems. However, this secondary salinization does not influence the quality of the irrigation water, since the river water is hardly used downstream of these diversion dams.

Sections 2.2 and 2.3 deal with production and transport of suspended and dissolved matter. The salty and sparsely vegetated Miocene formations are the main sources of these substances. Sheet and rill wash are the principal debris producing processes, whereas gully and tunnel erosion are common in salt plugs. Suspended matter concentrations up to 42 kg/m^3 have been measured, and the mean annual sediment yield in the basin is estimated to be $1200 \text{ t/km}^2/\text{yr}$.

The solutes are mainly derived from formation weathering (with acid-sulphate weathering being absent because of an abundance of calcium carbonate) and from salty groundwater contributed by spring, ghanats and drains.

The output of suspended and dissolved materials in the basin is closely related to the output of water. The seasonality in flood occurrence plays an important role. Only 10.5% of the water output and 3.5% of the sediment load of Shapur river leaves the catchment during the summer months (June to September).

Regression analysis is used to determine the relationship between concentrations of suspended and dissolved matter and river water discharge. A close positive relationship exists between the suspended matter concentration and discharge. As shown in Fig. 2.8, 90% of the variance was explained by a log-linear model. No significant improvement was achieved by using a polynomial model. In response to seasonal characteristics of flows, the relation between sediment concentration and river discharge has been subdivided according to season. No distinctive difference was found between the snowmelt period in spring (Fig. 2.11a) and the rainy winter season, because snowmelt is not very important in the study area. In summer the sediment is purely derived from the river bed and its banks; this explains the lack of correlation in this season (Fig. 2.11b).

Whereas the suspended sediment concentration strongly increases with increasing river flow, the dissolved matter behaves in an opposite way. Base flows, with high concentrations of NaCl originate mainly from groundwater issuing from springs and give rise to high river salinity in summer. During floods, the salinity is lower due to dilution of the base flow by the large quantities of surface runoff, although the salt loads are much higher during such events.

The resulting relationships are employed to estimate the sediment and TDS inputs into the future Jarreh Reservoir over a larger period.

Chapter 3 deals with salinity management in the basin. In the Shapur and Dalaki rivers, salinity can be reduced by engineering measures. Those investigated are: salt disposal to prevent salt entrance into the receiving water bodies and salt mitigation measures which reduce the salinity in the river water. Among the salt disposal measures, collection and evaporation of saline water in ponds appears to be a feasible option, in view of the high rate of evaporation in the region. After the full implementation of proposed schemes, the average annual salt loads of the Shapur and Dalaki rivers are expected to be reduced by 82 000 and 294 000 tons (that is 7.4 and 17.2% improvement), respectively.

Among the salt mitigation measures, the construction and management of a storage reservoir will be the most successful one. The planned Jarreh storage dam on Shapur river has been studied to evaluate this measure. A four-year simulation (1982-1985) of the reservoir as shown in Fig. 7 indicates that the high salinity of the river in spring and summer (up to 4200 ppm) is reduced to a range between 1500-2400 ppm. This lowering in salinity would allow the cultivation of cash crops, like sugarbeet in the coastal region.

The following three chapters deal with the behaviour, modelling and management of the salt-affected Jarreh Reservoir. The main characteristics of this reservoir will be: strongly stratified and warm-monomictic, with a residence time of 1.1 year, and oligo-mesotrophic (at least during the first years after construction). Stratification in reservoirs is greatly influenced by the climate and by three main properties of the inflowing water: temperature, soluble salts and suspended matter. The suspended

sediment affects the density of inflows considerably and influences mixing and stratification. However, the effect of suspended matter is seldom taken into account. In Section 4.2, a procedure is introduced to calculate the water density as influenced by temperature, soluble salts and suspended matter. Whereas changes in temperature and salinity cause a slowly varying seasonal fluctuation in the density of the river water, sharp peaks in density are caused by heavy sediment loads during floods (Fig. 2).

Chapter 5.1 presents the relationships that describe the fate of a sediment-laden inflow into a reservoir. This dense suspension will move along the bottom as a turbidity current. The suspended sediment of this underflow is not preserved; the turbidity current may deposit its sediment on the bed, or erode sediment from the bed, and in doing so it will affect its own dynamics. The resulting type of underflow mainly depends on the bed slope. An appreciable bed slope is required to maintain the current in a supercritical state (Richardson number $R_I < 1$), which is a necessary condition for erosion to occur. In most reservoirs, the bed slope is small and the turbidity currents are of depositing type, with R_I larger than one. The basic equations (eqs. 5.4-5.6) are applied to the Jarreh Reservoir for a flood on day 27/1/1980 and solved numerically. It is shown that R_I reaches a value close to unity over a very short distance near the entrance, after which the current becomes subcritical (Fig. 5.2a). The case of an eroding/depositing turbidity current was only observed when the bottom slope was fictitiously increased to 4% (Fig. 5.2b), far higher than the existing 0.35%.

The behaviour of turbidity currents on mild bed slopes has been investigated by various researchers. The current is characterized by a constant and large R_I ($R_I > 1$) and thus attains a "normal" state. Accordingly, the equations (5.4-5.6) can be simplified by assuming that the velocity of the underflow does not change with distance (uniform flow) and that the sediment particles in the current remain in suspension with negligible deposition and entrainment during the flow. A momentum equation is derived and compared with equations described in the literature (Table 5.1). It is shown that the resulting differences in the flow velocity are small. However, those equations that consider the settling tendency of sediment particles, V_s/U , resulted in a higher R_I and a slightly lower current velocity.

Turbidity currents are rare events and their direct measurement in the field is difficult and expensive. Therefore, there are few well-described observations of turbidity currents in reservoirs. A field measurement of a turbidity current in Latian Reservoir, Iran, as occurred during a flood on 25/4/1984, shown in Fig. 5.3, demonstrates the characteristics of a continuously-fed turbidity current. As the current advances, it decelerates and deposits the larger particles, but continues with smaller size fractions remaining in suspension. After losing particles greater than about 0.02 mm, it reaches an equilibrium state, and attains a uniform average velocity of about 6-8 cm/s. The current moves downward towards the dam wall with negligible deposition during this movement. The measured

velocity is in reasonable agreement with values obtained from momentum equations (Fig. 5.4).

In the last part of Chapter 5.1, the results calculated for turbidity currents are compared with those for sediment-free density currents. The results of two simulations, representing a flood and a normal flow, are presented in Fig. 5.5. It is evident that the sediment particles considerably enhance the velocity and buoyancy force of the underflow, especially at high river discharges. The sediment effect is mainly present near the point of inflow. It may be concluded that the behaviour of a turbidity current on a mild bed slope with negligible deposition or erosion fundamentally reduces to a conservative density current.

Chapter 5.2 deals with modelling of the Jarreh Reservoir water salinity, as affected by temperature, dissolved salt and suspended sediments.

The dynamic reservoir simulation model, DYRESM (Version 6.4), originally developed by Imberger et al. (1978) was adapted and modified to simulate the salinity distribution in the reservoir. Before applying a one-dimensional model like DYRESM, it is necessary to verify whether or not the reservoir conditions warrant such an approach. This analysis leads to the conclusion that the Jarreh Reservoir meets all theoretical constraints of one-dimensionality (Table 5.4).

An algorithm is developed for the behaviour of sediment-laden inflows, based on the relations described in Chapter 5.1. The sediment will affect the density of the current during inflow, its dilution with the reservoir water, and its intrusion into the reservoir. After the flow arrives at the dam wall, it will stop and the suspended sediment will settle on the reservoir bottom. The vertical and horizontal propagation of sediment has not been modelled in this approach. This confines the application of the model to those substances that are not reacting physically or (bio)chemically with suspended particles. Salinity may be supposed to be non-reacting in this respect.

DYRESM was run for the data of the wet year 1982 and for a four-year period (1982-1985), with and without sediment effects (Figs. 5.11 and 5.12). A physical explanation is given for the observed results. Winter flows are colder, less saline and are denser than the water in the reservoir. They lodge in deeper layers where they cause a drop in temperature (from 17.8 to 14.4 °C) and salinity (from 1950 to 1650 ppm). In this period, a weak stratification (999.6-1000.4 kg/m³) develops. In summer the reservoir becomes strongly stratified due to warming up of the surface water (temperature near bottom and top 14.5 & 35 °C, salinity 1470 & 1950 ppm, and density 1000.4 & 995.3 kg/m³, respectively). A thermocline forms, protecting the deeper cold waters from mixing with the upper layers. Warm and salty summer inflows remain near the top of the reservoir, where they form a relatively thin brackish water layer. In autumn the incident radiation decreases, the temperature of the epilimnion drops and its thickness increases. Finally an overturn occurs at the end of autumn (day

82340) and the reservoir becomes homogeneous again over the entire depth of 80 meters.

When the effect of sediment is introduced, the density of the inflowing water is notably increased, especially in winter. The inflow penetrates more rapidly to the bottom layer and tends to stay there longer than in the case of sediment-free inflow. This results in more salty and colder bottom water layers, an effect which persists throughout the year. For the simulation year 1982, the salinity of the lower layers increases with up to 200 ppm, temperature decreases with 0.5-2.5 °C, and density increases with up to 0.3 kg/m³. The sediment effect on the salinity of the water released from the reservoir- an increase up to 150 ppm at the bottom outlet - is hardly significant for its use in irrigation (Fig. 5.13). However, the total salt content of the reservoir is affected by the change in salinity distribution due to the inflowing sediment (Table 5.2 and 5.3).

The catchment of Shapur river is severely suffering from salinity, so that in an average year approximately 1.2×10^6 tons of salt will be brought into Jarreh Reservoir. Careful management is required to minimize the risk of a salinity build-up in the reservoir and if possible to improve the quality of the water impounded. In Chapter 6, DYRESM is used to investigate the response of Jarreh Reservoir to various management strategies, as well as to simulate the salinity trend over a long time-span. The simulations are based on the premise that in summer and early autumn as much water as possible should be either released from the reservoir (scouring policy) or be diverted (by-passing policy). On the other hand, the less saline high flows in winter should be retained as much as possible. Of course, these actions are subject to constraints regarding the safe yield of the reservoir.

Different values for release or diversion are examined by using the simulation program, RELEAS. For the simulation period 1982-1986, an amount of 158 Mm³ of water (corresponding to diverting all inflows with salinity greater than 3000 ppm) can be diverted without adversely affecting the reliability of supply (Fig. 6.3, Diversion IV).

Diversion of the most saline part of the inflow will result in significant quality improvement of the water in the reservoir. The diversion of inflows with salinity over 3000 mg/l (Table 6.1, Diversion IV), reduces the average salinity of the reservoir by 8.7% (equivalent to 198 mg/l TDS), whereas the supply salinity is lowered by 18% (equivalent to 387 mg/l TDS). At the end of the simulated period the total salt accumulation is reduced by 72 000 tons, 8.5% improvement on the "no policy" results. Implementing such a policy for Jarreh Reservoir does not require elaborate engineering measures.

Control by scouring at the presently planned outlet levels is not very effective (Table 6.1, SCOUR I, II and IIa). The maximum benefit is gained by SCOUR III, which allows removal of warm and salty summer inflows at a high outlet level prior to their mixing with deeper layers. At the end of the simulation period, this policy will reduce the salinity by about

4.6% (equivalent to 85 mg/l TDS); salt accumulation is reduced by 26 000 tons. A combination of by-passing and scouring policies, SCOUR IV, considerably reduces the salt accumulation in the reservoir, but this combination will involve such high water losses that the effects on the reservoir levels become intolerable. In SCOUR IV, maximum reduction is again achieved at the end of the simulation period: improvement of 13.7% (equivalent to 248 mg/l TDS) in reservoir salinity, 12.4% (equivalent to 248 mg/l TDS) in supply salinity, and 117 000 tons in salt accumulation. The large losses by diversion and scouring, however, endanger the reliability of water supply by the reservoir; therefore, this combination cannot be recommended.

For the simulation period 1982-1986, the extreme variation in river salinity (from 700 to 4000 ppm) is attenuated and reservoir salinity variation is limited to the range 1450-2415 ppm. The most promising management policy (diverting of inflows with a salinity greater than 3000 ppm) reduces this figure to about 1430-2200 ppm.

The long term salinity trend in Jarreh Reservoir is studied by using a 15-year (1975-1990) period of input data (Fig. 6.9). It is evident that the salinity in the reservoir is largely determined by annual variability in river discharge. The high and fresh flows of wet years flush out the reservoir, whereas the low and salty flows of dry years deteriorate the quality. Over the 15-year simulation period the reservoir salinity varies within a range of 1500-2600 ppm. Salt balance calculations indicate that only a small fraction of the salt input has accumulated in the reservoir, the main part being removed by spill and irrigation supply (Table 6.3). Diffusion of salt from the saline Miocene formations below the reservoir bottom appears to be negligible in the salt balance of Jarreh Reservoir (Appendix 4).

SAMENVATTING

Dit proefschrift behandelt de uitkomsten van een onderzoek naar de verzilting in het stroomgebied van de rivieren Shapur en Dalaki in zuidelijk Iran en beschrijft enkele maatregelen, die het zoutgehalte in het water van deze rivieren zouden kunnen verminderen. De bevloeiing van landbouwgronden met dit water zal in de toekomst sterk worden uitgebreid. De gegevens voor dit onderzoek werden verzameld in het tijdvak 1974-1990. Er wordt in het bijzonder aandacht besteed aan de oorsprong, de bronnen en de verbreiding van het zout en aan het vrijkomen en de verplaatsing ervan. Een belangrijk gedeelte van deze studie is gewijd aan het modelleren van een toekomstig stuwmeer, waarin de gelaagdheid van het water wordt beïnvloed door temperatuur, zoutgehalte en meegevoerd slib.

Hoofdstuk 1 bespreekt de algemene kenmerken van het stroomgebied en geeft de nodige achtergrond-informatie.

Het gebied wordt doorsneden door twee rivieren. De Shapur ontwatert het noordelijk gedeelte, de Dalaki het zuidelijke deel. De geologische gesteldheid van het gebied is gekenmerkt door zeer dikke pakketten van secundaire en tertiaire afzettingen, die in het Pliocen door plooiing zijn vervormd en opgeheven (Zagros orogeen). In deze geplooiden afzettingen hebben de rivieren diepe dalen uitgesleten, die gedeeltelijk door alluvia zijn opgevuld. Tot in het Oligoceen zijn voornamelijk dolomitische kalkstenen gevormd. Het Mioceen bestaat uit mariene kleischalies en mergels, waartussen zout- en gipslagen voorkomen. Op grote diepte (3-5 km) zijn precambrische evaporieten aanwezig. In de kernen van enkele anticlinalen, of bij breuken, zijn in het stroomgebied uit deze laag zes grote zoutpijlers opgestegen. Het huidige landschap is gevormd in een aried klimaat onder invloed van erosie, transport en afzetting. De rivieren ontspringen in gebieden met kalkstenen en mergels uit het Krijt tot Oligoceen, terwijl hun middenloop een gebied doorsnijdt dat vrijwel geheel uit zoute Miocene afzettingen bestaat (Annex 1). De gezamenlijke benedenloop van beide rivieren doorkruist een eveneens zoute alluviale kustvlakte. Als gevolg van deze opbouw worden de hoogste zoutgehalten in bodem en water in het benedenstroomse deel van het stroomgebied aangetroffen.

Het klimaat is zeer droog, met gematigde winters en zeer warme zomers. De neerslag valt grotendeels in de winter (december t/m maart), maar zij is veel geringer dan de potentiële evapo-transpiratie, zelfs zodanig dat het klimaat als ariede moet worden beschouwd. De verschillen tussen de jaargetijden zijn zeer groot, waardoor ook de rivier-afvoeren uiterst variabel zijn. Ongeveer 70-80% van de afvoer vindt plaats in de winter, vaak in zeer felle pieken met een duur van slechts enkele uren. In de alluviale vlakten is slechts weinig grondwater aanwezig, zodat alleen brak oppervlaktewater voor bevloeiing kan worden gebruikt. In de benedenstroomse vlakten, waar bodem en water het sterkst zijn verzilt, vormt de zout-tolerante dadelpalm het voornaamste gewas. In de vlakten verder bovenstrooms worden tarwe en gerst verbouwd, maar ook meer zout-gevoelige gewassen zoals fruit en groenten.

Hoofdstuk 2 beschrijft het verziltingsproces en de verbreiding van zout over het stroomgebied.

Na en Cl zijn de voornaamste ionen in het rivierwater, hetgeen wijst op een maritieme oorsprong van het zout. De voornaamste bronnen zijn de laat-precambrische evaporieten van de Hormuz formatie en de miocene afzettingen, in het bijzonder de Gachsaran formatie. De miocene zouten komen verspreid of laagsgewijs voor in de tertiaire afzettingen (Foto 3 en 4), de precambrische zouten daarentegen als grote koepels, die de top vormen van zout-diapiëren (Foto 5 en 6). De aanwezigheid van deze structuren heeft invloed uitgeoefend op de pliocene plooiing van het Zagros-gebergte.

Metingen, verricht aan een netwerk van waarnemingspunten laten zien dat in een gemiddeld jaar de rivieren Shapur en Dalaki omstreeks $2,5 \cdot 10^6$ ton zout afvoeren (Tabel 2.1). De belangrijkste aanvoer komt van enkele zeer zoute zijrivieren: Shekastian (in het stroomgebied van de Shapur) heeft een gemiddeld zoutgehalte van 6850 (3700-40000) mg/l en Shur (in het stroomgebied van Dalaki) zelfs van 58 000 (26 000-148 000) mg/l. Beide ontwateren gebieden, die vrijwel geheel uit de miocene Gachsaran formatie zijn opgebouwd. Hier en elders komen zeer zoute bronnen voor, die ontspringen uit Gachsaran lagen of die onder invloed staan van zoutkoepels van de Hormuz formatie.

Het water in de bovenlopen van Shapur en Dalaki is afkomstig uit kalksteenformaties en is van calcium-bicarbonaat type. Na de samenvloeiing met de eerste zoute zijrivieren wordt natrium chloride overheersend en bij intrede in de kustvlakte bestaat 75% van de ionen uit Na en Cl; de overige zouten zijn sulfaten van Ca en Mg en een geringe hoeveelheid bicarbonaten. Het aandeel van Na en Cl in het water van zoute bronnen en zijrivieren kan oplopen tot 88-97%, meer dan de 84% in zeewater (Fig. 2.5).

In het binnenland wordt de verzilting vrijwel uitsluitend bepaald door natuurlijke omstandigheden, die reeds gedurende geruime tijd werkzaam zijn. Secundaire verzilting wordt vooral aangetroffen in de kustvlakte, benedenstrooms van de uitkeerdammen te Saad-Abad en Sarghanat. De verzilting, die een gevolg is van bevloeiing in de Borazjan-vlakte, heeft aldaar tot ernstige moeilijkheden geleid. Zij heeft evenwel geen invloed op de kwaliteit van het bevoelingswater omdat benedenstrooms van genoemde dammen het rivierwater nauwelijks meer wordt gebruikt.

De secties 2.2 en 2.3 behandelen het vrijkomen en de verplaatsing van sediment en opgeloste stoffen. De zoute en spaarzaam begroeide Miocene formaties zijn de voornaamste bron van deze bestanddelen. Laminaire en ril-erosie zijn de voornaamste oorzaak, terwijl geul- en tunnel-erosie veelvuldig voorkomen in de zoutkoepels. In watermonsters zijn slib-concentraties tot 42 kg/m^3 gemeten en de jaarlijkse slib-afvoer in het stroomgebied wordt geschat op $1200 \text{ t/km}^2/\text{yr}$.

De opgeloste stoffen zijn vooral afkomstig van vertering (waarbij uit de veelvuldig aanwezige sulfiden geen kateklei wordt gevormd doordat koolzure kalk in overmaat aanwezig is) en uit zout grondwater dat wordt aangevoerd door bronnen en door drains, afvoersloten en ghanats.

De afvoer van slib en opgeloste stoffen houdt nauw verband met de afvoer van water. De verdeling van de afvoer over het jaar schommelt sterk. Slechts 10,5% van het water en 3,5% van het slib van de Shapur verlaat het stroomgebied in de zomermaanden (juni t/m september).

Om het verband tussen slibgehalte en rivierafvoer te bepalen werd een regressie-analyse uitgevoerd. Er bestaat een sterke positieve correlatie tussen slibconcentratie en afvoer. Uit Fig. 2.8 blijkt dat 90% van de variantie kan worden verklaard met een log-lineair model. Een benadering met veeltermen bracht geen verdere verbetering. In overeenstemming met het seizoens-karakter van de afvoer werd het verband onderverdeeld naar jaargetijde. Er werd geen duidelijk verschil gevonden tussen de periode van sneeuwsmelt in het voorjaar en de regentijd in de winter (Fig. 2.11a), omdat de sneeuwval in dit gebied niet erg belangrijk is. In de zomer is het sediment vrijwel uitsluitend afkomstig van de rivierbodem en de oevers; dit verklaart het ontbreken van correlatie in dit jaargetijde (Fig. 2.11b).

Terwijl het gehalte aan slib zeer sterk toeneemt met de afvoer van water, is het omgekeerde het geval voor de opgeloste stoffen. De basis-afvoeren, met hoge gehalten aan NaCl, zijn voornamelijk afkomstig uit bronnen en leiden tot afvoer van vrij zout rivierwater in de zomer. Bij grote afvoer zijn de zoutgehalten veel lager door verdunning met grote hoeveelheden oppervlakkig afgestroomd water, hoewel in dergelijke perioden de zoutvrachten veel hoger zijn.

De gevonden verbanden zijn gebruikt voor een schatting van de aanvoer van slib en opgeloste stoffen (TDS) naar het toekomstige Jarreh-stuwmeer in de jaren voor 1982, waarvoor alleen waarnemingen over de rivier-afvoeren beschikbaar waren.

Hoofdstuk 3 behandelt het beheer van het zout in het stroomgebied. In de rivieren Shapur en Dalaki kan het zoutgehalte worden verminderd door technische maatregelen. De volgende mogelijkheden zijn onderzocht: opslaan van zout om de aanvoer naar de rivieren en stuwmeren te verkleinen en maatregelen tot vermindering van het zoutgehalte in het rivierwater zelf. De opslag, door het zoutste water in vijvers te leiden, lijkt perspectief te bieden wegens de sterke evaporatie in dit droge klimaat. Na de uitvoering van alle daartoe voorgestelde maatregelen wordt verwacht dat de jaarlijkse zoutlast van Shapur en Dalaki met 82 000 resp. 294 000 ton zal verminderen, een verbetering met 7,4, resp. 17,2%.

Onder de maatregelen tot vermindering van het zoutgehalte in het rivierwater - althans in de zomer - biedt de aanleg van een stuwmeer de beste vooruitzichten. Het effect van de toekomstige Jarreh stuwdam in de Shapur is nader onderzocht. Een simulatie over een periode van vier jaar (1982 t/m 1985) geeft aan dat het hoge zoutgehalte in de zomer (tot 4200 mg/l) wordt teruggebracht tot het traject 1500-2400 mg/l (Fig. 7). Deze verlaging van het zoutgehalte zou in de kustvlakte de verbouw van gewassen als suikerbieten mogelijk maken.

De volgende drie hoofdstukken handelen over het gedrag, de modellering en het beheer van het toekomstige Jarreh-stuwmeer. De belangrijkste kenmerken van dit meer zullen zijn: sterk gelaagd, warm-monomictisch, met een verblijftijd van 1,1 jaar en oligo-mesotroof (althans gedurende de eerste jaren na de aanleg). Gelaagdheid in het water van stuwmeren wordt sterk bepaald door het klimaat en door drie kenmerken van het instromende water: temperatuur, zoutgehalte en gehalte aan zwevend slib. Slib dat in suspensie wordt meegevoerd draagt aanzienlijk bij tot de dichtheid van het water en beïnvloedt daardoor de menging en gelaagdheid in het stuwmeer. Deze invloed is echter nog slechts zelden in beschouwing genomen. In Sectie 4.2 is een berekeningswijze gegeven ter bepaling van de dichtheid als functie van temperatuur, zoutgehalte en zwevend slib.

Terwijl veranderingen in temperatuur en zoutgehalte van het rivierwater in de loop der seizoenen langzame veranderingen in dichtheid teweeg brengen, leiden de hoge gehalten aan zwevend slib tijdens hoge afvoeren tot scherpe pieken in dichtheid (Fig. 2).

Hoofdstuk 5.1 vermeldt de vergelijkingen, die het gedrag van een met slib beladen instroom in een stuwmeer beschrijven. Deze zware suspensie zal zich als een troebelingsstroming langs de bodem verplaatsen. Het zwevende sediment in deze onderstroom zal daarbij in het algemeen niet in suspensie blijven; er kan materiaal op de bodem worden afgezet, maar ook kan de bodem worden aangetast, processen die op hun beurt de dynamiek van de stroming zullen bepalen. Welk type stroming ontstaat, zal voornamelijk afhangen van de helling in de lengterichting van het reservoir. Er blijkt een aanzienlijke helling nodig te zijn om een superkritische stroming te veroorzaken (met getal van Richardson R_I kleiner dan 1), een noodzakelijke voorwaarde voor erosie van de bodem. In de meeste stuwmeren is deze helling daarvoor te gering en zal dus afzetting van sediment plaats vinden, waarbij R_I groter is dan 1. De basis-vergelijkingen (5.4-5.6) zijn toegepast op het Jarreh-stuwmeer gedurende een hoge afvoer op 27-1-1980 en numeriek opgelost. Aangetoond wordt dat over een kleine afstand nabij het punt van instroming de waarde van R_I dicht bij 1 ligt, maar dat daarna de stroming sub-kritisch wordt (Fig. 5.2a). Een eroderende onderstroom kan eerst worden verwacht bij een langshelling van 4% (Fig. 5.2b), veel groter dan de werkelijke 0,35%.

Het verloop van troebelingsstromingen over een zwak hellende bodem is door verscheidene onderzoekers bestudeerd. De stroming wordt gekenmerkt door een hoge en constante waarde van het getal van Richardson R_I (R_I groter dan 1) en bereikt een "normale" stromingstoestand. De vergelijkingen (5.4-5.6) kunnen dan worden vereenvoudigd door aan te nemen dat langs de bodem de stroomsnelheid niet verandert (eenparige stroming); de slibdeeltjes blijven daarbij in suspensie, hun bezinking is verwaarloosbaar en er wordt slechts weinig helder water in de stroming opgenomen. Voor dit type stroming werd een impulsvergelijking opgesteld, die is vergeleken met in de literatuur beschreven betrekkingen (Tabel 5.1). Aangetoond kan worden dat de verschillende vergelijkingen slechts geringe verschillen in stroomsnelheid te zien geven. De vergelijkingen, die ook de neiging tot bezinken van slib (bepaald door V_s/U) in beschouwing nemen, leiden echter tot een grotere R_I en een iets kleinere stroomsnelheid.

Dichtheidsstromingen in stuwmeren zijn vrij zeldzame verschijnselen en goede metingen ervan zijn moeilijk en kostbaar. Er zijn dan ook slechts weinig voorbeelden in de literatuur beschreven. De uitkomsten van een veldmeting in het Latian stuwmeer, Iran, verricht tijdens een langdurig hoge rivierafvoer op 25-4-1984, is weergegeven in Fig. 5.3. Bij de voortgang van de stroming vermindert aanvankelijk de snelheid en worden de grovere frakties van het sediment afgezet. Nadat deeltjes groter dan ongeveer 0,02 mm zijn bezonken wordt de stroming stationair, met een snelheid van 6-8 cm/s. Deze stroming loopt over de bodem tot aan de dam waarbij de afzetting van slib verwaarloosbaar is. De gemeten stroomsnelheid komt vrij goed overeen met de waarden welke uit de impulsvergelijkingen worden berekend (Fig. 5.4).

In het laatste gedeelte van Hfst. 5.1 worden berekende troebelingsstromingen vergeleken met berekende dichtheidsstromingen van helder water. Fig. 5.5 toont

de uitkomsten van twee simulaties, een voor een hoge rivierafvoer, de andere voor meer normale omstandigheden. Het is duidelijk dat de aanwezigheid van slib de stroomsnelheid en de optredende krachten als gevolg van dichtheidsverschillen verhoogt, vooral bij hoge afvoer. Het effect van sediment is het sterkst nabij het invoerpunt. Het gedrag van een troebelingsstroming met verwaarloosbare bezinking over een zwakke helling blijkt in beginsel overeen te komen met een conservatieve dichtheidsstroming.

Hoofdstuk 5.2 handelt over het modelleren van het zoutgehalte in het water van het Jarreh stuwmeer onder invloed van temperatuur, opgeloste stoffen en zwevend slib.

Het dynamische model DYRESM (Versie 6.4), oorspronkelijk ontwikkeld door Imberger et al. (1978) werd aangepast en gebruikt om de zoutverdeling in het water na te bootsen. Alvorens een een-dimensionaal model (zoals DYRESM) toe te passen, dient eerst te worden nagegaan of het betreffende meer op een dergelijke wijze mag worden beschreven. Deze analyse toonde aan dat het Jarreh-stuwmeer inderdaad aan alle theoretische voorwaarden voor een-dimensionaliteit voldoet (Tabel 5.4).

Op grond van de betrekkingen die zijn vermeld in Hfst. 5.1 werd een rekenwijze ontwikkeld om het gedrag van slibhoudende instroming te beschrijven. Het meegevoerde sediment zal invloed uitoefenen op de dichtheid van de onderstroom, op de verdunning ervan met reservoir-water en op het doordringen ervan in het reservoir. Als de voet van de dam is bereikt zal de stroming tot stilstand komen en zullen de zwevende slibdeeltjes op de bodem bezinken. De verticale en horizontale verplaatsing van sediment is niet verder nagegaan. De toepassing van het model blijft daarom beperkt tot stoffen die niet worden gebonden aan zwevend slib. De opgeloste zouten mogen bij benadering als niet-reagerend worden beschouwd.

Het model DYRESM werd toegepast op gegevens van het natte jaar 1982 en op een vierjarig tijdperk (1982-1985), zowel met als zonder de aanwezigheid van zwevend slib (Fig. 5.11 en 5.12). Voor de uitkomsten kunnen de volgende fysische verklaringen worden gegeven. De winterafvoeren zijn kouder en minder zout, maar hebben een grotere dichtheid dan het water in het stuwmeer. Zij blijven achter in diepere lagen, waar zij een daling veroorzaken van de temperatuur (van 17,8 naar 14,4 °C) en van het zoutgehalte (van 1950 naar 1650 ppm). In dit jaargetijde ontwikkelt zich een zwakke gelaagdheid (999,6-1000,4 kg/m³). In de zomer raakt het water sterk gelaagd door opwarming aan de oppervlakte (temperatuur nabij de bodem en bovenin resp. 14,5 & 35 °C, zoutgehalte 1470 & 1950 ppm en dichtheid 1000,4 & 995,3 kg/m³). Er vormt zich een thermocline, die de koude diepere lagen beschermt tegen vermenging met de bovenlagen. De warme en vrij zoute instroom in de zomer vormt bovenin het reservoir een vrij dunne laag brak water. In de herfst wordt de inkomende straling geringer, de temperatuur van het epilimnion neemt af en zijn dikte neemt toe. Tenslotte vindt in de late herfst (dag 82340) een omkering plaats waardoor het water over de gehele diepte van 80 m weer dezelfde samenstelling verkrijgt.

Wanneer ook de invloed van het sediment in de beschouwing wordt betrokken, dan wordt de dichtheid van de instroom duidelijk groter, met name in de winter. Deze instroom dringt nu sneller tot de bodemlaag door en verblijft daar langer dan bij toestroming van helder water. Dit leidt tot zouter en kouder water nabij de

bodem, een verschijnsel dat gedurende het gehele jaar merkbaar blijft. Voor het gesimuleerde jaar 1982 wordt in dat geval het zoutgehalte van de diepe lagen tot 200 ppm hoger, de temperatuur vermindert met 0,5-2,5 °C en de dichtheid stijgt met een bedrag tot 0,3 kg/m³. De invloed van het slib op de kwaliteit van het aan het meer onttrokken water - blijkens Fig. 5.13 een stijging tot 150 ppm indien de bodem-uitlaat wordt gebruikt - is nauwelijks van betekenis voor het gebruik daarvan voor bevoeiing. De totale hoeveelheid zout in het reservoir wordt evenwel duidelijk beïnvloed (Tabel 5.2 en 5.3).

Uit het stroomgebied van de Shapur komen zoveel zouten vrij dat in een gemiddeld jaar het stuwmeer daarvan $1,2 \cdot 10^6$ ton ontvangt. Door een zorgvuldig beheer dient accumulatie van dit zout te worden voorkomen en zo mogelijk de kwaliteit van het opgeslagen water te worden verbeterd. In Hoofdstuk 6 wordt het model DYRESM gebruikt om de gevolgen van verschillende beheersmaatregelen te onderzoeken. Ook wordt op deze wijze de ontwikkeling van het zoutgehalte over een langer tijdvak nagebootst. De simulaties berusten op de aanname dat hetzij in de zomer en vroege herfst zoveel mogelijk water uit het meer wordt gespuid ("scouring policy"), hetzij dat de zoute afvoeren in de zomer worden omgeleid naar een ver benedenstrooms gelegen punt ("diversion policy"). Anderzijds dienen de minder zoute winterafvoeren zoveel mogelijk in het meer te worden opgeslagen. Uiteraard zijn de opties onderhevig aan beperkingen opgelegd door de te leveren hoeveelheden water, ook in droge jaren ("safe yield").

Verschillende waarden voor de hoeveelheden te spuien of om te leiden water werden onderzocht met behulp van het programma RELEAS. Voor het tijdvak 1982-1986 kan een hoeveelheid van 158 Mm³ worden omgeleid zonder dat de betrouwbaarheid van de levering in gevaar komt; dit komt overeen met het omleiden van alle rivierafvoeren met een zoutgehalte van meer dan 3000 ppm (Fig. 6.3, Diversion IV).

Het afleiden van de meest zoute instroom geeft een duidelijke verbetering van het opgeslagen water. Omleiding van water met meer dan 3000 mg/l (Tabel 6.1, Diversion IV) vermindert het gemiddelde zoutgehalte in het stuwmeer met 8,7% (overeenkomend met 198 mg/l TDS), terwijl het zoutgehalte van het verstrekte water wordt verlaagd met 18% (overeenkomend met 387 mg/l TDS). Aan het eind van de beschouwde periode bedraagt de verlaging van de zoutvoorraad 72 000 ton, of 8,5% ten opzichte van "niets doen". Het maken van een dergelijke voorziening kan met betrekkelijk eenvoudige middelen geschieden en vergt geen grote kunstwerken.

Het aflaten van water via de geprojecteerde uitlaten in de stuwdam blijkt niet erg werkzaam te zijn (Tabel 6.1, SCOUR I, II en IIa). Het grootste nut wordt verkregen door SCOUR III, waarbij in de zomer water wordt gespuid door een hoog gelegen uitlaat, op een tijdstip dat het warme en zoute water zich nog niet heeft vermengd met diepere lagen. Aan het einde van de gesimuleerde tijdvak leidt dit tot een vermindering in zoutgehalte van ongeveer 4,6%, overeenkomend met 85 mg/l TDS; de zoutvoorraad in het stuwmeer is daarbij verminderd met 26 000 ton. Indien zowel water wordt om- als afgeleid (SCOUR IV), dan wordt de voorraad zout in het meer weliswaar veel minder, maar anderzijds gaat bij deze combinatie zoveel water verloren dat de daling van de meerpeilen ontoelaatbaar wordt. Bij SCOUR IV wordt de grootste verbetering wederom aan het eind van de periode bereikt: een vermindering van het zoutgehalte in het meer met 13,7% (overeenkomend met 248 mg/l TDS), 12,4% (248 mg/l TDS) in het afgeleverde water en 117 000 ton aan

zoutvoorraad in het meer. De grote verliezen door omleiding en aflaten brengen echter de betrouwbaarheid van de waterlevering in gevaar, waardoor deze combinatie niet kan worden aanbevolen.

Gedurende het tijdvak 1982-1986 werd de zeer grote schommeling in het zoutgehalte van het rivierwater (van 700 tot 4000 ppm) sterk gedempt en beperkt tot het traject 1450-2415 ppm. De meest belovende beheerswijze (het omleiden van aanvoeren met een zoutgehalte boven 3000 ppm) verlaagt dit traject tot ongeveer 1430-2200 ppm.

Het gedrag van het meer over een langer tijdvak is onderzocht door de invoergegevens over een periode van 15 jaar (1975-1990) te gebruiken (Fig. 6.9). Er blijkt duidelijk dat het zoutgehalte van het water in het stuwmeer voornamelijk afhangt van de jaarlijkse schommelingen in de aanvoer door de rivier. De hoge en betrekkelijk zoete instroming in natte jaren spoelt het reservoir schoon, terwijl de geringe en vrij zoute aanvoer in droge jaren de waterkwaliteit slechter maakt. Tijdens het gehele tijdvak schommelt het zoutgehalte van het water in het meer tussen 1500 en 2600 ppm. Berekeningen van de zoutbalans wijzen uit dat slechts een zeer klein deel van het aangevoerde zout in het meer achterblijft en dat het meeste is verwijderd door het overlopen van de overlaat in de dam en door de levering van bevoeiingswater (Tabel 6.3). Diffusie van zout uit de zoute miocene formaties onder de bodem van het meer blijkt in de zoutbalans een te verwaarlozen post te vormen (Appendix 4).

این رساله نتیجه تحقیقاتی است که روی شوری آب رودخانه های شاپورودالکی در جنوب ایران و راه حل های منطقه ای آن انجام شده است. در این تحقیقات، تاکید بخصوصی روی منشاء، منابع، دامنه و عوامل مؤثر در تولید و انتقال شوری انجام شده است. قسمت مهمی از این مطالعات شامل مدل کردن کیفیت (شوری) آب مخزن سدجره بر روی رودخانه شاپورتحت تاثیر عوامل حرارت، شوری و رسوب میباشد.

در فصل اول مشخصه های عمومی حوزه آبریز رودخانه های شاپورودالکی شامل اطلاعات اولیه لازم برای مطالعات ارائه شده است. سیمای کلی زمین شناسی این حوزه هاراتشکیلات ضخیم دوران دوم و سوم تشکیل میدهد که در آن رودخانه های شاپورودالکی و شاخه های فرعی آن، دره های آبرفتی را بریده اند. سادوره الیگوسن، تشکیلات زمین شناسی حوزه را اغلب آهک های دولومیتی تشکیل داده اند. ازدوره میوسن، شیل های دریائی و مارن دیده میشوند که در آن سنگ های نمکی و گچی بصورت لایه هائی وجود دارد. در مرکز برخی طاقدیس های ادرمسیرگسل ها، شش گنبد نمکی مربوط به دوره کامبرین از اعماق زیاد، ۳ تا ۵ کیلومتری بیرون زده است. مناطق ارتفاعی شامل سنگ های آهکی و مارن دوران کرتاسه تا الیگوسن میباشد، در صورتیکه پائین دست حوزه بطور کامل بوسیله تشکیلات نمکی دوره میوسن پوشانده شده است (نقشه ۱). در نتیجه حداکثر تمرکز نمک در خاک و آب در قسمت های پائین حوزه یافت میشود.

منطقه از نظر آب و هوائی خشک بوده و زمستانهای ملایم و خشک و تابستانهای خیلی گرم از ویژگیهای آب و هوائی آن است. تعریق و تبخیر پتانسیل خیلی بیش از کل بارندگی است. بارندگی محدود به ماههای زمستان (آذرالی اسفند) است. از نظر مشخصه های هیدرولوژیکی، تغییرات فعلی دبی رودخانه بسیار بالاست بطوریکه حدود ۷۰ الی ۸۰ درصد کل حجم سالیانه آب در ماههای زمستان جریان می یابد. دشت های آبرفتی از نظر آب زیرزمینی فقیر هستند و آبهای سطحی با املاح بالا تنه منابع آب آبیاری را تشکیل میدهد. زراعت آبی تحت تاثیر کیفیت آب رودخانه ها است. الگوی کشت بستگی به میزان شوری خاک و آب دارد. در دشت های پائین دست که منابع خاک و آب بیشتر شور هستند، عمدتاً "نخل کاشته میشود. در دشت های بالا دست گندم و جو و زراعتهای کم تحمل به شوری مانند درختان میوه و سبزیجات کشت میشود.

در فصل دوم، فرآیند شوری و وسعت آن در حوزه آبریز شرح داده شده است. سدیم و کلسیم عناصر غالب آب رودخانه را تشکیل میدهند که نشان دهنده منبع دریائی نمک است. رسوبات تبخیری کامبرین زیرین (تشکیلات هرمز) و تشکیلات دوره میوسن (بطور عمده گچسازان) منبع اصلی تولید نمک را تشکیل میدهند. نمک های دوره میوسن بصورت لایه هائی و یا پخش در لایه های دوران سوم قرار دارد (عکس ۳ و ۴) در حالیکه نمک های دوره کامبرین زیرین در سطح زمین، بصورت گنبد های نمکی ظاهر میشوند (عکس ۵ و ۶). بر اساس برآوردهای انجام شده، سالیانه ۳/۵ میلیون تن نمک بوسیله رودخانه های شاپورودالکی حمل میشود (جدول ۱-۲). شاخه های فرعی شورکستیان در حوزه رودخانه شاپوریا متوسط سالیانه شوری ۶۸۵ میلیگرم در لیتر و شاخه شور در حوزه رودخانه دالکی با متوسط سالیانه شوری ۵۸۰۰ میلیگرم در لیتر، منابع شورکننده اصلی میباشد. این شاخه ها جریان حوزه هائی را که کاملاً

از رسوبات شبخیری دوره میوسن (عمدتاً کچساران) پوشانده شده اند و چشمه های خیلی شور (شوری تا ۱۹۸ گرم در لیتر اندازه گیری شده است)، منشاء گرفته از تشکیلات کچساران و کنگبدهای نمکی راتخلیه میکنند.

آب رودخانه هادریالادست از نوع بی کربناته است و پس از الحاق اولین منبع شوری به کلرورسدیم تغییر میکند. در پائین دست، Na و Cl، ۷۵ درصد عناصر شیمیائی آب را تشکیل میدهند و بقیه املاح عبارتند از سولفات کلسیم و منیزیم و مقدار کمی بی کربنات، نسبت Na و Cl در منابع شور آلوده کننده بین ۸۸ الی ۹۷ درصد میباشد که از آب دریا (۸۴ درصد) بیشتر است (شکل ۵-۲).

تاقبل از دشت ساحلی برازجان شوری تحت شرایط طبیعی حادث میشود (شوری اولیه). در صورتیکه فعالیت کشاورزی در دشت برازجان بشدت سبب شور شدن منابع آب و خاک گردیده است (شوری ثانویه). بهر حال نظریه اینکه آب رودخانه های مذکور بندرت بعد از سد های انحرای سرقنات و سعد آباد مورد استفاده قرار میگیرد، نقش شوری ثانویه در تخریب کیفیت آب آبیاری دشت برازجان محسوس نخواهد بود.

قسمت ۲-۳ و ۳-۳ در رابطه با تولید و حمل مواد معلقه آب رودخانه و همچنین املاح محلول آب میباشد. تشکیلات شور و کم پوش دوره میوسن، منشاء اصلی مواد معلقه و املاح محلول است. فرسایش ورقه ای و ریل فرآیند اصلی تولید مواد معلق بوده و ایجاد گالی های فرسایشی در کنگبدهای نمکی مشاهده میشود. غلظت مواد معلق تا ۴۳ کیلوگرم در متر مکعب اندازه گیری شده است اما متوسط سالیانه رسوب حوزه ۱۲۰۰ تن در کیلومتر مربع در سال برآورد گردیده است.

تولید مواد معلقه و املاح محلول در حوزه آبریز، بستگی کامل به تولید و میزان رواناب دارد و جریانهای سیلابی در فصول خاص نقش مهمی را بازی میکند. فقط ۱۰/۵ درصد آب و ۳/۵ درصد مواد معلقه رودخانه شاپور در ماههای تابستان (خرداد تا شهریور) جریان می یابد.

تحلیل های همبستگی بین مواد معلقه و املاح محلول بادی رودخانه نشان میدهد که غلظت مواد معلقه با افزایش دبی زیاد میشود، در صورتیکه غلظت املاح محلول کاهش می یابد (شکل های ۸-۳ و ۱۳-۲). جریان پایه رودخانه که دارای غلظت بالایی از NaCl میباشد، بطور عمده از آبهای زیرزمینی (چشمه ها و قنوات) سرچشمه میگیرد و شوری آب رودخانه را در فعل تابستان افزایش می دهد. در مواقع سیلابی بعلت رفیق شدن جریان پایه، غلظت املاح محلول کاهش زیادی پیدا میکند.

فصل سوم، در رابطه با مدیریت شوری در حوزه آبریز میباشد. در حوزه آبریز رودخانه های شاپور و دالکی، میتوان با انجام اقدامات مهندسی، شوری آب رودخانه را کاهش داد. این اقدامات عبارتند از:

- جلوگیری از ورود منابع شور به رودخانه و حذف آن از حوزه.
 - اقداماتی که اثر شوری آب رودخانه را کاهش دهد.
- در بین اقدامات حذف منابع شور کننده، جمع آوری و تبخیر آبهای شور در راستخه های ذخیره و تبخیر آن، بعلت بالابودن نرخ تبخیر در منطقه از نظر اقلیمادی توجیه پذیرترین آنهاست. با اجرای طرح های پیشنهادی این روش، میزان نمک سالیانه رودخانه های شاپور و دالکی به ترتیب ۸۲۰۰۰ و ۲۹۴۰۰۰ (۷/۴ و ۱۷/۲ درصد) کاهش می یابد.
- در بین اقدامات کاهش اثر شوری، احداث سد مخزنی و مدیریت مخزن موفق ترین

آنهاست. سدمخزنی پیشنهادی جرعه روی رودخانه شاپور برای ارزیابی این روش مدیریت شوری مورد استفاده قرار گرفته است. محاسبات شبیه سازی دوره ۴ ساله ۸۵-۱۹۸۲ مخزن سدجره (مطابق شکل ۷) نشان میدهد که شوری زیاد آب رودخانه در فصول بهار و تابستان به حدود بین ۱۵۰۰ تا ۲۴۰۰ میلیگرم در لیتر کاهش می یابد. این کاهش شوری، امکان کشت محصولات پر در آمد مانند چغندر قند و صیفی جات را فراهم خواهد آورد. سه فصل بعدی رساله به رفتار، مدل سازی و مدیریت مخزن سدجره اختصاص دارد. پدیده ای که کیفیت آب رابه میزان قابل توجهی در مخزن سدمخزین می نماید، لایه ای شدن آب (Stratification) است. این پدیده تحت تاثیر عوامل آب و هوایی و سه خاصیت اصلی آب ورودی به مخزن میباشد: درجه حرارت، املاح محلول و مواد معلقه رسوبی. مواد معلقه رسوبی روی دانسیته آب ورودی تاثیر داشته و لذا روی اختلاط لایه ای شدن آب در مخزن اثر می گذارد. نقش مواد معلقه رسوبی بندرت در سیمولاسیون کیفی آب مخزن در نظر گرفته شده است. در بخش ۲-۴ یک روش برای محاسبه دانسیته آب تحت تاثیر حرارت، املاح محلول و مواد معلقه رسوبی معرفی شده است.

در قسمت اول فصل پنجم روابطی برای تشریح جریان آب ورودی حاوی مواد رسوبی ارائه شده است. این جریان در کف بستر مخزن حرکت نموده (جریان ثانویه، جریان غلیظ رسوبی Turbidity current نامیده میشود) و ممکن است مواد خود را روی کف بستر باقی گذاشته و یا مواد رسوبی را از کف بستر کنده و بدین ترتیب روی دینامیک خود اثر بگذارد. نوع جریان ثانویه عمدتاً "بستگی به شیب کف دارد. برای بوجود آمدن جریان فوق بحرانی که شرط لازم برای کندن مواد رسوبی از کف میباشد شیب کافی بستر ضروری است. در مخازن سدها معمولاً شیب کف بستر کم بوده و جریان غلیظ رسوبی از نوع رسوب گذار میباشد. اعمال روابط اساسی جریان غلیظ رسوبی (معادلات ۵/۴ تا ۵/۶) در مخزن سدجره نقش شیب کف بستر را در تعیین نوع جریان غلیظ مشخص می نماید (شکل ۲-۵).

رفتار جریان غلیظ رسوبی در شیب های ملایم بوسیله محققین مختلفی مورد بررسی قرار گرفته است. مشخصه جریان در شیب های ملایم، این است که عدد ریچاردسون بزرگتر از رقم ۱ میباشد و جریان در حالت نرمال میباشد. لذا معادلات ۵/۴ تا ۵/۶ را میتوان با فرضیات زیر ساده کرد:

سرعت جریان زیرین نسبت به مسافت مسیر آن تغییر عمده ای نمی کند (جریان یونیفرم) و ذرات مواد رسوبی با رسوب گذاری و یار رسوب کنی ناچیز در امتداد کف بستر بحالت معلق باقی می مانند. معادله مقدار حرکت (مونتگم) بدست آمده با سایر روابط پیشنهادی مقایسه شده است (جدول ۱-۵).

بمنظور مقایسه عملکرد معادلات مذکور در فوق با اندازه گیری های واقعی، جریان مواد رسوبی بدخل مخزن سدلتیان، ایران مربوط به سیلاب ۱۹۸۴/۴/۲۵ مورد بررسی قرار گرفته است (شکل ۳-۵). وقتی جریان غلیظ رسوبی در داخل مخزن پیش میرود، سرعت آن کاهش یافته و ابتدای ذرات درشت تر رسوب کرده ولی ذرات ریز تر به جریان خود ادامه میدهند تا اینکه پس از رسوب گذاری ذرات بزرگتر از ۰.۲ میلیمتر، جریان به یک حالت تعادل میرسد. در آن حالت سرعت متوسط آن در حدود ۶ تا ۸ سانتیمتر در ثانیه باقی می ماند و بالاخره جریان غلیظ رسوبی به سمت پائین و به طرف

دیواره سدبارسوبگذاری ناچیز حرکت می نماید. نتایج اندازه گیری های انجام شده بارقام بدست آمده از معادلات مومنت همخوانی دارد (شکل ۴-۵).

در قسمت آخر بخش ۱-۵ روابط جریان غلیظ رسوبی در مقایسه با جریان غلیظ بدون حاوی مواد معلقه (Density current) با اعمال آنها برای مخزن سدجره مورد بررسی قرار گرفته و نتایج شبیه سازی برای شرایط سیلابی و شرایط نرمال جریان در شکل ۵-۵ ارائه شده است. واضح است که وجود ذرات مواد معلقه بطور قابل ملاحظه ای سرعت و نیروی شناوری (Buoyancy) جریانهای زیرین را بویژه در بی های بالا، افزایش می دهد. اثر مواد رسوبی عمدتاً "در شرایط اولیه (نقطه شروع جریان زیرین) وجود دارد و میتوان نتیجه گرفت که رفتار جریان غلیظ رسوبی در شیب های ملایم و بارسوب گذاری و رسوب کنی ناچیز اساساً شبیه رفتار جریان غلیظ بدون مواد معلقه میباشد.

قسمت دوم فصل پنجم در رابطه با مدل ریاضی کیفیت آب مخزن سدجره با لانت تاثیر حرارت، املاح محلول و مواد رسوبی میباشد. مدل دینامیکی DYRESM (Version 6.4) که اصل آن بوسیله Imberger و دیگران در سال ۱۹۷۸ تهیه شده، مورد استفاده قرار گرفته و با تغییراتی جهت شبیه سازی توزیع شوری در مخزن سدجره با لایه کاربرد شده است. در کاربرد مدل یک بعدی DYRESM، ابتدا بایستی مشخص شود که آیا شرایط مخزن با مدل یک بعدی تطبیق میکند؟ با این تطبیق نتیجه گرفته میشود که مشخصات مخزن سدجره با محدودیت های تئوریک مدل یک بعدی مطابقت دارد (جدول ۴-۵).

یک الگوریتم برای جریان واردشونده حاوی مواد رسوبی بر اساس روابط شرح داده شده در قسمت ۱-۵ ساخته شده است. در این روش اثر ذرات رسوبی روی دانسیته جریان زیرین، رقیق شدن آن بوسیله آب مخزن و همچنین نفوذ آنقی آن (Intrusion) در بدنه مخزن در نظر گرفته شده است. توزیع عمودی مواد رسوبی در مخزن مدل نگردیده است. بدین ترتیب کاربرد مدل فقط برای پارامترهایی از کیفیت که با ذرات معلقه عکس العمل فیزیکی و بیوشیمیایی ایجاد نمایی نمایند (مانند شوری) توصیه میشود.

مدل DYRESM با آماریکاله ۱۹۸۳ و ۴ ساله ۸۵-۱۹۸۳ با و بدون اثر مواد رسوبی اجرا شده است (شکل های ۱۱-۵ و ۱۲-۵)، یک توضیح فیزیکی برای نتایج اجرای مدل وجود دارد: جریان آب زمستانی سرد و با شوری کمتر میباشد و لذا دانسیته آن از دانسیته آب مخزن بیشتر است. این آب در لایه های زیر مخزن فرومی راند و موجب تغییر حرارت از $17/8$ تا $14/4$ درجه سانتیگراد و شوری از ۱۹۵ تا ۱۶۵ میلیگرم در لیتر می گردند. در این دوره یک لایه بندی ضعیف در مخزن تشکیل میشود. در تابستان آب مخزن بشدت لایه ای میشود (درجه حرارت $14/5$ الی 25 درجه سانتیگراد، شوری بین ۱۴۷ تا ۱۹۵ میلیگرم در لیتر و دانسیته بین $998/3$ الی $1000/4$ کیلوگرم در مترمکعب). در این حالت ترموکلین (Thermocline) تشکیل میشود که مانع اختلاط لایه های زیرین (Hypolimnion) و روئین (Epilimnion) میگردد. جریان ورودی شور تابستانی در تراز ترموکلین وارد میشود و تشکیل یک لایه نسبتاً نازک آب شور در قسمت بالای مخزن میدهد. از پایش تا شب شعشع کاهش یافته و درجه حرارت لایه روئین پائین آمده وضامت آن افزایش می یابد. انهاییه در اوخر پایش این

حالت ناپایدار در مخزن ایجاد یک چرخش (Overturn) می نماید و مخزن تا عمق ۸ متر یکنواخت میگردد.

وقتی اثر مواد رسوبی را در نظر بگیریم، دانسیته آب ورودی به مخزن افزایش می یابد و جریان آب خیلی سریع در لایه های زیرین نفوذ میکند. بدین ترتیب لایه زیرین شورتر و سردتری بوجود می آید که در طول سال به همین شکل باقی می ماند. در محاسبات شبیه سازی سال ۱۹۸۲ شوری لایه های زیرین آب تا ۲۰۰ میلیگرم در لیتر و حرارت به میزان ۵/۵- تا ۲/۵ درجه سانتیگراد و دانسیته به میزان ۳/۴- کیلوگرم در متر مکعب افزایش می یابد. تغییر پروفیل شوری آب مخزن نیز باعث تغییر در شوری آب تخلیه شده (افزایش ۱۵۰ میلیگرم در لیتر در خروجی پائین) میگردد (شکل ۱۳-۵) که تاثیر مهمی در آبیاری ندارد، معذاکمل بار نمک مخزن تابع توزیع شوری ناشی از مواد رسوبی ورودی میباشد (جدول ۲-۵ و ۳-۵).

حوزه رودخانه شاپور به شدت از شوری آب رنج می برد. بنابراین در یک سال متوسط تقریباً ۱/۲ میلیون تن نمک وارد مخزن سد جره میشود. مدیریت دقیقی جهت کاهش شوری فزاینده آب و در صورت امکان بهبود کیفیت آب ذخیره شده در مخزن سد لازم میباشد.

در فعل ششم، مدل DYRESM جهت بررسی عکس العمل مخزن سد جره به استراژی های مختلف مدیریت مخزن و همچنین برای شبیه سازی روند شوری در یک دوره طولانی مدت بکار برده شده است. تلاش اولیه برای بهبود کیفیت آب مخزن سد بر این اساس است که در تابستان و اوائل پاییز و قبل از دبی های بالای زمستانی، حتی الامکان یابایستی آب از مخزن تخلیه شود (سیاست Scouring) و یا قبل از ورود جریان آب شور به مخزن به پائین دست انحراف داده شود (سیاست By-Passing) با استفاده از برنامه شبیه سازی RELEAS ارقام مختلفی برای تخلیه و یا انحراف آب امتحان شد و برای دوره شبیه سازی ۸۶-۱۹۸۲، مقدار ۱۵۸ میلیون متر مکعب از آب ورودی مربوط به شوری های بالاتر از ۳۰۰۰ میلیگرم در لیتر را میتوان بدون اینکه اثری در آب پائین دست داشته باشد، انحراف داد (شکل ۳-۶ انحراف IV).

انحراف شورترین قسمت آب ورودی موجب بهبود قابل توجه کیفیت آب تخلیه و مخزن خواهد شد. وقتی که انحراف آب بالای ۳۰۰۰ میلیگرم در لیتر انجام شود (جدول ۱-۶-۱، Diversion IV)، متوسط شوری مخزن تا ۸/۷ درصد (معادل ۱۹۸ میلیگرم در لیتر) و آب تخلیه شده تا ۱۸ درصد (معادل ۳۸۷ میلیگرم در لیتر) کاهش می یابد. در پایان محاسبات شبیه سازی، کل نمک انباشته شده به میزان ۷۲۰۰۰ تن کاهش و ۸/۵ درصد بهبود نتیجه عدم اعمال سیاست مدیریتی میباشد. با انجام چنین سیاستی برای مخزن جره اقدام مهندسی مهمی لازم نخواهد بود.

کنترل کیفیت آب مخزن با عمل Scouring با ترازهای پیشنهادی آبیگری اشکنتری دارد (جدول ۱-۶-۱ Scour I, II, IIa). حداکثر استفاده با Scour III بدست می آید که در آن تخلیه آبهای ورودی تابستانی در یک تراز بالا قبل از اختلاط با آب اطراف میباشد. نتیجه این سیاست حداکثر کاهش شوری مخزن و آب تخلیه (در پایان محاسبات شبیه سازی) حدود ۴/۶ درصد (معادل ۸۵ میلیگرم در لیتر) و کاهش انباشت نمک به میزان ۲۶۰۰۰ تن است. وقتی که ترکیب سیاست By-Passing و Scouring توأم " امتحان شد، Scour IV، انباشت نمک در مخزن به میزان قابل توجهی کاهش

می یابد. بابت آلودگی کاهش حداکثر (در پایان محاسبات شبیه سازی)، بهبود کیفیت آب برابر ۱۳/۷ درصد (معادل ۲۴۸ میلیگرم در لیتر) در شوری مخزن و ۱۳/۴ درصد (معادل ۲۴۸ میلیگرم در لیتر) در آب تخلیه و ۱۱۷۰۰۰ تن در کاهش انباشت نمک در مخزن خواهد بود. بهر حال اعمال این سیاست مستلزم تخلیه و انحراف آب به میزان زیادی خواهد بود که نتیجه "سطح آب مخزن در حد زیادی پائین انداخته میشود و اطمینان تامین آب مورد نیاز کاهش میدهد (شکل ۳-۶).

برای دوره شبیه سازی ۸۶-۱۹۸۲، تغییرات شوری آب ورودی (از ۷۰۰ تا ۴۰۰ میلیگرم در لیتر) کاهش یافته و تغییرات شوری مخزن محدود به طیف ۱۴۵ تا ۲۴۱۵ میلیگرم در لیتر میگردد. موثرترین سیاست مدیریتی، انحراف آب ورودی با شوری بیش از ۳۰۰ میلیگرم در لیتر این رقم را به حدود ۱۴۳ تا ۲۲۰ میلیگرم در لیتر کاهش میدهد.

روند طولانی مدت شوری در مخزن سدره با انجام محاسبات شبیه سازی دوره ۱۵ ساله ۹۰-۱۹۷۵ مورد مطالعه قرار گرفته است (شکل ۹-۶) و واضح است که شوری مخزن بطور عمده تابع تغییرات دبی سالیانه است. آب های زیاد با کیفیت بالای سالهای تر، مخزن را شستشو میدهد در حالیکه آبهای شور سالهای خشک کیفیت را خراب می نماید. در طول ۱۵ سال محاسبه شبیه سازی، شوری آب مخزن در طیفی بین ۱۵۰ تا ۲۶۰۰ میلیگرم در لیتر تغییر می نماید. محاسبات بیان نمک نشان میدهد که فقط یک جزء کوچکی از نمک ورودی در مخزن باقی مانده است و قسمت عمده آن با سرریز آن و آب آبیاری تخلیه شده است (جدول ۳-۶). در ضمیمه ۴ نشان داده شده است که بخش (Diffusion) نمک از تشکیلات شور میوسن کف مخزن ناچیز خواهد بود.

Appendix 1

SALINITY AND SALINIZATION

A1.1 Major properties of salt structures

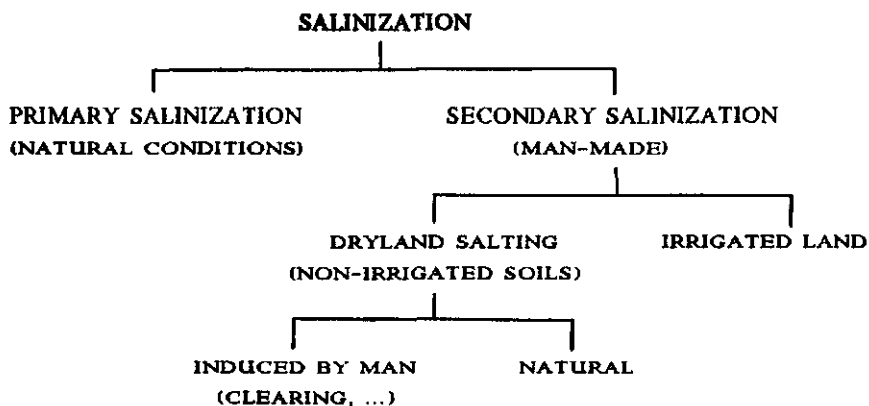
Salt has three major properties which cause it to play a dominant role in sedimentary basins (Lerche and O'Brien, 1987):

1) On a geological time scale salt flows as a nearly incompressible fluid under applied stress, thereby both distorting sedimentary patterns and influencing further basin evolution.

2) Salt has a density approximating 2.2 g/cm^3 , which is intermediate between sedimentary densities at deposition ($1.6\text{-}1.9 \text{ g/cm}^3$) and the densities of fully compacted sedimentary formations ($2.6\text{-}2.8 \text{ g/cm}^3$). The density of salt varies little during burial under an increasing overburden weight. Thus at some point in a basin's evolution the salt will become buoyant and will attempt to rise up through the overlying formations.

3) Salt has a thermal conductivity approx. 3 times greater than that of "typical" sedimentary formations and so salt bodies act as conduits for heat transport from depth. In the vicinity of the salt local thermal effects, caused or modified by this conductivity contrast, impact on chemical precipitation and dissolution, hydrocarbons maturity, and fluid flow.

A1.2 Cause of salinization



Primary salinization: non-man induced (under natural conditions) salinity is denoted as primary or natural salinization (van der Molen, 1985).

Secondary salinization: refer to areas where soluble salt accumulated as a consequence of irrigation, agricultural practices or the clearing of native vegetation.

A1.3 Water resources salinity classification

Table A1.1 Water resources salinity classification (W. Australian Water Resources Council, 1986)

Category	Resource salinity
Fresh	less than 500 mg/l TSS
Marginal	greater than 500 mg/l TSS but less than 1500 mg/l TSS
Brackish	greater than 1500 mg/l TSS but less than 5000 mg/l TSS
Saline	greater than 5000 mg/l TSS

Note: Usually there is a small difference between TDS and TSS (Total Soluble Salts), due to the non-major ions.

A1.4 References list on salt diapirism in the study area (more references are cited in the text, section 2.1)

Barton, D.C., 1933. Mechanics of formation of salt dome with special reference to Gulf Coast, salt domes of Texas and Louisiana. Amer. Assoc. Petrol. Geol. Bull., 17:1025-1083.

Berner, H., Ramberg, H., and Stefanson, O, 1972. Diapirism in theory and experiments. Tectonophysics, 15:197-218.

Bishop, R.S., 1978. Mechanism for emplacement of piercement diapirs. Amer. Assoc. Petrol. Geol. Bull., 62:1561-1583.

Dixon, J.M., 1975. Finite strain and progressive deformation in models of diapiric structures. Tectonophysics, 28:89-124.

Ewing, m., and Ewing, J.I., 1962. Rate of salt dome growth. Amer. Assoc. Petrol. Geol. Bull., 46:708-709.

Falcon, N.L., 1961. Major earth-flexuring in the Zagros Mountains of south-west Iran. Geol. Soc. London Quart. J., 117:367-376.

Furst, M., 1976. Tektonik und diapirismus der ostlichen Zagrosketten. Z. dt. Geol. Ges., 127:183-225.

- Gansser, A., 1960. Uber Schlammvulkane und Salzdomo. Vjschr. Naturf. Ges. Zurich, 105:1-46.
- Gray, K.W., 1950. A tectonic window in South-western Iran. Geol. Soc. London Quart. J., 105:189-223.
- Gussow, W.C., 1968. Salt Diapirism: Importance of temperature, and energy source of emplacement. In: Braunstein, J., and O'Brien, G.D., eds., Diapirism and Diapirs. Amer. Assoc. Petrol. Geol. Memoir, 8:16-52.
- Halbouty, M.T., 1979. Salt domes, Gulf region, United State and Mexico: Houston, Texas. Gulf Publishing Co., 561 pp.
- Harrison, J.V., 1930. The geology of some salt plugs in Laristan (Southern Persia). Geol. Soc. London Quart. J., 86:463-522.
- Harrison, J.V., 1931. Salt domes in Persia. J. Inst. Petrol. Tech., 17:300-320.
- Harrison, J.V., 1956. Comments on salt domes. Verh. Ned. Geol. Mijnb. Genoot., 14:1-8.
- Haynes, S.J., and McQuillan, H., 1974. Evolution of the Zagros suture zone, southern Iran. Geol. Soc. Amer. Bull., 85:739- 744.
- Humphery, W.E., 1958. Diapirs and Diapirism in Persia and North Africa. Review. Amer. Assoc. Petrol. Geol. Bull., 42:1736-1744.
- Kent, P.E., 1968. In review: Salt domes, Gulf region, United Stats and Mexico by M.T. Halbouty. J. Inst. Petrol. Techn., 54:531, 37A-38A.
- Kent, P.E., 1970. The salt plugs of the Persian Gulf region. Trans. Leicester Lit. & Phil. Soc., 64:56-88.
- King, W.B.R., 1930. Notes on the Cambrian fauna of Persia. Geol. Mag., 67:316-372.
- Lees, G.M., 1927. Salzgletscher in Persia. Mitt. Geol. Ges. Wien. 22:29-34.
- Lees, G.M., 1931. Salt dome depositional and deformational problems. J. Inst. Petrol. Tech., 17:259-280.
- Lehner, E., 1945. The Persian salt formations. Nat. Acad. Sci. India, Proc., Sect. b, 14:6, 249-258.
- Ramberg, H., 1966. Experiment and theoretical study of salt dome evolution. In: Rau, J.L., and Dellwig, L.F., eds., Symposium on salt, 3rd: Cleveland, Ohio, Northem Ohio Geological Society, pp. 261-270.
- Stocklin, J., 1968a. Salt deposits of Middle East. Geol. Soc. Amer. Spec. Pap., 88:157-181.

Stocklin, J., 1968b. Structural history and tectonics of Iran: a review. Amer. Assoc. Petrol. Geol. Bull., 52:1229-1258.

Talbot, C.J., 1978. Halokinesis and thermal convection. Nature, 273:5665, 739-741.

Talbot, C., 1979. Fold trains in a glacier of salt in Southern Iran. Structural Geology, 1:5-18.

Talbot, C.J., and Jarvis, R.J., 1984. Age, budget and dynamics of an active salt extrusion in Iran. Journal of Structural Geology, 6:521-533.

Talbot, C.J., and Rogers, E.A., 1980. Seasonal movements in a salt glacier in Iran. Science, 208:395-397.

Walther, H.W., 1968. The genesis of the Iron Ore of the Hormuz Series near Bandar Abbas (Cambrian, south-east Iran). Paper presented at 23th Int. Geol. Cong., Prague.

Appendix 2

TURBIDITY CURRENT RELATIONSHIPS

A2.1 Governing two-dimensional equations

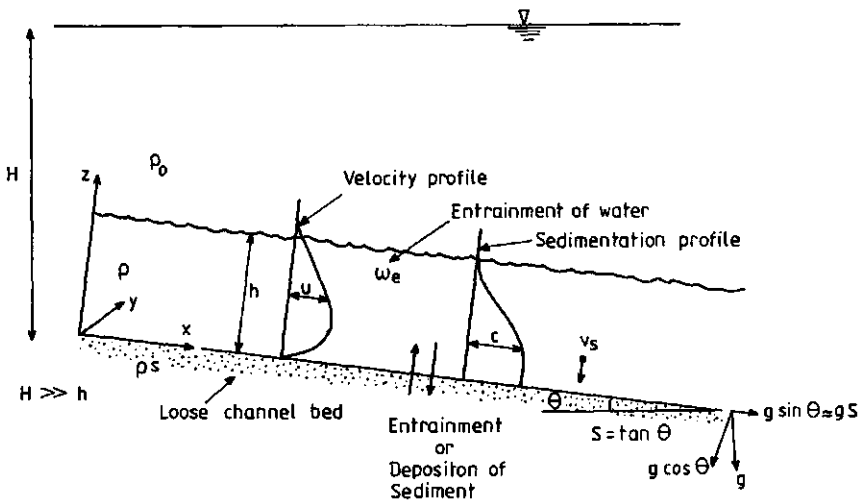


Fig. A2.1a Turbidity current and definition of parameters.

A rectangular cross-section is considered (Fig. A2.1). The sediment particles are assumed to be non-cohesive and to have uniform settling velocity. Moreover, sediment concentration is assumed to be small enough to treat the mixture as a Newtonian fluid ($\rho < 1.07 \text{ g/cm}^3$). The quiescent water above the current is assumed to be infinitely deep ($H \gg h$), consequently no account has been made for counter-currents in the overlying waters. The bed has a constant slope S ; the x -coordinate is directed downstream and parallel to the bed, the Z -coordinate is directed upward normal to the bed. Bed load transport and related phenomena such as additional shear stress due to bed transforms are not considered. Some more assumptions are made, which will be described during the derivation of relationships.

To analyse the turbidity current at least three basic relationships will be used: (1) a momentum equation; (2) conservation of fluid mass; and (3)

conservation of sediment mass. Parker (1982) and Akiyama and Stefan (1985) showed that the equation of the turbulent energy could be reduced to Bagnold's auto-suspension concept.

1) Equation of balance of momentum:

$$\frac{\partial \bar{\rho} \bar{u}_i}{\partial t} + \frac{\partial \bar{\rho} \bar{u}_j \bar{u}_i}{\partial x_j} = \frac{\partial \bar{F}_{ji}}{\partial x_j} + \bar{\rho} g_i \quad (\text{A2.1})$$

where \bar{u}_i denotes the instantaneous flow velocity of the mixture, F_{ij} denotes the stress tensor, $\bar{\rho}$ is the density of the mixture, and $g = (g \sin \theta, 0, -g)$ in which $g \cos \theta$ is approximated to g , because θ is very small. The constitutive equation for stress in incompressible fluid is

$$\bar{F}_{ij} = -\bar{P}^* \delta_{ij} + \mu \frac{\partial \bar{u}_i}{\partial x_j} \quad (\text{A2.2})$$

where \bar{P}^* is instantaneous pressure, μ the dynamic viscosity, and δ_{ij} the Kronecker delta. Substitute (A2.2) into (A2.1) to obtain the Navier-Stokes equation, (A2.3)

$$\frac{\partial \bar{\rho} \bar{u}_i}{\partial t} + \frac{\partial \bar{\rho} \bar{u}_i \bar{u}_j}{\partial x_j} = -\frac{\partial \bar{P}^*}{\partial x_i} + \mu \frac{\partial^2 \bar{u}_i}{\partial x_j \partial x_j} + \bar{\rho} g_i \quad (\text{A2.3})$$

The density of the suspension is given by $\bar{\rho} = \rho_0 + \rho_0 R \bar{c}$, where R is the submerged specific density of sediment particle, $R = (\rho^s - \rho_0) / \rho_0$, ρ_0 the reference density, and \bar{c} the volumetric concentration of suspended sediment.

$$\frac{\rho_0 \partial \bar{u}_i}{\partial t} + \frac{\rho_0 R \partial \bar{c} \bar{u}_i}{\partial t} + \frac{\rho_0 \partial \bar{u}_i \bar{u}_j}{\partial x_j} + \frac{\rho_0 R \partial \bar{c} \bar{u}_i \bar{u}_j}{\partial x_j} = -\frac{\partial \bar{P}^*}{\partial x_i} + \mu \frac{\partial^2 \bar{u}_i}{\partial x_j \partial x_j} + (\rho_0 + \rho_0 R \bar{c}) g_i$$

Introduce the kinematic viscosity $\nu = \mu / \rho_0$ to obtain (A2.4)

$$\frac{\partial \bar{u}_i (1 + R \bar{c})}{\partial t} + \frac{\partial \bar{u}_i \bar{u}_j (1 + R \bar{c})}{\partial x_j} = -\frac{1}{\rho_0} \frac{\partial \bar{P}^*}{\partial x_i} + \nu \frac{\partial^2 \bar{u}_i}{\partial x_j \partial x_j} + (1 + R \bar{c}) g_i \quad (\text{A2.4})$$

We assume that the pressure consists of a hydrostatic and a dynamic part, $\tilde{P}^* = \tilde{P} + P_s$, where hydrostatic pressure $\partial P_s / \partial x_i = \rho_0 \delta_{iz}$.

$$-\frac{1}{\rho_0} \frac{\partial \tilde{P}^*}{\partial x_i} = -\frac{1}{\rho_0} \left(\frac{\partial \tilde{P}}{\partial x_i} + \rho_0 g_z e_i^z \right) \quad e_i^z = \langle 0, 0, 1 \rangle$$

$$-\frac{1}{\rho_0} \frac{\partial \tilde{P}^*}{\partial x_i} + (1 + R\tilde{c}) g_i = -\frac{1}{\rho_0} \frac{\partial \tilde{P}}{\partial x_i} - g_z e_i^z + (1 + R\tilde{c}) g_z e_i^z$$

$$-\frac{1}{\rho_0} \frac{\partial \tilde{P}}{\partial x_i} + (1 + R\tilde{c}) g_i = -\frac{1}{\rho_0} \frac{\partial \tilde{P}}{\partial x_i} + R\tilde{c} g_i \quad (\text{A2.5})$$

Substitute (A2.5) in (A2.4) to obtain (A2.6)

$$\frac{\partial \tilde{u}_i (1 + R\tilde{c})}{\partial t} + \frac{\partial \tilde{u}_i \tilde{u}_j (1 + R\tilde{c})}{\partial x_j} = -\frac{1}{\rho_0} \frac{\partial \tilde{P}}{\partial x_i} + \nu \frac{\partial^2 \tilde{u}_i}{\partial x_j \partial x_j} + R\tilde{c} g_i \quad (\text{A2.6})$$

Using the Boussinesq approximation, it is allowed to neglect $R\tilde{c}$ compared to one in the left hand side of the equation (A2.6). Integrate (A2.6) over time using the following definitions to obtain (A2.7)

$$\tilde{u}(\tilde{t}, x) = u(t, x) + \hat{u}(\tilde{t}, x), \quad \tilde{P}(\tilde{t}, x) = P(t, x) + \hat{P}(\tilde{t}, x), \quad \tilde{c}(\tilde{t}, x) = c(t, x) + \hat{c}(\tilde{t}, x)$$

where u, P, c are the mean values and $\hat{u}, \hat{P}, \hat{c}$ are fluctuating parts.

$$\frac{\partial u_i}{\partial t} + \frac{\partial u_i u_j}{\partial x_j} + \overline{\frac{\partial \hat{u}_i \hat{u}_j}{\partial x_j}} = -\frac{1}{\rho_0} \frac{\partial P}{\partial x_i} + \nu \frac{\partial^2 u_i}{\partial x_j \partial x_j} + R c g_i \quad (\text{A2.7})$$

$$\tau_{ij} = -\overline{\hat{u}_i \hat{u}_j} \rho_0$$

τ_{ij} denotes the Reynolds stress.

$$\frac{\partial u_i}{\partial t} + \frac{\partial u_i u_j}{\partial x_j} = -\frac{1}{\rho_0} \frac{\partial P}{\partial x_i} + \frac{\partial}{\partial x_j} \left(\frac{\tau_{ij}}{\rho_0} + v \frac{\partial u_i}{\partial x_j} \right) + R C g_i \quad (\text{A2.8})$$

Assumptions: consider two-dimensional flow $x_i = (x, z)$ and $u_i = (\tilde{u}, \tilde{w})$; within the turbidity current $u \gg w$ and $\partial/\partial z \gg \partial/\partial x$; the turbidity current is assumed to be fully turbulent, with all viscous terms negligible except the viscous dissipation due to the turbulence and $|\tilde{c}w'| \gg |\tilde{c}'u|S$. Under these constraints, (A2.8) at z-component gives

$$\frac{\partial w}{\partial t} + \frac{\partial w u}{\partial x} + \frac{\partial w^2}{\partial z} = -\frac{1}{\rho_0} \frac{\partial P}{\partial z} + \frac{\partial}{\partial x} \left(\frac{\tau_{zx}}{\rho_0} + v \frac{\partial w}{\partial x} \right) +$$

①
②
③
④
⑤

$$\frac{\partial}{\partial z} \left(\frac{\tau_{zz}}{\rho_0} + v \frac{\partial w}{\partial z} \right) + R C g_z \quad (\text{A2.9})$$

⑥
⑦

Neglect all viscous terms (term 5 and 6) and inertial terms (term 1, 2, 3) and integrate from z to h to obtain (A2.10)

$$\frac{1}{\rho_0} (P|_h - P|_z) = R g_z \int_z^h c dz$$

$$P = \rho_0 R g \int_z^h c dz \quad (\text{A2.10})$$

(A2.8) at x-component gives

$$\frac{\partial u}{\partial t} + \frac{\partial u^2}{\partial x} + \frac{\partial u w}{\partial z} = -\frac{1}{\rho_0} \frac{\partial P}{\partial x} + \frac{\partial}{\partial x} \left(\frac{\tau_{xx}}{\rho_0} + \frac{\partial u}{\partial x} \right) +$$

$$\frac{\partial}{\partial z} \left(\frac{\tau_{xz}}{\rho_0} + \frac{\partial u}{\partial z} \right) + R C g_x \quad (\text{A2.11})$$

From viscous terms keep only $\partial \tau_{xz} / \partial z = \partial \tau / \partial z$, and $g_x = gS$

$$\frac{\partial u}{\partial t} + \frac{\partial u^2}{\partial x} + \frac{\partial uw}{\partial z} = -Rg \frac{\partial}{\partial x} \int_z^h cdz + \frac{\partial \tau}{\rho_0 \partial z} + Rcs_g \quad (\text{A2.12})$$

Integrate (A2.12) in z-direction (using Leibnitz rule)

$$\frac{\partial}{\partial t} \int_0^h u dz - u|_h \frac{\partial h}{\partial t} + \frac{\partial}{\partial x} \int_0^h u^2 dz - u^2|_h \frac{\partial h}{\partial x} + uw|_h - uw|_0 = \quad (\text{A2.13})$$

$$-Rg \frac{\partial}{\partial x} \int_0^h \left(\int_z^h cdz \right) dz + Rg \left(\int_z^h cdz \right) |_h \frac{\partial h}{\partial x} + \frac{\tau|_h - \tau|_0}{\rho_0} + RgS \int_0^h cdz$$

Introduce U , C as layer-averaged values (Fig. A2.1b), $U = 1/h \int_0^h u dz$, and $C = 1/h \int_0^h cdz$, and $\int_z^h cdz \approx (h-z)C$ to obtain (A2.14)

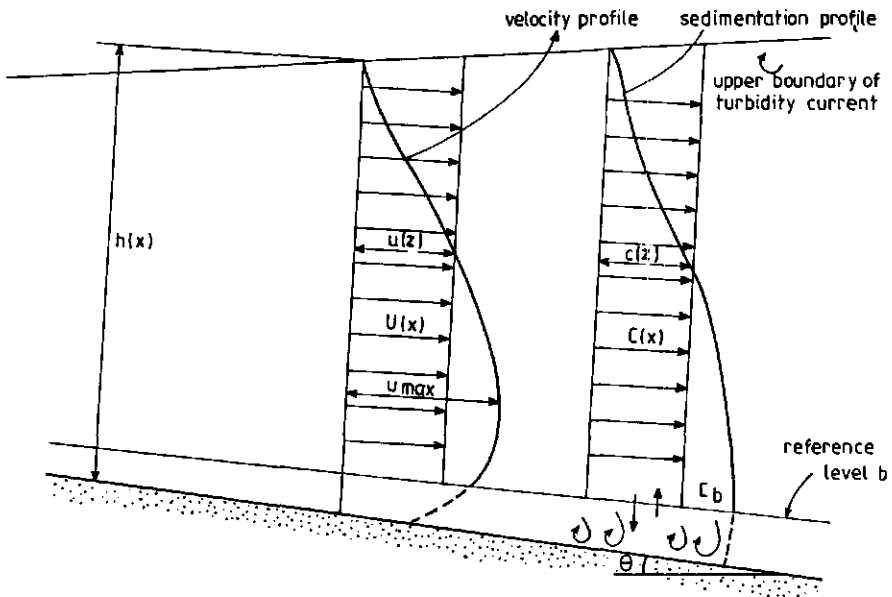


Fig. A2.1b Velocity and sediment concentration profiles and definition of layer-averaged values.

$$\frac{\partial uh}{\partial t} - u|_h \frac{\partial h}{\partial t} + \frac{\partial U^2 h}{\partial x} + \frac{\partial}{\partial x} (\overline{u'u'h}) - U^2|_h \frac{\partial h}{\partial x} + uw|_h - uw|_0 =$$

①
②
③
④
⑤
⑥
⑦

$$-\frac{1}{2} Rg \frac{\partial Ch^2}{\partial x} + \frac{\tau|_h}{\rho_0} - \frac{\tau|_0}{\rho_0} + RChgS \quad (\text{A2.14})$$

⑧
⑨
⑩
⑪

Terms 2, 4, 5, 6, 7, and 9 are negligible under the constraints described. Term 10 denotes the bed shear stress and is expressed as

$$\tau|_0 = \rho_0 u_*^2 = \rho_0 C_D U^2$$

where C_D is the drag coefficient, and u_* the shear velocity. (A2.15) is the two-dimensional, layer averaged equation of balance of momentum for a turbidity current.

$$\frac{\partial Uh}{\partial t} + \frac{\partial U^2 h}{\partial x} = -\frac{1}{2} Rg \frac{\partial (Ch^2)}{\partial x} - C_D U^2 + RChgS \quad (\text{A2.15})$$

2. Equation of balance of fluid mass :

$$\frac{\partial \bar{\rho}}{\partial t} + \nabla \cdot (\bar{\rho} \underline{U}) = 0 \quad (\text{A2.16})$$

Average (A2.16) over time and neglect $\rho'u'$ to obtain (A2.17)

$$\frac{\partial \bar{\rho}}{\partial t} + \nabla \cdot (\bar{\rho} \underline{U}) = 0 \quad (\text{A2.17})$$

and neglect the variation in y-direction

$$\frac{\partial \bar{\rho}}{\partial t} + \frac{\partial \bar{\rho} u}{\partial x} + \frac{\partial \bar{\rho} w}{\partial z} = 0 \quad (\text{A2.18})$$

Integrate (A2.18) over z (using Leibnitz rule), and introduce the layer-averaged $\bar{\rho}$ and U , $\bar{\rho} = 1/h \int_0^h \rho dz$ and $U = 1/(\bar{\rho}h) \int_0^h \rho u dz$ to obtain (A2.19)

$$\frac{\partial \bar{\rho} h}{\partial t} - \frac{\partial h}{\partial t} \rho|_h + \frac{\partial \bar{\rho} U h}{\partial x} - \frac{\partial h}{\partial x} \mu \rho|_h + \rho w|_h - \rho w|_0 = 0 \quad (\text{A2.19})$$

①
②
③
④
⑤
⑥

The first two terms can be omitted with the steady state assumption, the term 4 and 6 are negligible and term 5 denotes the entrainment velocity (ω_e) with negative direction along the z axis

$$w|_h = \omega_e = E_\omega U \quad (\text{A2.20})$$

3. Equation of balance of sediment mass :

$$\frac{\partial \tilde{c}}{\partial t} + \frac{\partial \tilde{V}_i \tilde{c}}{\partial x_i} = 0 \quad (\text{A2.21})$$

where \tilde{V}_i is the instantaneous velocity of sediment phase and is equal to velocity of fluid (\tilde{u}_i) minus the falling velocity of particles V_s

$$\frac{\partial \tilde{c}}{\partial t} + \frac{\partial [(\tilde{u}_i - V_s \delta_{i3}) \tilde{c}] }{\partial x_i} = 0 \quad (\text{A2.22})$$

Integrate (A2.22) over time to obtain (A2.23)

$$\frac{\partial c}{\partial t} + \frac{\partial u_i c}{\partial x_i} = - \frac{\partial}{\partial x_i} (F_i - V_s c \delta_{i3}) \quad (\text{A2.23})$$

where $F_i = \overline{u'_i c'}$ denotes the Reynolds flux of sediment. Neglect the variation in y -direction and the variation of F in x direction

$$\frac{\partial c}{\partial t} + \frac{\partial u c}{\partial x} + \frac{\partial w c}{\partial z} = - \frac{\partial}{\partial z} (F - V_s c) \quad (\text{A2.24})$$

$$F = F_3 = \overline{c\omega}$$

Integrate (A2.24) over z and introduce the layer-averaged values for u and c

$$\begin{aligned} \frac{\partial}{\partial t} \int_0^h c dz - \frac{\partial h}{\partial t} c|_h + \frac{\partial}{\partial x} \int_0^h u c dz - \frac{\partial h}{\partial x} u c|_h + c w|_h - c w|_0 = \\ \textcircled{1} \qquad \textcircled{2} \qquad \textcircled{3} \qquad \textcircled{4} \qquad \textcircled{5} \qquad \textcircled{6} \\ - (F - V_s c)|_h + (F - V_s c)|_0 \qquad \textcircled{7} \qquad \textcircled{8} \end{aligned} \quad (\text{A2.25})$$

Terms 2, 4, 5, 6 and 7 are negligible under the constraints described before and term 8 denotes the deposition and entrainment of particles at a depth b very close to the bed

$$|(F - V_s c)|_{z=b} = F_b - V_s C_b \qquad F_b = V_s E_s$$

(A2.26) is the equation of balance of sediment mass for a turbidity current.

$$\frac{\partial Ch}{\partial t} + \frac{\partial (UCh)}{\partial x} = V_s (E_s - C_b) \quad (\text{A2.26})$$

where E_s is the entrainment coefficient of sediment particles. $V_s E_s$ indicate the rate of sediment entrainment and $V_s C_b$ denotes the rate of deposition. (A2.27) represents the steady condition

$$\frac{\partial (UCh)}{\partial x} = V_s (E_s - C_b) \quad (\text{A2.27})$$

A2.2 Equations on mild bed slopes

Assumptions are made that the change in velocity of the turbid underflow ($du/dx=0$) and amount of deposition or entrainment of particles are negligible (Chap. 5 - Part 1). Under these constraints, (A2.20) and (A2.27) can be written as

$$\frac{dh}{dx} = E_w \quad (\text{A2.28})$$

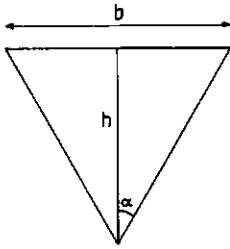
$$\frac{dC}{dx} = -\frac{E_w C}{h} \quad (\text{A2.29})$$

Substituting (A2.28) and (A2.29) into the momentum equation (A2.15), and introducing the Richardson number, $R_I = (RgCh)/U^2$ results in (A2.30) that describes the momentum equation of turbidity currents on mild bed slopes.

$$E_w + C_D = R_I \left(S - \frac{1}{2} E_w \right) \quad (\text{A2.30})$$

A2.3 Recasting the equations for triangular cross-section

For a triangular cross-section the following definitions can be made:



$$a(\text{area}) = h^2 \tan \alpha$$

$$b(\text{width}) = 2h \tan \alpha$$

$$P(\text{wetted perimeter}) = 2h \frac{\tan \alpha}{\sin \alpha}$$

The equations (A2.20), (A2.27), and (A2.15) for triangular cross-section can be written as

$$\frac{d(Ua)}{dx} = bE_w U \quad (\text{A2.31})$$

$$\frac{d(UaC)}{d} = bV_s(E_s - C_b) \quad (\text{A2.32})$$

$$\frac{d(U^2 a)}{dx} = -C_D U^2 P + RCg a S - \frac{1}{3} \frac{d(RCg a h)}{dx} \quad (\text{A2.33})$$

Substitute the definition of a, b, and P into (A2.31)-(A2.33), assuming $v_s E_s - v_s C_b = 0$ and $\partial u / \partial x = 0$, and $\partial \alpha / \partial x = 0$, and introduce the Richardson number as

$R_I = (RgCh)/2U^2$ to obtain

$$\frac{dh}{dx} = E_w \quad (\text{A2.34})$$

$$\frac{dC}{dx} = -2E_w \frac{C}{h} \quad (\text{A2.35})$$

$$E_w + \frac{C_D}{\sin \alpha} = R_I (S - (\frac{1}{3}) E_w) \quad (\text{A2.35})$$

A2.4 Dilution by entrainment (triangular cross-section)

The amount of dilution $\Delta Q/Q_0$ due to water entrainment along the river channel x can be obtained from (A2.31) and (A2.34) as follows:

$$Q = Uh^2 \cdot \tan \alpha$$

$$Q_0 = Uh_0^2 \cdot \tan \alpha$$

$$Q - Q_0 = \Delta Q = U[h^2 - h_0^2] \tan \alpha$$

$$\frac{\Delta Q}{Q_0} = \left(\frac{h}{h_0}\right)^2 - 1 \quad (\text{A2.36})$$

Appendix 3

NUMERICAL MODEL DYRESM

A3.1 Model description

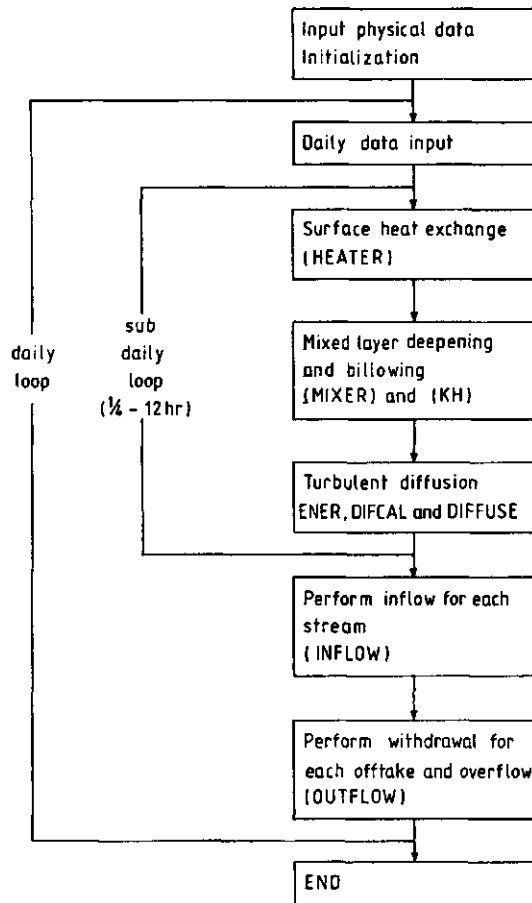
The dynamic reservoir simulation model DYRESM, is a one-dimensional numerical simulation model for the prediction of temperature and salinity in small to medium lakes and reservoirs. DYRESM was developed by Imberger et al. (1978), concentrating on parameterization of the physical processes rather than numerical solution of the appropriate differential equations. DYRESM makes use of a layer concept, in which it divides the reservoir into uniform horizontal slabs which form the computational building blocks of the model. These layers move up and down, adjusting their thickness in accordance with the volume-depth relationship, as inflow and withdrawal increase and decrease the reservoir volume. In this way the problems of numerical diffusion associated with computation of vertical advection above the levels of inflow and withdrawal are avoided. The model incorporates two time steps; a fixed basic time step of one day and a variable sub-daily (1/4-12hrs) time step for the mixing algorithm. This procedure allows small time steps when the dynamics so require; in less critical periods, the time step expands without loss in accuracy.

The outstanding features of DYRESM are: the accuracy by which the various components (salt and temperature) are modelled, its variable time step, its dependance on only physical interpretable calibration factors, and its Lagrangian structure. The one-dimensional assumption places certain restrictions on the applicability of the model. Therefore, one needs to validate the one-dimensionality criteria (as described in Chapter 5) for the lake or reservoir for which the model is used.

DYRESM was developed over the last decade. The development of the model is continuing, Version 6.4 is used for the present study. A brief description of the model is given here. Fig. A3.1 contains a scheme of the model and the major relationships that govern the different processes.

A3.2 Model structure

The model is constructed as a main program with subroutines which separately model each of the physical processes as inflow, outflow, mixed layer dynamics in epilimnion and vertical transport in the hypolimnion (Flowchart 1).



Flowchart 1. DYRESM mainline.

The main program inserts the fixed input data; physical dimensions, volume-area as a function of depth, physical properties of the inflowing streams, offtake locations, initial temperature and salinity profiles, and output control parameters.

The daily loop begins with the input of the inflow, outflow and meteorological data. After some output, the sub-daily loop commences. The heat exchanges through the surface are modeled by HEATER, which simulates radiation penetrative heating and evaporative, conductive, and long wave radiation exchanges at the surface. The updated slab structure is then adjusted for mixed layer deepening by MIXER and for Kelvin-Helmholtz

billowing at the interface by KH. The mixed layer dynamics are modelled in four distinct sections; deepening by convective overturn, deepening by stirring, deepening by shear production and mixing at the thermocline by Kelvin-Helmholtz billows. Once the new thermocline depth and thickness have been computed, the model then calculates the vertical turbulent diffusion in the hypolimnion by subroutines ENER, DIFCAL and DIFUSE. These subroutines calculate the eddy diffusivity, and the net heat and salt transport from the bottom through the hypolimnion into the epilimnion. This sub-daily loop has a time-step varying from 15 minutes to 12 hours.

At the end of the diffusion routine, which is carried out in the same time step as the mixed layer dynamics, a new structure for a particular day is obtained. This density structure is then used to route the inflowing water from the various contributing streams into the reservoir. The subroutine INFLOW allows for turbulent entrainment and subsurface intrusions (a modified version of INFLOW, Chapter 5, also allows for the sediment in the inflowing water). The outflow is calculated by the model using the structure left after the inflow has been added. The simulation models withdrawal from each submerged offtake, and if necessary, flow over the crest. Two idealized outflow structures are modelled. First, a two-dimensional flow into a line sink (Fig. A3.1), and second, a radial flow into a point sink, both of finite dimensions.

At this stage the predicted temperature and salinity structure is recorded as output. In the present work, the model is extended with the calculation of the average salinity of the withdrawal water at the offtakes and overflow, the total mass and salt content, and the average salinity of the reservoir. This routine is repeated for each day of the simulation.

A number of service routines which are called from the various segments of the main program and the dynamics subroutines complete the structure of DYRESM. The first is THICK, which maintains the model layer volumes between specific limits. The maximum and minimum volumes V_{MAX} and V_{MIN} as set in the present study are; $V_{MIN} = 0.01 * \text{storage volume}$ and $V_{MAX} = 2V_{MIN}$. DENSITY calculates the density of water for given temperature and salinity (it is modified to calculate the water density as a function of temperature, salt and sediment (Shiati, 1990). SATVAP evaluates the saturated vapor pressure of air corresponding to a given temperature, and RESINT provides an interpolation between depth, volumes and areas from the physical data input.

A3.3 Model constants

There are seven constants used in DYRESM, of which only one is adjustable, the others are related to well identified physical processes and are determined from experimental or field data. The constants are shown in Table A3.1.

Table A3.1 Values of constants used in DYRESM

process	constant	value	units	description
Rad. penetration (thermal) heating	ζ_1	0.35	1/m	extinction coefficient for short-wave radiation
Mixing in the epilimnion	C_K	0.125	-	the stirring efficiency of convective overturn
	C_S	0.20	-	the efficiency of shear production for entrainment
	C_T	0.51	-	constant determining rate of increase of kinetic energy
	ζ	1.23	-	the stirring efficiency of the wind
Mixing in the hypolimnion	α_1	0.048	-	the efficiency of mixing in the hypolimnion
Inflow	C_D	0.016*	-	drag coefficient for inflowing streams

* A value of $C_D=0.025$ is used in the present study.

Surface heat, mass and momentum exchanges :

$$\begin{aligned}\bar{H} &= -C_H \rho_a C_p U (\theta - \theta_a) \\ E &= -C_W \rho_a L_w U (q - q_s) \\ \tau &= C_D \rho_a U^2\end{aligned}$$

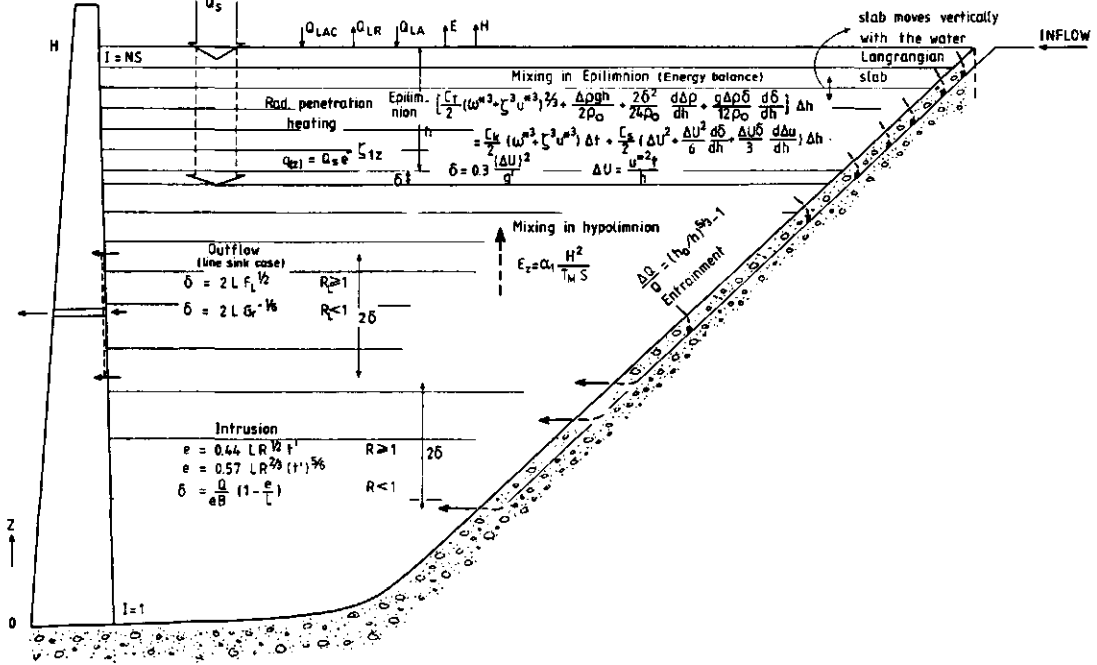


Fig. A3.1 A schematic of the numerical model DYRESM.

Notations :

- B = the reservoir width (m)
- C_D = drag coefficient (-)
- C_H = respective bulk transfer coefficients (-)
- C_K = coefficient of stirring efficiency (-)
- C_S = coefficient of the efficiency of shear production (-)
- C_T = temporal effects due to changes in surface wind stress or surface cooling (-)
- C_P = specific heat of air (J/kg °C)
- C_W = respective bulk transfer coefficient (-)
- E = evaporative heat transfer flux (W/m²)
- e = intrusion length (m)
- F_I = internal Froude number (Q/BNL²) (-)
- F_L = internal Froude number (q/NL²) (-)
- G_r = Grashof number (N²L⁴/ε₂²) (-)
- g = acceleration due to gravity (m/s²)
- g' = modified acceleration due to gravity, g(Δρ/ρ) (m/s²)

- H = the reservoir depth (m)
 \tilde{H} = conductive (sensible) heat transfer flux (W/m^2)
 h = depth of mixed layer (m)
 h = depth of underflow in eq. of entrainment (m)
 h_0 = initial depth of underflow (m)
 L = the reservoir length (m)
 L_w = latent heat of evaporation (J/kg)
 N = Brunt-Vaisala frequency $N = [gd\rho/(\rho_0 dz)]^{1/2}$ (1/s)
 NS = total number of slabs
 Q = discharge (m^3/s)
 Q_{LA} = Re-emitted back long-wave radiation from sky to earth ($J/m^2 s$)
 Q_{LAC} = clouds emit long-wave radiation ($J/m^2 s$)
 Q_{LR} = long-wave radiation emitted from the water surface ($J/m^2 s$)
 Q_S = solar radiation at surface ($J/m^2 s$)
 q = discharge per unit width (m)
 q = specific humidity (kg of water moisture/ kg of air-water moisture)
 q_s = saturation specific humidity (kg of water moisture/kg of air-water moisture)
 $q_{(Z)}$ = radiation remain at a height Z ($J/m^2 s$)
 R = non-dimensional number $R = F_I G_r^{1/3}$
 R_L = non-dimensional number $R_L = F_L G_r^{1/3}$
 S = normalized water column stability $S = (H/\Delta\rho)(d\rho/dz)$ (-)
 T_M = time scale for mixing (s)
 t = time (s)
 t' = non-dimensional time $tN/G_r^{1/6}$
 Δt = time step (s)
 U = wind speed (m/s)
 ΔU = mean shear velocity (m/s)
 u^* = current wind shear velocity (m/s)
 Z = the depth (m)
 α_1 = constant in eddy diffusivity in hypolimnion (-)
 δ = half thickness of intrusion or withdrawal layer (m)
 δ = billow thickness (m)
 ζ = coefficient measuring stirring efficiency of the wind (-)
 ζ_1 = the bulk extinction coefficient (1/m)
 θ = air temperature ($^{\circ}C$)
 θ_s = surface water temperature ($^{\circ}C$)
 ρ = density of water (kg/m^3)
 ρ_a = density of air (kg/m^3)
 ρ_0 = mean density of water reservoir (kg/m^3)
 $\Delta\rho$ = density difference between the mixed layer and the next layer of thickness Δh
 τ = shear stress ($kg/m/s^2$)
 ϵ_z = effective vertical diffusion coefficient (m^2/s)
 ω^* = turbulent velocity scale (m/s)

Appendix 4

DIFFUSION OF SALT FROM RESERVOIR BOTTOM

The Jarreh Reservoir will be formed in salty strata of the Agha-Jari formation. The salt will move by diffusion from the bottom formation towards the lake. If the lake remains fresh, this will finally result in desalinization of the bottom sediments, first of the top layers, later also at greater depth. Salt diffusion from the Jarreh reservoir bottom appears to be a slow process and is negligible after the first few years.

Macroscopically diffusion in soil is described by Fick's Law:

$$J = -\epsilon D \frac{\partial C}{\partial x} \quad (\text{A4.1})$$

where

J = flux density (areal mass flux density) in $(\text{kg m}^{-2} \text{s}^{-1})$ or $(\text{kg m}^{-2} \text{yr}^{-1})$

D = diffusion coefficient in $(\text{m}^2 \text{s}^{-1})$ or $(\text{m}^2 \text{yr}^{-1})$

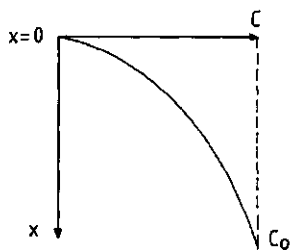
C = salt concentration in the pore water in (kg m^{-3})

x = distance in (m)

t = time in (s) or (yr)

ϵ = porosity of soil in (%).

The concentration (C) at any depth (x) and time (t) can be obtained by the following relation (Volker, 1942; Crank, 1967).



$$C = C_0 \operatorname{erf}(m) \quad (\text{A4.2})$$

$$m = \frac{x}{2\sqrt{Dt}}$$

$$\operatorname{erf}(m) = \frac{2}{\sqrt{\pi}} \int_0^m e^{-m^2} \cdot dm$$

where

C_0 = the initial salt concentration of the formations (pore water)

differentiation of eq. (A4.2) with respect to x gives:

$$\frac{\partial C}{\partial x} = C_0 \frac{2}{\sqrt{\pi}} e^{-\left(\frac{x}{2\sqrt{Dt}}\right)^2} \cdot \frac{1}{2\sqrt{Dt}} = \frac{2C_0}{\sqrt{\pi}} e^{-\frac{x^2}{4Dt}} \cdot \frac{1}{2\sqrt{Dt}}$$

$$\frac{\partial C}{\partial x} = \frac{C_0 \cdot e^{-\frac{x^2}{4Dt}}}{\sqrt{\pi Dt}} \quad (\text{A4.3})$$

substituting eq. (A4.3) in eq. (A4.1) gives for x=0:

$$J_{(x=0)} = eD \frac{\partial C}{\partial x} \Big|_{x=0} = \frac{eC_0\sqrt{D}}{\sqrt{\pi t}} \quad (\text{A4.4})$$

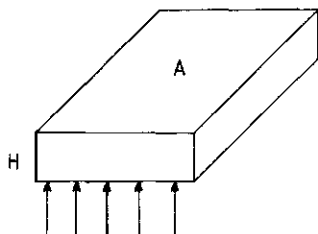
In the relation (A4.4), the upward flux is considered positive and the minus sign has been neglected.

The amount of salt entering the Jarreh reservoir (ΔM) in time step Δt can be calculated as follows:

$$\Delta M = JA \Delta t$$

$$\Delta M = \left[\int_t^{t+\Delta t} J(\tau) d\tau \right] A = A \int_t^{t+\Delta t} \frac{eC_0\sqrt{D}}{\sqrt{\pi\tau}} d\tau$$

$$= \frac{eAC_0\sqrt{D}}{\sqrt{\pi}} (2\tau^{1/2}) \Big|_t^{t+\Delta t} = \frac{2eAC_0\sqrt{D}}{\sqrt{\pi}} [\sqrt{t+\Delta t} - \sqrt{t}]$$



H= average depth
V= volume
V= A . H

Let ΔC be the increase in the salt concentration due to bottom diffusion in time step Δt then

$$\Delta C = \frac{\Delta M}{V} = \frac{\Delta M}{AH}$$

$$\Delta C = \alpha [\sqrt{E + \Delta E} - \sqrt{E}] \quad \alpha = \frac{2\epsilon C_0 \sqrt{D}}{\sqrt{\pi} H} \quad (A4.5)$$

For Jarreh Reservoir: $H = 24.1$ m, porosity of formation = 0.2, and $D = 0.018$ m²/Yr, Fig. A4.1 gives the increase in salt concentration due to salt diffusive flux for different initial salt concentrations of the bottom formation. As can be seen from Fig. A4.1 the amount of salt diffusive flux from the Jarreh R. bottom formation ($C_0 \approx 25$ kg/m³) is about 13 g/m³ in the first year and reduces to 4.8 and 3.4 g/m³ after 10 and 20 years, respectively. Apparently, this is not significant when compared with the average reservoir salinity of around 2000 g/m³. This is even the case if the salinity of the bottom formation would be as high as 100 kg/m³.

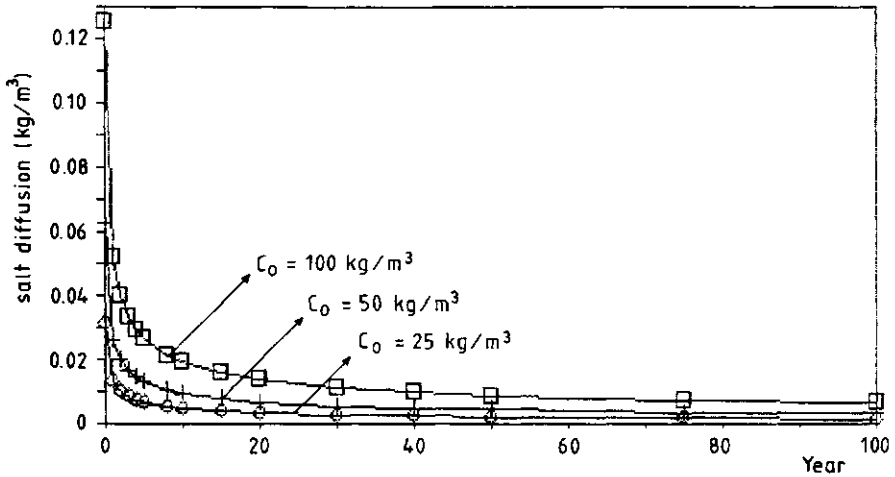


Fig. A4.1 The increase in salt concentration in Jarreh R. due to salt diffusion from the bottom.

CURRICULUM VITAE

Karim Shiati was born in Shiraz (Iran) on 24 April 1951. He is graduated in Agriculture (specialization Irrigation) from the Shiraz University (Iran) in 1973. In 1977 he received his M. Sc. in Agricultural Engineering (specialization Water Resources Engineering) from the University of Canterbury in New Zealand.

Since then, he has worked with Yekom Consulting Engineering Co. (Iran). During his career he has been involved in regional water resources studies, groundwater hydrology, irrigation, and drainage projects. He followed the training course, "Graduate Course in Hydrology", held in the University of New South Wales, School of Civil Engineering, Australia in March-June 1984 and made technical short-term visits to Pakistan, India, Japan and The Netherlands.

During the past four years, he has been working on the present research under the supervision of Professor Dr. W.H. van der Molen and Ir. J.H.G. Verhagen of the Wageningen Agricultural University.

His permanent address is: Yekom Consulting Engineers,
No. 77 North Saba Ave.
Tehran 14167, Iran
Tel: (98) -21- 899362
Fax: (98) -21- 893815



